Secondary Metabolites of Marine-Derived Fungi

Inaugural dissertation

for the attainment of the title of doctor
in the Faculty of Mathematics and Natural Sciences
at Heinrich Heine University Düsseldorf

presented by

Dina Faek Abdel-Kader Hassouna El-Kashef
from Egypt

Düsseldorf, November 2020

from the institute for Pharmaceutical Biology and Biotechnology
at Heinrich Heine University Düsseldorf

Published by permission of the
Faculty of Mathematics and Natural Sciences at
Heinrich Heine University Düsseldorf

Supervisor: Prof. Dr. Dres. h.c. Peter Proksch
Co-supervisor: Prof. Dr. Matthias Kassack

Date of the oral examination: 18.02.2021

Declaration of Academic Honesty/Erklärung

Hiermit erkläre ich ehrenwörtlich, dass ich die vorliegende Dissertation mit dem Titel “ Secondary Metabolites of Marine-Derived Fungi ” selbst angefertigt habe. Außer den angegebenen Quellen und Hilfsmitteln wurden keine weiteren verwendet. Diese Dissertation wurde weder in gleicher noch in abgewandelter Form in einem anderen Prüfungsverfahren vorgelegt.

Düsseldorf, den 02.11.2020

Dina F. A. Hassouna El-Kashef

(بِسْمِ اللَّـهِ الرَّحْمَـٰنِ الرَّحِيمِ)

Table of Contents

Abstract

Since ancient times, nature has served as an inspiration for and source of therapies for many diseases of mankind. Despite the development of many modern synthetic therapeutics, there is an immense need for finding bioactive natural compounds which could serve as lead compounds for drug discovery and development. The marine environment represents one of the most important resources of bioactive secondary metabolites. In particular, marine fungi exemplify an underexplored treasure and are producers of many promising natural products that could contribute to the development of new pharmaceuticals. Aiming to expand the potential of marine-derived fungi, the OSMAC approach (**O**ne **S**train **Ma**ny **C**ompounds) is implemented to activate silent biosynthetic gene clusters and eventually to expand the metabolic profile of fungi.

This dissertation includes two major projects described in three publications. The first project deals with the investigation of a marine-derived strain of the fungus *Metarhizium marquandii* obtained from a seawater sample collected from the North Sea, Germany. The second project deals with the investigation of the marine-derived fungus *Aspergillus falconensis* isolated from marine sediment collected at a depth of 25 m from the Canyon at Dahab, Red Sea, Egypt. In general, the work flow has focused on exploring the diverse cryptic fungal metabolites of these fungi in addition to some modifications in the culture conditions (OSMAC approach) with the purpose of diversifying the metabolic pattern of the fungi. For the isolation of the secondary metabolites from the aforementioned fungi, several chromatographic techniques have been utilized. The structures of the isolated compounds were unambiguously elucidated by 1D/2D nuclear magnetic resonance spectroscopy (NMR) analyses together with mass spectrometry data, while their stereochemical configurations were deduced based on optical rotations (OR) measurements and comparison with the literature values, modified Mosher's method (MMM), electronic circular dichroism (ECD) and vibrational circular dichroism (VCD) calculations or single-crystal X-ray diffraction analysis (XRD).

The results described in this dissertation are included in two published manuscripts and one manuscript which is currently under revision.

First Project: Investigation of the marine-derived strain of the fungus *Metarhizium marquandii*.

The results of the first project are published in the *Journal of Natural Products* in August, 2019, by Dina H. El-Kashef, Georgios Daletos, Malte Plenker, Rudolf Hartmann, Attila Mándi, Tibor Kurtán, Horst Weber, Wenhan Lin, Elena Ancheeva and Peter Proksch, and are included in **chapter 2** (Polyketides and a Dihydroquinolone Alkaloid from a Marine-Derived Strain of the Fungus *Metarhizium marquandii*). "Three new natural products (**1**–**3**), including two butenolide derivatives (**1** and **2**) and one dihydroquinolone derivative (**3**), together with nine known natural products were isolated from a marine-derived strain of the fungus *Metarhizium marquandii*. The structures of the new compounds were unambiguously deduced by spectroscopic means including HRESIMS and 1D/2D NMR spectroscopy, ECD, VCD, OR measurements, and calculations. The absolute configuration of marqualide (**1**) was determined by a combination of modified Mosher's method with TDDFT-ECD calculations at different levels, which revealed the importance of intramolecular hydrogen bonding in determining the ECD features. The (3*R*,4*R*) absolute configuration of aflaquinolone I (**3**), determined by OR, ECD, and VCD calculations, was found to be opposite of the (3*S*,4*S*) absolute configuration of the related aflaquinolones A–G, suggesting that the fungus *M. marquandii* produces aflaquinolone I with a different configuration (chiral switching). The absolute configuration of the known natural product terrestric acid hydrate (**4**) was likewise determined for the first time in this study. TDDFT-ECD calculations allowed determination of the absolute configuration of its chirality center remote from the stereogenic unsaturated *γ*-lactone chromophore. ECD calculations aided by solvent models revealed the importance of intramolecular hydrogen bond networks in stabilizing conformers and determining relationships between ECD transitions and absolute configurations." (El-Kashef *et al.* 2019).

Second Project: Investigation of the marine-derived fungus *Aspergillus falconensis*.

The results of the second project are included in two major publications based on the metabolic pattern of isolated compounds and the conducted bioassays. The first part is published in *Marine Drugs* in April, 2020 by Dina H. El-Kashef, Fadia S. Youssef, Rudolf Hartmann, Tim-Oliver Knedel, Christoph Janiak, Wenhan Lin, Irene Reimche, Nicole Teusch, Zhen Liu and Peter Proksch while, the other part is submitted to

Bioorganic & Medicinal Chemistry, Dina H. El-Kashef, Fadia S. Youssef, Werner E.G. Müller, Wenhan Lin, Marian Frank, Zhen Liu and Peter Proksch and currently is under revision. The results are included in **chapter 3** and **4**, respectively. (Azaphilones from the Red Sea Fungus *Aspergillus falconensis*). "The marine-derived fungus *Aspergillus falconensis*, isolated from sediment collected from the Canyon at Dahab, Red Sea, yielded two new chlorinated azaphilones, falconensins O and P (**1** and **2**) in addition to four known azaphilone derivatives (**3**−**6**) following fermentation of the fungus on solid rice medium containing 3.5% NaCl. Replacing NaCl with 3.5% NaBr induced accumulation of three additional new azaphilones, falconensins Q−S (**7**−**9**) including two brominated derivatives (**7** and **8**) together with three known analogues (**10**−**12**). The structures of the new compounds were elucidated by 1D and 2D NMR spectroscopy and HRESIMS data as well as by comparison with the literature. The absolute configuration of the azaphilone derivatives was established based on single-crystal X-ray diffraction analysis of **5**, comparison of NMR data and optical rotations as well as on biogenetic considerations. Compounds **1**, **3**−**9**, and **11** showed NF-κB inhibitory activity against the triple negative breast cancer cell line MDA-MB-231 with IC_{50} values ranging from 11.9 to 72.0 μM." (El-Kashef *et al.* 2020).

(A new dibenzoxepin and a new natural isocoumarin from the marine-derived fungus *Aspergillus falconensis*). "Fermentation of the marine-derived fungus *Aspergillus falconensis*, isolated from sediment collected from the Red Sea, Egypt on solid rice medium containing 3.5% NaCl yielded a new dibenzoxepin derivative (**1**) and a new natural isocoumarin (**2**) along with six known compounds (**3** - **8**). Changes in the metabolic profile of the fungus were induced by replacing NaCl with 3.5% $(NH_4)_2SO_4$ that resulted in the accumulation of three further known compounds (**9** – **11**), which were not detected when the fungus was cultivated in the presence of NaCl. The structures of the new compounds were elucidated by HRESIMS and 1D/2D NMR as well as by comparison with the literature. Molecular docking was conducted for all isolated compounds on crucial enzymes involved in the formation, progression and metastasis of cancer which included human cyclin-dependent kinase 2 (CDK-2), human DNA topoisomerase II (TOP-2) and matrix metalloproteinase 13 (MMP-13). Diorcinol (**7**), sulochrin (**9**) and monochlorosulochrin (**10**) displayed notable stability within the active pocket of CDK-2 with free binding energy (ΔG) equals to -25.72, -25.03 and -25.37 Kcal/mol, respectively whereas sulochrin (**9**) exerted the highest fitting score

within MMP-13 active center (ΔG = -33.83 Kcal/mol). *In vitro* cytotoxic assessment using MTT assay showed that sulochrin (**9**) exhibited cytotoxic activity versus L5178Y mouse lymphoma cells with an IC_{50} value of 5.1 μM.", (abstract taken from the submitted draft).

Zusammenfassung

Seit der Vorzeit dient die Natur als Ideengeber und Quelle für Arzneistoffe, die Menschen zur Behandlung von zahlreichen Krankheiten einsetzen. Wenngleich neue moderne, synthetische Arzneistoffe entwickelt werden, gibt es nach wie vor ein großes Bestreben bioaktive Naturstoffe zu entdecken, da diese als Leitstrukturen zur Entdeckung und Entwicklung neuer Therapeutika dienen können. Marine Habitate bilden eine der wichtigsten Quellen für die Suche nach bioaktiven Sekundärmetabolite. Marine Pilze stellen hierbei eine noch wenig erforschte Quelle für die Naturstoffforschung dar. Pilze sind u. a. Produzenten zahlreicher und vielversprechender Naturstoffe, die zur Entwicklung neuer Arzneistoffe beitragen können. Um das Potential mariner Pilze besser nutzen zu können, kann das OSMAC Prinzip (**O**ne **S**train **Ma**ny **C**ompounds für Ein Stamm viele Verbindungen) angewendet werden. Hierbei können sog. „schlafende“ Biosynthese-Gencluster reaktiviert werden. Die Aktivierung von diesen Biosynthese-Genclustern kann u. a. wiederum zu einer Änderung des metabolischen Profils führen.

Diese Dissertation ist in zwei Hauptprojekte gegliedert, aus denen insgesamt drei Publikationen hervorgegangen sind. Das erste Projekt befasst sich mit der Untersuchung des marinen Pilzes *Metarhizium marquandii*, welcher aus einer deutschen Nordseemeerwasserprobe isoliert worden war Das zweite Projekt befasst sich mit der Untersuchung des marinen Pilzes *Aspergillus falconensis*. Dieser wurde aus einer Probe Meeressediment isoliert. Die Probe stammte aus 25 m Tiefe des roten Meeres an der Schlucht von Dahab in Ägypten. Das generelle Arbeitsschema legt hierbei den Fokus auf die Entdeckung kryptischer Pilzmetaboliten. Es wurden Modifikationen an den Kultivierungsbedingungen vorgenommen (OSMAC Ansatz) um eine Diversifizierung der pilzlichen Metabolitmuster zu erreichen. Um Sekundärmetaboliten aus den zuvor genannten Pilzen zu isolieren, wurden verschiedene chromatographische Verfahren angewendet. Die planare Struktur der isolierten Verbindungen wurde durch das Zusammenspiel von ein- und zweidimensionaler Kernspinresonanzspektroskopie (NMR) und Massenspektrometrie eindeutig aufgeklärt. Die Stereochemie wurde durch Messungen und Literaturvergleich der optischen Aktivität (OR), modifizierter Mosher Methode (MMM), Messung und Berechnung von elektronischem Zirkulardichroismus (ECD) und Vibrations

Zirkulardichroismus (VCD), sowie der Interpretation von Röntgenkristallstrukturbeugungsmustern (XRD) abgeleitet.

Die in dieser Dissertation beschriebenen Ergebnisse sind Bestandteile von zwei Veröffentlichungen und einem bereits zur Veröffentlichung eingereichten Manuskript.

Erstes Projekt: Untersuchungen am marinen Pilz *Metarhizium marquandii*.

Die Ergebnisse des ersten Projektes wurden im August 2019 im *Journal of Natural Products* von Dina H. El-Kashef, Georgios Daletos, Malte Plenker, Rudolf Hartmann, Attila Mándi, Tibor Kurtán, Horst Weber, Wenhan Lin, Elena Ancheeva und Peter Proksch veröffentlicht. Sie sind im Original in **Kapitel 2** (Polyketides and a Dihydroquinolone Alkaloid from a Marine-Derived Strain of the Fungus *Metarhizium marquandii*) zu finden. "Drei neue Naturstoffe (**1**–**3**), inklusive zweier Butenolid Derivative (**1** und **2**) und einem Dihydrochinolon Derivativ (**3**), wurden zusammen mit neun bekannten Naturstoffen aus dem marinen Pilz *Metarhizium marquandii* isoliert. Die Struktur der neuen Verbindungen wurde durch den Einsatz spektroskopischer Methoden wie HRESIMS, 1D/2D NMR sowie Messungen und Berechnungen von ECD, VCD und OR eindeutig aufgeklärt. Die absolute Konfiguration von Marqualid (**1**) wurde durch eine Kombination aus modifizierter Mosher Methode und mehrstufigen TDDFT-ECD Berechnungen bestimmt. Hierbei wurde die intramolekulare Wasserstoffbrücke als das Strukturmerkmal identifiziert, welches das ECD bestimmt. Die absolute (3*R*,4*R*) Konfiguration von Aflachinolon I (**3**), bestimmt durch OR, ECD und VCD Berechnungen, stellte sich als chirales Gegenstück zur absoluten (3*S*,4*S*) Konfiguration der verwandten Aflachinolone A–G heraus. Dies legt nah, dass das vom Pilz *M. marquandii* produzierte Aflachinolon I einem chiralen Switch unterliegt. Außerdem wurde die absolute Konfiguration des bekannten Naturstoffs Terresticsäurehydrat (**4**) in dieser Studie zum ersten Mal beschrieben. TDDFT-ECD Berechnungen erlaubten die Bestimmung der absoluten Konfiguration des Chiralitätszentrums, welches sich entfernt von der stereogenen Einheit des ungesättigten γ-Lacton Chromophors befindet. ECD Berechnungen halfen hierbei im Lösemittelmodell dabei die Wichtigkeit des intramolekularen Wasserstoffbrückennetzwerks aufzuzeigen. Dieses stabilisiert Konformere und ist damit maßgeblich am der Beziehung zwischen ECD Übergängen und der absoluten Konfiguration beteiligt." (El-Kashef *et al.* 2019).

Zweites Projekt: Untersuchungen am marinen Pilz *Aspergillus falconensis*.

Die Ergebnisse des zweiten Projekts bilden den Inhalt von zwei Publikationen und beschäftigen sich mit der Einordnung der isolierten Verbindungen in ein metabolisches Muster und mit den damit durchgeführten Bioassays. Der erste Teil wurde im April 2019 in *Marine Drugs* von Dina H. El-Kashef, Fadia S. Youssef, Rudolf Hartmann, Tim-Oliver Knedel, Christoph Janiak, Wenhan Lin, Irene Reimche, Nicole Teusch, Zhen Liu und Peter Proksch veröffentlicht, während der zweite Teil zurzeit in Revision bei *Bioorganic & Medicinal Chemistry* ist. Das Manuskript wurde von Dina H. El-Kashef, Fadia S. Youssef, Werner E.G. Müller, Wenhan Lin, Marian Frank, Zhen Liu und Peter Proksch eingereicht. Die Ergebnisse befinden sich im Original in **Kapitel 3** und **4**. (Azaphilones from the Red Sea Fungus *Aspergillus falconensis*). "Der marine Pilz *Aspergillus falconensis*, der aus einer Sedimentprobe des roten Meers bei der Schlucht von Dahab isoliert worden war, produzierte bei einer Fermentation auf festem Reismedium unter Zusatz von 3.5 % NaCl, zwei neue chlorierte Azaphilone: Falconensine O und P (**1** und **2**) und außerdem vier bekannte Azaphilonderivate (**3**−**6**). Die Substitution von NaCl mit 3.5 % NaBr führte zur Akkumulation von drei zusätzlichen neuen Azaphilonen: Falconensine Q-S (**7**-**9**), und außerdem von drei bekannten Analoga (**10**-**12**). Unter den Verbindungen befanden sich zwei bromierte Derivative (**7** und **8**). Die neuen Strukturen wurden durch den Einsatz von 1D und 2D NMR, hochauflösender Massenspektrometrie, sowie den Vergleich mit Literaturdaten aufgeklärt . Die absolute Konfiguration der Azaphilonderivate wurde durch die Auswertung der Röntgenkristallstrukturanalye von **5**, sowie den Vergleich von NMR Daten und optischer Aktivät unter Berücksichtigung der Aspekte der Biosynthese bestimmt. Verbindungen **1**, **3**−**9**, und **11** zeigten NF-κB Inhibitionsaktivität gegen die tripelnegative Brustkrebszelllinie MDA-MB-231 mit IC_{50} Werten im Bereich von 11.9 bis 72.0 μM." (El-Kashef *et al.* 2020).

(A new dibenzoxepin and a new natural isocoumarin from the marine-derived fungus *Aspergillus falconensis*). "Die Fermentation des marinen Pilzes *Aspergillus falconensis*, welcher aus einer Sedimentprobe des roten Meers in Ägypten isoliert wurde, auf festem Reismedium unter Zusatz von 3.5% NaCl produzierte ein neues Dibenzoxepinderivat (**1**) und ein neues natürlich vorkommendes Isocumarin (**2**), neben sechs weiteren bekannten Verbindungen (**3 - 8**). Der Austausch des zugesetzten NaCl durch 3.5% $(NH_4)_2SO_4$ führte zu Veränderungen im metabolischen Profil und zur

Isolation von drei weiteren Verbindungen (**9 – 11**), welche in Anwesenheit von NaCl nicht detektiert wurden. Die Struktur der neuen Verbindungen wurden durch den Einsatz von HRESIMS und 1D/2D NMR, sowie durch den Vergleich mit Literaturdaten aufgeklärt. Mit allen Substanzen wurde molekulares Docking in Bindetaschen der Enzyme humane cyclin-abhängige Kinase 2 (CDK-2), humane DNA Topoisomerase II (TOP-2) und Matrix Metalloproteinase 13 (MMP-13) durchgeführt. Hierbei handelt es sich um für die Bildung, das Fortschreiten und die Metastasierung von Krebserkrankungen essentielle Enzyme. Diorcinol (**7**), Sulochrin (**9**) und Monochlorosulochrin (**10**) zeigten hierbei bemerkenswerte Stabilität in der aktiven Bindetasche von CDK-2 mit freien Bindungsenergien (ΔG) von jeweils -25.72, -25.03 und -25.37 Kcal/mol. Außerdem zeigte Sulochrin (**9**) einen hohen Fittingscore im aktiven Zentrum von MMP-13 (ΔG = -33.83 Kcal/mol). In der *in vitro* Zytotoxizitätsbestimmung durch MTT-Assay gegen Mauslymphomazelllinie L5178Yzeigte Sulochrin (**9**) Aktivität mit einem IC_{50} Wert von 5.1 µM.", (Der übersetzte Abstract stammt aus dem eingereichten Manuskript).

Chapter 1 - General Introduction

Natural products continue to be a prolific source of a wide array of molecular entities which exert a variety of biological activities and serve as lead compounds for drug discovery and development. The majority of natural product-derived drugs originate from terrestrial plants and microorganisms, particularly fungi (Newman *et al.* 2016). Nevertheless, marine-derived natural products have also many success stories (Jiménez 2018). Since the oceans cover around 70% of the earth's surface, it is not surprising that the marine environment contributes significantly to the discovery of new drugs and drug leads. Being an underexplored habitat, the marine environment harbours diverse microbes, many of which are untouched and the studied ones are proven to be producers of many interesting bioactive compounds (Cheung *et al.* 2015, Wiese *et al.* 2019).

1.1 Marine Natural Products: Bioprospecting the Future of Drug Discovery

The marine environment offers diverse organisms including invertebrates (sponges, tunicates, corals, etc.), algae and marine microorganisms (including phytoplankton), which are considered as an excellent source of fascinating new natural products with potential therapeutic effects (Hu *et al.* 2011). Strikingly, a growing interest towards marine natural products chemistry has started since the early 1950s, with the isolation of the unusual nucleosides, spongouridine and spongothymidine from the sponge *Cryptotethya crypta* by Bergmann and Feeny (Bergmann *et al.* 1951, Bergmann *et al.* 1955, Hu *et al.* 2011), which later served as lead structures for the antiviral and anticancer marine-derived drugs, Ara-A (vidarabine, Vira-A®) and Ara-C (cytarabine, Cytosar-U®), respectively (Mayer *et al.* 2010). However, after the approval of vidarabine by FDA (Food and Drug Administration of US) for the treatment of *Herpes simplex* virus in 1976, there was a decline in the clinical development of marine-derived drugs (Dyshlovoy *et al.* 2019). Few decades later, marine natural products chemistry got a more prominent status and entered a time of renaissance with the emergence of new techniques for sample collection and advances in analytical and spectroscopic (mainly NMR) methods (Gerwick *et al.* 2012, Jiménez 2018). More than 28,600 marine natural products have been reported till 2019 (Pereira *et al.* 2019). To acclimatize to the harsh marine conditions, marine organisms produce different unique molecules with different structural features including peptides, terpenes, alkaloids, polyketides,

diketopiperazines and many metabolites of mixed biosynthesis, which possess a variety of pharmacological properties such as antibacterial, antimalarial, antiviral, antifungal, anticancer activities etc. (Blunt *et al.* 2018, Jiménez 2018). Many marine natural products have success stories in reaching the pharmaceutical market and others have reached clinical trials exemplifying that marine natural products are potential candidates for drug discovery and development (Mayer *et al.* 2010, Ebada *et al.* 2015).

1.1.1 Marine Pharmaceuticals: FDA-Approved Drugs and Clinical Pipeline

By the beginning of 2020, the total number of FDA-approved marine-derived pharmaceuticals was 12 in addition to one drug approved in Australia in December 2018 (figure 1). Based on the report of marine pharmaceuticals, the marine clinical pipeline of Midwestern University (table 1), almost 24 marine natural compounds were in clinical development till June 2020 (4 in Phase III, 13 in Phase II and 7 in Phase I). Additionally, around 1,000 marine natural products are under pre-clinical trials with various pharmacological activities (https://www.midwestern.edu/departments/marinepharmacology/clinical-pipeline.xml). However, drug development is a dynamic field; a new drug candidate could enter pre-clinical trial or Phase I of clinical trials while others could drop out of the clinical pipeline after failing in one of the consecutive clinical trials (Dyshlovoy *et al.* 2019).

Clinical Status	Compound Name	Trademark isolated/ FDA Approved (Year)	Marine Organism	Chemical Class	Molecular Target	Disease Area
FDA-Approved	Lurbinectedin	Zepzelca™ (2020)	Tunicate	Alkaloid	RNA Polymerase II	Cancer
	Enfortumab Vedotin-ejfv	PADCEV™ (2019)	Mollusk/ cyanobacterium	ADC (MMAE)[a]	Nectin-4	Cancer
	Polatuzumab vedotin (DCDS-4501A)	Polivy™ (2019)	Mollusk/ cyanobacterium	ADC (MMAE)[a]	CD76b & microtubules	Cancer
	Trabectedin (ET-743)	Yondelis® (2015)	Tunicate	Alkaloid	Minor groove of DNA	Cancer
	Omega-3-carboxylic acid	Epanova® (2014)	Fish	Omega-3 fatty acids	Trygliceride-synthesizing enzymes	Hyper-triglyceridemia
	Eicosapenta-enoic acid ethyl ester	Vascepa® (2012)	Fish	Omega-3 fatty acids	Trygliceride-synthesizing enzymes	Hyper-triglyceridemia
	Brentuximab vedotin (SGN-35)	Adcetris® (2011)	Mollusk/ cyanobacterium	ADC (MMAE)[a]	CD30 & microtubules	Cancer
	Eribulin Mesylate (E7389)	Halaven® (2010)	Sponge	Macrolide	Microtubules	Cancer

	Omega-3-acid ethyl esters	Lovaza® (2004)	Fish	Omega-3 fatty acids	Trygliceride-synthesizing enzymes	Hyper-triglyceridemia
	Ziconotide	Prialt® (2004)	Cone snail	Peptide	N-Type Ca^{+2} channel	Chronic Pain
	Vidarabine (Ara-A)	Vira-A® (1976)	Sponge	Nucleoside	Viral DNA polymerase	Antiviral
	Cytarabine (Ara-C)	Cytosar-U® (1969)	Sponge	Nucleoside	DNA polymerase	Cancer
Australia Dec 2018 Approved	Plitidepsin	Aplidin® (2018)	Tunicate	Depsipeptide	eEF1A2	Cancer
Phase III	Plinabulin (NPI-2358)	NA	Fungus	Diketo-piperazine	Microtubules	Cancer
	Tetrodotoxin	Halneuron™	Pufferfish	Guanidinium alkaloid	Sodium Channel	Chronic Pain
	Lurbinectedin (PM01183)	Zepsyre®	Tunicate	Alkaloid	RNA Polymerase II	Cancer
	Marizomib (Salinosporamide A; NPI-0052)	NA	Bacterium	Beta-lactone-gamma lactam	20S proteasome	Cancer
Phase II	GTS-21 (DMXBA)	NA	Worm	Alkaloid	α7 nicotinic acetylcholine receptor	Schizophrenia, Alzheimer Disease, Attention Deficit Hyperactivity Disorder, Endotoxemia, Sepsis, Vagal Activity
	AGS-16C3F	NA	Mollusk/ cyanobacterium	ADC (MMAF)[b]	ENPP3 & microtubules	Cancer
	Plocabulin (PM184)	NA	Sponge	Polyketide	Minor groove of DNA	Cancer
	Tisotumab Vedotin	HuMax®-TF-ADC	Mollusk/ cyanobacterium	ADC (MMAE)[a]	Tissue Factor & microtubules	Cancer
	GSK2857916	NA	Mollusk/ cyanobacterium	ADC (MMAF)[b]	BCMA	Cancer
	Ladiratuzumab vedotin (SGN-LIV1A)	NA	Mollusk/ cyanobacterium	ADC (MMAE)[a]	LIV-1 & microtubules	Cancer
	Bryostatin	NA	Bryozoan	Macrolide lactone	Protein kinase C	Alzheimer's Disease
	Telisotuzumab vedotin (ABBV-399)	NA	Mollusk/ cyanobacterium	ADC (MMAE)[a]	c-Met	Cancer
	Enapotamab vedotin (HuMax-AXL)	NA	Mollusk/ cyanobacterium	ADC (MMAE)[a]	Axl RTK	Cancer
	RC-48	NA	Mollusk/ cyanobacterium	ADC (MMAE)[a]	HER2	Cancer
	CAB-ROR2 (BA-3021)	NA	Mollusk/ cyanobacterium	ADC (MMAE)[a]	ROR2	Cancer
	CX-2029 (ABBV-2029)	NA	Mollusk/ cyanobacterium	ADC (MMAE)[a]	CD71	Cancer
	W0101	NA	Mollusk/ cyanobacterium	ADC (MMAE)[a]	IGF-1R	Cancer
Phase I	ARX-788	NA	Mollusk/ cyanobacterium	ADC (MMAE)[a]	HER2 & microtubules	Cancer
	XMT-1536	NA	Mollusk/ cyanobacterium	ADC (Dolaflexin)	NaPi2b & microtubules	Cancer
	ALT-P7	NA	Mollusk/ cyanobacterium	ADC (MMAE)[a]	HER2 & microtubules	Cancer
	MORAb-202	NA	Sponge	ADC (Macrolide)	Microtubules	Cancer
	PF-06804103	NA	Mollusk/ cyanobacterium	ADC (Auristatin variant)	HER2	Cancer
	Griffithsin	NA	Red alga	Lectin	Carbohydrate-binding	HIV prevention

	ZW-49	NA	Mollusk/ cyanobacterium	ADC (Auristatin variant)	HER2	Cancer

[a]ADC (MMAE) Antibody-Drug Conjugate (Monomethyl auristatin E)

[b]ADC (MMAF) Antibody-Drug Conjugate (Monomethyl auristatin F)

Table 1: Marine derived drugs, FDA approved, in pre-clinical and clinical trials. Table is modified after (A.M.S. Mayer, Marine pharmaceuticals: the clinical pipeline, Midwestern University, Last Rev. June, 2020)

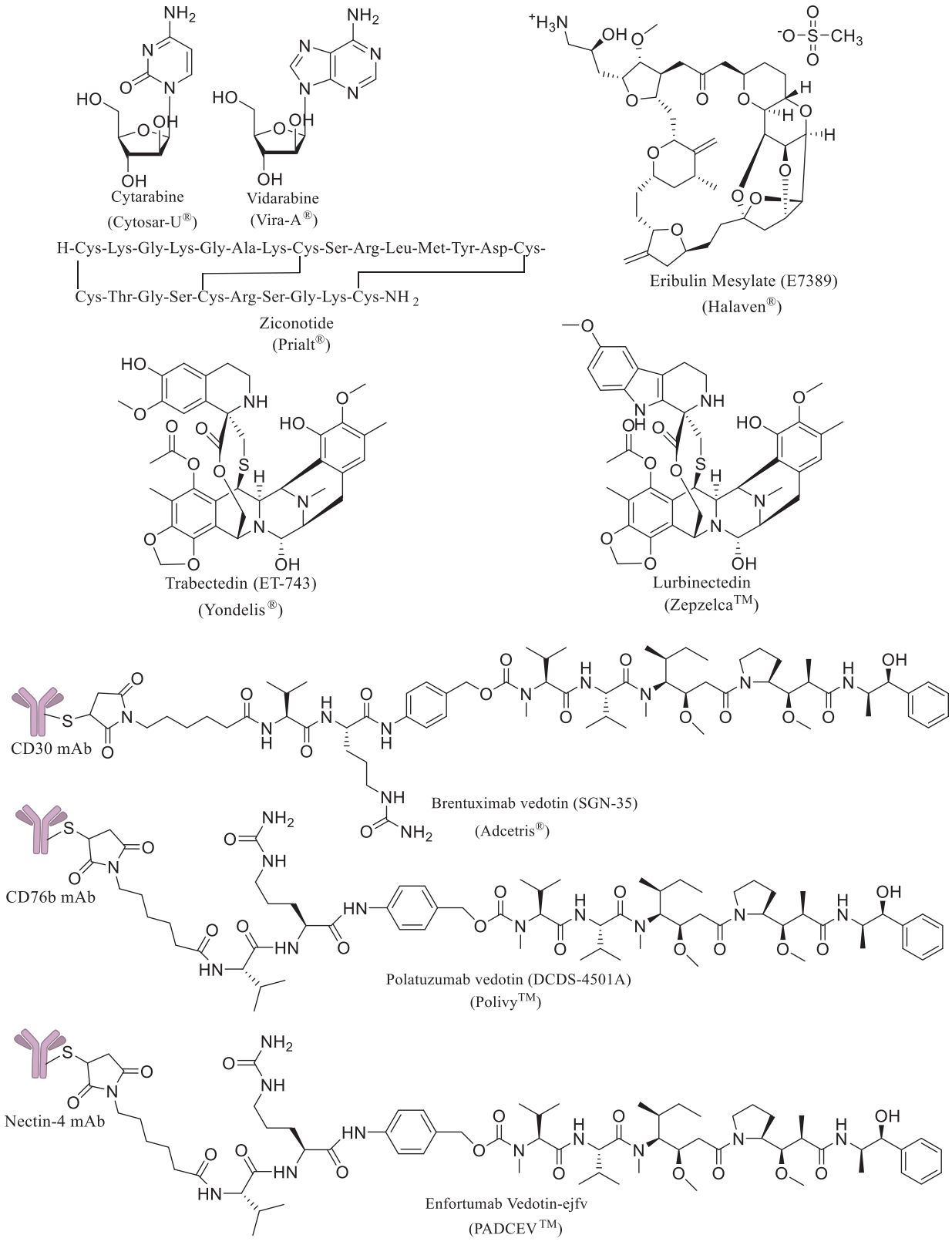

Figure 1: Structures of US FDA-approved marine-derived drugs (excluding Omega-3 fatty acids)

1.1.2 Marine Fungi as Producers of Interesting Natural Products

Marine fungi represent a relatively untapped source of structurally interesting secondary metabolites with significant biological activities including, antibacterial, antiviral, and cytotoxic activities (Shin 2020). Marine fungi are found in nearly every possible marine habitat including soil and sediment, driftwood, sessile and mobile invertebrates, marine vertebrates and algae. In addition, they are distributed from surface waters to kilometres below (deep sea) (Amend *et al.* 2019). It is important to mention that marine fungi play a significant role in aquatic ecosystems as they are involved in decomposition of woody and herbaceous substrates and degradation of dead animals. Some marine fungi are pathogenic to marine plants and animals, while others form symbiotic relationships with other organisms (Hyde *et al.* 1998).

During the last few decades, great attention from natural products' chemists was given to marine-derived fungi with respect to compounds isolated and activities exerted (Ebada *et al.* 2015). Remarkably, the reported new marine-derived fungal natural products in 2018 have increased by 38% compared to 2017. Additionally, compared to the average number of natural products reported for the previous three years, the new marine-derived fungal natural products have increased by 85%, resulting in a total cumulative number of 4,708 new metabolites reported so far from marine fungi (Carroll *et al.* 2020). Some marine-derived fungi have offered promising drug leads for drug discovery. For instance, the antibiotic cephalosporin C, was the first isolated bioactive compound from a marine-derived fungus, *Cephalosporium* sp., obtained off the Sardinian coast (Florey 1955, Newton *et al.* 1955). Currently, the only candidate that showed remarkable activities during *in vitro* and *in vivo* studies and successfully reached phase III of clinical trials is plinabulin. Plinabulin (NPI 2358) is a synthetic analogue of the fungal marine natural product halimide, a diketopiperazine alkaloid, obtained from the marine-derived fungus *Aspergillus* sp. It acts as a microtubule-disturbing agent and has a direct pro-apoptotic effect. It is in phase III of clinical pipeline in a combination therapy with docetaxel for the treatment of non-small-cell lung cancer (NSCLC) in addition to prevention of chemotherapy-induced neutropenia (CIN) (Nicholson *et al.* 2006, Ebada *et al.* 2015, Jiménez 2018).

Although the majority of the reported marine natural products are produced by marine invertebrates, marine fungi are estimated to hold the key for development of

many new pharmaceuticals and drug leads from marine environment in the future due to the diversity of fungal metabolites and the relative ease of collection and cultivation of marine fungi (Jiménez 2018). Marine fungi will overcome the problem of limited yields associated with other marine organisms by mass production of desired bioactive compounds through mass fermentation. Hence, marine fungi will be able to provide bioactive secondary metabolites in huge amounts in order to supply different clinical phases in addition to supplying future production of marine-derived pharmaceuticals to face market needs (Ebada *et al.* 2015, Jiménez 2018).

1.2 Activation of Silent Gene Clusters- Strategies

Nowadays, the rate of discovery of new microbial secondary metabolites is suffering a decline whereas, the rate of re-isolation of already known compounds is increasing (Daletos *et al.* 2017). This can be attributed to the silencing of many biosynthetic gene clusters under standard laboratory conditions as proven by genome sequencing of microorganisms. Genome sequencing revealed the difference between the high number of natural product gene clusters and the observed lower number of isolated secondary metabolites under standard cultivation conditions (Arora *et al.* 2020). Thus, in order to activate silent biogenetic gene clusters, many strategies have been developed and successfully aided in isolating new microbial secondary metabolites or increasing the yield of a desired metabolite. These strategies among others include, OSMAC approach (**O**ne **S**train **Ma**ny **C**ompounds), co –cultivation, and epigenetic modification (Romano *et al.* 2018).

1.2.1 OSMAC

OSMAC approach is recognized as an important and a powerful tool in inducing many silent biosynthetic gene clusters. This term was first introduced by Zeeck and co-workers in 1997 (Fuchser *et al.* 1997). The OSMAC approach reveals how fungi could produce many secondary metabolites from a single strain by simple changes in the cultivation conditions and parameters such as media composition, cultivation vessels and other physical or chemical factors (Bode *et al.* 2002). Many examples demonstrated how these changes in the cultivation conditions have a great impact in activating silent gene clusters and changing the metabolic profile of fungi resulting in the production of interesting new secondary metabolites (Pan *et al.* 2019).

1.2.1.1 Variations of Medium

Alteration of medium composition including nitrogen and carbon sources, the main components of a culture medium, is verified to have a significant impact on fungal secondary metabolism (Pan *et al.* 2019). From a marine sediment-derived strain of the fungus *Aspergillus niger*, a new cytotoxic ester furan derivative was obtained when the fungus was cultivated on MPDB medium (malt peptone dextrose broth), whereas the fungus failed to produce the same metabolite when it was cultivated on PDB (potato dextrose broth) and PDYB (potato dextrose yeast broth) (Uchoa *et al.* 2017).

In marine microbes, salinity plays an important role in activating enzymes involved in the expression of marine secondary metabolites. Therefore, natural product scientists tried to mimic marine conditions in cultivating marine microbes in order to enhance the secondary metabolite production. (Romano *et al.* 2018). When the marine-derived fungus *Aspergillus terreus* PT06-2 isolated from sediment of the Putian Sea Saltern, Fujian, China, was cultured at 0%, 3% and 10% salinity, the biomass production and the chemical diversity of the secondary metabolites of the 10% salinity culture was the highest followed by the 3% and the least was for the 0% salinity demonstrating the effect of salinity on secondary metabolites production in marine microbes. Interestingly, the two compounds methyl 3,4,5-trimethoxy-2-(2-(nicotinamido) benzamido) benzoate, and (+)-terrein were only isolated from the 10% salinity culture (Wang *et al.* 2011).

Incorporation of trace elements and inorganic salts such as halides in the culture media of microorganisms also triggers activation of hidden biogenetic gene clusters and influences secondary metabolites production (Romano *et al.* 2018). When the marine-derived fungus *Aspergillus unguis* CRI282-03 isolated from an unidentified marine sponge CRI282, collected from the Royal Navy Base at Tub-La-Mu bay, Pang-nga Province, Thailand, was cultured in potato dextrose broth (PDB) prepared in seawater instead of preparing in distilled H_2O, chlorinated depsidones were obtained. Furthermore, cultivating the fungus in media containing other halogens such as KBR and KI, led to the isolation of brominated unnatural natural depsidones and non-halogenated depsidone, unguinol, respectively (Sureram *et al.* 2013).

1.2.1.2 Cultivation Conditions

Microorganisms can only grow under appropriate cultivation conditions which have a direct impact on enzyme activity and hence play a major role in secondary metabolites production. These conditions include, temperature, pH, oxygen supply and even the shape of the culture vessel which affects biofilm formation (Romano *et al.* 2018). Nevertheless, under standard cultivation conditions, some secondary gene clusters are not expressed (cryptic) and remain silent. Thus, OSMAC approach with changing these cultivation conditions aids in diversifying the secondary metabolites production through activation of the silent clusters (Bode *et al.* 2002).

1.2.1.3 Cultivation Status

Cultivation status has a great impact on the secondary metabolites production in fungi. Some fungi favour growing under static (non-shaking) conditions with the formation of a mycelium cake while others favour the cultivation under dynamic (shaking conditions) that ensures a better aeration and oxygen supply for the culture. In addition, changing from solid medium to liquid medium and *vice versa* is also considered as an OSMAC approach that affects the metabolic production of fungi (Bode *et al.* 2002, Romano *et al.* 2018).

When the marine-derived fungus *Aspergillus terreus* was cultured on 11 different culture conditions utilizing solid agar, broth cultures and grain based media in a comparative metabolomic study, it was found that the static agar condition was the best for the production of the antifungal compounds lovastatin and lovastatin mevinolinic acid methyl ester, whereas both compounds were detected only in minor amounts in the shaking cultures (Adpressa *et al.* 2016). Contrastingly, with changing from static to agitated fermentation with shakers in PYG (peptone yeast glucose broth) medium, five new nitrogen containing sorbicillinoids, namely sorbicillamines A−E and the known compounds sorbicillinoids bisvertinolone and rezishanone C, were isolated from the deep-sea-derived fungus *Penicillium* sp. F23−2 (Guo *et al.* 2013).

1.2.2 Co-cultivation

Contrary to OSMAC approach which involves axenic cultivation of a fungus with varying the media, cultivation conditions and status, co-cultivation involves the

cultivation of two or more microorganisms within the same culture (Marmann *et al.* 2014). These organisms could be different fungi, different bacteria or fungi with bacteria (Netzker *et al.* 2015). The principle behind co–cultivation (mixed fermentation) relies on mimicking the ecological conditions where different microorganisms co-exist in a microbial ecosystem communicating and competing for nutritional sources and space (Marmann *et al.* 2014). Hence, microorganisms are subjected to stress conditions which provoke activation of hidden biosynthetic gene clusters that remained silent under luxurious cultivation conditions. Eventually, this competition leads to accumulation of cryptic metabolites which were not detected in the axenic culture of the organism and/or upregulation of constitutively present compounds (Daletos *et al.* 2017). In 1982, Watanabe *et al*. demonstrated the ability of the antibiotic producing bacterium *Gluconobacter* Sp. W-315 to produce antibacterial compounds against gram-positive and gram-negative bacteria only when co-cultivated with fungi *Aspergillus oryzae* or *Neurospora crassa* (Watanabe *et al.* 1982). Since then, many studies have demonstrated the power of co-cultivation in diversifying secondary metabolite production in microorganisms (Marmann *et al.* 2014, Pan *et al.* 2019).

1.2.3 Epigenetic Modification

Another strategy for triggering transcription of silent biogenetic clusters without altering DNA is epigenetic modification or chromatin remodelling (Bertrand *et al.* 2014). Basically, inhibition of the fungal enzymes histone deacetylases (HDAC), or DNA methyl transferase (DNMT) represents a target for unlocking silent gene clusters which in turn leads to isolating new and/or previously unexpressed (cryptic) secondary metabolites (Cichewicz 2010, Marmann *et al.* 2014). Enzyme inhibitors which act as epigenetic modulators include, suberoylanilide hydroxamic acid (SAHA), suberoyl bishydroxamic acid (SBHA), and nicotinamide for HDAC inhibition as well as, 5-Azacytidine (5-AC) for DNMT inhibition (Pan *et al.* 2019).

1.3 Absolute Configuration Determination

Natural products have served as productive source of drug leads for drug discovery and development. A major challenge that natural product chemists face after elucidation of the planar structures of compounds lies in the assignment of the absolute configuration of the respective compounds (Li *et al.* 2010). In drug development, the

correct assignment of the stereochemistry of drugs has an indispensable importance since binding of drugs to receptors is dependent on their stereochemistry. All human receptors are chiral thus, two enantiomers of a chiral drug would have different interactions with the receptors and consequently have different pharmacological effects (Pescitelli *et al.* 2009). Many examples in the literature demonstrate the different therapeutic usage of the enantiomers of the same drug. For instance, from the Cinchona alkaloids, quinine is used as antimalarial and muscle relaxant drug while, its isomer quinidine is used as an antiarrhythmic drug (Song 2009).

In 1992, the FDA released a policy statement for the development of new stereoisomeric drugs (chiral drugs) stating that the isomeric composition of a drug bearing chiral centres should be specified and for the enantiomeric mixtures, both enantiomers should be clinically evaluated. When both enantiomers are pharmacologically active but differ in potency, specificity, or have different pharmacokinetics then development of a single isomer is a must before being released to the market (FDA 1992). As a consequence, for a complete structural characterization of new or novel natural product, determination of relative configuration (RC) and absolute configuration (AC) is crucial for drug development (Kong *et al.* 2013).

Many methods are available for (AC) assignment of chiral centres of natural products. Some are relative (indirect) including NMR based methods and the use of chiral derivatizing agents, analytical methods and optical rotation (OR) measurement, while others are absolute (direct) methods such as X-ray crystallography, chemical synthesis and chiroptical methods (Li *et al.* 2010, Ling-Yi *et al.* 2013).

The relative methods for assigning the absolute configuration are based on the existence of a reference with a known AC either contained in the compound itself (if previously characterized), a chemically related compound with a known and characterized AC or the use of a chiral derivatizing agent with known AC. NMR-based methods including scalar *J*-couplings and NOE effects are well known relative methods for AC determination. In addition, measurement of optical rotation (OR, or $[\alpha]_D$) and comparison with the reported literature values of pure compounds is also considered as a relative method for AC assignment. In contrary to those relative methods, absolute methods for determining the AC have a wider scope and application being independent from the existence of any reference compound. The most reliable techniques belonging

to this method are X-ray analysis and chiroptical spectroscopic techniques (Pescitelli *et al.* 2009).

1.3.1 Nuclear Magnetic Resonance (NMR)-Based Methods

1.3.1.1 Nuclear Overhauser Effect, Rotating-Frame Nuclear Overhauser Effect and *J* Coupling (^{1}H–^{1}H)

Generally, nuclear magnetic resonance spectroscopy (NMR) is the most important tool for a planar structure elucidation of natural products. However, determining the three-dimensional structure of bioactive natural products is crucial for the study of structure activity relationships (Matsumori *et al.* 1995, Molinski *et al.* 2012). 1D and 2D nuclear Overhauser effect spectroscopy (NOESY) and rotating-frame nuclear Overhauser effect correlation spectroscopy (ROESY) experiments together with the analysis of NMR (*J*) coupling constants (^{1}H–^{1}H), are widely utilized for characterizing the conformation and RC of small molecules (Molinski *et al.* 2012). It is noteworthy to mention that for flexible compounds such as acyclic or macrocyclic compounds in which minor conformations can influence NOE intensities, it is difficult to determine the dominant conformation from NOE assignment (Matsumori *et al.* 1995).

1.3.1.2 Murata's Method: *J*-Based Configurational Analysis

This method involves the analysis of the ^{1}H-^{1}H and ^{1}H-^{13}C *J* couplings with the purpose of designating the relationships of vicinally substituted chains. The interproton/homonuclear ($^3J_{H\text{-}H}$) and heteronuclear ($^{2,3}J_{H\text{-}C}$) coupling constants are measured through a combination of NMR experiments as a weighted average derived from each conformer of the compound thus, the dihedral angels obtained from these coupling data together with NOE are more reliable for flexible molecules unlike NOE measurements alone. This method is commonly used for RC assignment of acyclic molecules with contiguous or 1,3-skipped stereogenic centers (with 1,2 or 1,3 relative positions) based on measuring $^3J_{H\text{-}H}$ and $^{2,3}J_{H\text{-}C}$ around the bond(s) which connect the stereocenters (Matsumori *et al.* 1995, Molinski *et al.* 2012, Menna *et al.* 2019). However, for molecules with isolated stereocenters this method is not applicable for RC assignment due to lacking of NMR correlations (Molinski *et al.* 2012).

1.3.1.3 Comparative Studies Using Databases (Universal NMR Database)

Another NMR-based method for assignment of RC is the use of databases which allow comparison of NMR parameters of molecules with unknown RC of stereocenters with libraries of model compounds with already known and characterized configuration of the stereocenters. This idea was introduced by the work group of Kishi during structure elucidation and stereochemical assignment of complex polyketides prepared by synthesis which came to be the first database for NMR (Universal NMR Database or UDB). UDB is useful for RC assignment of acyclic molecules with many stereocenters including contiguous polyols (Molinski *et al.* 2012, Menna *et al.* 2019).

1.3.1.4 Mosher's Method: Utilizing Chiral Derivatizing Agents

Mosher's method is an NMR-based method for determination of AC of natural products. This well-known indirect method of determining the AC, which is known as Mosher ester (amide) analysis, was originally introduced by Dale and Mosher in 1973 (Dale *et al.* 1973). Later in the late 1980's, Ohtani *et al*. refined and developed the previous method into the modified (or advanced) Mosher's method (MMM) (Ohtani *et al.* 1989). This method is the most widely used method for AC deduction of stereogenic secondary alcohols R^1R^2CHOH or the analogous stereogenic amines $R^1R^2CHNH_2$ (where R1 ≠ R2 in both cases) (Hoye *et al.* 2007).

Since enantiomers have identical NMR spectra, NMR cannot distinguish between them. Therefore, the basic principle for this method relies on transforming a chiral substrate into two diastereomers with different and distinct NMR spectra using chiral derivatizing agents (CDAs). Afterwards, the ^{1}H NMR chemical shift differences ($\Delta\delta^{RS}$) of the substituents (L1 and L2) attached to the stereogenic center of the substrate are analysed and the AC of the original secondary alcohol or amine is then deduced from the signs (+ or -) of the difference in chemical shifts of the analogous pairs of protons (Hoye *et al.* 2007, Kong *et al.* 2013).

The most widely used chiral derivatizing agents (CDAs), which are known as Mosher's regents, are enantiometrically pure MTPA (*α*-methoxy-*α*-trifluoromethylphenylacetic acid), its acid chloride MTPA-Cl or methoxyphenylacetic acid (MPA) which is considered as a more reliable CDA (Molinski *et al.* 2012). The CDA incorporates: (1) a functional group (*e.g.* carboxyl) for covalent attachment with

the chiral substrate and formation of ester, (2) a bulky or polar group which fixes a particular conformation and (3) a group which produces space-oriented anisotropic effect that affects the different substituents L1 and L2 of the substrate (*e.g.* aromatic, carbonyl moiety). The overall resultant of this shielding or deshielding ensures chemical shift differences of L1 and L2 in the two diastereomers which is then used for AC determination (Seco *et al.* 2004).

Attention should be paid to the absolute configuration of the used reagent in Mosher ester analysis as (*R*)-MTPA reagent produces the (*R*)-MTPA ester, while its acid chloride (*R*)-MTPA-Cl produces the (*S*)-MTPA ester (Kong *et al.* 2013) as shown in figure 2.

This method works perfectly with assigning the AC of monofunctional compounds such as alcohols, amine or carboxylic acids while, for polyfunctional molecules the process is much more complex and could be performed only with two possibilities; either by using appropriate protection/deprotection steps for a selective derivatization of each hydroxyl group or derivatizing the two hydroxyl groups in a single reaction (Seco *et al.* 2004).

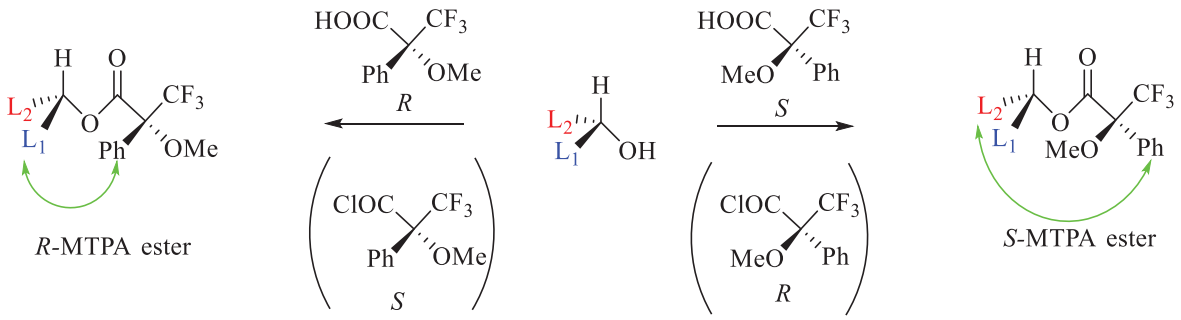

Figure 2: *R* and *S* Mosher esters produced from the generic secondary alcohol, the green arrow indicates the phenyl group shielding effect. Figure is modified after (Hoye *et al.* 2007).

After the relative configuration of the sesquiterpene eutyperemophilane F, isolated from the deep-sea fungus *Eutypella* sp., was established by NOE correlations, the AC at the stereocenter C-9 was assigned by the modified Mosher's method utilizing MPA as the CDA. After esterification with (*R*)- and (*S*)-MPA and obtaining the corresponding (*R*)- and (*S*)-MPA esters, the differences in the chemical shifts in ^{1}H

NMR raised from (*R*)- and (*S*)-MPA esters ($\Delta\delta^{RS} = \delta^{R}$-$\delta^{S}$) assigned the AC at C-9 to be 9*S* configuration as shown in figure 3 (Niu *et al.* 2018).

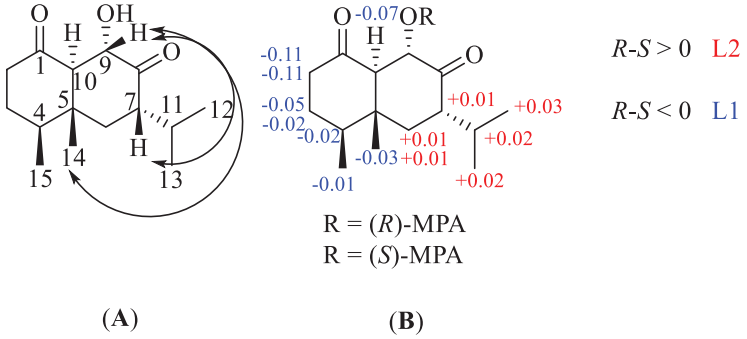

Figure 3: (**A**) Some NOE correlations for eutyperemophilane F, (**B**) $\Delta\delta^{H}$ ($\Delta\delta^{RS} = \delta^{R}$-$\delta^{S}$) data of MPA esters of eutyperemophilane F. Figure is modified after (Niu *et al.* 2018).

1.3.2 Single Crystal X-ray Diffraction Analysis (XRD)

Single X-ray diffraction analysis using anomalous dispersion is considered to be the most reliable and powerful absolute method for determining AC of crystalline natural products. Moreover, it provides a solid state confirmation of the measured compound. Nevertheless, the requirement of a good quality crystal with certain dimensions at low temperature represents a severe limitation for the application of this method in AC determination of many natural products (Mándi *et al.* 2019). As long as X-ray crystallography in AC assignment is not always applicable, many alternative versatile methods have been developed for stereochemical analysis of chiral natural products including chiroptical methods (Pescitelli *et al.* 2009). The X-ray diffraction analysis can be used in combination with ECD analyses for AC determination where they strengthen each other (Mándi *et al.* 2019).

The absolute configurations of pimarane diterpenes, isolated from the marine fungus *Cryptosphaeria eunomia* var. *eunomia*, obtained by recrystallization experiments using chloroform, were unambiguously determined by X-ray crystallography utilizing anomalous scattering (Yoshida *et al.* 2007).

1.3.3 Chiroptical Methods

Chiroptical spectroscopic methods are very powerful absolute methods for configurational assignment of chiral non-racemic natural products. These methods are

based on the interaction between the chiral compound and the left- and right-circularly polarized light (Mándi *et al.* 2019). They include several different techniques, the selection of which is dependent on the chemical structure of the chiral substrate together with the limitations and scope of each technique (Petrovic *et al.* 2010). Fortunately, chiroptical methods are non-destructive and can be applied for compounds in solution without the need of crystallization as in the case of X-ray analysis, which makes these methods more applicable and widely used for AC assignment of many natural products (Menna *et al.* 2019).

1.3.3.1 Optical Rotation (OR) or Specific Optical Rotation (SOR)

Optical rotation or specific optical rotation $[\alpha]_D$ is a physical constant which is commonly used for characterization of optically active molecules and determination of optical purity of compounds (Molinski *et al.* 2012, Kong *et al.* 2013). It is based on measuring the difference in refractive indices of left and right polarized light, which is measured at a specific single wavelength, usually at 589.3 nm (the yellow sodium D line). Historically, this method was the first used method for distinguishing enantiomers of chiral compounds and dates back to the early 19th century (Mándi *et al.* 2019). SOR measurement could be easily used for AC assignment of a natural product only by having a reference SOR literature data of one of the enantiomers with the specified wavelength, solvent, temperature and concentration (Mándi *et al.* 2019). Unfortunately, due to the absence of independent measurement of the OR of natural products, this method relies completely on trusting the reported literature values and that the conducted measurements were conducted with pure samples (Molinski *et al.* 2012).

1.3.3.2 Optical Rotatory Dispersion (ORD)

ORD is the change in the optical rotation angle as a function of wavelength. The successive measurement of OR at multiple wavelengths gives ORD spectrum (Mándi *et al.* 2019). ORD measurement can be applied for AC assignment of natural products with no UV/Vis active chromophores, an advantage over ECD measurements (Li *et al.* 2010). However, for flexible compounds, ORD is only applicable under certain conditions (Petrovic *et al.* 2010).

1.3.3.3 UV-Vis and Electronic Circular Dichroism (ECD)

ECD represents the most widely used chiroptical method over the past decade for stereochemical and conformational analysis of chiral natural products. It is derived from the differential absorption of the left- and right-circularly polarized light components in the UV-Vis region (180-800 nm) during electronic excitation (Mándi *et al.* 2019).

Among other chiroptical methods such as SOR and VCD, ECD has the advantage of the higher sensitivity which allows recording a high quality ECD spectra for samples of 50-100 µg (Mándi *et al.* 2019). In addition, running online HPLC-ECD analysis of stereoisomeric mixtures, which have a weak or baseline ECD spectrum, is applicable by coupling ECD as a detector with chiral HPLC (Mándi *et al.* 2019).

On the other hand, the main limitation of ECD is that it requires the presence of at least one UV/Vis active chromophore such as aromatic, carbonyl, diene or a conjugated system. Nevertheless, since most biologically active natural products have one or more degree of unsaturation, the solid-state ECD method is the most useful method for assigning AC of natural products (Pescitelli *et al.* 2009, Li *et al.* 2010). Another limitation is that flexible compounds would have difficulties in conformational analysis and in *ab initio* calculations due to the presence of many conformers with different populations. Other limitations include the required long computational time which results in high costs in computation (Petrovic *et al.* 2010, Kong *et al.* 2013). Therefore, rigid molecules and molecules with distinct chromophores or with a single stereogenic center afford more reliable and easily predicted ECD spectra (Li *et al.* 2010, Menna *et al.* 2019).

The absolute configuration of the xanthone derivative, (1*R*,2*R*)-AGI-B4, isolated from the marine-derived fungus *Scopulariopsis* sp. obtained from the Red Sea hard coral *Stylophora* sp., was unambiguously determined as 1*R*, 2*R* using TDDFT-ECD calculations (Elnaggar *et al.* 2016).

1.3.3.4 The Exciton Chirality CD Method (ECCD)

The exciton chirality CD method is considered to be a non-empirical chiroptical method in assigning the AC of chiral molecules (Kong *et al.* 2013). It applies only to molecules with at least two or more separate UV/Vis chromophores which are located

close to each other in space and form a chiral system. As a result, there will be an exciton coupling between the transitions on the two chromophores giving rise to an interpretable bisignate exciton couplet in the ECD spectrum (Pescitelli *et al.* 2009, Petrovic *et al.* 2010, Mándi *et al.* 2019). ECCD method represents a successful widely used approach for establishing the AC of bis-and muti-chromophoric compounds because of its high sensitivity, reliability and simplicity. The limitation of this method are the interferences that could result from other chromophores that reside in the compound (Pescitelli *et al.* 2009, Mándi *et al.* 2019).

ECCD method aided in an unambiguous assignment of the (*R*) configuration of the long-chain polyacetylenic diol, faulkneryne A, isolated from the sponge, *Diplastrella* sp., collected from the surface of coral in the Bahamas (Ko *et al.* 2011).

1.3.3.5 Vibrational Circular Dichroism (VCD)

Vibrational Circular Dichroism (VCD) arises from differential absorption of left- and right- circularly polarized infrared radiation (IR) (mid-infrared; 4000-650 cm^{-1}) during vibrational excitation. VCD has a shorter history than ECD, and it was introduced in the late 1990s with the manufacture of the first instrument (Mándi *et al.* 2019).

VCD has many advantages over ECD in AC determination of natural products. Although both methods are based on the same phenomenon of the difference in absorption, VCD relies on the vibrational transitions of chemical bonds unlike ECD which relies on excitation of electrons. Therefore, VCD does not require the presence of a UV-Vis chromophore in the molecule and even fully saturated chiral natural products can be studied. As a consequence, it has a larger scope of assigning AC than ECD. Moreover, VCD requires calculations performed within the electronic ground state. Therefore, it is easier to model in normal Density functional theory (DFT) computations and there is no need for Time-dependent Density functional theory (TDDFT) calculations which results in less computational resources (Petrovic *et al.* 2010, Mándi *et al.* 2019). Furthermore, being related to IR, VCD spectra show a larger number of transitions than ECD which is reflected in higher resolution, easier *ab initio* calculations of VCD spectra and hence a higher reliability (Kong *et al.* 2013).

Nevertheless, a wider spread application of VCD in AC analysis of natural products may be hindered because of its low sensitivity. Thus, for experimental measurements

at least 5-15 mg of the compound are needed and hours of acquisition time are required (Mándi *et al.* 2019).

The AC of C-2′ and C-3′ of the azaphilone derivative pleosporalone D, isolated from the modified potato dextrose broth (PDB) culture medium of the marine-derived fungus *Pleosporales* sp. CF09-1, was assigned to be (2′*S*,3′*R*) by implementing VCD method. The calculated VCD signals of (2′*S*,3′*R*)-pleosporalone D had better agreement with the experimental VCD signals of the compound, indicating the (2′*S*,3′*R*) configuration for pleosporalone D (Cao *et al.* 2019).

1.3.4 Analytical Methods (GLC/ HPLC analysis)

For determination of the AC of certain classes of natural products, some analytical chemistry-based methods can be used including GLC and HPLC analyses. These analytical methods are remarkably useful in assigning the AC of sugar units of glycosides and amino acid constituents of peptides (Li *et al.* 2010).

1.3.4.1 The Use of Marfey's Reagent

After hydrolysis of peptides followed by derivatization of the resulting amino acids with the pre-column derivatizing reagent, Marfey's reagent (1-fluoro-2,4-dinitrophenyl-5-L-alanine amide, FDAA), the amino acids are converted into UV active diastereomers. Thus, the separation of D- and L-amino acids on a non-chiral HPLC column is possible. This method has many advantages as an analytical method for AC determination of amino acid constituents of peptides such as, the simplicity and effectiveness (B'Hymer *et al.* 2003, Bhushan *et al.* 2004).

1.3.4.2 GLC and HPLC Analysis for Sugar Residues of Polysaccharides

For the determination of absolute configuration of small amounts of sugar residues (D or L), gas-liquid chromatography (GLC) or high-performance liquid chromatography (HPLC) could be employed. GLC separation of sugar enantiomers on an OV-17 capillary column could be achieved after converting the sugars to the chiral derivatives, trimethylsilyl (TMS) ethers of methyl 2-(polyhydroxyalkyl)-thiazolidine-4(*R*)-carboxylates, obtained by the reaction of aldoses with L-cysteine methyl ester (Hara *et al.* 1987). Moreover, as a modification of the previous method utilizing GLC, one-pot reactions of aldoses with L-cysteine methyl ester and *o*-tolyl isothiocyanate

yielding methyl 2-(polyhydroxyalkyl)-3-(*o*-tolylthiocarbamoyl)-thiazolidine-4(*R*)-carboxylates followed by direct analysis using C_{18}-reversed phase HPLC equipped with a UV detector, represent a widely used analytical method in determining AC of monosaccharides (Tanaka *et al.* 2007).

1.3.5 Chemical Synthesis

Total synthesis of all the possible stereoisomers represents an ultimate solution to a stereochemical problem followed by comparison of their spectroscopic data to the compound with unknown AC. Nevertheless, this approach has many challenges. Thus, it is usually sufficient and more favourable to synthesize the 'key' fragments for comparative studies with the databases (Kong *et al.* 2013, Menna *et al.* 2019).

It is worth to mention that there is no general method for determining the absolute configuration of all chiral natural products even for those compounds with only one chiral centre. Each method has its particular limitations with regard to the different structural features of compounds. Thus, the absolute configuration has to be determined on a case-by-case basis and sometimes this require a combination of two or more methods as shown in figure 4 (Li *et al.* 2010, Molinski *et al.* 2012).

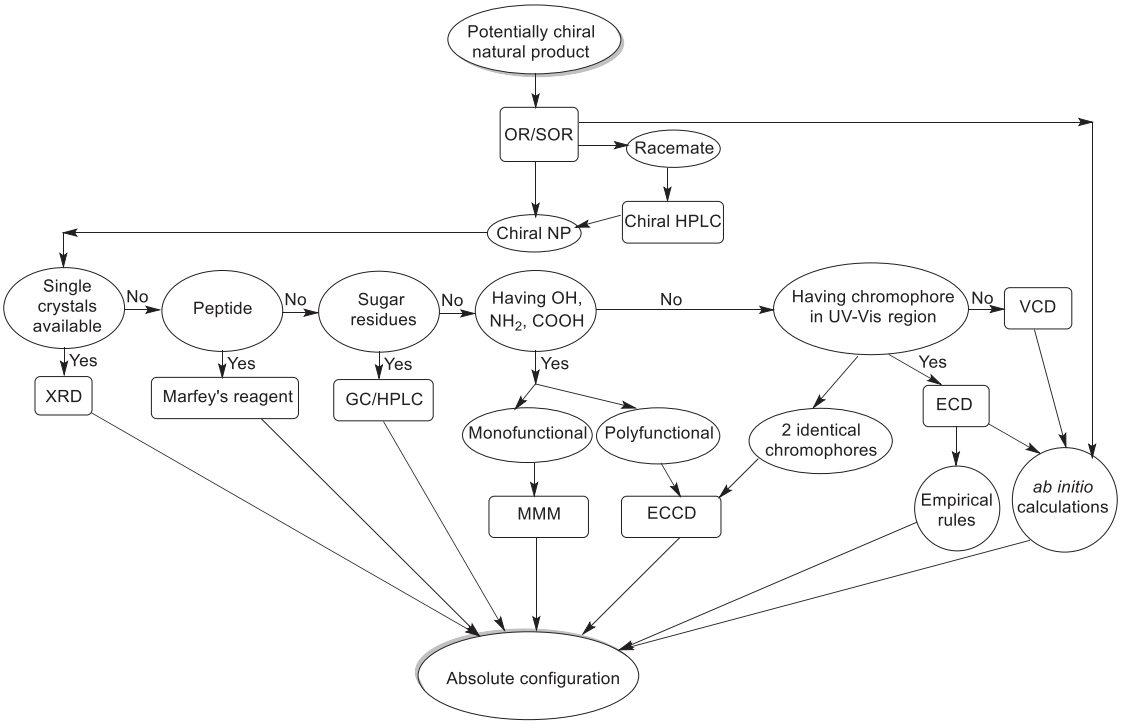

OR/SOR: Optical Rotation/ Specific Optical Rotation.

XRD: X-ray Diffraction Analysis

GC/HPLC: Gas-liquid chromatography/ High-performance liquid chromatography.

MMM: Modified Mosher's method.

ECD: Electronic Circular Dichroism.

ECCD: Exciton Chirality Circular Dichroism.

VCD: Vibrational Circular Dichroism.

Figure 4: Strategies of absolute configuration determination of chiral natural products. Figure is modified after (Kong *et al.* 2013).

1.4 NF- κB Inhibition and Anti-inflammatory Activity

The term inflammation comes from the Latin word *inflammare* and means "to set on fire", a term which would describe the four cardinal signs of inflammation including redness and swelling accompanied with heat and pain. These signs would fit with what we would today recognise as acute inflammation which is beneficial and has therapeutic importance. However, on the other hand, chronic inflammation is considered as a causative factor for many chronic diseases including cancer, arthritis, diabetes and obesity (Scott *et al.* 2004, Gupta *et al.* 2018) and is known to be implicated in various aspects of cancer initiation and development starting from cellular transformation,

proliferation, invasion, metastasis, angiogenesis and drug resistance (Gupta *et al.* 2018, Rajagopal *et al.* 2018). 150 years ago, the link between cancer and inflammation was recognized after Virchow noted the presence of leucocytes in neoplastic tissues reflecting that the sites of chronic inflammation are origins of cancer (Balkwill *et al.* 2001). The molecular link between inflammation and chronic diseases such as cancer lies within the inflammatory molecules and transcription factors such as cytokines, NF-κB, COX-2, STAT3, and vascular endothelial growth factor (VEGF) (Gupta *et al.* 2018). The nuclear factor kappa B (NF-κB), a pro-inflammatory transcription factor, has been shown to be a crucial regulator in inflammatory diseases and is also linked to cancer development (Rajagopal *et al.* 2018). Moreover, it has been reported to be involved in regulation of expression of more than 500 cancer related genes that are involved in cellular transformation, proliferation, invasion, angiogenesis, metastasis, and inflammation (Gupta *et al.* 2010).

1.5 Aims and Significance of the Study

Fungi from unusual sources (*e.g.* marine habitat) have proven themselves as a reservoir for many interesting metabolites with respect to structural novelty together with new modes of bioactivities (Sashidhara *et al.* 2009). The aim of this study was to explore fungi from such sources as producers of diverse secondary metabolites with potential different biological activities. Two different marine-derived fungi were chosen for study in this doctoral thesis; *Metarhizium marquandii* and *Aspergillus falconensis*. In addition, in order to diversify the conditions affecting fungi, these two marine fungi were collected from two different locations. One was collected from the North Sea, Germany and the other was collected from the Red Sea, Egypt. Both fungi succeeded to produce various secondary metabolites with new structural features from the initial cultivation and isolation procedures. Moreover, aiming to diversify the metabolic pattern, different OSMAC experiments were conducted and eventually aided in activating silent biosynthetic gene clusters as proven with the additional isolation of diverse new secondary metabolites. All the isolated compounds were structurally elucidated by 1D/2D NMR spectroscopy, mass-spectrometry, modified Mosher's method, ECD, VCD, optical rotation measurements and calculations and single-crystal X-ray diffraction analysis. The isolated compounds were also evaluated for their cytotoxic and anti-inflammatory activity. Additionally, molecular docking helped in

predicting the binding of compounds to possible targets. The distinguished results obtained in this study are either published or submitted as shown in **chapters 2-4**.

Chapter 2 - Polyketides and a Dihydroquinolone Alkaloid from a Marine-Derived Strain of the Fungus *Metarhizium marquandii*

Reprint from "**Dina H. El-Kashef**, Georgios Daletos, Malte Plenker, Rudolf Hartmann, Attila Mándi, Tibor Kurtán, Horst Weber, Wenhan Lin, Elena Ancheeva, and Peter Proksch (2019). Polyketides and a dihydroquinolone alkaloid from a marine-derived strain of the fungus *Metarhizium marquandii*. *Journal of natural products*, 82 (9), 2460-2469.", by the permission of American Chemical Society (ACS) publications (https://pubs.acs.org/)

2.1 Publication Manuscript

Published in "Journal of Natural Products" 82 (9): 2460-2469 (2019).

Impact Factor: 3.779 (2019)

Overall contribution to this publication: First author, laboratory work including, compound isolation, structure elucidation, and preparation of manuscript.

JOURNAL OF NATURAL PRODUCTS

Article

Cite This: J. Nat. Prod. 2019, 82, 2460−2469

pubs.acs.org/jnp

Polyketides and a Dihydroquinolone Alkaloid from a Marine-Derived Strain of the Fungus *Metarhizium marquandii*

Dina H. El-Kashef,[†,‡] Georgios Daletos,[†,¶] Malte Plenker,[§] Rudolf Hartmann,[§] Attila Mándi,[⊥] Tibor Kurtán,[⊥] Horst Weber,[∥] Wenhan Lin,[#] Elena Ancheeva,[*,†] and Peter Proksch[*,†]

[†]Institut für Pharmazeutische Biologie und Biotechnologie, Heinrich-Heine-Universität Düsseldorf, Universitätsstrasse 1, 40225 Düsseldorf, Germany

[‡]Department of Pharmacognosy, Faculty of Pharmacy, Minia University, 61519 Minia, Egypt

[§]Institute of Complex Systems: Strukturbiochemie, Forschungszentrum Jülich GmbH, ICS-6, 52425 Jülich, Germany

[⊥]Department of Organic Chemistry, University of Debrecen, P.O.B. 400, 4002 Debrecen, Hungary

[∥]Institut für Pharmazeutische und Medizinische Chemie, Heinrich-Heine-Universität Düsseldorf, Universitätsstrasse 1, 40225 Düsseldorf, Germany

[#]State Key Laboratory of Natural and Biomimetic Drugs, Peking University, Beijing 100191, China

Supporting Information

ABSTRACT: Three new natural products (**1**−**3**), including two butenolide derivatives (**1** and **2**) and one dihydroquinolone derivative (**3**), together with nine known natural products were isolated from a marine-derived strain of the fungus *Metarhizium marquandii*. The structures of the new compounds were unambiguously deduced by spectroscopic means including HRESIMS and 1D/2D NMR spectroscopy, ECD, VCD, OR measurements, and calculations. The absolute configuration of marqualide (**1**) was determined by a combination of modified Mosher's method with TDDFT-ECD calculations at different levels, which revealed the importance of intramolecular hydrogen bonding in determining the ECD features. The (3*R*,4*R*) absolute configuration of aflaquinolone I (**3**), determined by OR, ECD, and VCD calculations, was found to be opposite of the (3*S*,4*S*) absolute configuration of the related aflaquinolones A−G, suggesting that the fungus *M. marquandii* produces aflaquinolone I with a different configuration (chiral switching). The absolute configuration of the known natural product terrestric acid hydrate (**4**) was likewise determined for the first time in this study. TDDFT-ECD calculations allowed determination of the absolute configuration of its chirality center remote from the stereogenic unsaturated γ-lactone chromophore. ECD calculations aided by solvent models revealed the importance of intramolecular hydrogen bond networks in stabilizing conformers and determining relationships between ECD transitions and absolute configurations.

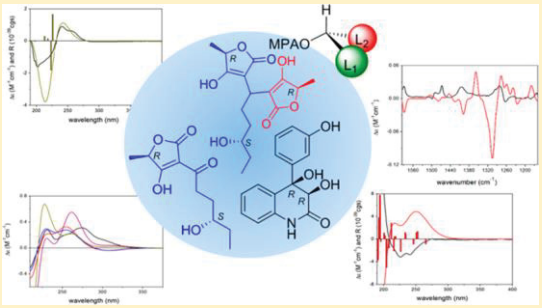

Marine-derived fungi have gained considerable attention among natural product chemists due to the chemical diversity and pharmacological properties of their secondary metabolites.[1−3] Cephalosporin C, an antibiotic, was the first bioactive compound reported from a marine-derived strain of the fungus *Acremonium chrysogenum*, the chemical structure of which was established in 1961.[1,4] During the last 15 years, the number of studies focused on marine-derived fungal metabolites has increased sharply, leading to the characterization of a plethora of new natural products.[2,5] Notably, these efforts resulted in the discovery of the lead compound (−)-phenylahistin (halimide) obtained from *Aspergillus ustus*, which acts as a tubulin depolymerizing agent.[2,6] Its closely related synthetic analogue plinabulin (NPI-2358) successfully passed phase II clinical trials and has currently entered phase III trials in combination therapy with docetaxel for the treatment of non-small-cell lung cancer (NSCLC).[2,6−8]

Fungi of the genus *Metarhizium* are among the most common entomopathogens that are commercially used worldwide as a biological control agent (biopesticide) against several insect pests.[9,10] Employment of entomopathogenic fungi as biopesticides is becoming increasingly important as an alternative to chemical pesticides, and these fungi are currently part of several agricultural pest and disease-vector control programs.[11,12] A literature review on secondary metabolites from the genus *Metarhizium* yielded several compound classes, including insecticidal cyclohexadepsipeptides (destruxins),[13−15] heptapeptides (serinocyclins A and B),[16] macro-

Received: February 10, 2019
Published: August 21, 2019

DOI: 10.1021/acs.jnatprod.9b00125
J. Nat. Prod. 2019, 82, 2460−2469

lides,[17] polyketides (aurovertins),[18] nor-terpenoids (helvolic acid[17,19] and viridoxins[20]), alkaloids (swainsonine[21] and hydroxyfungerins A and B[22]), macrocycles (metacridamides A and B),[23] and sesquiterpenes (12-hydroxyovalicin).[24] However, only a few natural products, including an unusual ureido derivative of sorbicillinol, as well as phytotoxic and antibiotic leucinostatin-peptide congeners, have been characterized from the fungus *Metarhizium marquandii* (syn. *Paecilomyces marquandii*).[25,26] Accordingly, as a part of our continuing studies on marine natural products[27−29] we have now investigated a strain of *M. marquandii* that was obtained from a seawater sample collected from the North Sea, Germany. We isolated 12 compounds including three new natural products (**1**−**3**). Additionally, the previously unknown absolute configuration of terrestric acid hydrate (**4**) was determined in this study.

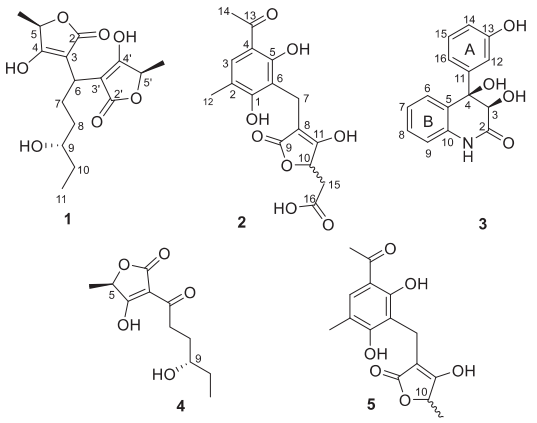

RESULTS AND DISCUSSION

Compound **1** was isolated as a dark yellow, amorphous powder. Its molecular formula was determined as $C_{16}H_{22}O_7$ based on the protonated molecule peak at *m*/*z* 327.1439 $[M + H]^+$ obtained by HRESIMS, which requires six degrees of unsaturation. The ^{1}H NMR spectrum indicated the presence of three methyl groups resonating at δ_H 0.77 (t, *J* = 7.4 Hz, H_3-11), 1.20 (d, *J* = 6.7 Hz, 5′-CH_3), and 1.23 (d, *J* = 6.7 Hz, 5-CH_3), three methylene groups at δ_H 1.12/1.16 (m, H_2-8a; m, H_2-8b), 1.20/1.26 (H-10a; m, H-10b), and 1.39/1.49 (m, H-7a; m, H-7b), and one aliphatic methine at δ_H 3.06 (t, *J* = 7.7 Hz, H-6), in addition to three oxymethine protons appearing at 3.20 (m, H-9), 4.37 (q, *J* = 6.7 Hz, H-5), and 4.42 (q, *J* = 6.7 Hz, H-5′) (Table 1). The ^{13}C NMR spectrum resolved 16 carbon signals, which were assigned based on HSQC NMR data to four nonprotonated olefinic carbons, C-3/3′ (δ_C 97.2/97.6) and C-4/4′ (δ_C 184.6/184.1), two carbonyl groups C-2/2′ (δ_C 175.9/176.1), and 10 further either oxygenated or nonoxygenated aliphatic carbon signals. Analysis of the COSY spectrum revealed a continuous spin system of an unbranched hexyl chain starting from H-6 until H-11. On the basis of the HMBC correlations from the methyl protons H_3-11 and from the methylene protons H_2-7, H_2-8, and H_2-10 to C-9 (δ_C 71.2), the alkyl side chain is hydroxylated at position 9 (Figure 1). Two additional spin systems of H_3-5/H-5 and H_3-5′/H-5′ along with the observed HMBC correlations from two methyl groups, 5-CH_3/5′-CH_3 to C-4/4′ and to C5/C5′, and from two oxymethine protons, H-5, H-5′, to the carbonyl carbons C-2/C-2′ and to the oxygenated olefinic carbons C-4/C-4′, respectively, suggested the presence of two butenolide moieties (α,β-unsaturated γ-lactone rings) (Figure 1, Table 1), which was in agreement with the required six degrees of unsaturation of **1**. The connection of the aliphatic side chain with the two butenolide moieties was corroborated by HMBC correlations from H-6 to C-2/2′, C-3/3′, and C-4/4′. The absolute configuration of the stereocenter at C-9 was successfully determined as (*S*) utilizing the modified Mosher's method (Figure 2).[30]

In order to elucidate the absolute configurations at C-5 and C-5′, the solution time-dependent density functional theory−electronic circular dichroism (TDDFT-ECD) method was applied to the (5*R*,9*S*,5′*R*) and (5*S*,9*S*,5′*S*) diastereomers assuming the same absolute configurations in the two γ-lactone rings.[31,32] The initial MMFF (Merck Molecular Force Field) conformational searches resulted in 135 and 147 conformers in a 21 kJ/mol energy window, which were reoptimized at the B3LYP/6-31+G(d,p) and CAM-B3LYP/TZVP PCM/MeCN levels, separately. In the lowest-energy B3LYP/6-31+G(d,p) conformer of (5*R*,9*S*,5′*R*)-**1** (conformer A, 58.1%), the

Table 1. ^{1}H (600 MHz), ^{13}C (150 MHz), and HMBC NMR Data (DMSO-d_6, δ in ppm) for Compound 1

position	δ_C, type	δ_H (*J* in Hz)	HMBC
1			
2	175.9, C		
3	97.2, C[a]		
4	184.6, C		
5	74.0, CH[a]	4.37, q (6.7)	2, 4, 5-CH_3
5-CH_3	18.3, CH_3	1.23, d (6.7)	4, 5
6	26.6, CH	3.06, t (7.7)	2, 2′, 3, 3′, 4, 4′, 7, 8
7a	30.5, CH_2	1.39, m	3, 3′, 6, 8, 9
7b		1.49, m	3, 3′, 6, 8, 9
8a	34.8, CH_2	1.12, m	6, 7, 9
8b		1.16, m	
9	71.2, CH	3.20, m	10, 11
9-OH		4.17, br s	
10a	29.7, CH_2	1.20[b]	8, 9, 11
10b		1.26, m	8, 9, 11
11	9.9, CH_3	0.77, t (7.4)	9, 10
1′			
2′	176.1, C		
3′	97.6, C[a]		
4′	184.1, C		
5′	74.1, CH[a]	4.42, q (6.7)	2′, 4′, 5′-CH_3
5′-CH_3	18.5, CH_3	1.20, d (6.7)[b]	4′, 5′

[a]Signals could be interchangeable. [b]Overlapped signals.

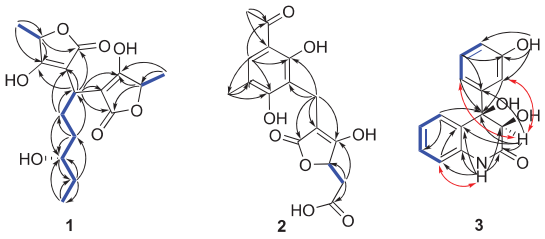

Figure 1. Key HMBC (arrows), COSY (blue bold lines), and ROESY (red arrows) correlations of new natural products **1**−**3**.

DOI: 10.1021/acs.jnatprod.9b00125
J. Nat. Prod. 2019, 82, 2460−2469

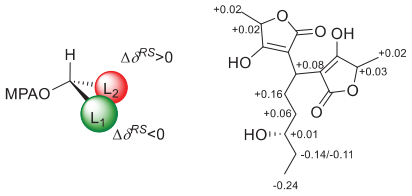

Figure 2. Mosher's model for methoxyphenylacetic acid (MPA) esters and $\Delta\delta$ ($\delta_R - \delta_S$) values derived from chemical shifts of the (*R*)-MPA and (*S*)-MPA esters of compound **1**.

hydroxy group of the right lactone ring was hydrogen-bonded to the carbonyl oxygen of the left lactone moiety and the hydroxy of the left lactone ring was bound to the oxygen atom of the C-9 hydroxy group, when the hydroxyalkyl side chain was oriented downward and the C-6 methine proton was pointing forward (Figure 3).

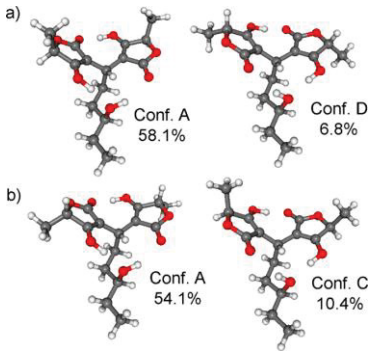

Figure 3. Geometry and population of low-energy gas-phase B3LYP/6-31+G(d,p) conformers of (a) (5*R*,9*S*,5′*R*)-**1** with different hydrogen bond networks. (b) (5*S*,9*S*,5′*S*)-**1** with different hydrogen bond networks.

The two hydrogen bonds rendered the two originally identical C-6 lactone substituents as different groups, which were reflected well in the different ECD spectra and were in accordance with the magnetically distinct NMR signals of these units (Table 1). Conformers B (13.9%) and C (8.1%) had the same hydrogen-bonding network with minor differences in the orientation of the alkyl groups, and they have near identical computed ECD spectra. In contrast, conformer D had a different hydrogen bond network, resulting in different orientations of the lactone rings; the hydroxy group of the left lactone ring formed a hydrogen bond with the carbonyl oxygen of the right lactone ring, and the hydroxy proton of the right lactone moiety bound to the oxygen of the 9-OH. The computed ECD of conformer D was a near mirror-image of that of conformers A–C. The B3LYP/6-31+G(d,p) conformers of (5*S*,9*S*,5′*S*)-**1** showed similar results; the lowest-energy conformer had the same hydrogen bond pattern as that of (5*R*,9*S*,5′*R*)-**1**, and their computed ECD spectra was also near identical.

The Boltzmann-weighted ECD spectra computed at various levels (B3LYP/TZVP, BH&HLYP/TZVP, CAM-B3LYP/TZVP, and PBE0/TZVP) for the B3LYP/6-31+G(d,p) gas-phase conformers of the (5*R*,9*S*,5′*R*) and (5*S*,9*S*,5′*S*) diastereomers were very similar and gave a moderate to good fit with the experimental spectrum (Figure S21). These conformers and their computed ECD spectra could not be used to distinguish between the (5*R*,9*S*,5′*R*) and (5*S*,9*S*,5′*S*) diastereomers and determine the absolute configuration of the lactone rings.

The CAM-B3LYP PCM/MeCN conformers of (5*R*,9*S*,5′*R*)-**1** and (5*S*,9*S*,5′*S*)-**1** showed the same two hydrogen-bonding networks, and their lowest-energy conformer was near identical with the previous B3LYP/6-31+G(d,p) conformer A (Figure 4). However, the Boltzmann-weighted computed solution

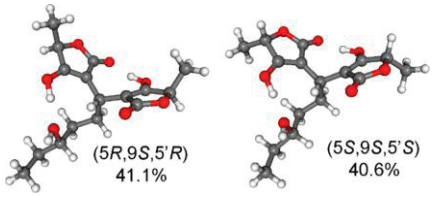

Figure 4. Lowest-energy conformers of (5*R*,9*S*,5′*R*)-**1** and (5*S*,9*S*,5′*S*)-**1** obtained at the CAM-B3LYP/TZVP PCM/MeCN level of theory.

ECD spectra of the diastereomers were markedly different, and they gave opposite Cotton effects (CEs) for the high-wavelength ECD transition (Figure 5). The Boltzmann-weighted ECD spectra of (5*R*,9*S*,5′*R*)-**1** reproduced well the main features of the experimental ECD, while those of (5*S*,9*S*,5′*S*)-**1** gave a mismatch, on the basis of which the (5*R*,9*S*,5′*R*) absolute configuration was assigned to **1**.

Geometry reoptimizations of the initial MMFF conformers were also carried out with B97D/TZVP PCM/MeCN and CAM-B3LYP/TZVP SMD/MeCN methods separately, and solution ECD spectra were computed with four methods for each set of conformational ensemble. These results clearly confirmed the above conclusion, and the B97D/TZVP PCM/MeCN conformers provided the best agreement (Figure 5). Vibrational circular dichroism (VCD) measurement of **1** was attempted with 5 mg of the sample in MeOH-d_4, but the resulting spectrum was too weak and noisy for utilization.

Thus, compound **1** was identified as a new natural product, for which the trivial name marqualide is proposed.

Compound **2** was obtained as an amorphous powder and displayed the molecular formula $C_{16}H_{16}O_8$ on the basis of the HRESIMS protonated molecule peak at *m*/*z* 337.0920 $[M + H]^+$ requiring nine degrees of unsaturation. The ^{1}H and ^{13}C NMR data displayed signals similar to those of the known compound peniphenone D,[33] indicating the presence of an identical clavatol unit[33] and an α,β-unsaturated carbonyl function of a butenolide moiety as in the case of compound **1** (Table 2). The HMBC correlations from the methylene H_2-7 (δ_H 3.17, br s) to C-5 (δ_C 160.9), C-6 (δ_C 115.8), C-8 (δ_C 91.5), C-9 (δ_C 176.4), and C-11 (188.9) confirmed the connectivity between these two moieties. However, broadening of signals in the ^{1}H NMR spectrum of **2** when recorded in DMSO-d_6 hindered the complete assignment of substituent signals at position 10 of the butenolide moiety. Additional NMR measurements of **2** recorded in D_2O resulted in sharper signals, thus affording key HMBC correlations (Figure 1) from H-15a/H-15b to C-10 (δ_C 78.8), C-11, and C-16 (δ_C 178.8), the latter signal denoting the presence of a carboxylic acid group, which is in accordance with the molecular formula of **2**.

DOI: 10.1021/acs.jnatprod.9b00125
J. Nat. Prod. 2019, 82, 2460−2469

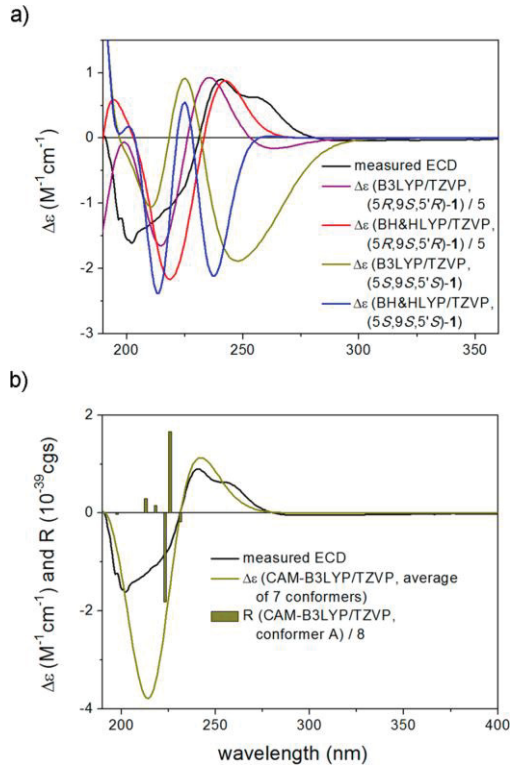

Figure 5. (a) Experimental ECD spectrum of **1** in MeCN compared with the Boltzmann-weighted B3LYP/TZVP PCM/MeCN and BH&HLYP/TZVP PCM/MeCN spectra of (5*R*,9*S*,5′*R*)-**1** and (5*S*,9*S*,5′*S*)-**1** computed for the CAM-B3LYP/TZVP PCM/MeCN conformers. (b) Experimental ECD spectrum of **1** in MeCN compared with the Boltzmann-weighted CAM-B3LYP/TZVP PCM/MeCN spectrum of (5*R*,9*S*,5′*R*)-**1** computed for the B97D/TZVP PCM/MeCN conformers.

The zero specific rotation suggested that **2** is a racemate. Thus, the structure of the new compound **2** was established as shown in Figure 1, for which the trivial name (±)-peniphenone E is proposed.

Compound **3** was obtained as an orange, amorphous powder. Its molecular formula was established as $C_{15}H_{13}NO_4$ (10 degrees of unsaturation) by HRESIMS. The ^{1}H and ^{13}C NMR data of **3** (Table 3) exhibited signals similar to those of the known compound 14-hydroxyaflaquinolone F with an exception of the substitution pattern of ring A, which in the case of **3** corresponded to a 1,3-disubstituted aromatic spin system.[34] Accordingly, a hydroxy group was placed at C-13 on the basis of the HMBC correlations from the phenolic proton 13-OH (δ_H 9.31) to C-12 (δ_C 114.3), C-13 (δ_C 156.8), and C-14 (δ_C 113.8) (Table 3, Figure 1). Further correlations from H-3 to C-11 (δ_C 144.2) as well as from H-12 to C-4 confirmed the connection with the phenyl ring A through the C4−C11 bond, thus forming a 4-phenyl-3,4-dihydroquinolone core structure.[34] Analysis of the ROESY data of **3** revealed the presence of a key correlation between H-3 and the aromatic protons at δ_H 6.83 (br t, J = 2.1 Hz, H-12) and 6.78 (ddd, J = 7.9, 2.1, 0.9 Hz, H-16), indicating their cofacial orientation, as previously shown for known analogues, such as aflaquinolone A and 22-*O*-(*N*-Me-L-valyl)-aflaquinolone B.[35,36]

The ECD spectrum of **3** in MeCN showed positive CEs at 278 and 195 nm and a negative one at 226 nm with shoulders, and the two high-energy CEs had opposite signs to the corresponding transitions of aflaquinolone F.[35] The ECD spectrum of compound **3** was also significantly different from that of the related 14-hydroxyaflaquinolone F, but they were far from a mirror-image relationship.[34] The solution TDDFT-ECD protocol was applied on the arbitrarily chosen (3*S*,4*S*)-**3** enantiomer to determine the absolute configuration. The Boltzmann-weighted ECD spectra of (3*S*,4*S*)-**3** were computed at various levels for the gas-phase B3LYP/6-31+G(d,p), CAM-

Table 2. ^{1}H (600 MHz), ^{13}C (150 MHz), and HMBC NMR Data (DMSO-d_6, δ in ppm) for Compound 2

position	δ_C, type	δ_H (J in Hz)	HMBC
1	165.7, C		
2	118.3, C		
3	129.7, CH	7.42, s	1, 5, 12, 13
4	110.9, C		
5	160.9, C		
5-OH		12.98, s	
6	115.8, C		
7	14.7, CH_2	3.17, br s	5, 6, 8, 9, 11
8	91.5, C		
9	176.4, C		
10	78.8, CH	4.57, br dd (9.3, 3.8)	
11	188.9, C		
12	16.6, CH_3	2.05, s	1, 2, 3
13	201.9, C		
14	26.0, CH_3	2.47, s	4, 13
15a	40.0, CH_2[b]	1.97, m	10, 11, 16[c]
15b		2.50[b]	10, 16[c]
16	178.8, C[c]		

[a]Chemical shift values are extracted from HMBC and HSQC spectra. [b]Overlapped signals. [c]Signals detected in NMR spectra recorded in D_2O.

Table 3. ^{1}H (600 MHz), ^{13}C (150 MHz), HMBC, and ROESY NMR Data (DMSO-d_6, δ in ppm) for Compound 3

position	δ_C, type	δ_H (J in Hz)	HMBC	ROESY
1-NH		10.26, s	2, 3, 5, 9, 10	9
2	170.4, C			
3	74.4, CH	4.46, d (5.4)	2, 4, 5, 11	12, 16
3-OH		5.14, d (5.4)	2, 3, 4	
4	76.8, C			
4-OH		5.51, s	3, 4, 5, 11	
5	129.3, C			
6	128.2, CH	6.75, dd (7.6, 1.3)	4, 7, 8, 10	
7	122.0, CH	6.88, td (7.6, 1.3)	5, 9, 10	
8	128.7, CH	7.21, td (7.6, 1.3)	6, 7, 9, 10	
9	115.3, CH	6.91, dd (7.6, 1.3)	4, 5, 7, 10	1-NH
10	137.1, C			
11	144.2, C			
12	114.3, CH	6.83, br t (2.1)	4, 11, 13, 14, 16	3
13	156.8, C			
13-OH		9.31, s	12, 13, 14	12, 14
14	113.8, CH	6.66, ddd (7.9, 2.1, 0.9)	11, 12, 13, 16	
15	128.6, CH	7.12, t (7.9)	11, 13, 14, 16	
16	117.7, CH	6.78, ddd (7.9, 2.1, 0.9)	4, 12, 13	3

DOI: 10.1021/acs.jnatprod.9b00125
J. Nat. Prod. 2019, 82, 2460−2469

B3LYP/TZVP PCM/MeCN, CAM-B3LYP/TZVP SMD/MeCN, and the B97D/TZVP PCM/MeCN conformers with four methods, and except for the gas-phase B3LYP/6-31+G(d,p) method, they gave consistently mirror-image agreement with the experimental ECD spectrum, which allowed determining the (3*R*,4*R*)-**3** absolute configuration (Figure 6). The B97D functional gave a better agreement than

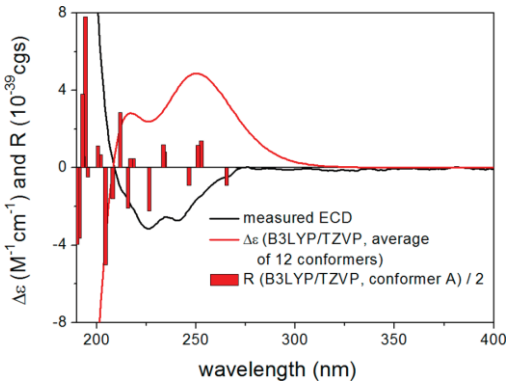

Figure 6. Experimental ECD spectrum of **3** in MeCN compared with the Boltzmann-weighted B3LYP/TZVP PCM/MeCN spectrum of (3*S*,4*S*)-**3** computed for the B97D/TZVP PCM/MeCN conformers.

the CAM-B3LYP. With the B97D/TZVP PCM/MeCN reoptimization, the C-4 aryl and the 3-OH groups adopted an equatorial orientation in the four low-energy conformers (>2.0%), which had a total population of 82.9% (Figure 7). The equatorial 3-OH proton was coordinated to the lactam carbonyl oxygen, which had probably an important role in stabilizing the diequatorial orientation of the C-3 and C-4 substituents. The C-4 aryl group can adopt different orientations by rotating around the C-4−C-11 σ bond. When the C-4 aryl group was equatorial, its benzene ring was always coplanar with the C-4−O σ bond, which could be achieved by two ways. In conformers A and B, the 16-H was cofacial with 3-H and the 13-OH was pointing to the other direction (type A), while in conformers C and D, the 12-H was cofacial with 3-H and the 13-OH was oriented in the same direction (type B).

Although all four of these low-energy conformers gave mirror-image computed ECD curves of the experimental ECD spectrum, the computed individual ECD spectra of the different conformers had distinct differences in the shape, intensities, and shifts of the transitions. Conformers A and B were responsible for the ROE correlation between 16-H and 3-H, while the 3-H/12-H ROE correlation was derived from conformers C and D. With the different orientations of the 13-OH, the electric transition moment of the C-4 aryl group changes, which explains the different computed ECD spectra of the conformers. Low-energy type A and type B CAM-B3LYP/TZVP SMD/MeCN conformers are shown in Figure 8, and their computed ECDs are compared to the experimental

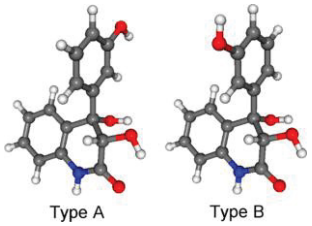

Figure 8. Lowest-energy representatives of type A and type B conformers of (3*S*,4*S*)-**3** obtained at the CAM-B3LYP/TZVP SMD/MeCN level of theory.

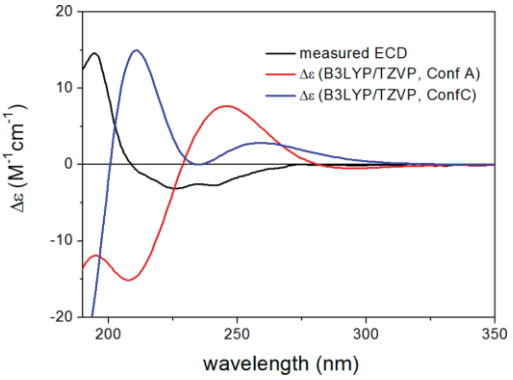

Figure 9. Experimental ECD spectrum of **3** in MeCN compared with the B3LYP/TZVP SMD/MeCN spectra of conformers A and C of (3*S*,4*S*)-**3** computed for the CAM-B3LYP/TZVP SMD/MeCN conformers.

ECD curves in Figure 9. All three solvent model conformational optimization methods including the CAM-B3LYP/TZVP SMD/MeCN produced mirror-image Boltzmann-weighted ECD spectra in the TDDFT-ECD calculations of (3*S*,4*S*)-**3**, which confirmed the (3*R*,4*R*) configurational assignment.

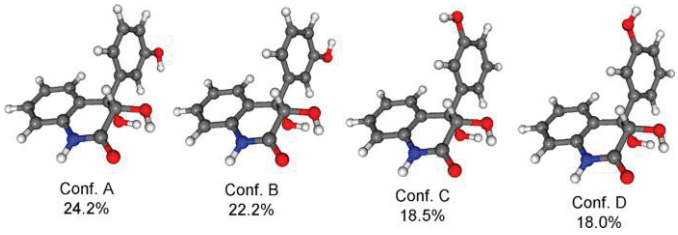

Figure 7. Four low-energy conformers (≥2%) of (3*S*,4*S*)-**3** obtained at the B97D/TZVP PCM/MeCN level of theory.

DOI: 10.1021/acs.jnatprod.9b00125
J. Nat. Prod. 2019, 82, 2460−2469

Interestingly, the gas-phase B3LYP/6-31+G(d,p) method did not allow a solid conclusion on the absolute configuration. In order to confirm the determination of the absolute configuration independently, specific optical rotation (SOR) calculations of (3*S*,4*S*)-**3** were performed for all three solvent model conformational ensembles at four different levels.[37] The Boltzmann-averaged SOR values were obtained in the range of −126 to −93 (experimental $[\alpha]^{23}_{D}$ value: +24), and all low-energy CAM-B3LYP conformers with solvent models and all the B97D/TZVP PCM/MeCN conformers above 2% had negative SOR values, unambiguously verifying the (3*R*,4*R*) absolute configuration of ECD calculations.[38] In contrast to ECD calculation results, the signs of the computed SOR values of conformers with different orientation of the C-4 aryl group were always negative, and thus this conformational difference was not manifested in the sign of the SOR. The related (3*S*,4*S*)-aflaquinolone F had an $[\alpha]^{25}_{D}$ value of +10 (*c* 0.19, MeOH),[35] while the (3*S*,4*S*)-14-hydroxyaflaquinolone F had a −33 $[\alpha]^{20}_{D}$ value (*c* 0.15, MeOH).[34]

VCD spectroscopy in combination with DFT calculations has been utilized to elucidate the absolute configuration of various natural products.[39−43] Due to the larger number of transitions in a VCD spectrum compared to those in an ECD spectrum, the VCD can be supplementary and more reliable in problematic cases.[44] Furthermore, numerical comparison methods and softwares of experimental and calculated spectra have been developed and implemented recently to help users estimate the agreement between experimental and computed data and minimize the possibility of human error.[45−49] In order to confirm the absolute configuration, the VCD spectrum of **3** was measured in MeOH-d_4 and computed at the B3LYP/TZVP PCM/MeOH level for the B3LYP/TZVP PCM/MeOH reoptimized conformers.[50,51] With the B3LYP/TZVP PCM/MeOH VCD spectrum of (3*S*,4*S*)-**3**, Gaussian broadening and a manual scaling factor of 0.98[51] gave an acceptable mirror-image agreement with the experimental curve by shifting the 1280 and 1260 cm^{-1} transitions to higher wavenumbers (Figure S23). The VCD spectra were also broadened with Lorentzian band type, and the best fit was automatically determined with a sweep of 0.0005 step size between 0.94 and 1.01 as default settings of the CDSpecTech package.[48,49] The best fit for the IR spectra was found between 0.974 and 0.9745, and thus computed VCD and IR spectra with Lorentzian broadening created with the CDSpecTech package were scaled by 0.974 and plotted together with the experimental data in Figure 10. A 6.8% confidence level was found for the wrong (3*S*,4*S*) enantiomer and 98.5% for the good (3*R*,4*R*) enantiomer by using the spectral range of 1170−1590 cm^{-1} of the experimental VCD and IR spectra. A maximum value for the enantiomeric similarity index (ESI_{max}) was found to be 0.456 with ESI-VCD values of 0.585 for the (3*R*,4*R*) and 0.129 for the (3*S*,4*S*) enantiomer. Characteristic transitions were ascribed as follows: 1 (∼1605 cm^{-1}) and 2 (∼1590 cm^{-1}) are aromatic C═C stretching vibrational modes of rings A and B, respectively, 3 (∼1500 cm^{-1}) is a stretching vibration of the aromatic C═C bonds of ring A combined with the deformation vibrations of the aromatic C−H and phenolic OH of ring A, 5 (∼1470 cm^{-1}) and 7 (∼1405 cm^{-1}) are aromatic C−H and N−H in-plane deformation vibrations combined with aromatic C═C stretching vibrations of ring B, 8 (∼1375 cm^{-1}) is a C−C stretching vibrations of ring C combined with the deformation vibration of H-3 and 3-OH, 9 (∼1350−1320 cm^{-1}) is a stretching vibrations of ring C

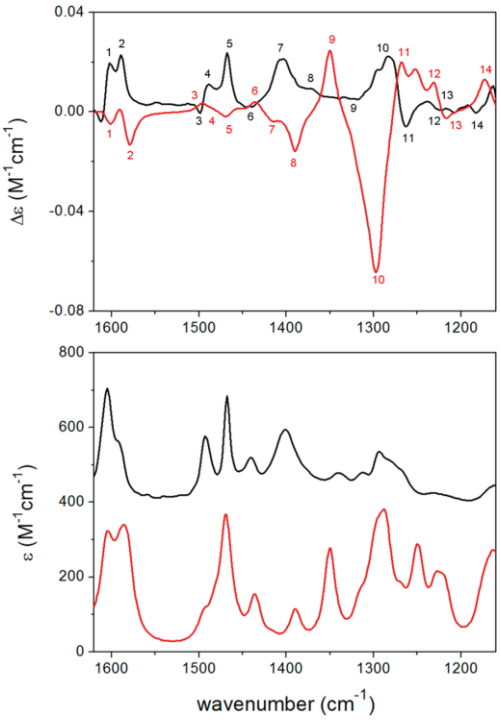

Figure 10. Experimental VCD (up, black line) and IR (down, black line) spectra of **3** in MeOH-d_4 compared with the B3LYP/TZVP PCM/MeOH VCD (up, red line) and IR (down, red line) spectra of (3*S*,4*S*)-**3** computed for the B3LYP/TZVP PCM/MeOH conformers and generated with Lorentzian broadening and a scaling factor of 0.974.

combined with the deformation vibration of H-3, 3-OH, 4-OH, and N−H, 10 (∼1285 cm^{-1}) is combined C−C stretching vibrations of rings B, C, and A, 11 (∼1260 cm^{-1}) and 12 (∼1225 cm^{-1}) are in-plane C−H deformation vibrations of rings B and A combined with the deformation vibrations of H-3 and 4-OH/3-OH, 13 (∼1215 cm^{-1}) is an in-plane C−H deformation vibration of ring B combined with the deformation vibration of H-3 and 3-OH, 14 (∼1180 cm^{-1}) is an in-plane deformation vibration of the aromatic hydrogens and the phenolic OH of ring A combined with the deformation vibration of H-3 and 4-OH.

Thus, the structure of compound **3** was determined as (3*R*,4*R*)-13-hydroxyaflaquinolone F, for which the trivial name aflaquinolone I is proposed. The (3*R*,4*R*) absolute configuration of aflaquinolone I is opposite that of (3*S*,4*S*) aflaquinolone F. Moreover, the C-4 aryl group of aflaquinolone I (**3**) has an equatorial orientation in solution according to our conformational analysis and ECD calculations, while the aryl group of the related aflaquinolones A−E and aniduquinolones A−C was proved to adopt an axial position in solution (ECD calculations) and in the solid state (single-crystal X-ray diffraction).[34,35] It has to be mentioned that aflaquinolone I represents an example for a chiral switch between different organisms, when closely related natural products are synthesized with opposite absolute configurations.[29]

DOI: 10.1021/acs.jnatprod.9b00125
J. Nat. Prod. 2019, 82, 2460−2469

Compound **4** was obtained as a yellow, amorphous powder, and based on detailed 1D, 2D, and mass-spectroscopic analysis as well as literature data,[52] it was identified as the known compound terrestric acid hydrate, the latter being a plausible biosynthetic precursor of **1**. However, the absolute configurations of the stereocenters at C-5 and C-9 of **4** had not been established so far. As compound **4** failed to convert into Mosher esters, we attempted to assign the configurations using the ECD approach.

Compound **4** is a fragment or subunit of **1**, and hence it was assumed that it has the same (9*S*) absolute configuration as determined for C-9 of **1**. Thus, (5*R*,9*S*)-**4** and (5*S*,9*S*)-**4** were chosen for solution ECD calculations. It was expected that the C-5 chirality center of the α,β-unsaturated lactone chromophore governs the ECD spectrum and the remote C-9 chirality center does not have much contribution. Thus, ECD calculation was expected to determine the absolute configuration of the C-5 chirality center. The 139 and 141 initial MMFF conformers of (5*R*,9*S*)-**4** and (5*S*,9*S*)-**4** were reoptimized at the B3LYP/6-31+G(d,p) and CAM-B3LYP/TZVP PCM/MeCN levels, and ECD spectra were calculated for the low-energy conformers similarly to **1** and **3**. In all low-energy conformers, the 4-OH was hydrogen-bonded to the C-6 carbonyl oxygen (six-membered chelate), and the 9-OH formed an nine-membered chelate by hydrogen bonding to the C-6 carbonyl oxygen. The computed conformers differed in the geometry of the nine-membered chelate, which included the ketone carbonyl and the C-9 chirality center, and computed ECD spectra of the individual conformers reflected the conformation of this chelate and hence the C-9 configuration. The lowest-energy CAM-B3LYP/TZVP PCM/MeCN conformers of (5*R*,9*S*)-**4** and (5*S*,9*S*)-**4** had the same geometry for the nine-membered chelate (Figure 11), and their

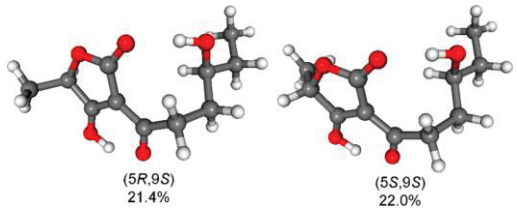

Figure 11. Lowest-energy conformers of (5*R*,9*S*)-**4** and (5*S*,9*S*)-**4** obtained at the CAM-B3LYP/TZVP PCM/MeCN level of theory.

computed ECD spectra were also very similar regardless of the different absolute configuration of C-5. The Boltzmann-weighted ECD spectra of the CAM-B3LYP/TZVP PCM/MeCN conformers of both (5*R*,9*S*)-**4** and (5*S*,9*S*)-**4** reproduced quite well the experimental ECD spectrum (Figure 12), on the basis of which the (9*S*) absolute configuration could be determined unambiguously. Based on the larger magnitude of the higher-wavelength positive CE reproduced better by the computed ECDs of (5*R*,9*S*)-**4**, the (5*R*) absolute configuration can be tentatively assigned, which also corroborates the (5*R*,5′*R*) configuration of the related **1**. Moreover, our configurational assignment for **4** is consistent with the reported (5*R*,9*S*) absolute configuration for the closely related natural product terrestric acid (dehydrated form).[53−55] The ECD calculation of **4** drew our attention in that a flexible side chain with a remote chirality center and a

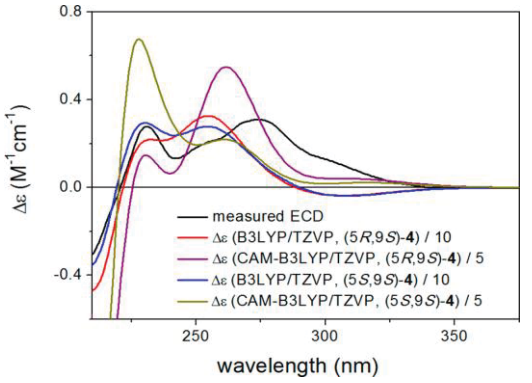

Figure 12. Experimental ECD spectrum of **4** in MeCN compared with the Boltzmann-weighted B3LYP/TZVP PCM/MeCN and CAM-B3LYP/TZVP PCM/MeCN spectra of (5*R*,9*S*)-**4** and (5*S*,9*S*)-**4** computed for the CAM-B3LYP/TZVP PCM/MeCN conformers.

chelating group should not be truncated or neglected to simplify the ECD calculation.

Compound **5** was obtained as an amorphous powder. The ^{1}H and ^{13}C NMR data of **5** were identical to those of the known compound peniphenone D.[33] Peniphenone D was reported to have a negative specific rotation value ($[\alpha]^{25}_{D}$ −72), and the stereocenter at C-10 was determined as *R*. However, in this study compound **5** was obtained as a racemate ($[\alpha]^{25}_{D}$ +0.5).

The remaining known compounds were identified as viridicatin,[56] clavatol,[57] penilactone A,[58] cyclopenol,[59] dehydrocyclopeptine,[60] chaetobutenolide C,[30] and WF-3681,[30] respectively by comparison of their spectroscopic data with those reported in the literature.

All isolated compounds were examined for their inhibitory effect on the growth of L5178Y mouse lymphoma cells utilizing the MTT assay, but none of them showed significant activity when investigated at a dose of 10 μg/mL. These compounds were also evaluated for their antibacterial activities against *Mycobacterium tuberculosis*, *Staphylococcus aureus* (ATCC 29213), *Staphylococcus aureus* (ATCC 700699), *Acinetobacter baumanii* (BAA1605), and *Pseudomonas aeruginosa* (27853); however, they were found to be inactive, with MIC > 100 μM.

Compound **1** is the first example of a natural product containing a methylenebistetronic acid unit. Moreover, there are only a few reports on the synthesis of this unusual structural motif.[61,62] Natural product **1** is proposed to be derived through an aldol condensation between terrestric acid hydrate and 5-methyltetronic acid followed by reduction (Scheme S1).

In summary, chemical investigation of a marine-derived strain of the fungus *M. marquandii* resulted in the isolation of 12 secondary metabolites. These compounds can be classified into three groups: polyketides (**1**, **2**, **4**, **5**, clavatol and penilactone A), alkaloids (**3**, viridicatin, cyclopenol, and dehydrocyclopeptine) originated from phenylalanine and anthranilic acid, as well as butenolides (chaetobutenolide C and WF-3681), which were postulated to be biosynthesized by NRPS-like enzymes.[30] Compounds **1**−**3** were found to be new natural products, including a new terrestric acid hydrate

DOI: 10.1021/acs.jnatprod.9b00125
J. Nat. Prod. 2019, 82, 2460−2469

derivative, marqualide (**1**), featuring an unusual methylenebistetronic acid moiety, which is unprecedented in nature.

EXPERIMENTAL SECTION

General Experimental Procedures. A Jasco P-2000 polarimeter was used for the measurement of the optical rotations of chiral compounds after being dissolved in optically pure solvents Uvasol (spectroscopic grade solvents, Merck). ECD spectra were recorded on a JASCO J-810 spectropolarimeter. VCD spectra were recorded on a BioTools Chiral*IR*-2X at a resolution of 4 cm^{-1} under ambient temperature for 18 × 3000 scans, respectively. Samples were dissolved in MeOH-d_4 at a concentration of 0.10 M (**1**) and 0.17 M (**3**), and the solution was placed in a 100 μm BaF_2 cell. FT-IR measurements were carried out on a Bruker TENSOR 37 IR spectrometer at ambient temperature in a KBr pellet in the range 4000−400 cm^{-1} with a 4 cm^{-1} resolution (16 scans per measurement). 1D and 2D NMR spectra were recorded on Bruker Avance III 600 MHz NMR spectrometers. An Ion-Trap-API Finnigan LCQ Deca (Thermo Quest) mass spectrometer was used for recording low-resolution mass spectra (ESI), while HRESIMS spectra were measured on a FTHRMS-Orbitrap (Thermo-Finnigan) mass spectrometer. HPLC analysis was carried out on a Dionex UltiMate-3400 SD with an LPG-3400SD pump equipped with a photodiode array detector (DAD3000RS). The detection was set routinely at 235, 254, 280, and 340 nm. The HPLC separation column (125 mm × 4 mm, L × i.d.) was prefilled with Eurosphere-10 C_{18}, and the following gradient was applied for analysis: (MeOH, 0.1% HCOOH in H_2O): 0 min (10% MeOH); 5 min (10% MeOH); 35 min (100% MeOH); 45 min (100% MeOH). Compounds were purified using semipreparative HPLC on the VWR Hitachi Chromaster HPLC system, 5160 pump; 5410 UV detector UV detector; Eurosphere-100 C_{18}, 300 mm × 8 mm) with a flow rate of 5 mL/min. The stationary phases used for column chromatography included Merck MN silica gel 60 M (0.04−0.063 mm), Sephadex LH-20, and silica gel 60 RP-18 (40−63 μm). For monitoring fractions resulting from column chromatography, TLC plates precoated with silica gel 60 F_{254}(Merck) were used and detection was by UV absorption at 254 and 366 nm or by spraying the plates with anisaldehyde reagent.

Fungal Material. The fungal strain was isolated from a seawater sample collected from the North Sea coast (Germany) close to St. Peter in spring 2016 and identified as *Metarhizium marquandii* SW2-B (GenBank accession no. MK014827). Fungal identification was carried out through sequencing of the ITS region as previously described,[63] followed by BlastN search in the NCBI database. The fungal strain *M. marquandii* was deposited in one of author's laboratory (P.P.)

Fermentation of the Fungus. The fungus was cultivated on solid rice medium in five 1 L Erlenmeyer flasks. To each flask were added 100 g of commercially available rice and 100 mL of demineralized H_2O. Afterward, the flasks were autoclaved at 121 °C for 20 min and later inoculated with the culture of *M. marquandii*. The fermentation of the fungus was conducted under static conditions for 21 days at 20 °C.

Extraction and Isolation. After fermentation on solid rice medium the fungal cultures were extracted with EtOAc (1 L × 3). The extracts were filtered, combined, and evaporated under vacuum to dryness to obtain 5 g of organic extract. The obtained extract was first fractionated by vacuum liquid chromatography (VLC) on silica gel using a gradient with increasing solvent polarity consisting of mixtures of *n*-hexane−EtOAc−CH_2Cl_2−MeOH, to yield 10 fractions (Mm-1 to Mm-10). Fraction Mm-2 (183.2 mg) was further separated by column chromatography on Sephadex LH-20 with MeOH as mobile phase, affording three subfractions (Mm-2-1 to Mm-2-3). Mm-2-3 was further purified by preparative TLC using a mixture of *n*-hexane−EtOAc (80:20) with addition of 1% NH_3 as a mobile phase to afford clavatol (1.5 mg). Fraction Mm-4 (519.4 mg) was subjected to column chromatography over Sephadex LH-20 with methanol as mobile phase, to yield seven subfractions (Mm-4-1 to Mm-4-7). Subfraction Mm-4-3 (47.6 mg) was further purified by semi-preparative HPLC using gradient elution with MeOH−H_2O mixtures (from 50:50 to 65:35 over 30 min) to afford **5** (3.4 mg), viridicatin (1.9 mg), penilactone A (1.6 mg), dehydrocyclopeptine (1 mg), chaetobutenolide C (4.8 mg), and WF-3681 (3.7 mg). Fractions Mm-6 (686.5 mg) and Mm-8 (349 mg) were submitted to an RP-VLC column using H_2O−MeOH gradient elution to yield seven subfractions, Mm-6-1 to Mm-6-7 and Mm-8-1 to Mm-8-8, respectively. Semipreparative HPLC purification of Mm-6-2 (56.2 mg) using MeOH−H_2O isocratic elution (34:66) yielded compounds **3** (16.5 mg) and cyclopenol (14.6 mg). Compound **2** (1.9 mg) was obtained as a MeOH-insoluble residue from subfraction Mm-8-2 (42.6 mg). The rest of this fraction, which was soluble in MeOH (36.6 mg), was purified by semipreparative HPLC using MeOH−H_2O gradient elution (from 10:90 to 45:55 over 30 min) to afford **1** (8.9 mg) and **4** (1.7 mg).

*Marqualide (**1**):* dark yellow, amorphous powder; $[\alpha]^{23}_D$ +17 (*c* 0.5, MeOH); UV (MeOH) λ_{max} 236 nm; ECD (0.306 mM, MeCN), λ_{max} ($\Delta\varepsilon$) 258sh (+0.60), 241 (+0.90), 218sh (−1.08) nm; IR (KBr) ν_{max} 3397, 1714, 1630, 1404, 1027 cm^{-1}; ^1H and ^{13}C NMR data, Table 1; HRESIMS *m*/*z* 327.1439 $[M + H]^+$ (calcd for $C_{16}H_{23}O_7$, 327.1438).

*(±)-Peniphenone E (**2**):* amorphous powder; $[\alpha]^{23}_D$ 0 (*c* 0.5, MeOH); UV (MeOH) λ_{max} 218, 262, 283, 331 nm; ^1H and ^{13}C NMR data, Table 2; HRESIMS *m*/*z* 337.0920 $[M + H]^+$ (calcd for $C_{16}H_{17}O_8$ 337.0918)

*Aflaquinolone I (**3**):* orange, amorphous powder; $[\alpha]^{23}_D$ +24 (*c* 0.5, MeOH); UV (MeOH) λ_{max} 200, 255 nm; ECD (0.186 mM, MeCN), λ_{max} ($\Delta\varepsilon$) 291sh (+0.11), 278 (+0.28), 274sh (0.25), 240sh (−2.73), 226 (−3.16), 215sh (−1.87), 195 (+14.6) nm; ECD (0.180 mM, MeOH), λ_{max} ($\Delta\varepsilon$) 290sh (+0.16), 280 (+0.24), 275sh (+0.17), 243sh (−1.07), 224 (−3.85), positive CE below 205 nm; IR (KBr) ν_{max} 3240, 1700, 1593, 1488, 1271, 1141, 771 cm^{-1}; ^1H and ^{13}C NMR data, Table 3; HRESIMS *m*/*z* 294.0737 $[M + Na]^+$ (calcd for $C_{15}H_{13}NNaO_4$ 294.0737).

*Terrestric acid hydrate (**4**):* yellow, amorphous powder; $[\alpha]^{23}_D$ −56 (*c* 0.5, MeOH); UV (MeOH) λ_{max} 206, 275 nm; ECD (0.438 mM, MeCN), λ_{max} ($\Delta\varepsilon$) 303sh (+0.12), 274 (+0.31), 255sh (+0.21), 231 (+0.28) nm, negative CE below 220 nm.

*(±)-Peniphenone D (**5**):* white powder; $[\alpha]^{25}_D$ +0.5 (*c* 0.5, MeOH).

Mosher's Reaction of Compound 1. To obtain the (*S*)- and (*R*)-MPA esters of **1**, 1 mg (0.00306 mmol) of **1** was treated with (*S*)- and (*R*)-α-methoxyphenylacetic acid (3 mg, 0.01807 mmol) and *N*,*N*′-dicyclohexylcarbodiimide (6 mg, 0.02912 mmol and 3 mg, 0.02459 mmol) in CH_2Cl_2 with continuous stirring at room temperature for 6 h. The formed reaction products were later submitted to semipreparative HPLC for purification using MeOH−H_2O as the mobile phase to afford 0.47 mg and 0.40 mg of (*S*)-MPA and (*R*)-MPA esters, respectively.

(S)-MPA ester of 1: ^1H NMR (DMSO-d_6, 600 MHz) δ_H 4.63 (m, H-9), 4.40/4.36 (q, *J* = 6.7 Hz, H-5′/5; q, *J* = 6.7 Hz, H-5/5′), 2.99 (t, *J* = 7.3 Hz, H-6), 1.41/1.46 (m, H-10a; m, H-10b), 1.27 (m, H_2-8), 1.21 (m, H_2-7), 1.21/1.19 (d, *J* = 6.7 Hz, 5/5′-CH_3; d, *J* = 6.7 Hz, 5′/5-CH_3), 0.70 (t, *J* = 7.4 Hz, H_3-11); ESIMS *m*/*z* 475 $[M + H]^+$.

(R)-MPA ester of 1: ^1H NMR (DMSO-d_6, 600 MHz) δ_H 4.64 (m, H-9), 4.43/4.38 (q, *J* = 6.6 Hz, H-5′/5; q, *J* = 6.6 Hz, H-5/5′), 3.07 (t, *J* = 7.1 Hz, H-6), 1.37 (m, H_2-7), 1.33 (m, H_2-8), 1.27/1.35 (m, H-10a; m, H-10b), 1.23/1.21 (d, *J* = 6.7 Hz, 5/5′-CH_3; d, *J* = 6.7 Hz, 5′/5-CH_3), 0.46 (t, *J* = 7.4 Hz, H_3-11); ESIMS *m*/*z* 475 $[M + H]^+$.

Antibacterial Assay. The performed antibacterial assay was carried out using the broth microdilution method according to the guidelines of the Clinical and Laboratory Standards Institute (CLSI).[64] Mueller-Hinton broth (0.20%, w/v, beef extract; 1.75%, w/v, acid digest of casein; 0.15%, w/v, starch) was used to propagate the bacterial strains. Moxifloxacin was used as a positive control for *Staphylococcus aureus*, whereas rifampicin was used as a positive control against *Mycobacterium tuberculosis* and the Gram-negative bacteria *Acinetobacter baumanii* and *Pseudomonas aeruginosa*. Compounds were added from stock solution (10 mg/mL in DMSO), resulting in a final DMSO amount of 0.64% at the highest antibiotic

DOI: 10.1021/acs.jnatprod.9b00125
J. Nat. Prod. 2019, 82, 2460−2469

concentration tested (64 μg/mL). Serial 2-fold dilutions of antibiotics were prepared with DMSO being diluted along with the compounds.

Cytotoxicity Assay. Cytotoxicity was tested against L5178Y mouse lymphoma cells using the MTT assay, in comparison to untreated controls, as described previously.[65] As negative controls, media with 0.1% ethylene glycol monomethyl ether/DMSO were utilized in these experiments. For the positive control, the depsipeptide kahalalide F, isolated from *Elysia grandifolia*, was used. Experiments were repeated three times and carried out in triplicate.

Computational Methods. Mixed torsional/low-mode conformational searches were carried out by means of the Macromodel 10.8.011 software using the MMFF with an implicit solvent model for $CHCl_3$ applying a 21 kJ/mol energy window.[66] Geometry reoptimizations of the resultant conformers [B3LYP/6-31+G(d,p) level in vacuo, B97D/TZVP[67,68] and CAM-B3LYP/TZVP[69] with PCM solvent model for MeCN and MeOH, B3LYP/TZVP with PCM for MeOH, and CAM-B3LYP/TZVP with SMD solvent model for MeCN] and DFT VCD, TDDFT ECD, and SOR calculations were performed with Gaussian 09 for ECD and SOR using various functionals (B3LYP, BH&HLYP, CAM-B3LYP, PBE0) and the TZVP basis set with the same or no solvent model as in the preceding DFT optimization step.[70] ECD spectra were generated as the sum of Gaussians with 3000, 3600, and 4200 cm^{-1} half-height widths, using dipole-velocity-computed rotational strengths.[71] VCD spectra were calculated with 8 cm^{-1} half-height width and scaled by a factor of 0.98.[72] Boltzmann distributions were estimated from the B3LYP, B97D, and CAM-B3LYP energies. The MOLEKEL software package was used for visualization of the results.[73]

■ ASSOCIATED CONTENT

Supporting Information

The Supporting Information is available free of charge on the ACS Publications website at DOI: 10.1021/acs.jnatprod.9b00125.

HPLC chromatograms, UV, HRESIMS, and NMR spectra of **1**–**3**, IR spectra of **1** and **3**, ECD calculations data, and ITS sequence of *M. marquandii* SW2-B (PDF)

■ AUTHOR INFORMATION

Corresponding Authors

*Tel: +49 211 81 14175. E-mail: elena.ancheeva@uni-duesseldorf.de (E. Ancheeva).

*Tel: +49 211 81 14163. Fax: +49 211 81 11923. E-mail: proksch@uni-duesseldorf.de (P. Proksch).

ORCID

Georgios Daletos: 0000-0002-1636-6424

Attila Mándi: 0000-0002-7867-7084

Wenhan Lin: 0000-0002-4978-4083

Elena Ancheeva: 0000-0002-2440-4427

Present Address

¶(G. Daletos) Department of Chemical Engineering, Massachusetts Institute of Technology, 25 Ames Street, Cambridge, Massachusetts 02139, United States.

Notes

The authors declare no competing financial interest.

■ ACKNOWLEDGMENTS

D.H.E. gratefully acknowledges the Egyptian Government (Ministry of Higher Education) for awarding the doctoral scholarship. Financial support by the Manchot Foundation to P.P. is gratefully acknowledged. We are thankful to Prof. R. Kalscheuer (Univ. of Düsseldorf) for carrying out the antibacterial assays and to Prof. W. E. G. Müller (Univ. Mainz) for cytotoxicity assays. Furthermore, we wish to thank Dr. M. Proksch for help during fungal isolation. The Hungarian authors were supported by the EU and cofinanced by the European Regional Development Fund under the project GINOP-2.3.2-15-2016-00008. T.K. thanks the National Research, Development and Innovation Office (NKFI K120181) and A.M. the János Bolyai Research Scholarship of the Hungarian Academy of Sciences. The Governmental Information-Technology Development Agency (KIFÜ) is acknowledged for CPU time. We are grateful to Prof. Dr. J. B. Gloer for kindly providing the original ECD spectrum of aflaquinolone F for comparison with that of **3**.

■ REFERENCES

(1) Bugni, T. S.; Ireland, C. M. *Nat. Prod. Rep.* **2004**, *21*, 143–163.

(2) Rateb, M. E.; Ebel, R. *Nat. Prod. Rep.* **2011**, *28*, 290–344.

(3) Blunt, J. W.; Copp, B. R.; Munro, M. H. G.; Northcote, P. T.; Prinsep, M. R. *Nat. Prod. Rep.* **2011**, *28*, 196–268.

(4) Abraham, E. P.; Newton, G. G. F. *Biochem. J.* **1961**, *79*, 377–393.

(5) Blunt, J. W.; Copp, B. R.; Keyzers, R. A.; Munro, M. H. G.; Prinsep, M. R. *Nat. Prod. Rep.* **2017**, *34*, 235–294.

(6) Kanoh, K.; Kohno, S.; Asari, T.; Harada, T.; Katada, J.; Muramatsu, M.; Kawashima, H.; Sekiya, H.; Uno, I. *Bioorg. Med. Chem. Lett.* **1997**, *7*, 2847–2852.

(7) Millward, M.; Mainwaring, P.; Mita, A.; Federico, K.; Lloyd, G. K.; Reddinger, N.; Nawrocki, S.; Mita, M.; Spear, M. A. *Invest. New Drugs* **2012**, *30*, 1065–1073.

(8) Beyondspring Home Page. https://www.beyondspringpharma.com/en/pipeline/plinabulin/nsclc/ (accessed Jul 23, 2019).

(9) Scholte, E.-J.; Knols, B. G. J.; Samson, R. A.; Takken, W. *J. Insect Sci.* **2004**, *4*, 19.

(10) Bidochka, M. J.; Kamp, A. M.; Lavender, T. M.; Dekoning, J.; De Croos, J. N. A. *Environ. Microbiol.* **2001**, *67*, 1335–1342.

(11) Senthil-Nathan, S. A review of biopesticides and their mode of action against insect pests. In *Environmental Sustainability: Role of Green Technologies*; Thangavel, P.; Sridevi, G., Eds.; Springer India: New Delhi, 2015; pp 49–63.

(12) Carollo, C. A.; Calil, A. L. A.; Schiave, L. A.; Guaratini, T.; Roberts, D. W.; Lopes, N. P.; Braga, G. U. L. *Fungal Biol.* **2010**, *114*, 473–480.

(13) Wang, C.; Skrobek, A.; Butt, T. M. *J. Invertebr. Pathol.* **2004**, *85*, 168–174.

(14) Seger, C.; Eberhart, K.; Sturm, S.; Strasser, H.; Stuppner, H. *J. Chromatogr. A* **2006**, *1117*, 67–73.

(15) Dornetshuber-Fleiss, R.; Heffeter, P.; Mohr, T.; Hazemi, P.; Kryeziu, K.; Seger, C.; Berger, W.; Lemmens-Gruber, R. *Biochem. Pharmacol.* **2013**, *86*, 361–377.

(16) Krasnoff, S. B.; Keresztes, I.; Gillilan, R. E.; Szebenyi, D. M. E.; Donzelli, B. G. G.; Churchill, A. C. L.; Gibson, D. M. *J. Nat. Prod.* **2007**, *70*, 1919–1924.

(17) Kozone, I.; Ueda, J.-y.; Watanabe, M.; Nogami, S.; Nagai, A.; Inaba, S.; Ohya, Y.; Takagi, M.; Shin-Ya, K. *J. Antibiot.* **2009**, *62*, 159–162.

(18) Azumi, M.; Ishidoh, K.-i.; Kinoshita, H.; Nihira, T.; Ihara, F.; Fujita, T.; Igarashi, Y. *J. Nat. Prod.* **2008**, *71*, 278–280.

(19) Lee, S. Y.; Kinoshita, H.; Ihara, F.; Igarashi, Y.; Nihira, T. *J. Biosci. Bioeng.* **2008**, *105*, 476–480.

(20) Gupta, S.; Krasnoff, S. B.; Renwick, J. A. A.; Roberts, D. W.; Steiner, J. R.; Clardy, J. *J. Org. Chem.* **1993**, *58*, 1062–1067.

(21) Patrick, M.; Adlard, M. W.; Keshavarz, T. *Biotechnol. Lett.* **1993**, *15*, 997–1000.

(22) Uchida, R.; Imasato, R.; Yamaguchi, Y.; Masuma, R.; Shiomi, K.; Tomoda, H.; Ōmura, S. *J. Antibiot.* **2005**, *58*, 804–809.

(23) Krasnoff, S. B.; Englich, U.; Miller, P. G.; Shuler, M. L.; Glahn, R. P.; Donzelli, B. G. G.; Gibson, D. M. *J. Nat. Prod.* **2012**, *75*, 175–180.

(24) Kuboki, H.; Tsuchida, T.; Wakazono, K.; Isshiki, K.; Kumagai, H.; Yoshioka, T. *J. Antibiot.* **1999**, *52*, 590–593.

DOI: 10.1021/acs.jnatprod.9b00125
J. Nat. Prod. 2019, 82, 2460–2469

(25) Cabrera, G. M.; Butler, M.; Rodriguez, M. A.; Godeas, A.; Haddad, R.; Eberlin, M. N. *J. Nat. Prod.* **2006**, *69*, 1806−1808.
(26) Radics, L.; Kajtar-Peredy, M.; Casinovi, C. G.; Rossi, C.; Ricci, M.; Tuttobello, L. *J. Antibiot.* **1987**, *40*, 714−716.
(27) Elnaggar, M. S.; Ebada, S. S.; Ashour, M. L.; Ebrahim, W.; Müller, W. E. G.; Mándi, A.; Kurtán, T.; Singab, A.; Lin, W.; Liu, Z.; Proksch, P. *Tetrahedron* **2016**, *72*, 2411−2419.
(28) Mokhlesi, A.; Hartmann, R.; Kurtán, T.; Weber, H.; Lin, W.; Chaidir, C.; Müller, W. E. G.; Daletos, G.; Proksch, P. *Mar. Drugs* **2017**, *15*, 356.
(29) Küppers, L.; Ebrahim, W.; El-Neketi, M.; Özkaya, F.; Mándi, A.; Kurtán, T.; Orfali, R. S.; Müller, W. E. G.; Hartmann, R.; Lin, W.; Song, W.; Liu, Z.; Proksch, P. *Mar. Drugs* **2017**, *15*, 359.
(30) Ancheeva, E.; Küppers, L.; Akone, S. H.; Ebrahim, W.; Liu, Z.; Mándi, A.; Kurtán, T.; Lin, W.; Orfali, R.; Rehberg, N.; Kalscheuer, R.; Daletos, G.; Proksch, P. *Eur. J. Org. Chem.* **2017**, *2017*, 3256−3264.
(31) Mándi, A.; Mudianta, I. W.; Kurtán, T.; Garson, M. J. *J. Nat. Prod.* **2015**, *78*, 2051−2056.
(32) Superchi, S.; Scafato, P.; Gorecki, M.; Pescitelli, G. *Curr. Med. Chem.* **2018**, *25*, 287−320.
(33) Li, H.; Jiang, J.; Liu, Z.; Lin, S.; Xia, G.; Xia, X.; Ding, B.; He, L.; Lu, Y.; She, Z. *J. Nat. Prod.* **2014**, *77*, 800−806.
(34) An, C.-Y.; Li, X.-M.; Luo, H.; Li, C.-S.; Wang, M.-H.; Xu, G.-M.; Wang, B.-G. *J. Nat. Prod.* **2013**, *76*, 1896−1901.
(35) Neff, S. A.; Lee, S. U.; Asami, Y.; Ahn, J. S.; Oh, H.; Baltrusaitis, J.; Gloer, J. B.; Wicklow, D. T. *J. Nat. Prod.* **2012**, *75*, 464−472.
(36) Chen, M.; Shao, C.-L.; Meng, H.; She, Z.-G.; Wang, C.-Y. *J. Nat. Prod.* **2014**, *77*, 2720−2724.
(37) Polavarapu, P. L.; Donahue, E. A.; Shanmugam, G.; Scalmani, G.; Hawkins, E. K.; Rizzo, C.; Ibnusaud, I.; Thomas, G.; Habel, D.; Sebastian, D. *J. Phys. Chem. A* **2011**, *115*, 5665−5673.
(38) Sun, P.; Yu, Q.; Li, J.; Riccio, R.; Lauro, G.; Bifulco, G.; Kurtán, T.; Mándi, A.; Tang, H.; Li, T.-J.; Zhuang, C.-L.; Gerwick, W. H.; Zhang, W. *J. Nat. Prod.* **2016**, *79*, 2552−2558.
(39) Pardo-Novoa, J. C.; Arreaga-González, H. M.; Gómez-Hurtado, M. A.; Rodríguez-García, G.; Cerda-García-Rojas, C. M.; Joseph-Nathan, P.; del Río, R. E. *J. Nat. Prod.* **2016**, *79*, 2570−2579.
(40) Arreaga-González, H. M.; Pardo-Novoa, J. C.; del Río, R. E.; Rodríguez-García, G.; Torres-Valencia, J. M.; Manríquez-Torres, J. J.; Cerda-García-Rojas, C. M.; Joseph-Nathan, P.; Gómez-Hurtado, M. A. *J. Nat. Prod.* **2018**, *81*, 63−71.
(41) Rehman, N. U.; Hussain, H.; Al-Shidhani, S.; Avula, S. K.; Abbas, G.; Anwar, M. U.; Górecki, M.; Pescitelli, G.; Al-Harrasi, A. *RSC Adv.* **2017**, *7*, 42357−42362.
(42) Mizutani, S.; Komori, K.; Taniguchi, T.; Monde, K.; Kuramochi, K.; Tsubaki, K. *Angew. Chem., Int. Ed.* **2016**, *55*, 9553−9556.
(43) Ye, Y.; Minami, A.; Mandi, A.; Liu, C.; Taniguchi, T.; Kuzuyama, T.; Monde, K.; Gomi, K.; Oikawa, H. *J. Am. Chem. Soc.* **2015**, *137*, 11846−11853.
(44) Polavarapu, P. L.; Jeirath, N.; Kurtan, T.; Pescitelli, G.; Krohn, K. *Chirality* **2009**, *21*, E202−E207.
(45) Debie, E.; De Gussem, E.; Dukor, R. K.; Herrebout, W.; Nafie, L. A.; Bultinck, P. *ChemPhysChem* **2011**, *12*, 1542−1549.
(46) *Compare VOA*; BioTools, Inc.: Jupiter, FL, USA.
(47) Bruhn, T.; Schaumlöffel, A.; Hemberger, Y.; Bringmann, G. *Chirality* **2013**, *25*, 243−249.
(48) Covington, C. L.; Polavarapu, P. L. CDSpecTech: Computer programs for calculating similarity measures of comparison between experimental and calculated dissymmetry factors and circular intensity differentials. https://sites.google.com/site/cdspectech1/, version 22.0, 2017.
(49) Covington, C. L.; Polavarapu, P. L. *Chirality* **2017**, *29*, 178−192.
(50) Covington, C. L.; Junior, F. M. S.; Silva, J. H. S.; Kuster, R. M.; de Amorim, M. B.; Polavarapu, P. L. *J. Nat. Prod.* **2016**, *79*, 2530−2537.
(51) Kasamatsu, K.; Yoshimura, T.; Mándi, A.; Taniguchi, T.; Monde, K.; Furuta, T.; Kawabata, T. *Org. Lett.* **2017**, *19*, 352−355.
(52) da Silva, J. V.; Fill, T. P.; da Silva, B. F.; Rodrigues-Fo, E. *Nat. Prod. Res.* **2013**, *27*, 9−16.
(53) Birkinshaw, J. H.; Raistrick, H. *Biochem. J.* **1936**, *30*, 2194−2200.
(54) Boll, P. M.; Sørensen, E.; Balieu, E. *Acta Chem. Scand.* **1968**, *22*, 3251−3255.
(55) Jacobsen, J. P.; Reffstrup, T.; Cox, R. E.; Holker, J. S. E.; Boll, P. M. *Tetrahedron Lett.* **1978**, *19*, 1081−1084.
(56) Indriani, I. D. *Biodiversity of marine-derived fungi and identification of their metabolites*. Ph.D. Dissertation, Heinrich-Heine-Universität, Düsseldorf, 2007.
(57) Zhang, C.-L.; Zheng, B.-Q.; Lao, J.-P.; Mao, L.-J.; Chen, S.-Y.; Kubicek, C. P.; Lin, F.-C. *Appl. Microbiol. Biotechnol.* **2008**, *78*, 833−840.
(58) Wu, G.; Ma, H.; Zhu, T.; Li, J.; Gu, Q.; Li, D. *Tetrahedron* **2012**, *68*, 9745−9749.
(59) Fremlin, L. J.; Piggott, A. M.; Lacey, E.; Capon, R. J. *J. Nat. Prod.* **2009**, *72*, 666−670.
(60) Ishikawa, N.; Tanaka, H.; Koyama, F.; Noguchi, H.; Wang, C. C.; Hotta, K.; Watanabe, K. *Angew. Chem., Int. Ed.* **2014**, *53*, 12880−12884.
(61) Aragón, D. T.; López, G. V.; García-Tellado, F.; Marrero-Tellado, J. J.; de Armas, P.; Terrero, D. *J. Org. Chem.* **2003**, *68*, 3363−3365.
(62) Zhang, Z.-Z.; Zhang, N.-T.; Hu, L.-M.; Wei, Z.-Q.; Zeng, C.-C.; Zhong, R.-G.; She, Y.-B. *RSC Adv.* **2011**, *1*, 1383−1388.
(63) Kjer, J.; Debbab, A.; Aly, A. H.; Proksch, P. *Nat. Protoc.* **2010**, *5*, 479−90.
(64) CLSI. Methods for Dilution Antimicrobial Susceptibility Tests for Bacteria That Grow Aerobically. *CLSI Document M07-A10, Approved Standard* (10th ed.); Clinical and Laboratory Standards Institute: Wayne, PA, USA, 2015.
(65) Ashour, M.; Edrada, R.; Ebel, R.; Wray, V.; Wätjen, W.; Padmakumar, K.; Müller, W. E. G.; Lin, W. H.; Proksch, P. *J. Nat. Prod.* **2006**, *69*, 1547−1553.
(66) *MacroModel*; Schrödinger, LLC, 2015, https://www.schrodinger.com/MacroModel.
(67) Grimme, S. *J. Comput. Chem.* **2006**, *27*, 1787−1799.
(68) Sun, P.; Xu, D.-X.; Mándi, A.; Kurtán, T.; Li, T.-J.; Schulz, B.; Zhang, W. *J. Org. Chem.* **2013**, *78*, 7030−7047.
(69) Yanai, T.; Tew, D. P.; Handy, N. C. *Chem. Phys. Lett.* **2004**, *393*, 51−57.
(70) Frisch, M. J.; Trucks, G. W.; Schlegel, H. B.; Scuseria, G. E.; Robb, M. A.; Cheeseman, J. R.; Scalmani, G.; Barone, V.; Mennucci, B.; Petersson, G. A.; Nakatsuji, H.; Caricato, M.; Li, X.; Hratchian, H. P.; Izmaylov, A. F.; Bloino, J.; Zheng, G.; Sonnenberg, J. L.; Hada, M.; Ehara, M.; Toyota, K.; Fukuda, R.; Hasegawa, J.; Ishida, M.; Nakajima, T.; Honda, Y.; Kitao, O.; Nakai, H.; Vreven, T.; Montgomery, J. A., Jr.; Peralta, J. E.; Ogliaro, F.; Bearpark, M.; Heyd, J. J.; Brothers, E.; Kudin, K. N.; Staroverov, V. N.; Kobayashi, R.; Normand, J.; Raghavachari, K.; Rendell, A.; Burant, J. C.; Iyengar, S. S.; Tomasi, J.; Cossi, M.; Rega, N.; Millam, J. M.; Klene, M.; Knox, J. E.; Cross, J. B.; Bakken, V.; Adamo, C.; Jaramillo, J.; Gomperts, R.; Stratmann, R. E.; Yazyev, O.; Austin, A. J.; Cammi, R.; Pomelli, C.; Ochterski, J. W.; Martin, R. L.; Morokuma, K.; Zakrzewski, V. G.; Voth, G. A.; Salvador, P.; Dannenberg, J. J.; Dapprich, S.; Daniels, A. D.; Farkas, Ö.; Foresman, J. B.; Ortiz, J. V.; Cioslowski, J.; Fox, D. J. *Gaussian 09*, Revision B.01; Gaussian, Inc.: Wallingford, CT, 2010.
(71) Stephens, P. J.; Harada, N. *Chirality* **2009**, *22*, 229−33.
(72) Mándi, A.; Swamy, M. M. M.; Taniguchi, T.; Anetai, M.; Monde, K. *Chirality* **2016**, *28*, 453−459.
(73) Varetto, U. *MOLEKEL*; Swiss National Supercomputing Centre: Manno, Switzerland, 2009.

DOI: 10.1021/acs.jnatprod.9b00125
J. Nat. Prod. 2019, 82, 2460−2469

2.2 Supporting Information

(Excluding the tables of Cartesian coordinates. Full version is available online under https://pubs.acs.org/doi/abs/10.1021/acs.jnatprod.9b00125).

Polyketides and a Dihydroquinolone Alkaloid from a Marine-Derived Strain of the Fungus *Metarhizium marquandii*

Dina H. El-Kashef,[†,‡] Georgios Daletos,[†] Malte Plenker,[§] Rudolf Hartmann,[§] Attila Mándi,[⊥] Tibor Kurtán,[⊥] Horst Weber,[∥] Wenhan Lin,[▽] Elena Ancheeva,[*,†] and Peter Proksch[*,†]

[†]Institut für Pharmazeutische Biologie und Biotechnologie, Heinrich-Heine-Universität Düsseldorf, Universitätsstrasse 1, 40225 Düsseldorf, Germany

[‡]Department of Pharmacognosy, Faculty of Pharmacy, Minia University, 61519 Minia, Egypt

[§]Institute of Complex Systems: Strukturbiochemie, Forschungszentrum Jülich GmbH, ICS-6, 52425 Jülich, Germany

[⊥]Department of Organic Chemistry, University of Debrecen, P.O.B. 400, 4002 Debrecen, Hungary

[∥]Institut für Pharmazeutische und Medizinische Chemie, Heinrich-Heine-Universität Düsseldorf, Universitätsstrasse 1, 40225 Düsseldorf, Germany

[▽]State Key Laboratory of Natural and Biomimetic Drugs, Peking University, Beijing 100191, China

Corresponding Authors

*E-mail: elena.ancheeva@uni-duesseldorf.de

*E-mail: proksch@uni-duesseldorf.de

Table of Content*

* The ^{1}H and ^{13}C NMR spectra for this study were recorded at 600 MHz and 150 MHz, respectively.

4

Figure S1. HPLC chromatogram (A), UV (B) and HRESIMS spectrum (C) of compound **1**.

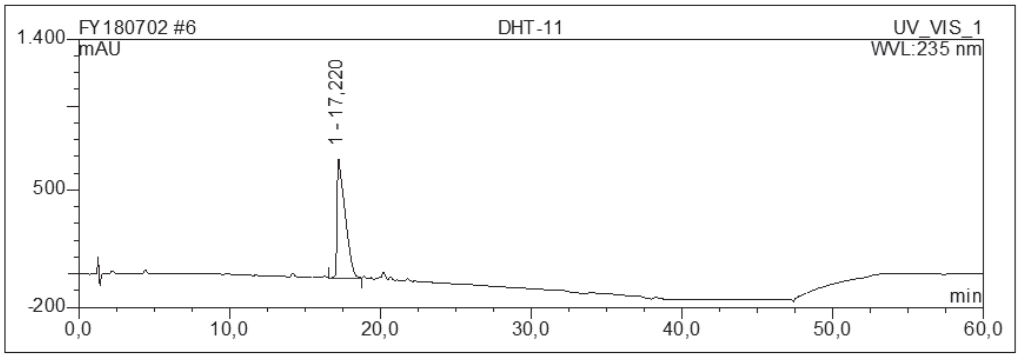

A)

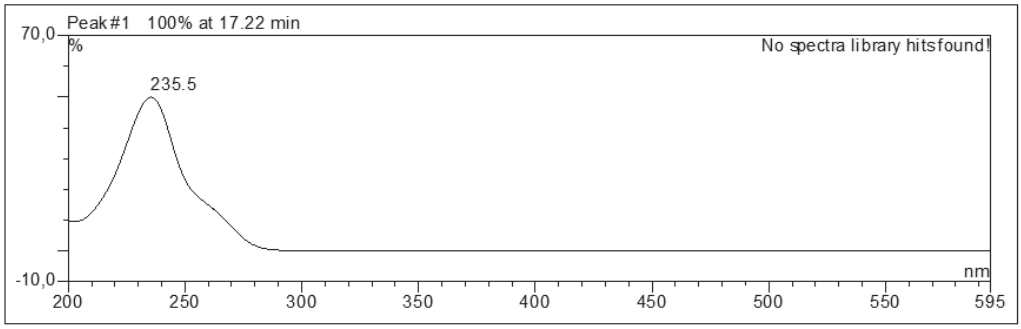

B)

C)

Mass Spectrum SmartFormula Report

Analysis Info

Analysis Name	D:\Data\spektren 2017\PRO17HR000014.d	Acquisition Date	8/28/2017 10:27:48 AM
Method	tune_low_new.m	Operator	Peter Tommes
Sample Name	D. Hassouna Mm-8-2-P5 (CH3OH)	Instrument	maXis 288882.20213
Comment	10 ul in 1 ml		

Acquisition Parameter

Source Type	ESI	Ion Polarity	Positive	Set Nebulizer	0.3 Bar
Focus	Not active	Set Capillary	4000 V	Set Dry Heater	180 °C
Scan Begin	50 m/z	Set End Plate Offset	-500 V	Set Dry Gas	4.0 l/min
Scan End	1500 m/z	Set Collision Cell RF	600.0 Vpp	Set Divert Valve	Source

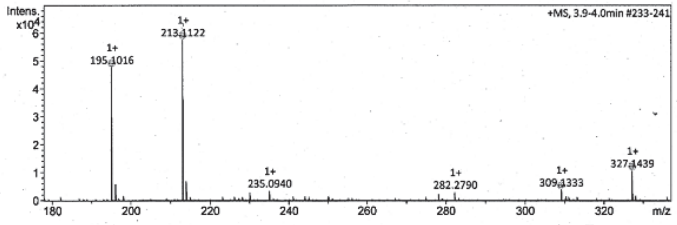

Meas. m/z	#	Ion Formula	m/z	err [ppm]	mSigma	# mSigma	Score	rdb	e⁻ Conf	N-Rule
195.1016	1	C11H15O3	195.1016	-0.3	3.3	1	100.00	4.5	even	ok
213.1122	1	C11H17O4	213.1121	-0.1	0.9	1	100.00	3.5	even	ok
309.1333	1	C16H21O6	309.1333	0.0	15.5	1	100.00	6.5	even	ok
327.1439	1	C16H23O7	327.1438	-0.1	4.1	1	100.00	5.5	even	ok

Figure S2. ^{1}H NMR spectrum of compound **1** in DMSO-d_6

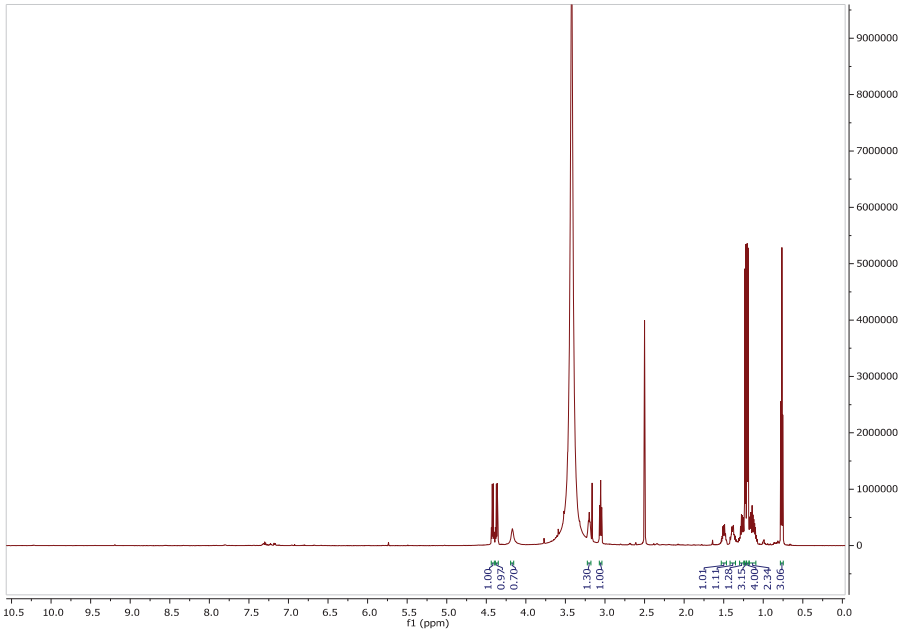

Figure S3. ^{13}C NMR spectrum of compound **1** in DMSO-d_6

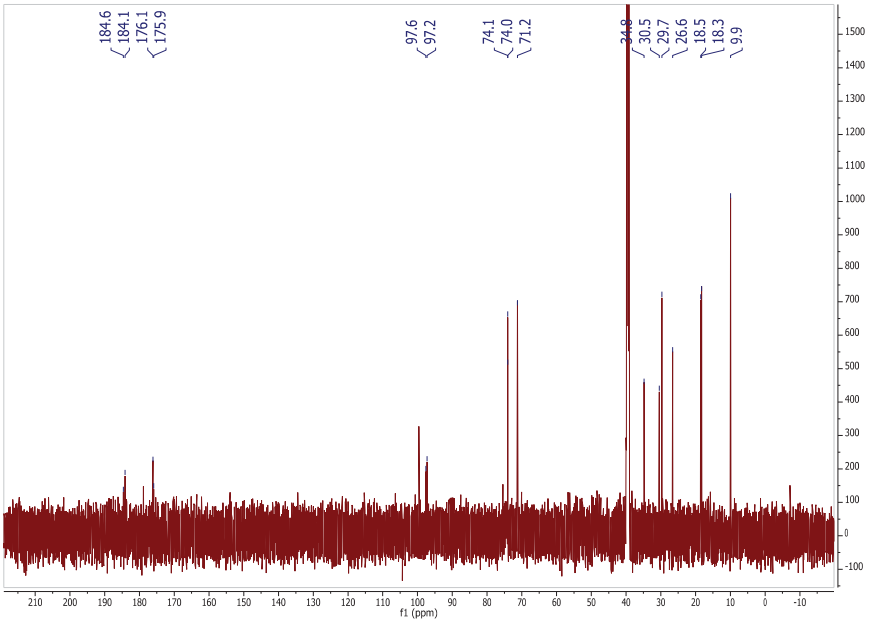

6

Figure S4. COSY spectrum of compound **1** in DMSO-d_6

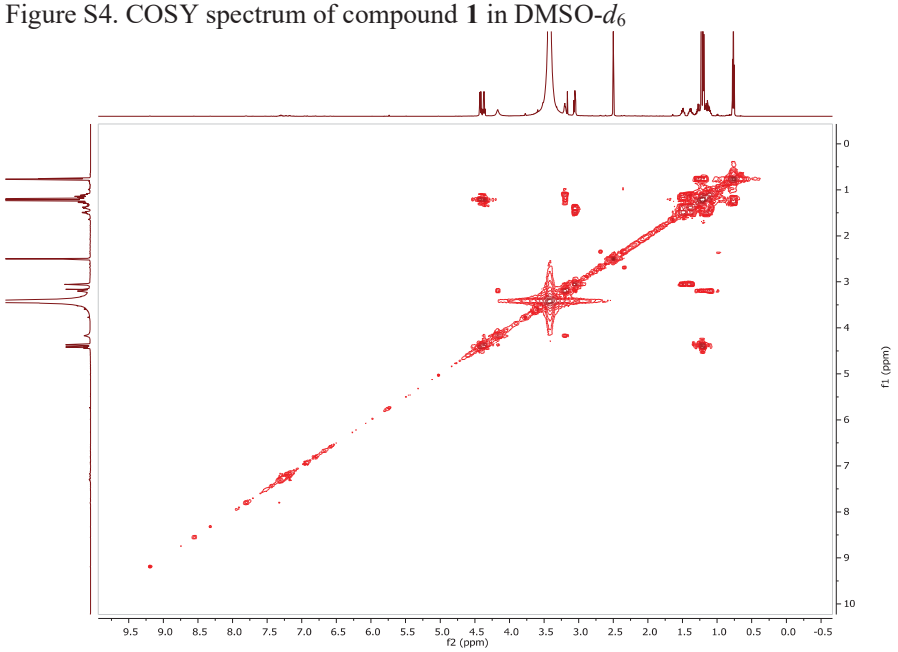

Figure S5. HSQC spectrum of compound **1** in DMSO-d_6

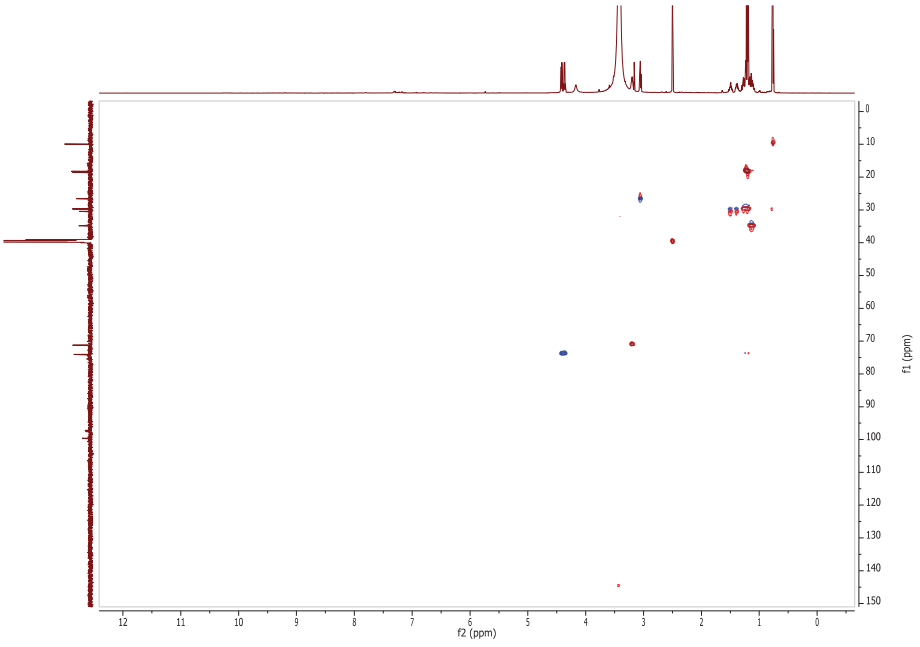

Figure S6. HMBC spectrum of compound **1** in DMSO-d_6

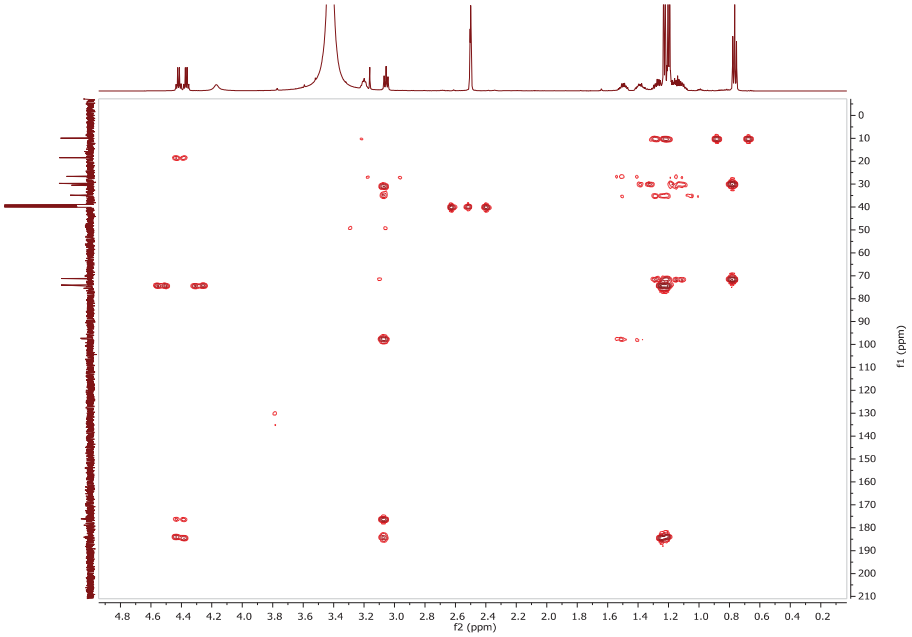

Figure S7. Comparison of ^{1}H NMR spectra of (*S*)-MPA and (*R*)-MPA esters of compound **1**

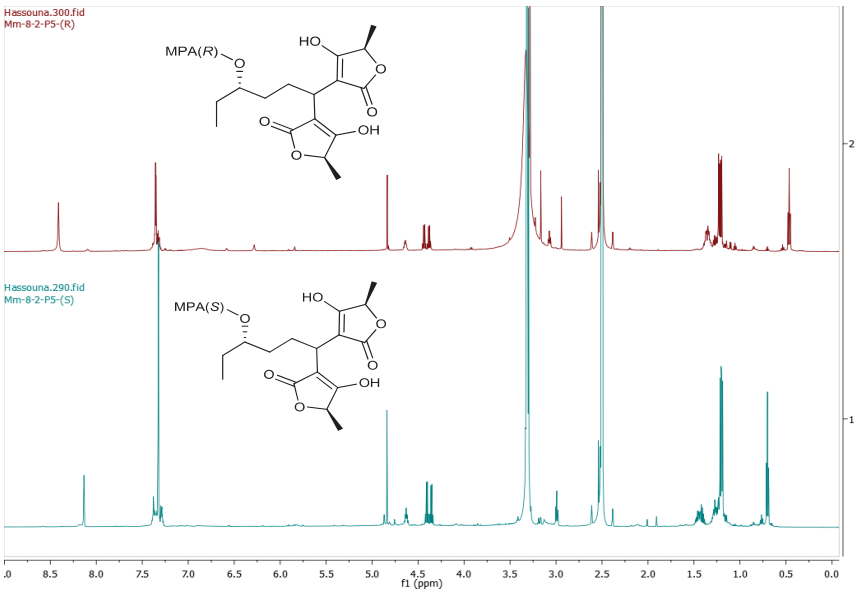

8

Figure S8. HPLC chromatogram (A), UV (B) and HRESIMS spectrum (C) of compound **2**

A)

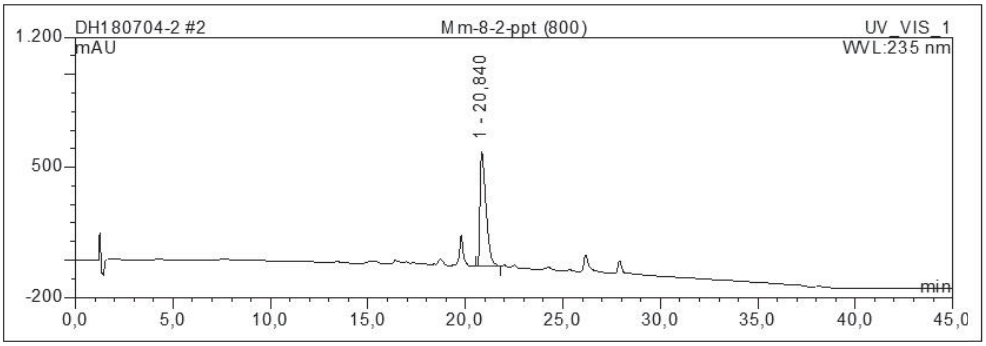

B)

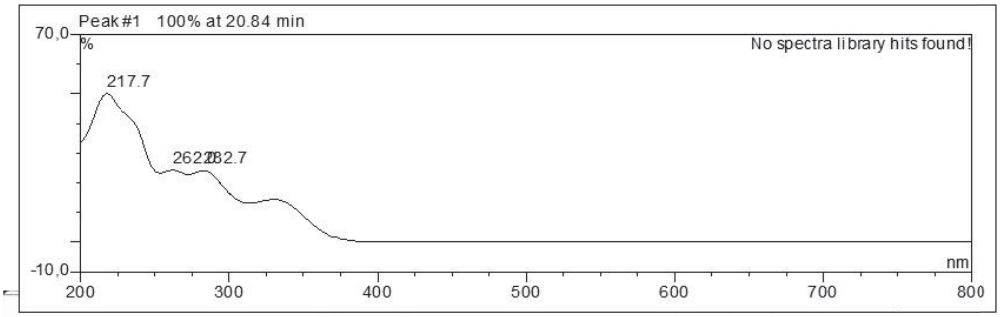

C)

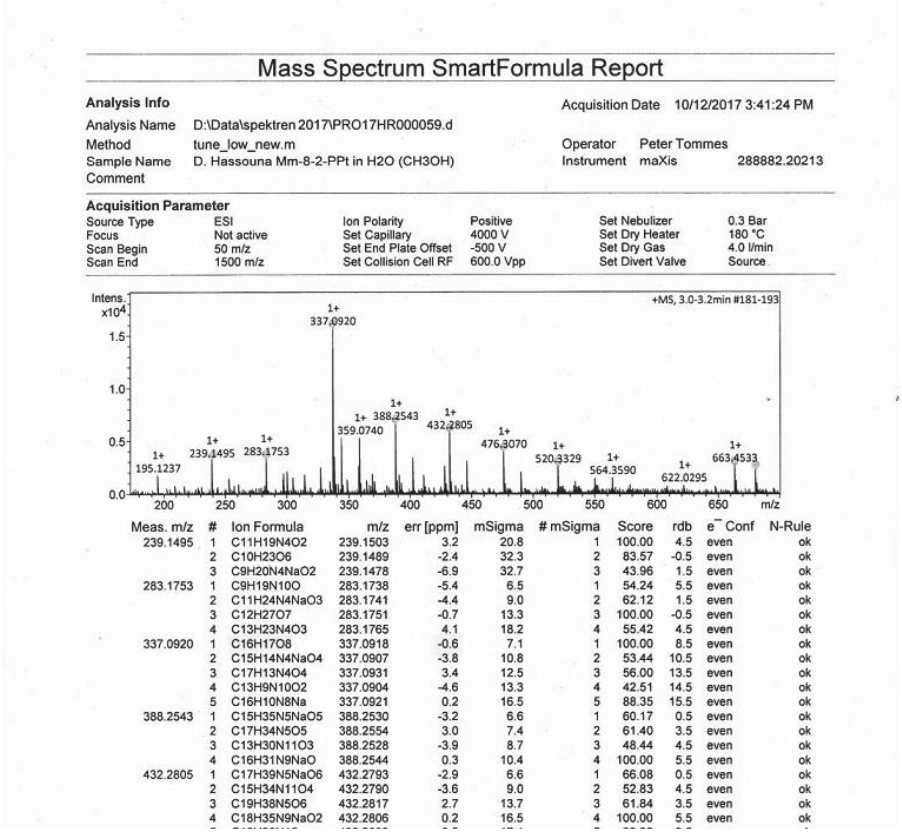

Mass Spectrum SmartFormula Report

Analysis Info

Analysis Name	D:\Data\spektren 2017\PRO17HR000059.d	Acquisition Date	10/12/2017 3:41:24 PM
Method	tune_low_new.m	Operator	Peter Tommes
Sample Name	D. Hassouna Mm-8-2-PPt in H2O (CH3OH)	Instrument	maXis 288882.20213
Comment			

Acquisition Parameter

Source Type	ESI	Ion Polarity	Positive	Set Nebulizer	0.3 Bar
Focus	Not active	Set Capillary	4000 V	Set Dry Heater	180 °C
Scan Begin	50 m/z	Set End Plate Offset	-500 V	Set Dry Gas	4.0 l/min
Scan End	1500 m/z	Set Collision Cell RF	600.0 Vpp	Set Divert Valve	Source

Meas. m/z	#	Ion Formula	m/z	err [ppm]	mSigma	# mSigma	Score	rdb	e⁻ Conf	N-Rule
239.1495	1	C11H19N4O2	239.1503	3.2	20.8	1	100.00	4.5	even	ok
	2	C10H23O6	239.1489	-2.4	32.3	2	83.57	-0.5	even	ok
	3	C9H20N4NaO2	239.1478	-6.9	32.7	3	43.96	1.5	even	ok
283.1753	1	C9H19N10O	283.1738	-5.4	6.5	1	54.24	5.5	even	ok
	2	C11H24N4NaO3	283.1741	-4.4	9.0	2	62.12	1.5	even	ok
	3	C12H27O7	283.1751	-0.7	13.3	3	100.00	-0.5	even	ok
	4	C13H23N4O3	283.1765	4.1	18.2	4	55.42	4.5	even	ok
337.0920	1	C16H17O8	337.0918	-0.6	7.1	1	100.00	8.5	even	ok
	2	C15H14N4NaO4	337.0907	-3.8	10.8	2	53.44	10.5	even	ok
	3	C17H13N4O4	337.0931	3.4	12.5	3	56.00	13.5	even	ok
	4	C13H9N10O2	337.0904	-4.6	13.3	4	42.51	14.5	even	ok
	5	C16H10N8Na	337.0921	0.2	16.5	5	88.35	15.5	even	ok
388.2543	1	C15H35N5NaO5	388.2530	-3.2	6.6	1	60.17	0.5	even	ok
	2	C17H34N5O5	388.2554	3.0	7.4	2	61.40	3.5	even	ok
	3	C13H30N11O3	388.2528	-3.9	8.7	3	48.44	4.5	even	ok
	4	C16H31N9NaO	388.2544	0.3	10.4	4	100.00	5.5	even	ok
432.2805	1	C17H39N5NaO6	432.2793	-2.9	6.6	1	66.08	0.5	even	ok
	2	C15H34N11O4	432.2790	-3.6	9.0	2	52.83	4.5	even	ok
	3	C19H38N5O6	432.2817	2.7	13.7	3	61.84	3.5	even	ok
	4	C18H35N9NaO2	432.2806	0.2	16.5	4	100.00	5.5	even	ok

Figure S9. ^{1}H NMR spectrum of compound **2** in DMSO-d_6

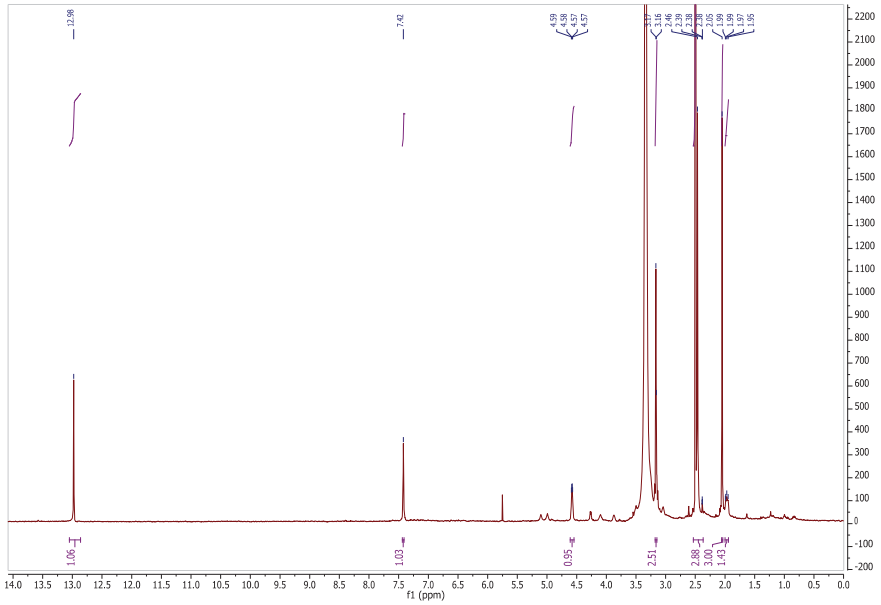

Figure S10. COSY spectrum of compound **2** in DMSO-d_6

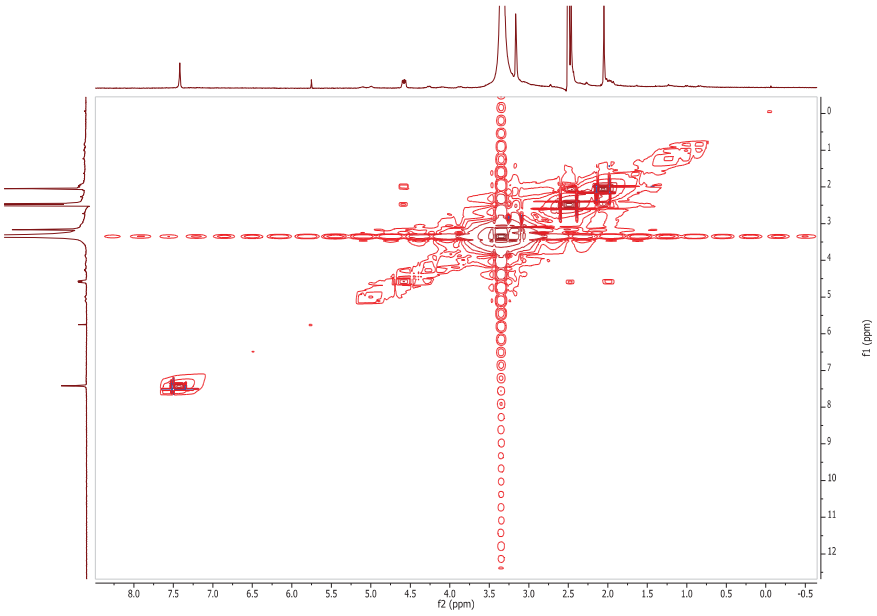

10

Figure S11. HSQC spectrum of compound **2** in DMSO-d_6

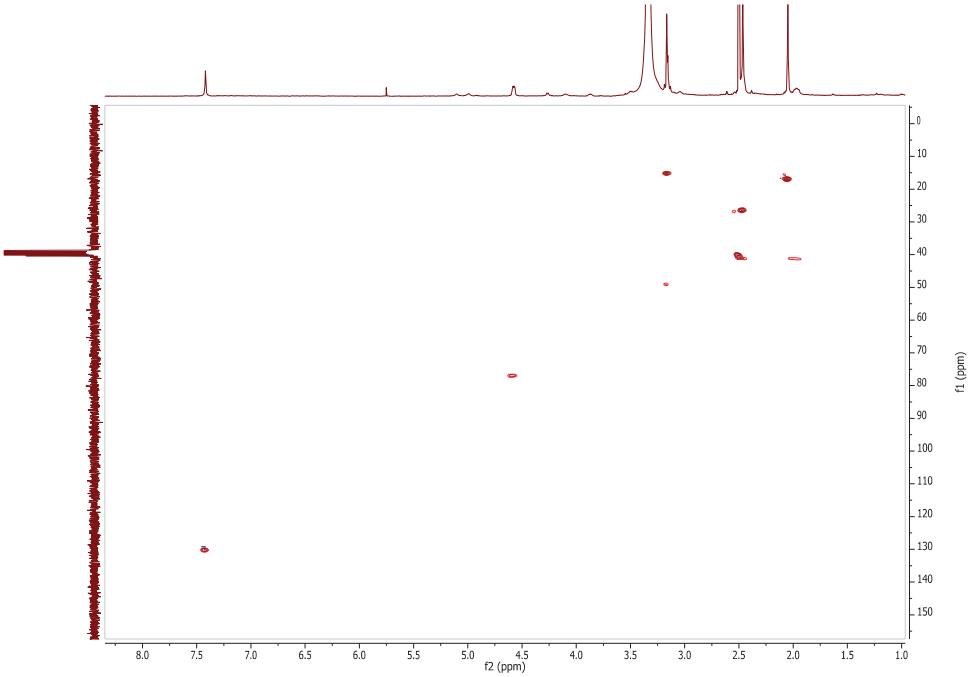

Figure S12. HMBC spectrum of compound **2** in DMSO-d_6

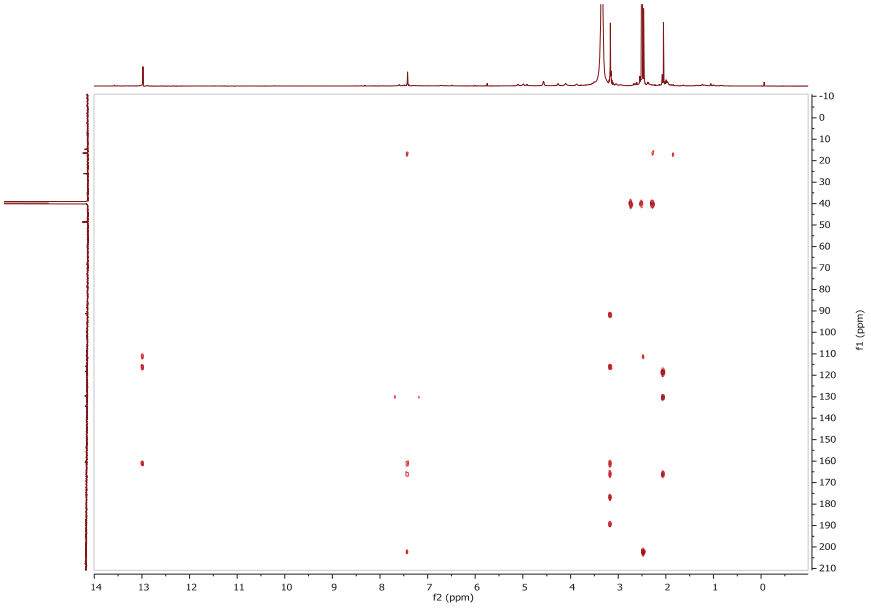

11

Figure S13. HMBC spectrum of compound **2** in D_2O

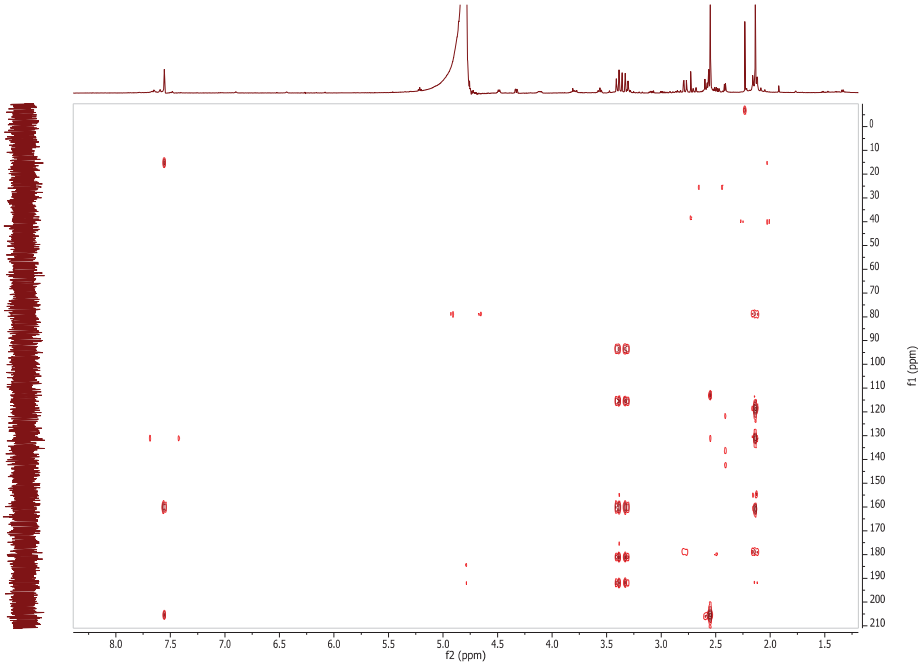

Figure S14. HPLC chromatogram (A), UV (B) and HRESIMS spectrum (C) of compound **3**

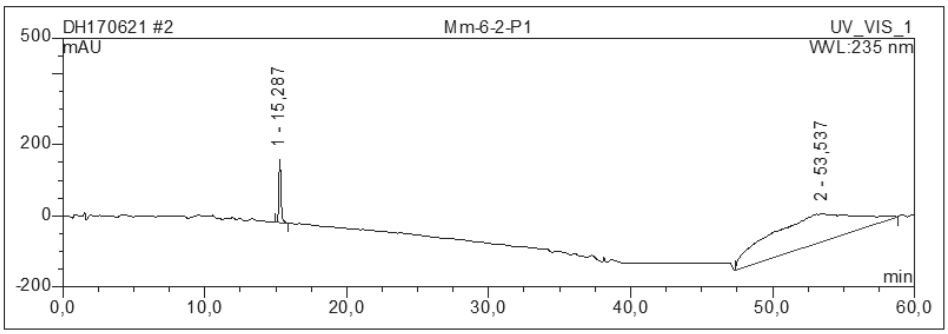

A)

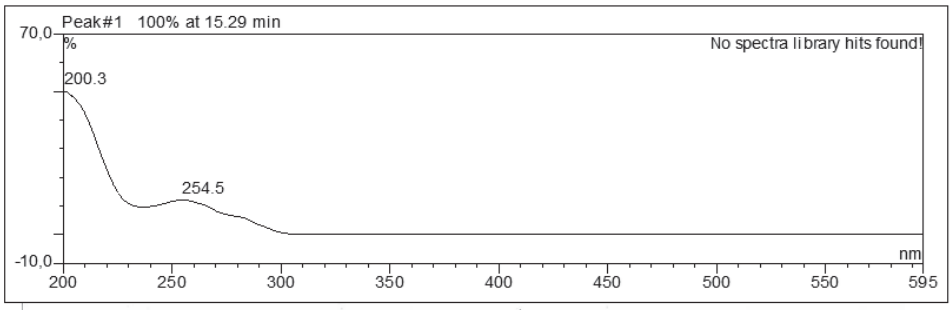

B)

C)

Mass Spectrum SmartFormula Report

Analysis Info

Analysis Name	D:\Data\spektren 2017\Proksch17HR000291.d	Acquisition Date	6/30/2017 12:49:46 PM
Method	tune_low_new.m	Operator	Peter Tommes
Sample Name	D. Hassouna Mm-6-2-P1 (CH3OH)	Instrument	maXis 288882.20213
Comment	5 ul in 1 ml		

Acquisition Parameter

Source Type	ESI	Ion Polarity	Positive	Set Nebulizer	0.3 Bar
Focus	Not active	Set Capillary	4000 V	Set Dry Heater	180 °C
Scan Begin	50 m/z	Set End Plate Offset	-500 V	Set Dry Gas	4.0 l/min
Scan End	1500 m/z	Set Collision Cell RF	600.0 Vpp	Set Divert Valve	Source

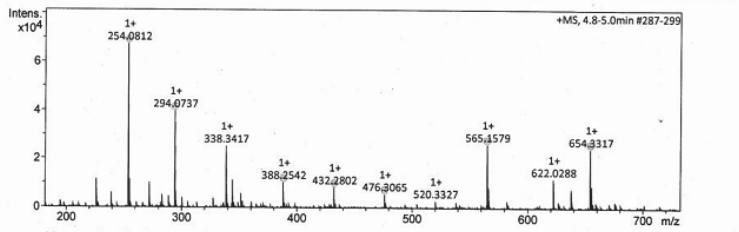

Meas. m/z	#	Ion Formula	m/z	err [ppm]	mSigma	# mSigma	Score	rdb	e⁻ Conf	N-Rule
254.0812	1	C15H12NO3	254.0812	-0.2	3.8	1	100.00	10.5	even	ok
294.0737	1	C15H13NNaO4	294.0737	-0.2	1.3	1	100.00	9.5	even	ok
	2	C13H8N7O2	294.0734	-1.1	1.6	2	88.24	13.5	even	ok
388.2542	1	C16H31N9NaO	388.2544	0.6	16.6	1	100.00	5.5	even	ok
432.2802	1	C18H35N9NaO2	432.2806	1.0	20.5	1	90.38	5.5	even	ok
	2	C16H30N15	432.2803	0.3	21.6	2	100.00	9.5	even	ok
476.3065	1	C19H43N5NaO7	476.3055	-2.1	13.7	1	85.70	0.5	even	ok
	2	C20H39N9NaO3	476.3068	0.7	27.2	2	88.71	5.5	even	ok
	3	C18H34N15O	476.3065	0.2	27.2	3	100.00	9.5	even	ok
	4	C33H38N3	476.3060	-0.9	82.4	4	19.31	16.5	even	ok
565.1579	1	C30H26N2NaO8	565.1581	0.4	8.3	1	94.66	18.5	even	ok
	2	C28H21N8O6	565.1579	-0.1	8.3	2	100.00	22.5	even	ok
	3	C27H18N12NaO2	565.1568	-2.0	11.1	3	55.49	24.5	even	ok
	4	C44H21O	565.1587	1.3	81.4	4	8.65	34.5	even	ok
654.3317	1	C26H37N19NaO	654.3321	0.6	14.0	1	100.00	17.5	even	ok
	2	C28H49N5NaO11	654.3321	0.6	20.8	2	86.48	6.5	even	ok
	3	C26H44N11O9	654.3318	0.2	22.0	3	95.53	10.5	even	ok
	4	C27H53NNaO15	654.3307	-1.4	32.3	4	51.56	1.5	even	ok
	5	C41H41N7Na	654.3316	-0.1	52.6	5	43.34	24.5	even	ok
	6	C42H44N3O4	654.3326	1.5	52.7	6	27.98	22.5	even	ok

Figure S15.[1]H NMR spectrum of compound **3** in DMSO-*d*6

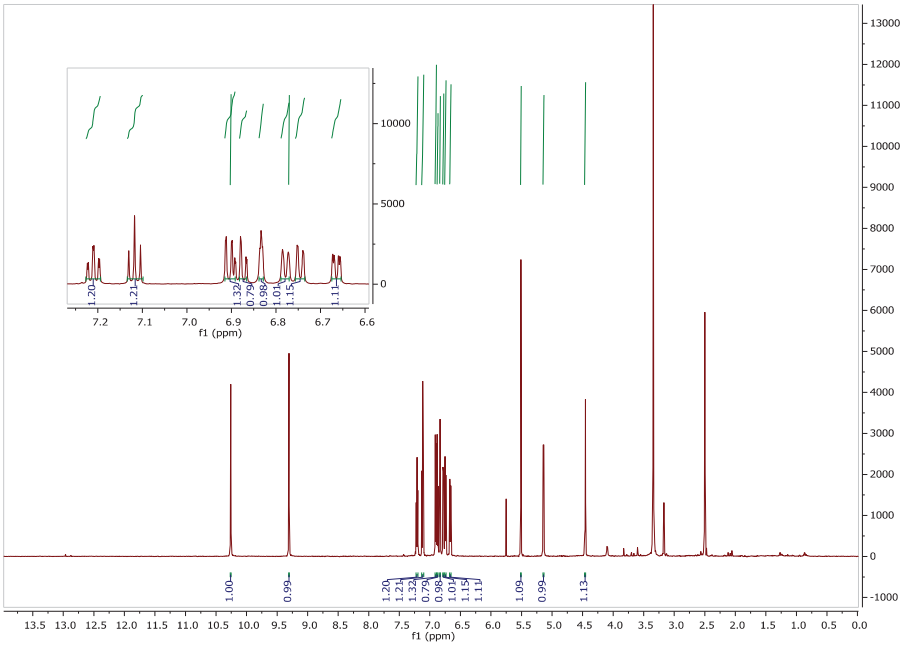

Figure S16.[13]C NMR spectrum of compound **3** in DMSO-*d*6

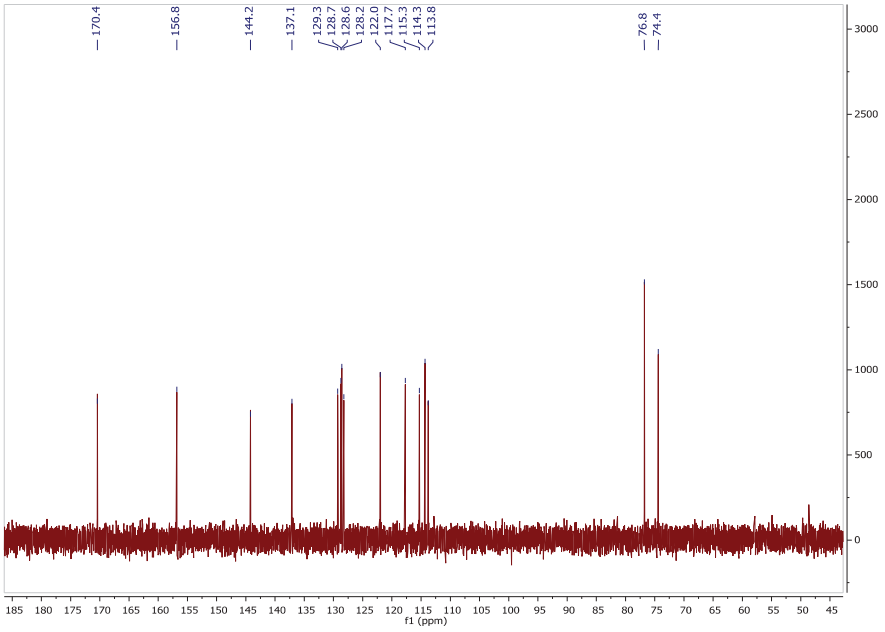

Figure S17. COSY spectrum of compound **3** in DMSO-d_6

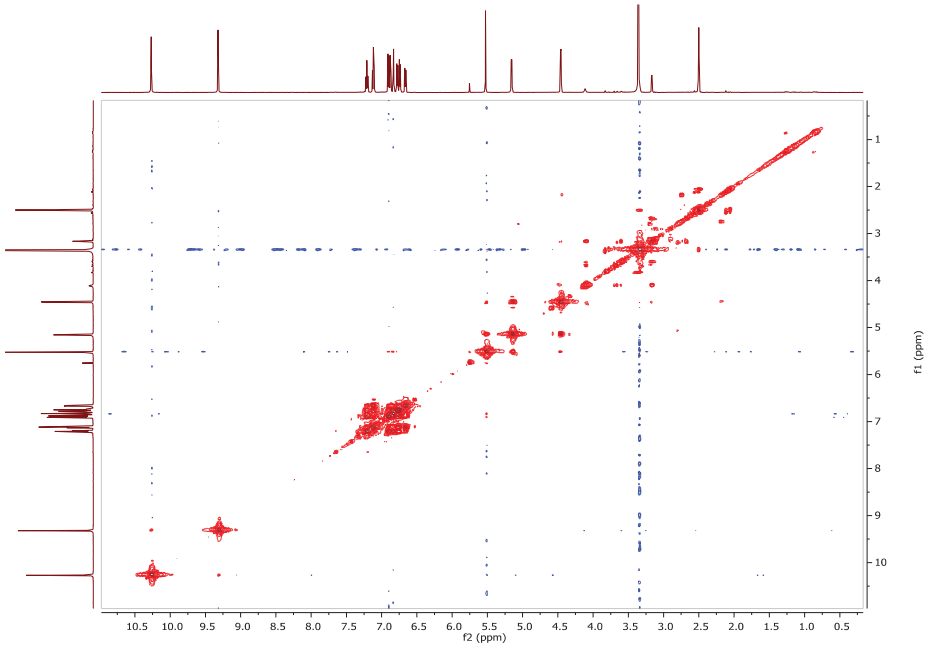

Figure S18. HSQC spectrum of compound **3** in DMSO-d_6

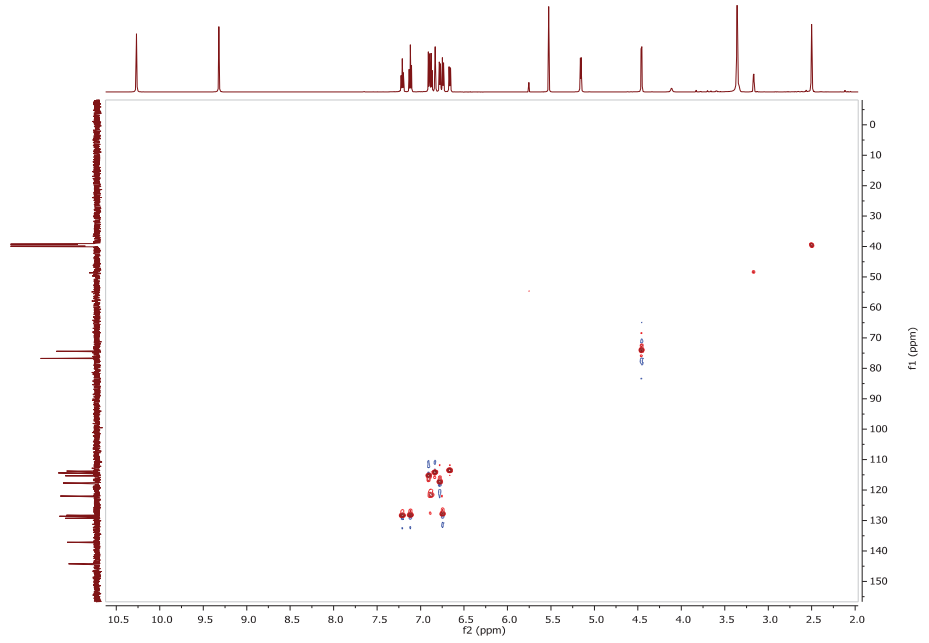

Figure S19. HMBC spectrum of compound **3** in DMSO-d_6

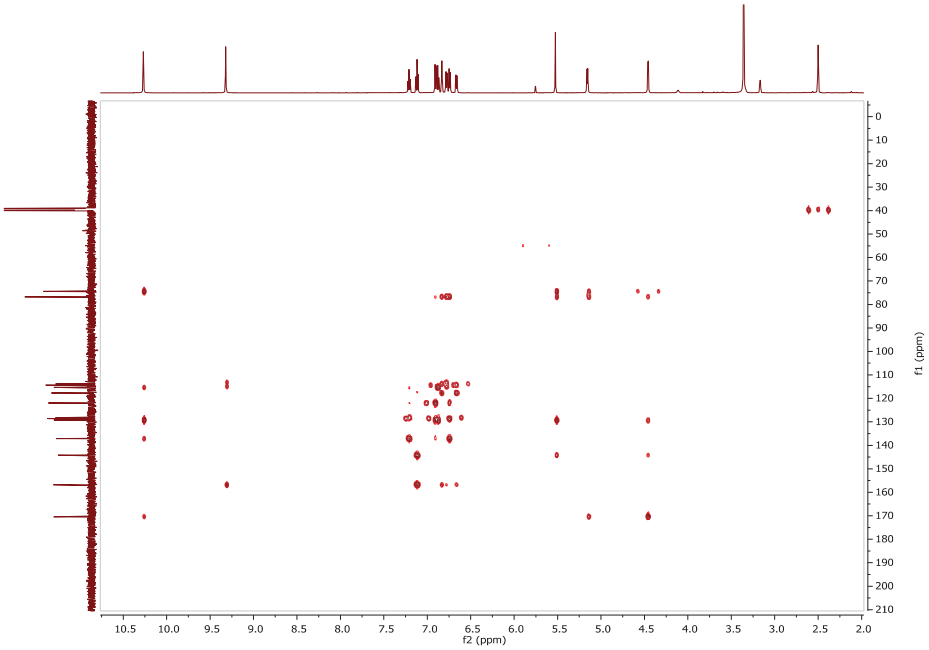

Figure S20. ROESY spectrum of compound **3** in DMSO-d_6

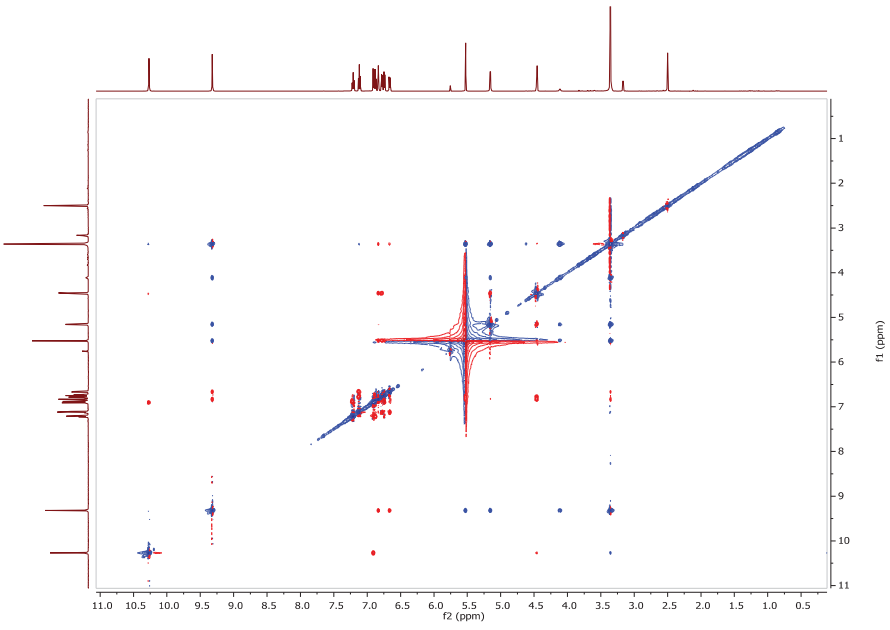

Figure S21. Experimental ECD spectrum of **1** in MeCN compared with the Boltzmann-weighted BH&HLYP/TZVP PCM/MeCN spectra of (5*R*,9*S*,5'*R*)-**1** and (5*S*,9*S*,5'*S*)-**1** computed for the gas-phase B3LYP/6-31+G(d,p) conformers.

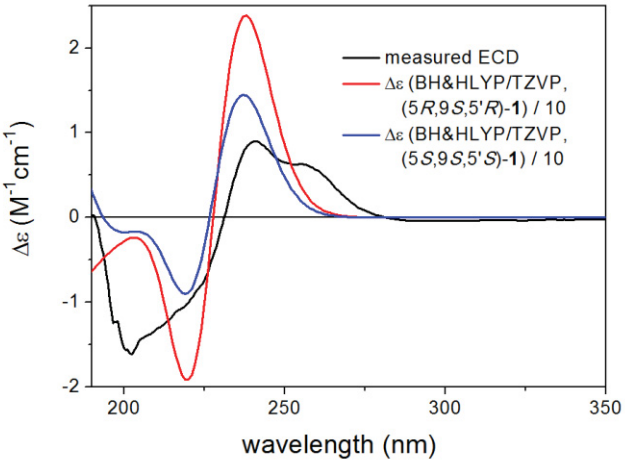

Figure S22. Low-energy conformers (≥ 1%) of (3*S*,4*S*)-**3** obtained at the B97D/TZVP PCM/MeCN level of theory.

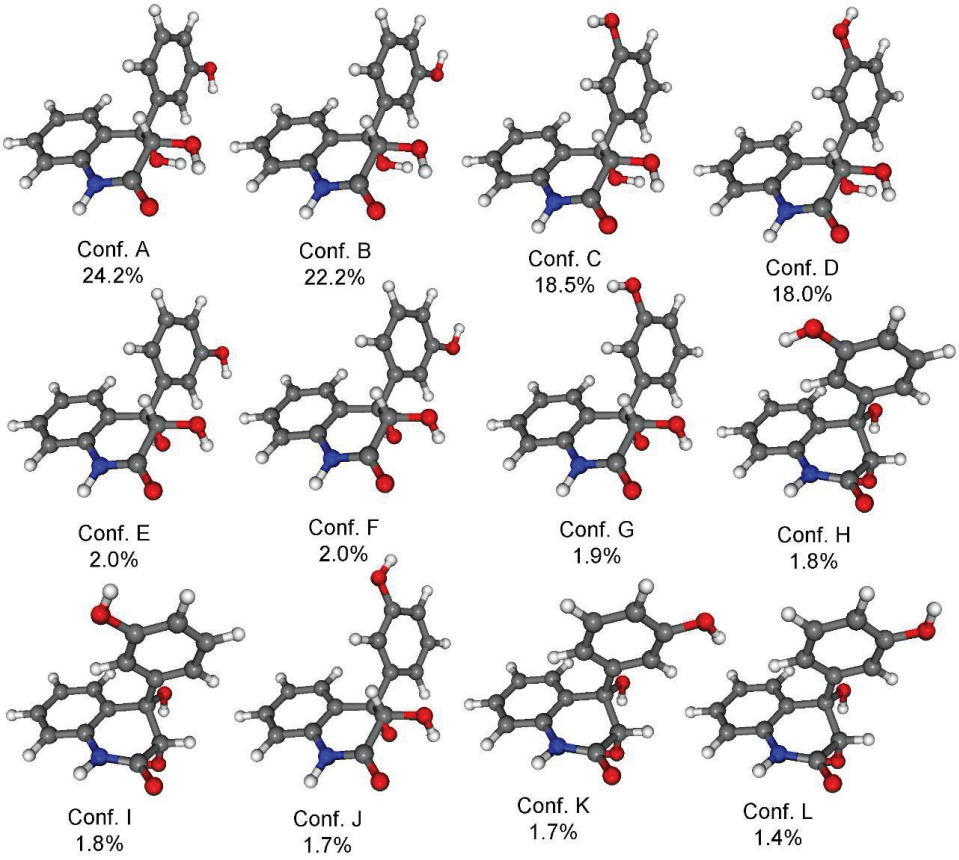

Figure S23. Experimental VCD spectrum (black) of 3 in MeOH-d_4 compared with the B3LYP/TZVP PCM/MeOH spectrum (red) of (3*S*,4*S*)-3 computed for the B3LYP/TZVP PCM/MeOH conformers; generated with Gaussian broadening and a manual scaling factor of 0.98.

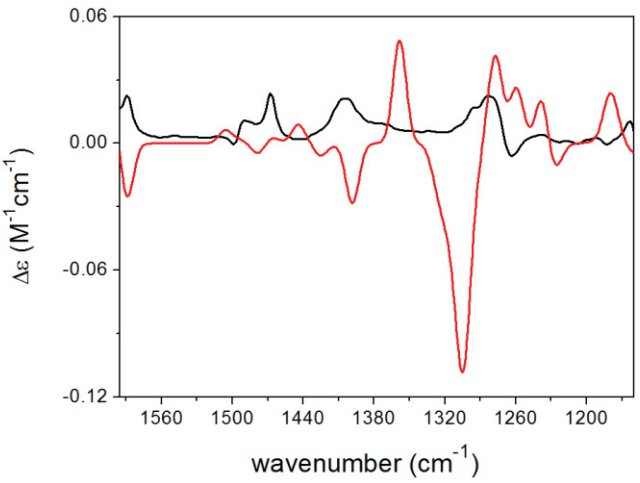

Table S1. Boltzmann populations and optical rotations of the low-energy conformers of (3*S*,4*S*)-**3** computed at various levels for the B97D/TZVP PCM/MeCN optimized MMFF conformers.

Conformer	Boltzmann population	B3LYP/TZVP	BH&HLYP/TZVP	CAM-B3LYP/TZVP	PBE0/TZVP
Conf. A	24.30	-157.50	-122.98	-136.90	-153.78
Conf. B	22.24	-153.00	-119.13	-133.32	-149.56
Conf. C	18.55	-98.02	-79.90	-90.18	-97.52
Conf. D	18.04	-102.64	-83.68	-93.86	-101.81
Conf. E	1.95	-81.88	-85.77	-87.95	-80.27
Conf. F	1.95	-84.79	-87.41	-90.02	-82.80
Conf. G	1.85	-43.13	-58.33	-58.77	-43.81
Conf. H	1.80	8.29	3.55	5.91	7.00
Conf. I	1.76	14.11	7.98	10.40	12.44
Conf. J	1.72	-46.95	-61.59	-61.55	-47.27
Conf. K	1.68	37.50	21.85	28.74	35.50
Conf. L	1.43	27.88	14.29	20.57	26.23
Average	N/A	-115.59	-93.60	-103.97	-113.69

Table S2. Boltzmann populations and optical rotations of the low-energy conformers of (3*S*,4*S*)-**3** computed at various levels for the CAM-B3LYP/TZVP PCM/MeCN optimized MMFF conformers.

Conformer	Boltzmann population	B3LYP/TZVP	BH&HLYP/TZVP	CAM-B3LYP/TZVP	PBE0/TZVP
Conf. A	27.89	-153.03	-118.05	-131.82	-149.17
Conf. B	27.03	-148.93	-114.56	-128.62	-145.34
Conf. C	21.37	-102.69	-81.83	-91.65	-101.12
Conf. D	19.25	-96.52	-76.63	-86.70	-95.33
Conf. E	1.47	-57.04	-60.30	-61.24	-56.96
Conf. F	1.21	-27.49	-39.84	-37.60	-28.98
Conf. G	1.10	-24.21	-37.17	-35.36	-26.13
Average	N/A	-125.75	-98.57	-110.30	-123.16

Table S3. Boltzmann populations and optical rotations of the low-energy conformers of (3*S*,4*S*)-**3** computed at various levels for the CAM-B3LYP/TZVP SMD/MeCN optimized MMFF conformers.

Conformer	Boltzmann population	B3LYP/TZVP	BH&HLYP/TZVP	CAM-B3LYP/TZVP	PBE0/TZVP
Conf. A	21.48	-156.95	-119.74	-134.06	-154.12
Conf. B	21.09	-147.03	-114.03	-127.94	-144.53
Conf. C	18.07	-126.17	-99.89	-111.52	-124.31
Conf. D	17.66	-124.55	-98.14	-110.18	-122.93
Conf. E	4.72	-69.63	-70.20	-72.53	-70.24
Conf. F	4.11	-86.52	-83.91	-88.14	-85.54
Conf. G	3.93	-51.91	-58.52	-59.30	-53.71
Conf. H	3.58	-66.90	-71.20	-73.75	-67.29
Conf. I	3.52	-66.24	-70.88	-73.88	-66.95
Average	N/A	-125.44	-101.12	-112.07	-123.75

Figure S24. HPLC chromatograms of the known compounds isolated from *M. marquandii*

Terrestric acid hydrate (**4**)

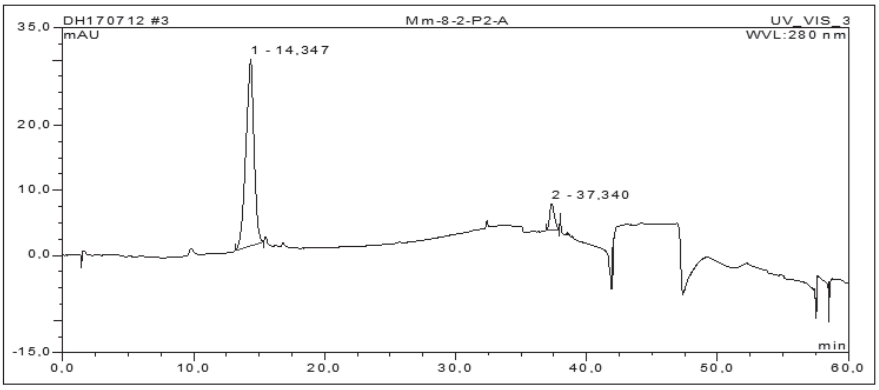

Peniphenone D (**5**)

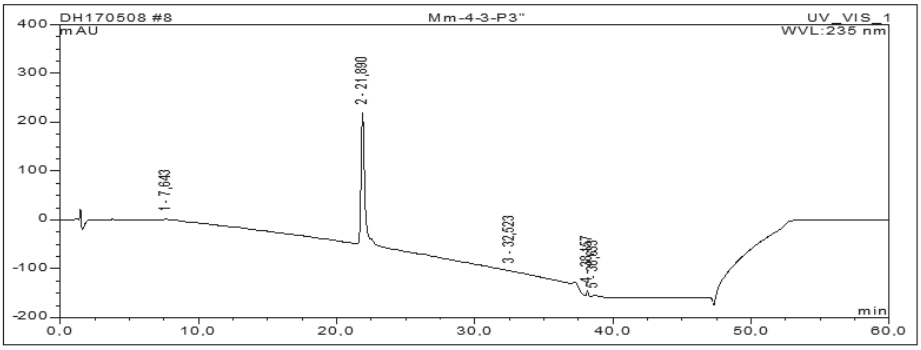

Viridicatin

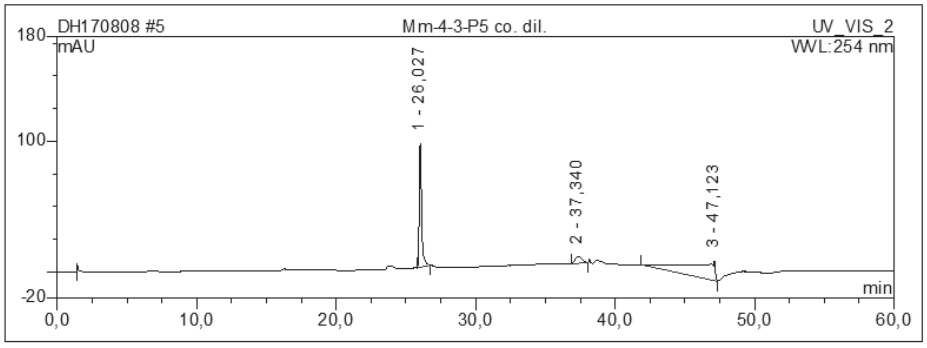

Clavatol

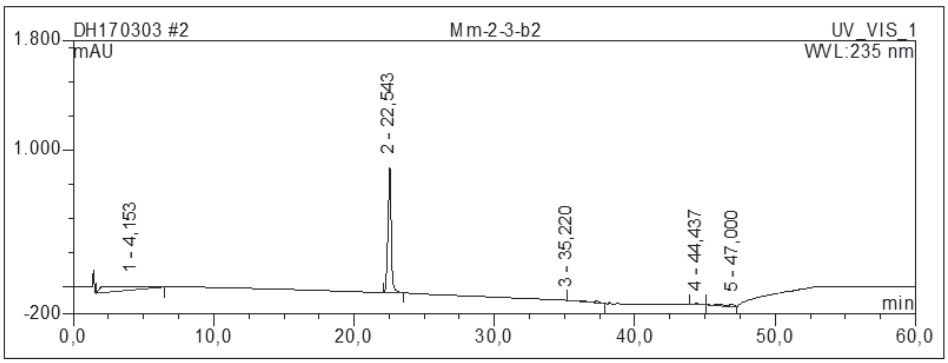

Penilactone A

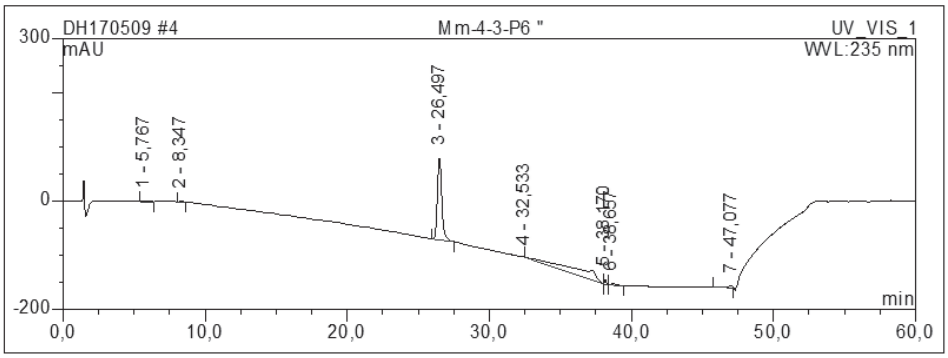

Cyclopenol

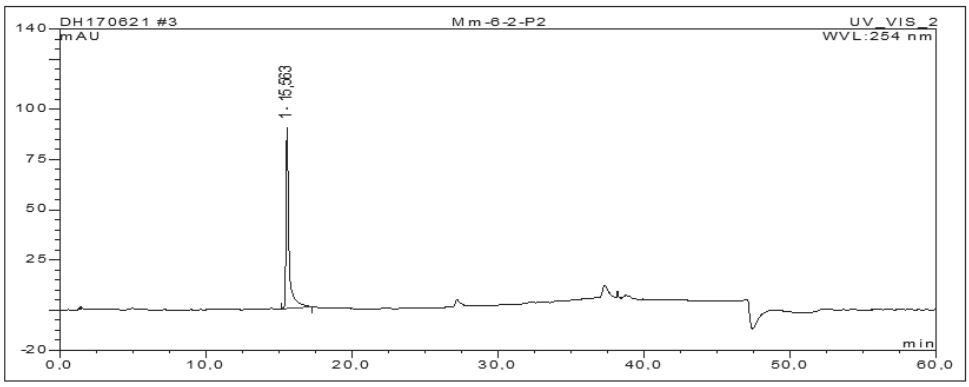

22

Dehydrocyclopeptine

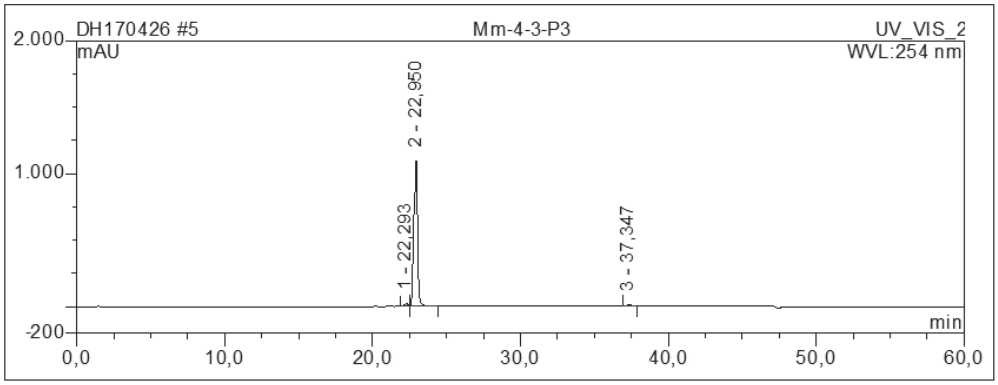

Chaetobutenolide C

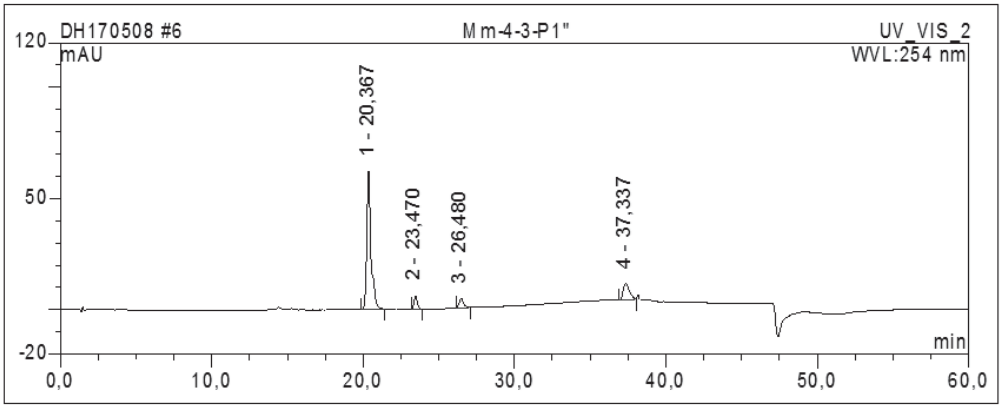

WF-3681

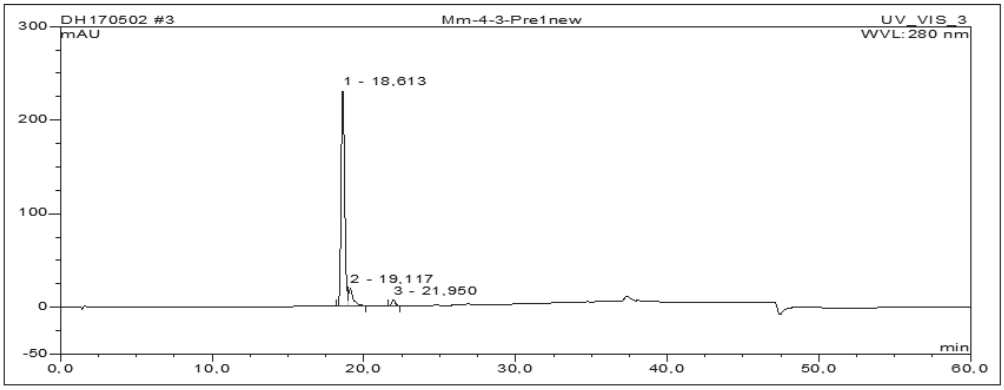

Figure S25. IR spectrum of compound **1**

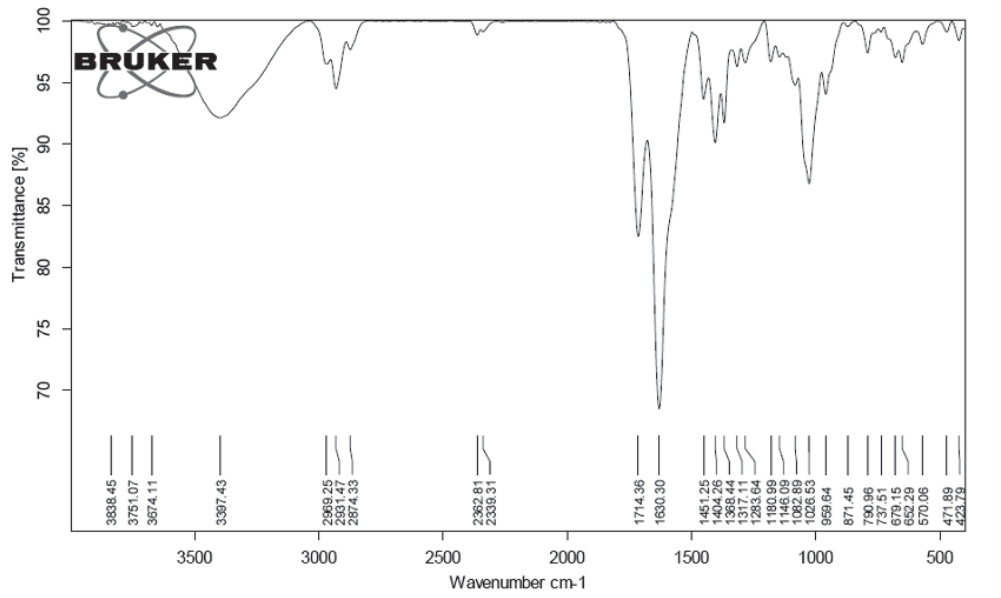

Figure S26. IR spectrum of compound **3**

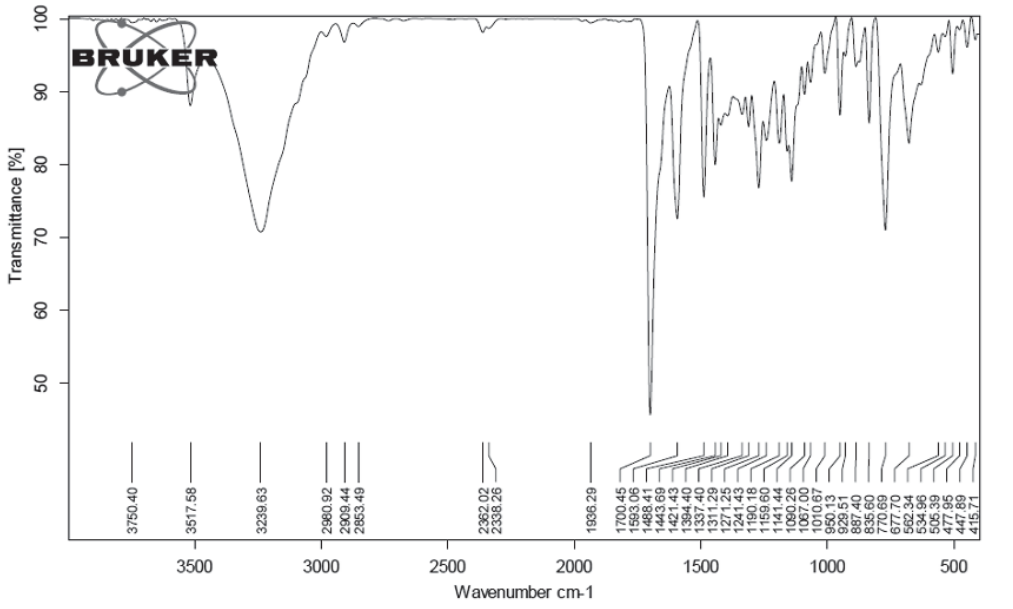

Figure S27. ITS sequence and identification of *Metarhizium marquandii*.

ITS 1 sequencing results

CTCCCAACCNACTGTGACATATACCATTTGTTTATTCGTTGCCTCGGCGGGTTCTACCCCCTGGAGACA
GGGCGGCCAGCCCCCGCCGGCGTAACACCAAAAACCCTGAATGTGTACCCGTTACACGGCAGTATTAC
TCTGAGTCACATCATTTTAAATGAATCAAAACTTTCAACAACGGATCTCTTGGTTCTGGCATCGATGAA
GAACGCAGCGAAATGCGATAAGTAATGTGAATTGCAGAATTCAGTGAATCATCGAATCTTTGAACGCA
CATTGCGCCCGCCAGTATTCTGGCGGGCATGCCTGTTCGAGCGTCATTTCAACCCTCAGGTCCCCCTTT
TCGGAGGGGGAGACACCCTGGTGTTGGGGGACGGCATCCTGGCCCGCTGTCTCACAGTGTGCCACGCC
GCCCCCGAAATGAATTGGCGGCCTCGTCGCGTGCCACCCCTGCGTAGTAGCACAACCTCGCAACGGGA
GCCCGACGCGGCCACTGCCGTAAAACGCCCAACTTTTACCGAGTTGACCTCGAATCAGGTAGGAATAC
CCGCTGAACTTAAGCATATCAATAAGCNGGAGGAA

Strain Identification Information

Sample No.	Sequencing Primer Name	Sequencing No.
SW2-B	ITS1	24AH61

Phylogenic Tree of the Fungus

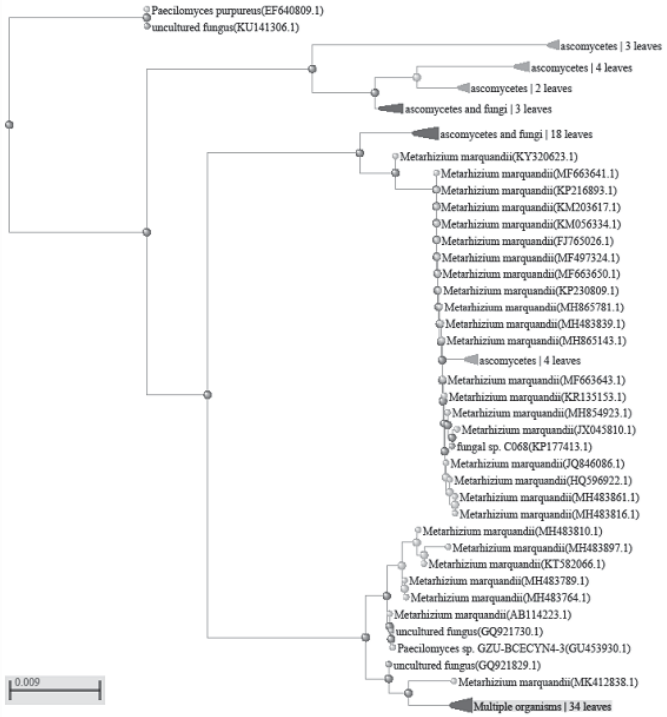

25

Scheme S1. Proposed biosynthetic pathway of **1**

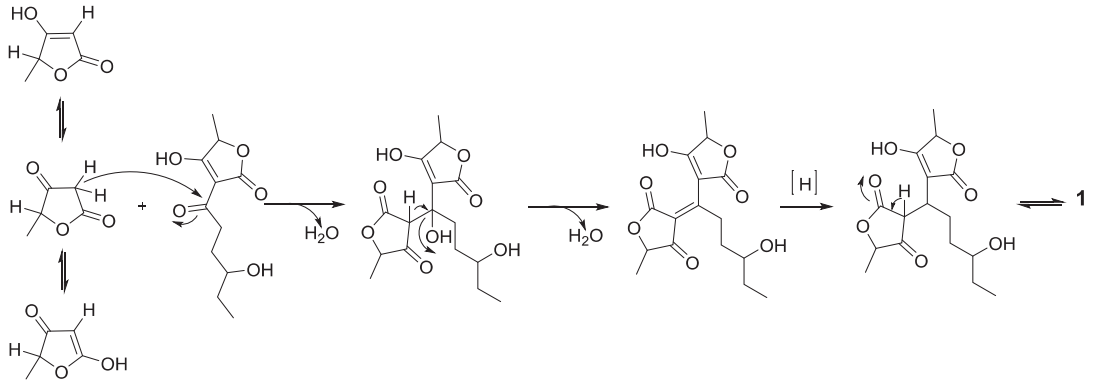

Chapter 3 - Azaphilones from the Red Sea Fungus *Aspergillus falconensis*

3.1 Publication Manuscript

Published in "Marine Drugs" 18 (4): 204 (2020).

Impact Factor: 4.073 (2019); 5-Year Impact Factor: 4.877 (2019)

Overall contribution to this publication: First author, laboratory work including, cultivation and extraction, compound isolation, structure elucidation, and preparation of manuscript.

marine drugs

MDPI

Article

Azaphilones from the Red Sea Fungus *Aspergillus falconensis*

Dina H. El-Kashef [1,2], Fadia S. Youssef [1,3], Rudolf Hartmann [4], Tim-Oliver Knedel [5], Christoph Janiak [5], Wenhan Lin [6], Irene Reimche [7], Nicole Teusch [7], Zhen Liu [1,*] and Peter Proksch [1,8,*]

1 Institute of Pharmaceutical Biology and Biotechnology, Heinrich-Heine-University Duesseldorf, 40225 Duesseldorf, Germany; dina.elkashef@mu.edu.eg (D.H.E.-K.); fadiayoussef@pharma.asu.edu.eg (F.S.Y.)
2 Department of Pharmacognosy, Faculty of Pharmacy, Minia University, 61519 Minia, Egypt
3 Department of Pharmacognosy, Faculty of Pharmacy, Ain Shams University, Abbassia, 11566 Cairo, Egypt
4 Institute of Complex Systems: Strukturbiochemie, Forschungszentrum Jülich GmbH, ICS-6, 52425 Jülich, Germany; r.hartmann@fz-juelich.de
5 Institut für Anorganische Chemie und Strukturchemie, Heinrich-Heine-Universität Düsseldorf, 40225 Düsseldorf, Germany; tim-oliver.knedel@hhu.de (T.-O.K.); janiak@uni-duesseldorf.de (C.J.)
6 State Key Laboratory of Natural and Biomimetic Drugs, Peking University, Beijing 100191, China; whlin@bjmu.edu.cn
7 Department of Biomedical Sciences, Institute of Health Research and Education, University of Osnabrück, 49074 Osnabrück, Germany; irene.reimche@uni-osnabrueck.de (I.R.); nicole.teusch@uni-osnabrueck.de (N.T.)
8 Hubei Key Laboratory of Natural Products Research and Development, College of Biological and Pharmaceutical Sciences, China Three Gorges University, Yichang 443002, China
* Correspondence: zhenfeizi0@sina.com (Z.L.); proksch@uni-duesseldorf.de (P.P.); Tel.: +49-211-81-14163 (Z.L. & P.P.)

Received: 4 March 2020; Accepted: 5 April 2020; Published: 10 April 2020

Abstract: The marine-derived fungus *Aspergillus falconensis*, isolated from sediment collected from the Canyon at Dahab, Red Sea, yielded two new chlorinated azaphilones, falconensins O and P (**1** and **2**) in addition to four known azaphilone derivatives (**3**–**6**) following fermentation of the fungus on solid rice medium containing 3.5% NaCl. Replacing NaCl with 3.5% NaBr induced accumulation of three additional new azaphilones, falconensins Q–S (**7**–**9**) including two brominated derivatives (**7** and **8**) together with three known analogues (**10**–**12**). The structures of the new compounds were elucidated by 1D and 2D NMR spectroscopy and HRESIMS data as well as by comparison with the literature. The absolute configuration of the azaphilone derivatives was established based on single-crystal X-ray diffraction analysis of **5**, comparison of NMR data and optical rotations as well as on biogenetic considerations. Compounds **1**, **3**–**9**, and **11** showed NF-κB inhibitory activity against the triple negative breast cancer cell line MDA-MB-231 with IC_{50} values ranging from 11.9 to 72.0 μM.

Keywords: *Aspergillus falconensis*; OSMAC; azaphilones; X-ray diffraction; NF-κB inhibition

1. Introduction

In the last two decades, marine-derived fungi have gained considerable attention for drug discovery due to their ability to produce a vast diversity of bioactive secondary metabolites [1]. Up until today, hundreds of secondary metabolites have been characterized from marine-derived fungi exhibiting promising biological and pharmacological properties [2,3]. In particular, the diketopiperazine alkaloid halimide, obtained from a marine-derived fungus *Aspergillus* sp., was the lead structure for the putative

anticancer drug plinabulin, which has entered Phase III of clinical trials against non-small cell lung cancer [4–6]. Interestingly, genomic sequencing revealed that under conventional culture conditions, many biosynthetic fungal gene clusters remain silent and transcriptionally suppressed [7,8]. Changing the cultivation conditions of fungi may activate silent biosynthetic gene clusters and eventually lead to either upregulation of constitutively present compounds or accumulation of new natural products [9]. The OSMAC (One Strain MAny Compounds) approach, first described by Zeeck et al. [10], represents one of the strategies which triggers diversification of the metabolic profile of fungi by altering the cultivation conditions. Fungi of the genus *Aspergillus* are rich sources of numerous bioactive secondary metabolites [11–13]. Consequently, as a part of our ongoing research on marine-derived fungi [14–16], we have investigated the fungus *Aspergillus falconensis* (formerly known as *Emericella falconensis* [17]) that was isolated from sea sediment collected at a depth of 25 m from the Canyon at Dahab, Red Sea, Egypt. The previously isolated soil-derived fungus, *Emericella falconesis*, is known as a producer of anti-inflammatory azaphilone derivatives [18–21]. Herein, we report the isolation, structure elucidation, and bioactivity of azaphilones obtained from *A. falconensis* following fermentation of the fungus on solid rice medium that contained either 3.5% NaCl or 3.5% NaBr. Following this approach, we were able to obtain two new chlorinated azaphilones (**1** and **2**) together with four known azaphilone derivatives (**3**–**6**) when the fungus was cultivated in the presence of NaCl and three additional new azaphilone derivatives (**7**–**9**) including two brominated analogues (**7** and **8**) in addition to three known derivatives (**10**–**12**) in the presence of NaBr. Compounds **1**, **3**–**9**, and **11** were examined with regard to their nuclear factor kappa B (NF-κB) inhibitory activity in the triple negative breast cancer (TNBC) cell line MDA-MB-231. In TNBC, constitutive activation of the proinflammatory NF-κB is associated with tumor aggressiveness [22]. All tested compounds revealed inhibition of NF-κB signaling with IC_{50} values at two-digit micromolar concentrations.

2. Results and Discussion

After fermentation of *A. falconensis* on solid rice medium containing 3.5% NaCl (similar to the salinity of sea water), chromatographic separation of the EtOAc extract of the fungus yielded two new chlorinated azaphilone derivatives (**1**–**2**). In addition, four known azaphilones (**3**–**6**) were identified including falconensins A (**3**) [18], M (**4**) [23], N (**5**) [23], and H (**6**) [19] by comparison of their spectroscopic data with the literature.

Compound **1** was isolated as a yellow oil. Its HRESIMS analysis showed an isotope pattern characteristic for two chlorine atoms in the molecule at *m*/*z* 511/513/515 (9:6:1), corresponding to the molecular formula $C_{24}H_{24}Cl_2O_8$ with 12 degrees of unsaturation. The UV pattern and NMR data of **1** (Tables 1 and 2) were similar to those of the co-isolated known falconensin M (**4**), which was previously reported from *Emericella falconensis* [23], suggesting **1** to be an azaphilone derivative [24]. However, the ^{1}H NMR spectrum of **1** displayed the signal of an additional methyl group at δ_H 2.07 (s) when compared to **4**. The Heteronuclear Multiple Bond Correlation (HMBC) correlations from the protons of this additional methyl and H-8 to a carbonyl carbon at δ_C 170.0 together with the obvious deshielded chemical shift of H-8 (δ_H 6.11) indicated the replacement of the hydroxy group by an acetoxy group at C-8 in **1**. Detailed analysis of the 2D NMR spectra of **1** indicated that the remaining substructure of **1** was identical to that of **4**. The large values of $^3J_{H\text{-}8,H\text{-}8a}$ (10.7 Hz) and $^3J_{H\text{-}1b,H\text{-}8a}$ (13.0 Hz) and the small value of $^3J_{H\text{-}1a,H\text{-}8a}$ (5.0 Hz) obtained from the ^{1}H NMR spectrum of **1**, indicated *trans*-diaxial orientation between H-8a (δ_H 2.98) and H-8 and between H-8a and H-1b (δ_H 3.96) and *cis*-orientation between H-8a and H-1a (δ_H 4.34). The NOE correlations from H-8a to H-1a and Me-9 (δ_H 1.56) as well as between H-8 and H-1b confirmed that H-1a, H-8a and Me-9 were on the same side of the ring (α-oriented) whereas H-1b and H-8 were on the opposite side (β-oriented). Thus, compound **1** was elucidated as 8-*O*-acetyl analogue of **4**, representing a new falconensin derivative, for which the trivial name falconensin O is proposed. Incubation of putative precursors of **1** such as **4** in EtOAc over three days failed to generate the corresponding acetates, thus ruling out the possibility that the acetylated azaphilones isolated in this study are artefacts generated during chromatographic workup.

Table 1. ^{13}C NMR data of compounds **1**, **2**, **7**, **8**, and **9** in $CDCl_3$.

No.	1 [a,c]	2 [a,c]	7 [b]	8 [a,c]	9 [b]
1	67.8, CH_2	68.2, CH_2	68.5, CH_2	68.4, CH_2	68.0, CH_2
3	160.2, C	168.2, C	160.5, C	160.2, C	160.2, C
4	102.4, CH	100.9, CH	102.8, CH	102.6 CH	102.8, CH
4a	149.4, C	149.2, C	150.3, C	149.9, C	148.9, C
5	116.6, CH	115.7, CH	116.6, CH	116.6, CH	117.1, CH
6	192.3, C	192.7, C	193.8, C	193.4, C	193.3, C
7	83.4, C	83.4, C	85.6, C	85.4, C	82.5, C
8	70.1, CH	70.4, CH	69.8, CH	69.7, CH	70.7, CH
8a	38.1, CH	38.0, CH	37.8, CH	37.5, CH	38.2, CH
9	17.9, CH_3	18.2, CH_3	16.8, CH_3	16.6, CH_3	18.2, CH_3
10	124.9, CH	36.4, CH_2	125.4, CH	125.3, CH	125.2, CH
11	134.1, CH	20.0, CH_2	133.9, CH	133.6, CH	133.9, CH
12	18.2, CH_3	13.6, CH_3	18.4, CH_3	18.2, CH_3	18.4, CH_3
1′	164.3, C	164.4, C	165.3, C	164.9, C	166.2, C
2′	122.2, C	122.3, C	117.4, C	117.2, C	115.5, C
3′	152.8, C	152.9, C	156.2, C	157.3, C	159.0, C
4′	112.9, C	112.8, C	97.1, CH	93.8, CH	96.9, CH
5′	149.2, C	149.8, C	154.0, C	155.8, C	157.6, C
6′	117.0, C	117.1, C	105.3, C	106.6, C	109.2, CH
7′	134.3, C	134.5, C	137.4, C	138.1, C	140.0, C
8′	16.9, CH_3	17.1, CH_3	20.2, CH_3	20.1, CH_3	19.6, CH_3
8-OAc	170.0, C	170.1, C			169.7, C
	20.5, CH_3	20.8, CH_3			20.8, CH_3
3′-OMe	62.4, CH_3	62.6, CH_3	56.5, CH_3	56.3, [d] CH_3	56.0, CH_3
5′-OMe				56.4, [d] CH_3	

[a] Measured at 150 MHz; [b] Measured at 175 MHz; [c] Data extracted from the HSQC (Heteronuclear Single Quantum Coherence) and HMBC spectra; [d] interchangeable.

Table 2. ^{1}H NMR data of compounds **1**, **2**, **7**, **8**, and **9** in $CDCl_3$.

No.	1 [a]	2 [a]	7 [b]	8 [a]	9 [b]
1	4.34, dd (11.0, 5.0); 3.96, dd (13.0, 11.0)	4.29, dd (11.0, 5.1); 3.93, dd (13.2, 11.0)	4.77, dd (10.5, 5.1); 3.84, dd (13.0, 10.5)	4.77, dd (10.6, 5.0); 3.84, dd (13.0, 10.6)	4.32, dd (10.8, 5.0); 3.93, dd (13.0, 10.8)
4	5.59, s	5.53, s	5.56, s	5.57, s	5.57, s
5	5.86, d (1.7)	5.79, d (1.9)	5.80, d (1.6)	5.80, d (1.8)	5.85, d (1.9)
8	6.11, d (10.7)	6.09, d (10.7)	4.74, d (10.7)	4.75, d (10.7)	6.11, d (10.7)
8a	2.98, dddd (13.0, 10.7, 5.0, 1.7)	2.94, dddd (13.2, 10.7, 5.1, 1.9)	2.88, dddd (13.0, 10.7, 5.1, 1.6)	2.88, dddd (13.0, 10.7, 5.0, 1.8)	2.96, dddd (13.0, 10.7, 5.0, 1.9)
9	1.56, s	1.56, s	1.47, s	1.47, s	1.54, s
10	5.91, dq (15.4, 1.3)	2.20, m	5.90, dq (15.4, 1.4)	5.90, dd (15.4, 1.5)	5.90, dd (15.3, 1.6)
11	6.45, dq (15.4, 7.0)	1.58, m	6.47, dq (15.4, 7.0)	6.46, dd (15.4, 7.0)	6.42, dd (15.3, 7.0)
12	1.88, dd (7.0, 1.3)	0.94, t (7.4)	1.87, dd (7.0, 1.4)	1.88, dd (7.0, 1.5)	1.87, dd (7.0, 1.6)
4′			6.52, s	6.38, s	6.23, s
6′					6.22, s
8′	2.50, s	2.50, s	2.48, s	2.51, s	2.39, s
8-OAc	2.17, s	2.16, s			2.15, s
3′-OMe	3.83, s	3.83, s	3.83, s	3.92, [c] s	3.74, s
5′-OH	6.04, s	6.04, s			
5′-OMe				3.89, [c] s	

[a] Measured at 600 MHz; [b] Measured at 700 MHz; [c] interchangeable.

The molecular formula of compound **2** was deduced as $C_{24}H_{26}Cl_2O_8$, containing two additional protons when compared to **1**. Investigation of the ^{1}H and ^{13}C NMR data of **2** (Tables 1 and 2) demonstrated the close structural similarity between **1** and **2** except for signals of the side chain at C-3. In particular, the resonances for the olefinic methine protons at δ_H 5.91 (H-10) and 6.45 (H-11) of **1** were replaced by two methylene groups at δ_H 2.20 (H_2-10) and 1.58 (H_2-11) in **2**. The COSY correlations between H_2-10/H_2-11/Me-12 together with the HMBC correlations from H_2-11 to C-3 (δ_C 168.2) and

from H_2-10 to C-3 and C-4 (δ_C 100.9) confirmed the attachment of a *n*-propyl moiety at C-3 in **2**. The remaining substructure of **2** was determined to be identical to that of **1** by comparison of the 2D NMR data of **1** and **2**. The similar coupling constants and NOE relationships between **1** and **2** indicated that both share the same relative configuration.

When 3.5% NaCl as a constituent of the rice medium was replaced with 3.5% NaBr, a profound change in the metabolic profile of the fungus was observed. In total, two new brominated azaphilone derivatives (**7** and **8**), one new non-halogenated azaphilone (**9**), in addition to the known falconensins K (**10**) [23] and I (**11**) [23] were obtained.

The ^{1}H and ^{13}C NMR spectra of **7** (Tables 1 and 2) were comparable to those of the co-isolated known compound, falconensin K (**10**) [23]. The HRESIMS data of **7** established the molecular formula $C_{22}H_{23}BrO_7$, differing from that of **10** by the replacement of the chlorine with a bromine atom. The HMBC correlations from Me-8′ (δ_H 2.48) to C-2′ (δ_C 117.4), C-6′ (δ_C 105.3), and C-7′ (δ_C 137.4), from H-4′ to C-2′, C-6′, C-3′ (δ_C 156.2), and C-4′ (δ_C 154.0), from 3′-OMe (δ_H 3.83) to C-3′ together with the NOE correlation between 3′-OMe and Me-9 (δ_H 1.47) indicated the position of the bromine atom at C-6′ in **7.** The remaining azaphilone core structure including the relative configuration of **7** was confirmed to be identical to that of **10** after further inspection of the 2D NMR spectra of **7**. Thus, the structure of **7** was elucidated as shown (Figure 1), and the trivial name falconensin Q is proposed for this compound.

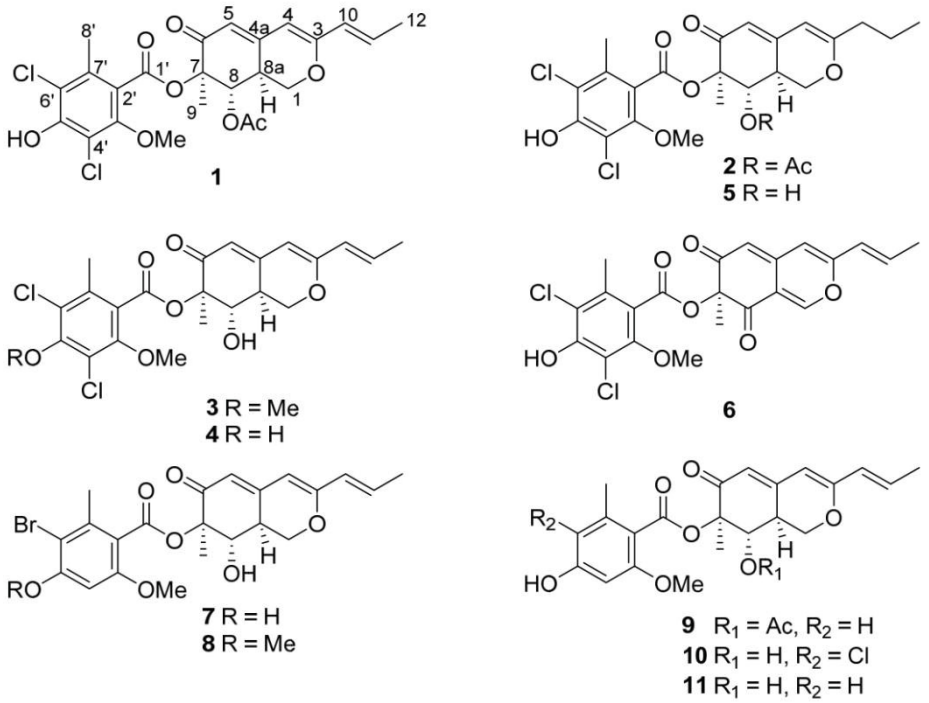

Figure 1. Structures of azaphilones isolated from *A. falconensis*.

Falconensin R (**8**) was isolated as a yellow oil. Its molecular formula was determined as $C_{23}H_{25}BrO_7$ by HRESIMS, containing an additional methyl group when compared to **7**. The NMR data of **8** (Tables 1 and 2) were similar to those of **7** except for the appearance of two methoxy groups at δ_C 56.4 and 56.3, and at δ_H 3.89 (5′-OMe) and 3.92 (3′-OMe) instead of one methoxy group in **7**. The location of the additional methoxy group at C-5′ in **8** was confirmed by the HMBC correlations from 3′-OMe to C-3′ (δ_C 157.3), from 5′-OMe to C-5′ (δ_C 155.8), and from H-4′ to C-2′ (δ_C 117.2), C-6′ (δ_C 106.6), C-3′ and C-5′, as well as based on the NOE correlations from H-4′ to 3′-OMe and 5′-OMe.

The molecular formula of **9** was determined as $C_{24}H_{26}O_8$ by HRESIMS, indicating 42 amu more than that of the co-isolated known falconensin I (**11**) ($C_{22}H_{24}O_7$) [23]. Comparison of the ^1H and ^{13}C NMR spectra revealed that the structure of **9** was closely related to that of **11**, except for the appearance of an additional acetoxy group at δ_H 2.15 and δ_C 20.8 and 169.7 in **9**. The location of this additional acetoxy group at C-8 was confirmed by the COSY correlations between H-1ab/H-8a/H-8 and the HMBC correlations from H-8 to the carbon of the additional acetoxy group. The similar NOE correlations of **9** and **11** suggested that they shared the same configuration. Thus, compound **9** was elucidated as 8-*O*-acetyl analogue of falconensin I (**11**).

The specific optical rotation values of **1**, **2**, **7**, **8**, and **9** are positive (+99 − +233), which is in agreement with the positive values reported for other known falconensin derivatives with 7*R*, 8*S*, and 8a*S* configuration, suggesting that the new compounds share the same absolute configuration as the known derivatives [18,20,25]. Although the absolute configuration of other falconensin derivatives had been determined previously by Mosher's reaction and observation of Cotton effects of CD curves [18,20,25], no crystal structure had so far been reported for these compounds. To independently assign the absolute configuration of the isolated compounds, a single crystal X-ray diffraction analysis through anomalous dispersion of the known falconensin N (**5**), for which crystals of sufficient quality were obtained, was conducted. Herein, we present for the first time the crystal structure of falconensin N (**5**) (Figure 2). From the single-crystal structure refinement, the absolute structure assignment was based on the Flack parameter of 0.016(5) (Table S1) [26–29]. The crystal structure of falconensin N (**5**) is in agreement with the previously reported absolute configuration [18,20,25]. Based on these data, all falconensin derivatives isolated in this study are suggested to share the same 7*R*, 8*S*, and 8a*S* absolute configuration.

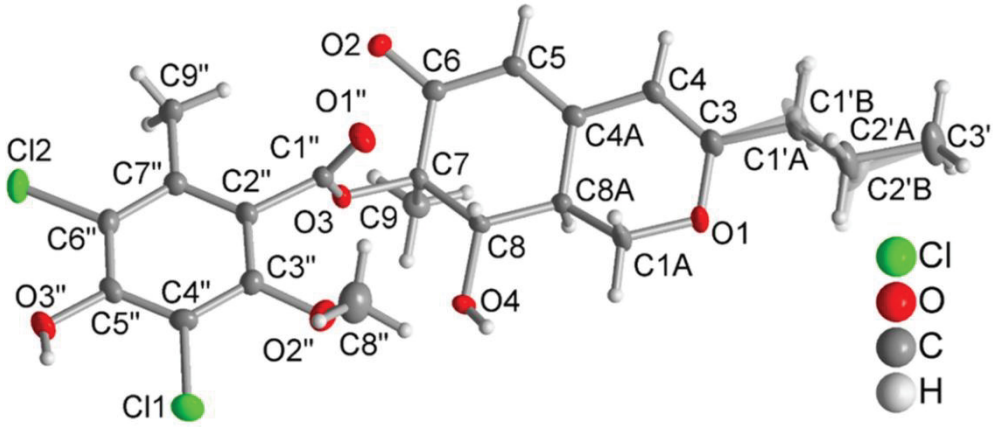

Figure 2. Molecular structure of **5** from a single-crystal X-ray structure determination (50% thermal ellipsoids; H atoms with arbitrary radii). The propyl group is disordered, and the two respective atom positions were refined with equal occupation factors.

Azaphilones constitute a class of fungal metabolites possessing various biological activities, including antiviral, antibacterial, antioxidant, hypolipidemic, cytotoxic, and anti-inflammatory properties [24,30]. For falconensins in particular, anti-inflammatory activity against 12-*O*-tetradecanoylphorbol-13-acetate-induced inflammatory ear edema in mice had been reported [21]. Compounds **1**, **3**–**9**, and **11** were evaluated for their anti-inflammatory activity in the triple negative breast cancer cell line NF-κB-MDA-MB-231. The IC_{50} values were calculated based on inhibition of the NF-κB-dependent luciferase activity and revealed NF-κB blockade for all compounds (Table 3). To exclude that cytotoxicity caused reduction of NF-κB activity, cell viability was determined in parallel. Compounds **1**, **4**–**7**, **9**, and **11** did not influence cell viability within the selected concentration range, whereas compound **8** reduced cell viability with an IC_{50} of 126.8 ± 5.4 µM, thus showing about

9-times higher potency in NF-κB-blockade compared to its cytotoxicity. Compound **3** with an IC_{50} of 89.7 ± 9.1 μM in the cytotoxicity assay only showed around 2-times higher potency in NF-κB-blockade. Plotting the pIC_{50}, which is calculated as the negative decadic logarithm of IC_{50}, of the cell viability against the pIC_{50} of NF-κB inhibition, illustrates a greater anti-inflammatory potential of the examined compounds compared to their cytotoxic potential (Figure S40). In conclusion, inhibition of NF-κB signaling in the TNBC cell line MDA-MB-231 could be induced by **1**, **3** − **9**, and **11**, with **7** being the most potent compound.

Table 3. IC_{50} values (μM) of the compounds tested in MDA-MB-231 cells for NF-κB inhibition and inhibition of cell viability. [a]

Compound	NF-κB inhibition	Cell viability inhibition
Falconensin O (1)	15.7 ± 0.7	> 200
Falconensin A (3)	53.2 ± 21.4	89.7 ± 9.1
Falconensin M (4)	56.5 ± 8.3	> 200
Falconensin N (5)	71.0 ± 7.3	> 200
Falconensin H (6)	72.0 ± 28.1	> 400
Falconensin Q (7)	11.9 ± 2.1	> 200
Falconensin R (8)	14.6 ± 1.7	126.8 ± 5.4
Falconensin S (9)	20.1 ± 5.6	> 200
Falconensin I (11)	19.5 ± 2.5	> 400

[a] Average IC_{50} of at least three individual experiments ± SD tested in the concentration range of 400 μM to 0.78 μM (**3**, **6**, and **11**) and 200 μM to 0.78 μM (**1**, **4**, **5**, **7**, **8**, and **9**) in a two-fold serial dilution.

3. Materials and Methods

3.1. General Experimental Procedures

Optical rotations were measured using a Jasco P-2000 polarimeter. The compounds were dissolved in optically pure solvents Uvasol® (spectroscopic grade solvents, Merck). 1D and 2D NMR spectra were recorded on Bruker Avance III 300 or 600 or 700 MHz NMR spectrometers (Bruker BioSpin, Rheinstetten, Germany). Low-resolution mass spectra were recorded with an Ion-Trap-API Finnigan LCQ Deca (Thermo Quest) mass spectrometer, while high-resolution mass data were measured on a FTHRMS-Orbitrap (Thermo-Finnigan) mass spectrometer. HPLC analysis was conducted using a Dionex UltiMate-3400 SD with an LPG-3400SD pump coupled to a photodiode array detector (DAD3000RS) and employing a Knauer Eurospher C_{18} analytical column (125 × 4 mm i.d., 5 μm). Purification of the compounds was performed using semipreparative HPLC on the VWR Hitachi Chromaster HPLC system, 5160 Pump; 5410 UV detector; Eurosphere-100 C_{18}, 300 mm × 8 mm i.d., 10 μm, Knauer, Germany) with MeOH and H2O as eluents utilizing a flow rate of 5 mL/min. Column chromatography was performed using different stationary phases including Merck MN silica gel 60 M (0.04−0.063 mm), silica gel 60 RP-18 (40–63 μm), and Sephadex LH-20 (Merck). TLC plates precoated with silica gel 60 F_{254} (Merck) were used for monitoring fractions resulting from column chromatography. Detection of spots on the TLC was done by UV absorption at 254 and 365 nm followed by anisaldehyde spray reagent.

3.2. Fungal Material

The fungus was isolated from marine sediment which was collected at a depth of 25 m from the Canyon at Dahab, Red Sea, Egypt in November 2016. The fungus was identified as *A. falconensis* (GenBank accession No. MN905375) through amplification and sequencing of the internal transcribed spacer region including the 5.8S ribosomal DNA following by a subsequent BLAST search in NCBI as described before [31]. A deep-frozen specimen of the fungal strain has been deposited in one of the author's laboratory (P.P.).

3.3. Fermentation, Extraction, and Isolation

Initial fermentation of the fungus was conducted in ten 1L Erlenmeyer flasks. To each flask, 100 g of rice (Oryza Milchreis), 100 mL of demineralized water, and 3.5 g of NaCl were added. Thereafter, the flasks were autoclaved at 121 °C for 20 min and after cooling to room temperature, the fungus was inoculated on the rice medium. Fermentation of the fungus was continued under static conditions for 21 days at 20 °C until the fungus had totally overgrown the medium. Then, each flask was extracted with 600 mL EtOAc. After overnight soaking in EtOAc, the rice medium was cut into small pieces and shaken for 8 h at 150 rpm followed by evaporation of EtOAc, yielding around 16 g of EtOAc extract. For the OSMAC experiment, the same cultivation and extraction procedures of the initial cultivation were conducted except for the replacement of the added 3.5% NaCl with 3.5% NaBr and the cultivation on three flasks instead of ten. Eventually, the OSMAC experiment yielded approximately 2 g of EtOAc extract.

The initial crude extract of the large scale cultivation of the fungus obtained in presence of NaCl (16 g) was fractionated by vacuum liquid chromatography (VLC) on silica gel as a stationary phase utilizing a step gradient of solvents consisting of mixtures of *n*-hexane/EtOAc and CH_2Cl_2/MeOH, to yield 12 fractions (V1 to V12). Fraction V4 (874 mg) was further separated by Sephadex LH20 column chromatography using CH_2Cl_2-MeOH (1:1) as mobile phase affording eight subfractions (V4-S1 to V4-S8). Subfraction V4-S4 (162.8 mg) was purified by semi-preparative HPLC using acetonitrile-H_2O containing 0.1% formic acid (from 60:40 to 95:5 in 22 min) to afford **1** (1.8 mg), **2** (1.5 mg), and **3** (11.8 mg). Subfraction V4-S5 (139.6 mg) was further purified by semi-preparative HPLC using gradient elution with acetonitrile-H_2O containing 0.1% formic acid (60:40 to 95:5 in 22 min) affording **4** (6.3 mg) and **5** (2.2 mg). Fraction V6 (686.1 mg) was submitted to RP-VLC column using H_2O-MeOH gradient elution to yield 10 subfractions (V6-R1 to V6-R10). Subfraction V6-R7 (110 mg) was further purified using semi-preparative HPLC with a gradient of MeOH-H_2O containing 0.1% formic acid (67:33 to 80:20 in 20 min) to afford **6** (15.1 mg).

The EtOAc extract (2 g) obtained from the OSMAC experiment with addition of 3.5% NaBr, was also fractionated by VLC on silica gel as described before to give 13 fractions (BrV1 to BrV13). Subsequent purification of BrV5 (157 mg), BrV6 (32 mg), and BrV10 (140 mg) using Sephadex LH20 column chromatography with CH_2Cl_2-MeOH (1:1) as mobile phase and semi-preparative HPLC with a gradient of MeOH-H_2O containing 0.1% formic acid to afford **7** (3.1 mg), **8** (2.1 mg), **9** (1.2 mg), **10** (0.9 mg), and **11** (2.0 mg).

Falconensin O (**1**): Yellow oil; $[\alpha]_D^{20}$ +176 (*c* 0.2, MeOH); UV (MeOH) λ_{max} 355 and 206 nm; ^{1}H and ^{13}C NMR data, Tables 1 and 2; HRESIMS *m*/*z* 511.0923 $[M + H]^+$ (calcd for $C_{24}H_{25}Cl_2O_8$, 511.0921).

Falconensin P (**2**): Yellow amorphous powder; $[\alpha]_D^{20}$ +233 (*c* 0.2, MeOH); UV (MeOH) λ_{max} 329 and 216 nm; ^{1}H and ^{13}C NMR data, Tables 1 and 2; HRESIMS *m*/*z* 513.1073 $[M + H]^+$ (calcd for $C_{24}H_{27}Cl_2O_8$, 513.1077).

Falconensin Q (**7**): Yellow oil; $[\alpha]_D^{20}$ +182 (*c* 0.2, MeOH); UV (MeOH) λ_{max} 354 and 205 nm; ^{1}H and ^{13}C NMR data, Tables 1 and 2; HRESIMS *m*/*z* 479.0702 $[M + H]^+$ (calcd for $C_{22}H_{24}BrO_7$, 479.0700).

Falconensin R (**8**): Yellow oil; $[\alpha]_D^{20}$ +99 (*c* 0.2, MeOH); UV (MeOH) λ_{max} 353 and 206 nm; ^{1}H and ^{13}C NMR data, Tables 1 and 2; HRESIMS *m*/*z* 493.0853 $[M + H]^+$ (calcd for $C_{23}H_{26}BrO_7$, 493.0856).

Falconensin S (**9**): Yellow oil; $[\alpha]_D^{20}$ +105 (*c* 0.2, MeOH); UV (MeOH) λ_{max} 355 and 201 nm; ^{1}H and ^{13}C NMR data, Tables 1 and 2; HRESIMS *m*/*z* 443.1700 $[M + H]^+$ (calcd for $C_{24}H_{27}O_8$, 443.1700).

3.4. Crystallographic Analysis of Compound **5**

Crystals were obtained by solvent evaporation (MeOH). Data Collection: compound **5** was measured with a Bruker Kappa APEX2 CCD diffractometer with a microfocus tube and Cu-Kα radiation (λ = 1.54178 Å). APEX2 was used for data collection, SAINT for cell refinement and data reduction [32], and SADABS for experimental absorption correction [33]. The structure was solved by intrinsic phasing using SHELXT [34], and refinement was done by full-matrix least-squares on F^2 using SHELXL-2016/6 [35]. The hydrogen atoms were positioned geometrically (with C-H = 0.95 Å for

aromatic CH, 1.00 Å for aliphatic CH, 0.99 Å for CH_2, and 0.98 Å for CH) and refined using riding models (AFIX 43, 13, 23, 137, respectively), with Uiso(H) = 1.2 Ueq(CH, CH_2), and 1.5 Ueq(CH_3). The absolute structure configuration of **5** was solved using anomalous dispersion from Cu-Kα, resulting in a Flack parameter of 0.016(5) using Parsons quotient method. All graphics were drawn using DIAMOND [36]. The structural data have been deposited in the Cambridge Crystallographic Data Center (CCDC No. 1976223).

3.5. Triple Negative Breast Cancer Studies

3.5.1. Cell Culture and Chemicals

Culture medium and supplements were purchased from Gibco (Fisher Scientific, Schwerte, Germany). Cell plates were obtained from Greiner bio-one (Frickenhausen, Germany). Cells were grown and incubated in a humidified 5% CO_2 atmosphere at constant 37 °C. The metastatic breast cancer cell line, MDA-MB-231, was purchased from the European Collection of Authenticated Cell Cultures (ECACC) (Salisbury, UK). Sub-culturing was performed in RPMI 1640 medium (#21875-034) supplemented with 15% (v/v) fetal calf serum (FCS) and 1% (v/v) penicillin-streptomycin (pen-strep) (10,000 U/mL). The MDA-MB-231 cell line stably expressing a plasmid with the NF-κB response element and the gene sequence for the firefly-luciferase protein (NF-κB- MDA-MB-231) was purchased from Signosis (Santa Clara, CA, USA; #SL-0043). For selection, 100 µg/mL hygromycin B (Life Technologies, Darmstadt, Germany; #10687010) was applied in high glucose DMEM (#41966-029) supplemented with 10% (v/v) FCS, 1% (v/v) pen-strep. Starvation medium for the NF-κB inhibition assay contained 1% (v/v) FCS, 1% (v/v) pen-strep, and 100 µg/mL hygromycin B. Cell detachment occurred by trypsinization in 0.25% trypsin-EDTA and cell counting was performed at 1:1 (v/v) dilution in Erythrosin B (BioCat, Heidelberg, Germany; #L13002) using the LUNA II automated cell counter (BioCat). Compounds **1**, **4**, **5**, **7**, **8**, and **9** were dissolved in dimethyl sulfoxide (DMSO) to a final concentration of 10 mM, whereas the compounds **3**, **6**, **11** were dissolved at 20 mM in DMSO. Further dilutions in cell culture medium contained maximal 2% DMSO.

3.5.2. NF-κB Inhibitory Assay

3×10^4 NFκB-MDA-MB-231 cells were seeded in total 100 µL medium per well in a 96-well plate (Greiner; #655098). On the next day, medium was exchanged, and triplicates were pre-incubated for 20 min without (negative control) or with compounds in total 100 µL starvation medium. Final concentration of the compounds ranged a twofold serial dilution starting from 400 µM (compound **3**, **6**, and **11**) or 200 µM (compound **1**, **4**, **5**, **7**, **8**, and **9**) to 0.78 µM. To activate NF-κB signaling, untreated cells (positive control) or compound treated cells were subsequently stimulated for 24 h with 20 ng/mL TNFα (Peprotech, Hamburg, Germany; #300-01A). Finally, cell lysis and measurement were done according to the manufacturer's instruction of the Luciferase Assay System (Promega, Mannheim, Germany; #E1500). Injection of equal volume of luciferase substrate with 10 s integration time and subsequent luminescence measurement was performed using the Spark® microplate reader (TECAN, Männedorf, Switzerland).

3.5.3. Cell Viability Assay

Using the CyBio® Well vario pipetting robot (Analytik Jena, Jena, Germany; #OL3381-24-730), 18 µL of the MDA-MB-231 cell suspension (2.8×10^5 cells/mL) were seeded per well in a 384-well plate (Greiner; #781074) and incubated for 24 h. The final concentration of the compounds ranged in twofold serial dilution steps starting from 400 µM (compound **3**, **6**, and **11**) or 200 µM (compound **1**, **4**, **5**, **7**, **8**, and **9**) to 0.78 µM. After 24 h compound stimulation in quadruples, cell lysis and measurement were done as prescribed in the manufacturer's instruction of the CellTiter-Glo® Luminescent Cell Viability Assay (Promega; #G7570). In short, it was applied equal volume of the CellTiter-Glo® reagent and luminescence was measured using the Spark® microplate reader (TECAN).

3.5.4. Statistical Analysis

Data of the NF-κB inhibitory assay and cell viability assay represent at least three individual experiments and were analyzed using GraphPad Prism (GraphPad Software, San Diego, USA; Version 8.1.2). For the NF-κB inhibitory assay, data below the relative light unit (RLU) of the negative control were excluded for further analysis. Half maximal inhibitory concentration (IC_{50}) values were determined by nonlinear regression analysis based on the dose–response inhibition calculation "log(inhibitor) vs. response–variable slope (four parameters)" without curve fitting.

Supplementary Materials: The following are available online at http://www.mdpi.com/1660-3397/18/4/204/s1, UV, HRMS, 1D and 2D NMR spectra of all the new compounds **1**, **2** and **7**–**9** as well as NF-κB inhibitory potential of the tested compounds and crystal data for compound **5**.

Author Contributions: Investigation, D.H.E.-K., F.S.Y., R.H., T.-O.K., C.J., W.L., I.R., and N.T.; writing—original draft preparation, D.H.E.-K.; writing—review and editing and supervision, Z.L. and P.P. All authors have read and agreed to the published version of the manuscript.

Funding: This project was supported by grants of the DFG (GRK 2158, project number 270650915) and the Manchot Foundation to P.P.

Acknowledgments: D.H.E. gratefully acknowledges the Egyptian Government (Ministry of Higher Education) for awarding a doctoral scholarship. Furthermore, we wish to thank Dr. Dent. Abdel Rahman O. El Mekkawi, EFR, PADI IDC staff instructor, founder of I Dive Tribe, Dahab, South Sinai – Egypt, for collecting the sediment sample.

Conflicts of Interest: The authors declare no conflict of interest.

References

1. Jimenez, C. Marine natural products in medicinal chemistry. *ACS Med. Chem. Lett.* **2018**, *9*, 959–961. [CrossRef] [PubMed]
2. Blunt, J.W.; Carroll, A.R.; Copp, B.R.; Davis, R.A.; Keyzers, R.A.; Prinsep, M.R. Marine natural products. *Nat. Prod. Rep.* **2018**, *35*, 8–53. [CrossRef]
3. Wang, Y.T.; Xue, Y.R.; Liu, C.H. A brief review of bioactive metabolites derived from deep-sea fungi. *Mar. Drugs* **2015**, *13*, 4594–4616. [CrossRef] [PubMed]
4. Fenical, W.; Jensen, P.R.; Cheng, X.C. Halimide, A Cytotoxic Marine Natural Product, and Derivatives Thereof. U.S. Patent No. 6,069,146, 30 May 2000.
5. Petersen, L.E.; Kellermann, M.Y.; Schupp, P.J. Secondary metabolites of marine microbes: From natural products chemistry to chemical ecology. In *YOUMARES 9-The oceans: Our Research, our Future*; Jungblut, S., Liebich, V., Bode-Dalby, M., Eds.; Springer International Publishing: Cham, Switzerland, 2020; pp. 159–180.
6. Available online: https://www.beyondspringpharma.com/ChannelPage/index.aspx (accessed on 6 November 2019).
7. Zhang, Z.; He, X.; Wu, G.; Liu, C.; Lu, C.; Gu, Q.; Che, Q.; Zhu, T.; Zhang, G.; Li, D. Aniline-tetramic acids from the deep-sea-derived fungus *Cladosporium sphaerospermum* L3P3 cultured with the HDAC inhibitor SAHA. *J. Nat. Prod.* **2018**, *81*, 1651–1657. [CrossRef] [PubMed]
8. Hertweck, C. Hidden biosynthetic treasures brought to light. *Nat. Chem. Biol.* **2009**, *5*, 450–452. [CrossRef]
9. Daletos, G.; Ebrahim, W.; Ancheeva, E.; El-Neketi, M.; Lin, W.; Chaidir, C. Microbial co-culture and OSMAC approach as strategies to induce cryptic fungal biogenetic gene clusters. In *Chemical Biology of Natural Products*; Grothaus, P., Cragg, G.M., Newman, D.J., Eds.; CRC press: Boca Raton, FL, USA, 2017; pp. 233–284.
10. Hofs, R.; Walker, M.; Zeeck, A. Hexacyclinic acid, a polyketide from *Streptomyces* with a novel carbon skeleton. *Angew. Chem. Int. Ed.* **2000**, *39*, 3258–3261. [CrossRef]
11. Zhang, M.; Wang, W.L.; Fang, Y.C.; Zhu, T.J.; Gu, Q.Q.; Zhu, W.M. Cytotoxic alkaloids and antibiotic nordammarane triterpenoids from the marine-derived fungus *Aspergillus sydowi*. *J. Nat. Prod.* **2008**, *71*, 985–989. [CrossRef]
12. Saleem, M.; Ali, M.S.; Hussain, S.; Jabbar, A.; Ashraf, M.; Lee, Y.S. Marine natural products of fungal origin. *Nat. Prod. Rep.* **2007**, *24*, 1142–1152. [CrossRef]
13. Ge, H.M.; Yu, Z.G.; Zhang, J.; Wu, J.H.; Tan, R.X. Bioactive alkaloids from endophytic *Aspergillus fumigatus*. *J. Nat. Prod.* **2009**, *72*, 753–755. [CrossRef]

14. Frank, M.; Ozkaya, F.C.; Muller, W.E.G.; Hamacher, A.; Kassack, M.U.; Lin, W.; Liu, Z.; Proksch, P. Cryptic secondary metabolites from the sponge-associated fungus *Aspergillus ochraceus*. *Mar. Drugs* **2019**, *17*, 99. [CrossRef]
15. El-Kashef, D.H.; Daletos, G.; Plenker, M.; Hartmann, R.; Mandi, A.; Kurtan, T.; Weber, H.; Lin, W.; Ancheeva, E.; Proksch, P. Polyketides and a dihydroquinolone alkaloid from a marine-derived strain of the fungus *Metarhizium marquandii*. *J. Nat. Prod.* **2019**, *82*, 2460–2469. [CrossRef] [PubMed]
16. Kuppers, L.; Ebrahim, W.; El-Neketi, M.; Ozkaya, F.C.; Mandi, A.; Kurtan, T.; Orfali, R.S.; Muller, W.E.G.; Hartmann, R.; Lin, W.H.; et al. Lactones from the sponge-derived fungus *Talaromyces rugulosus*. *Mar. Drugs* **2017**, *15*, 359. [CrossRef] [PubMed]
17. Samson, R.A.; Visagie, C.M.; Houbraken, J.; Hong, S.B.; Hubka, V.; Klaassen, C.H.; Perrone, G.; Seifert, K.A.; Susca, A.; Tanney, J.B.; et al. Phylogeny, identification and nomenclature of the genus *Aspergillus*. *Stud. Mycol.* **2014**, *78*, 141–173. [CrossRef]
18. Itabashi, T.; Nozawa, K.; Miyaji, M.; Udagawa, S.; Nakajima, S.; Kawai, K. Falconensins A, B, C, and D, new compounds related to azaphilone from *Emericella falconensis*. *Chem. Pharm. Bull.* **1992**, *40*, 3142–3144. [CrossRef]
19. Itabashi, T.; Nozawa, K.; Nakajima, S.; Kawai, K. A new azaphilone, falconensin H, from *Emericella falconensis*. *Chem. Pharm. Bull.* **1993**, *41*, 2040–2041. [CrossRef]
20. Itabashi, T.; Ogasawara, N.; Nozawa, K.; Kawai, K. Isolation and structures of new azaphilone derivatives, falconensins E−G, from *Emericella falconensis* and absolute configurations of falconensins A−G. *Chem. Pharm. Bull.* **1996**, *44*, 2213–2217. [CrossRef]
21. Yasukawa, K.; Itabashi, T.; Kawai, K.; Takido, M. Inhibitory effects of falconensins on 12-*O*-tetradecanoylphorbol-13-acetate-induced inflammatory ear edema in mice. *J. Nat. Med.* **2008**, *62*, 384–386. [CrossRef]
22. Agrawal, A.K.; Pielka, E.; Lipinski, A.; Jelen, M.; Kielan, W.; Agrawal, S. Clinical validation of nuclear factor kappa B expression in invasive breast cancer. *Tumour Biol.* **2018**, *40*. [CrossRef]
23. Ogasawara, N.; Kawai, K.I. Hydrogenated azaphilones from *Emericella falconensis* and *E. fruticulosa*. *Phytochemistry* **1998**, *47*, 1131–1135. [CrossRef]
24. Gao, J.M.; Yang, S.X.; Qin, J.C. Azaphilones: Chemistry and biology. *Chem. Rev.* **2013**, *113*, 4755–4811. [CrossRef]
25. Huang, H.; Wang, F.; Luo, M.; Chen, Y.; Song, Y.; Zhang, W.; Zhang, S.; Ju, J. Halogenated anthraquinones from the marine-derived fungus *Aspergillus* sp. SCSIO F063. *J. Nat. Prod.* **2012**, *75*, 1346–1352. [CrossRef]
26. Flack, H.D. On enantiomorph-polarity estimation. *Acta Crystallogr. Sect. A* **1983**, *39*, 876–881. [CrossRef]
27. Flack, H.D.; Bernardinelli, G. Absolute structure and absolute configuration. *Acta Crystallogr. Sect. A* **1999**, *55*, 908–915. [CrossRef] [PubMed]
28. Flack, H.D.; Bernardinelli, G. The use of X-ray crystallography to determine absolute configuration. *Chirality* **2008**, *20*, 681–690. [CrossRef] [PubMed]
29. Flack, H.D.; Sadki, M.; Thompson, A.L.; Watkin, D.J. Practical applications of averages and differences of Friedel opposites. *Acta Crystallogr. Sect. A* **2011**, *67*, 21–34. [CrossRef]
30. Osmanova, N.; Schultze, W.; Ayoub, N. Azaphilones: A class of fungal metabolites with diverse biological activities. *Phytochem. Rev.* **2010**, *9*, 315–342. [CrossRef]
31. Kjer, J.; Debbab, A.; Aly, A.H.; Proksch, P. Methods for isolation of marine-derived endophytic fungi and their bioactive secondary products. *Nat. Protoc.* **2010**, *5*, 479–490. [CrossRef]
32. Bruker. *Bruker AXS: Apex2, data collection program for the CCD area-detector system; SAINT, data reduction and frame integration program for the CCD area-detector system*; Bruker: Billerica, MA, USA, 2014−2015.
33. Sheldrick, G.M. *SADABS: Area-Detector Absorption Correction*; University of Goettingen: Goettingen, Germany, 1996.
34. Sheldrick, G.M. SHELXT–Integrated space-group and crystal-structure determination. *Acta Crystallogr. Sect. A Found. Adv.* **2015**, *71*, 3–8. [CrossRef]
35. Sheldrick, G.M. Crystal structure refinement with SHELXL. *Acta Crystallogr. Sect. C Struct. Chem.* **2015**, *71*, 3–8. [CrossRef]
36. Brandenburg, K. *Diamond (Version 4), Crystal and Molecular Structure Visualization*; Crystal Impact−K, Brandenburg & H. Putz Gbr: Bonn, Germany, 2009.

3.2 Supporting Information

Support Information

Azaphilones from the Red Sea Fungus *Aspergillus falconensis*

Dina H. El-Kashef [1,2], Fadia S. Youssef [1,3], Rudolf Hartmann [4], Tim-Oliver Knedel [5], Christoph Janiak [5], Wenhan Lin [6], Irene Reimche [7], Nicole Teusch [7], Zhen Liu [1,*] and Peter Proksch [1,8,*]

[1] Institute of Pharmaceutical Biology and Biotechnology, Heinrich-Heine-University Duesseldorf, 40225 Duesseldorf, Germany; dina.elkashef@mu.edu.eg (D.H.E.); fadiayoussef@pharma.asu.edu.eg (F.S.Y.)
[2] Department of Pharmacognosy, Faculty of Pharmacy, Minia University, 61519 Minia, Egypt;
[3] Department of Pharmacognosy, Faculty of Pharmacy, Ain Shams University, Abbassia, 11566 Cairo, Egypt;
[4] Institute of Complex Systems: Strukturbiochemie, Forschungszentrum Jülich GmbH, ICS-6, 52425 Jülich, Germany; r.hartmann@fz-juelich.de (R.H.)
[5] Institut für Anorganische Chemie und Strukturchemie, Heinrich-Heine-Universität Düsseldorf, 40225 Düsseldorf, Germany; tim-oliver.knedel@hhu.de (T.O.K.); janiak@uni-duesseldorf.de (C.J.)
[6] State Key Laboratory of Natural and Biomimetic Drugs, Peking University, Beijing 100191, China; whlin@bjmu.edu.cn (W.L.)
[7] Department of Biomedical Sciences, Institute of Health Research and Education, University of Osnabrück, Germany; irene.reimche@uni-osnabrueck.de (I.R.); nicole.teusch@uni-osnabrueck.de (N.T.)
[8] Hubei Key Laboratory of Natural Products Research and Development, College of Biological and Pharmaceutical Sciences, China Three Gorges University, Yichang 443002, People's Republic of China;
* Correspondence: zhenfeizi0@sina.com (Z.L.); proksch@uni-duesseldorf.de (P.P.); Tel.: +49-211-81-14163

Contents

Figure S1. UV spectrum of compound **1**.

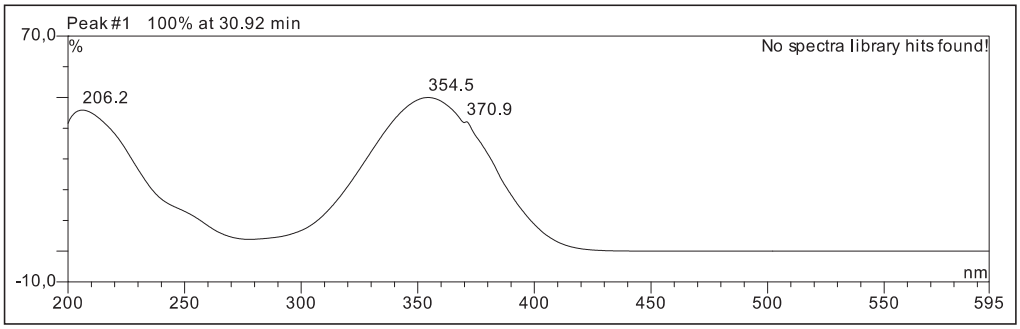

Figure S2. HRESIMS of compound **1**.

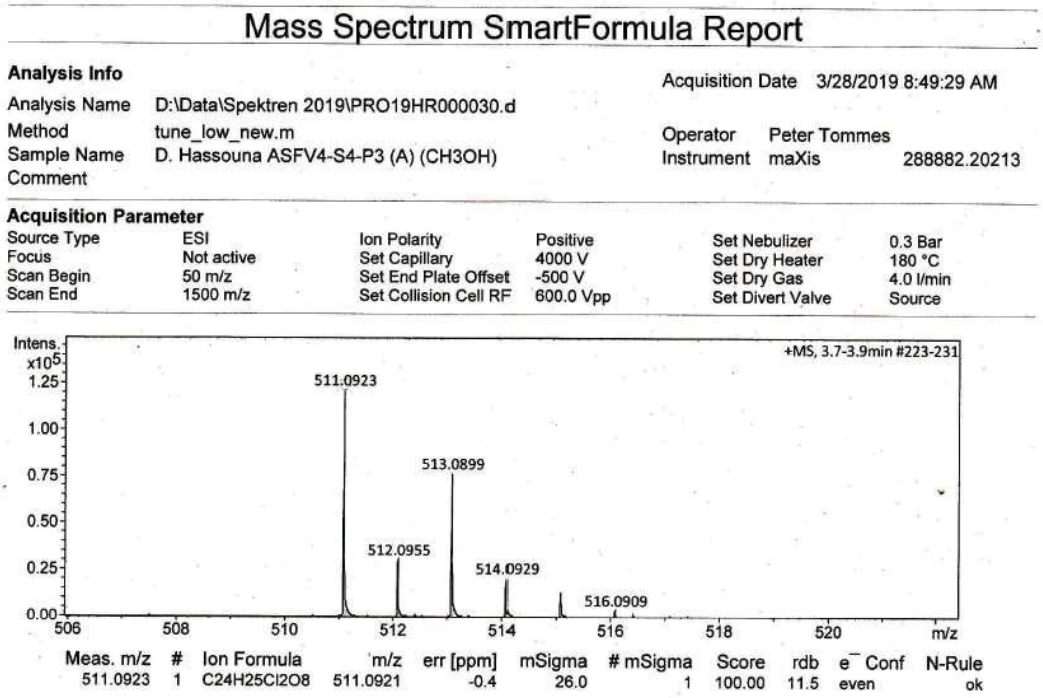

Figure S3. ^{1}H NMR (600 MHz, $CDCl_3$) spectrum of compound **1**.

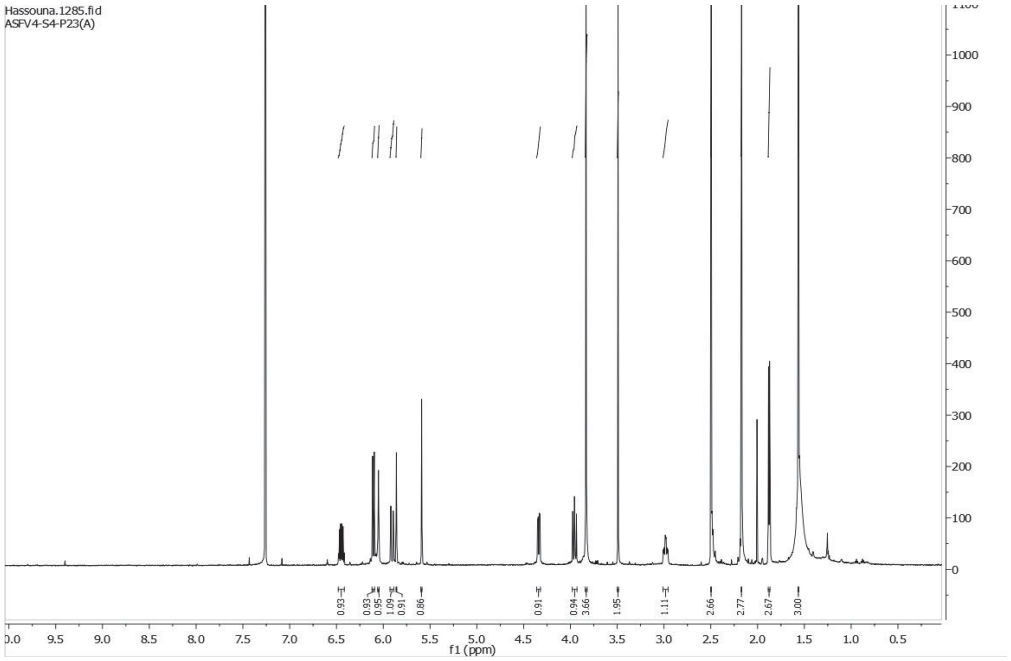

5

Figure S4. COSY (600 MHz, $CDCl_3$) spectrum of compound **1**.

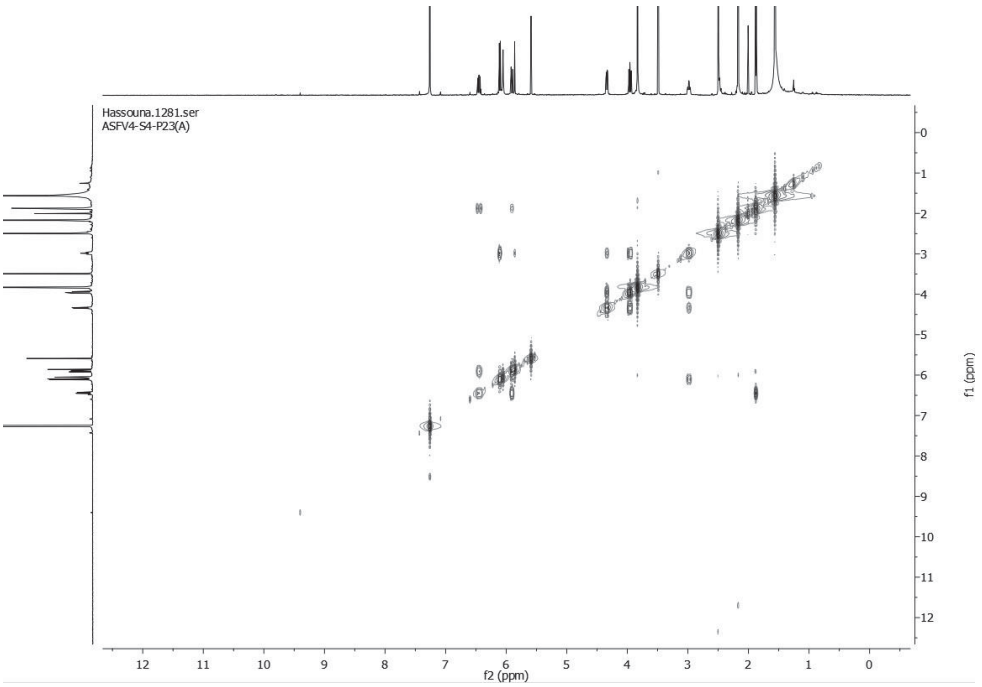

6

Figure S5. HSQC (600 MHz/150 MHz, $CDCl_3$) spectrum of compound **1**.

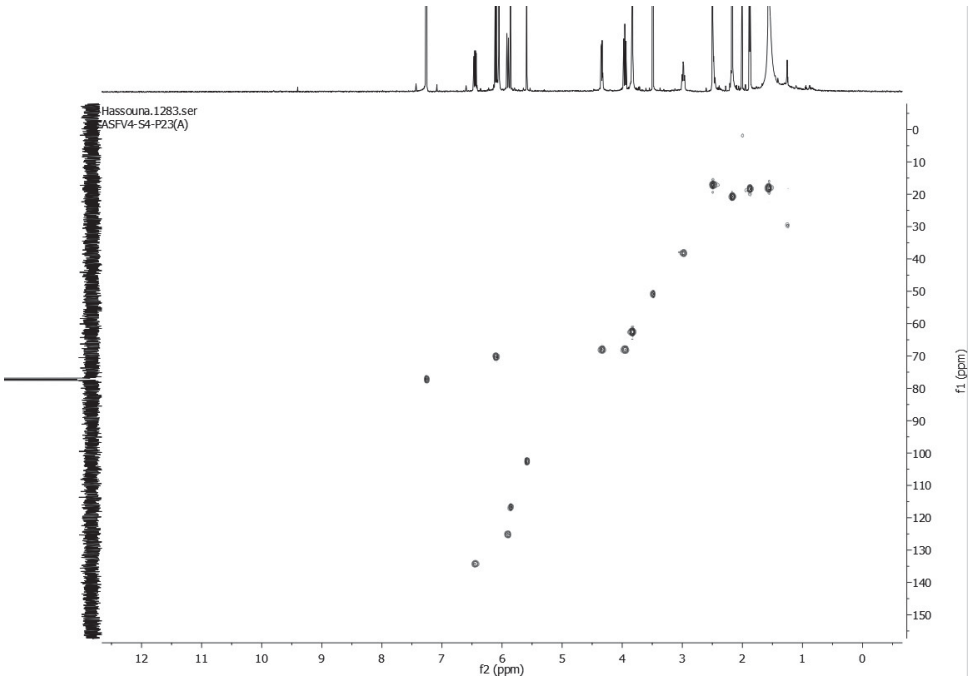

7

Figure S6. HMBC (600 MHz/150 MHz, $CDCl_3$) spectrum of compound **1**.

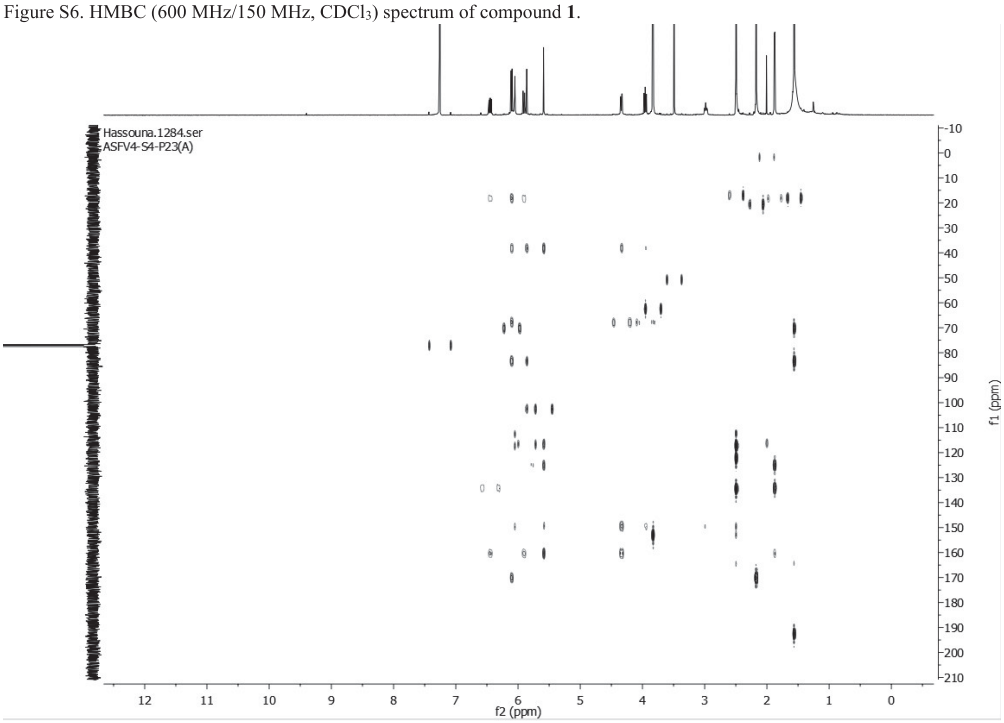

8

Figure S7. ROESY (600 MHz, $CDCl_3$) spectrum of compound **1**.

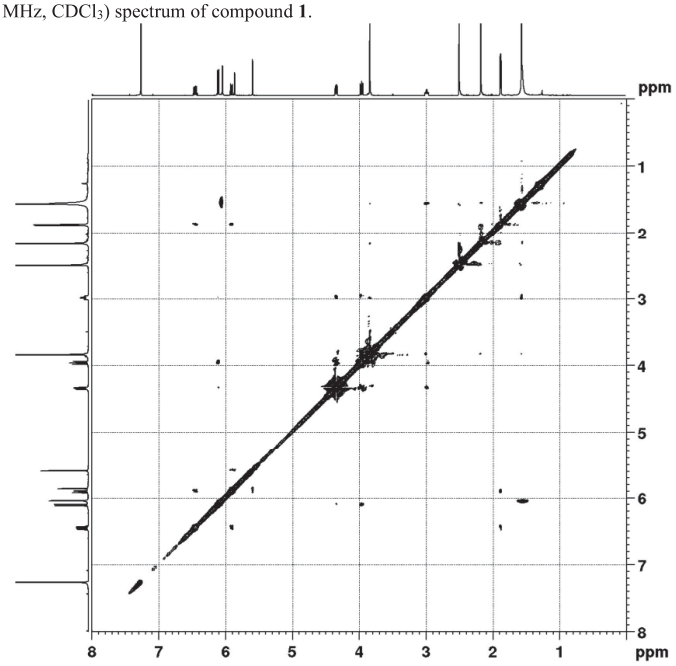

Figure S8. UV spectrum of compound **2**.

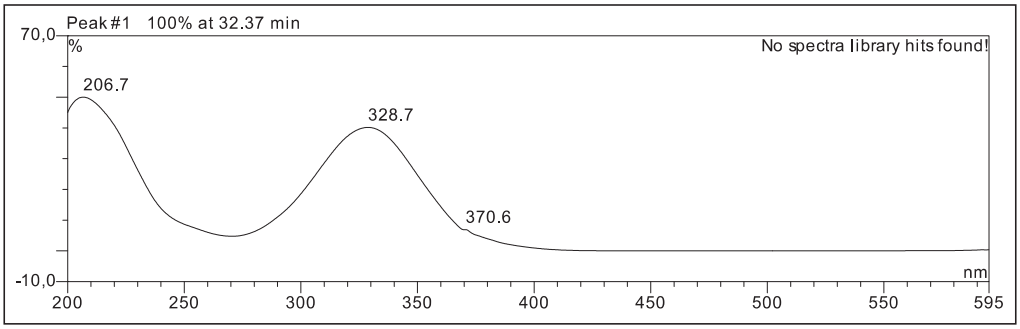

Figure S9. HRESIMS of compound **2**.

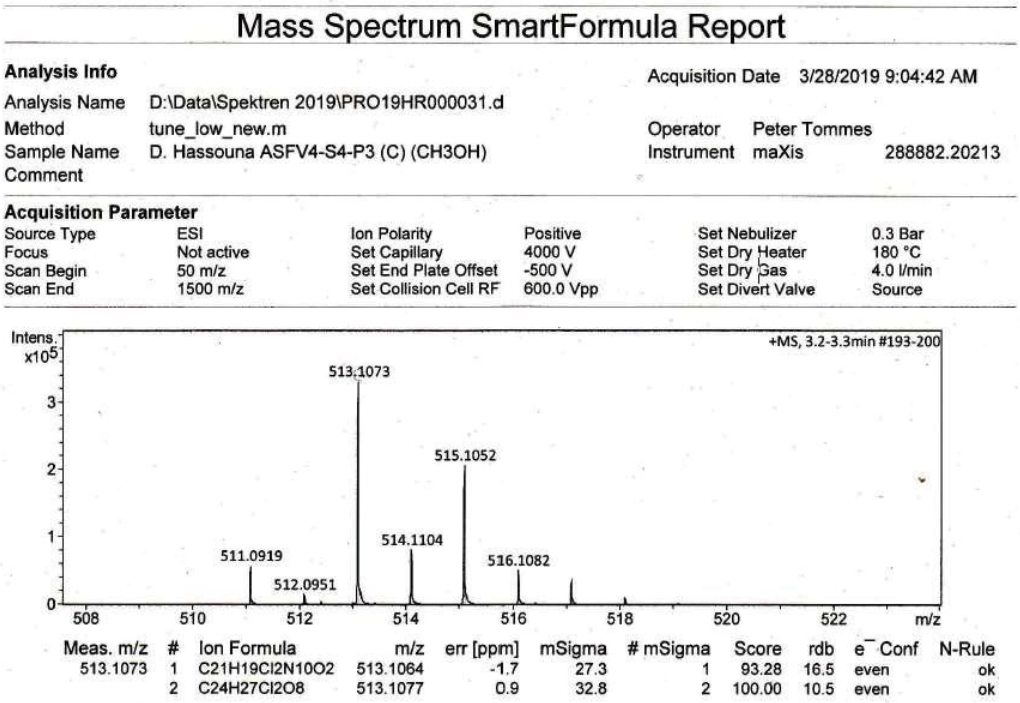

Mass Spectrum SmartFormula Report

Analysis Info

Analysis Name	D:\Data\Spektren 2019\PRO19HR000031.d	Acquisition Date	3/28/2019 9:04:42 AM
Method	tune_low_new.m	Operator	Peter Tommes
Sample Name	D. Hassouna ASFV4-S4-P3 (C) (CH3OH)	Instrument	maXis 288882.20213
Comment			

Acquisition Parameter

Source Type	ESI	Ion Polarity	Positive	Set Nebulizer	0.3 Bar
Focus	Not active	Set Capillary	4000 V	Set Dry Heater	180 °C
Scan Begin	50 m/z	Set End Plate Offset	-500 V	Set Dry Gas	4.0 l/min
Scan End	1500 m/z	Set Collision Cell RF	600.0 Vpp	Set Divert Valve	Source

Meas. m/z	#	Ion Formula	m/z	err [ppm]	mSigma	# mSigma	Score	rdb	e⁻ Conf	N-Rule
513.1073	1	C21H19Cl2N10O2	513.1064	-1.7	27.3	1	93.28	16.5	even	ok
	2	C24H27Cl2O8	513.1077	0.9	32.8	2	100.00	10.5	even	ok

Figure S10. ^{1}H NMR (600 MHz, $CDCl_3$) spectrum of compound **2**.

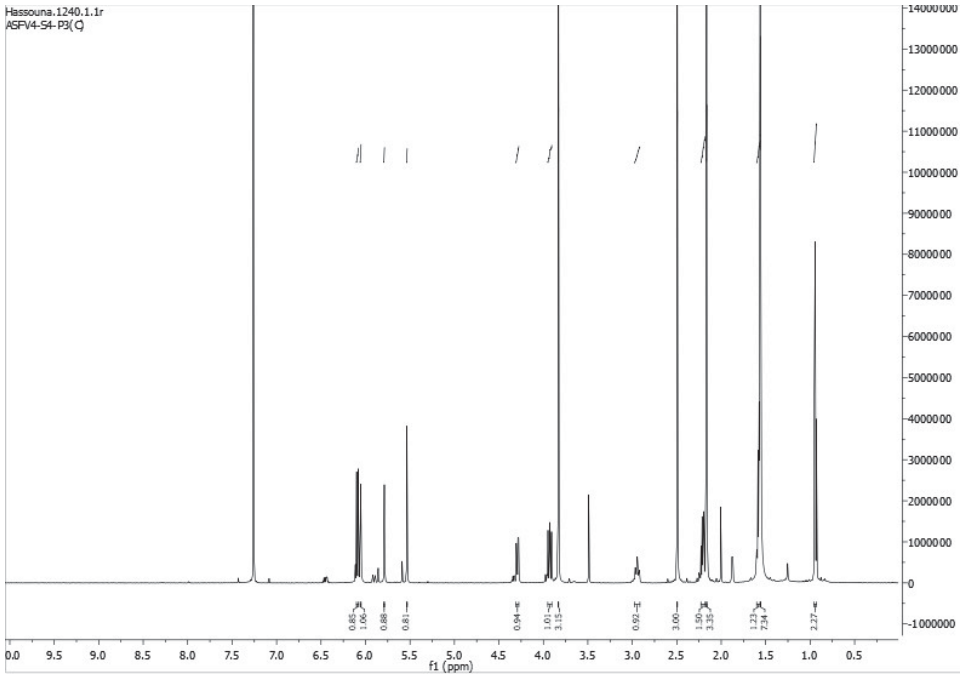

11

Figure S11. COSY (600 MHz, $CDCl_3$) spectrum of compound **2**.

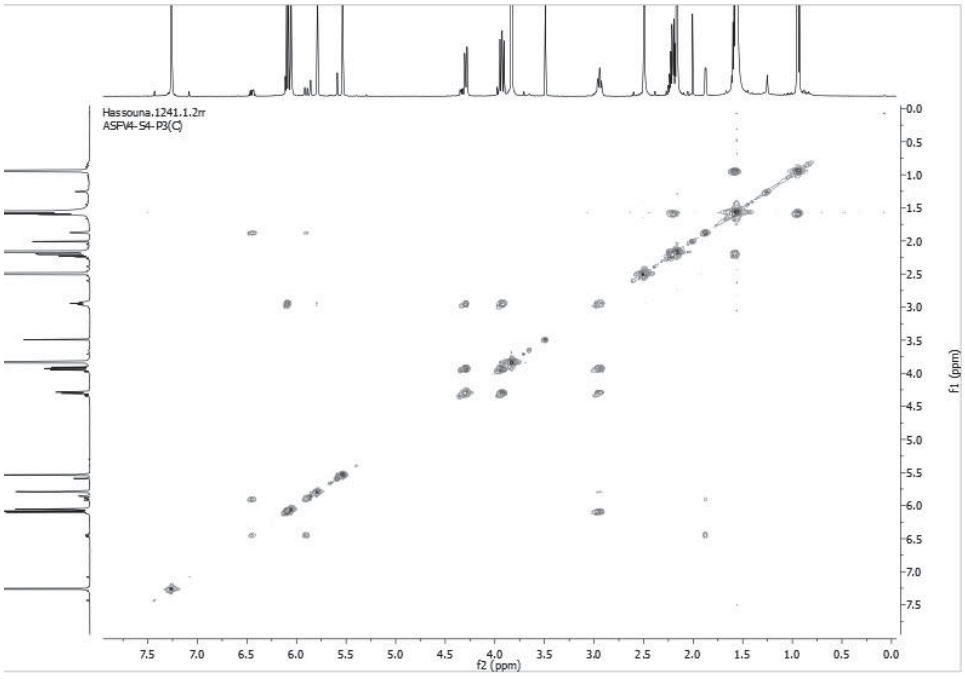

12

Figure S12. HSQC (600 MHz/150 MHz, $CDCl_3$) spectrum of compound **2**.

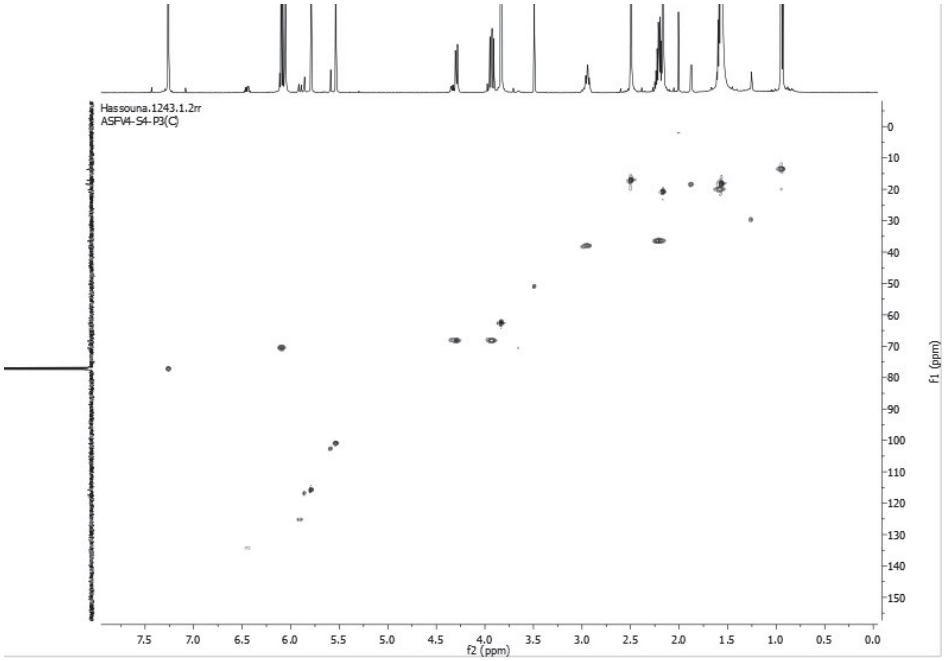

13

Figure S13. HMBC (600 MHz/150 MHz, $CDCl_3$) spectrum of compound **2**.

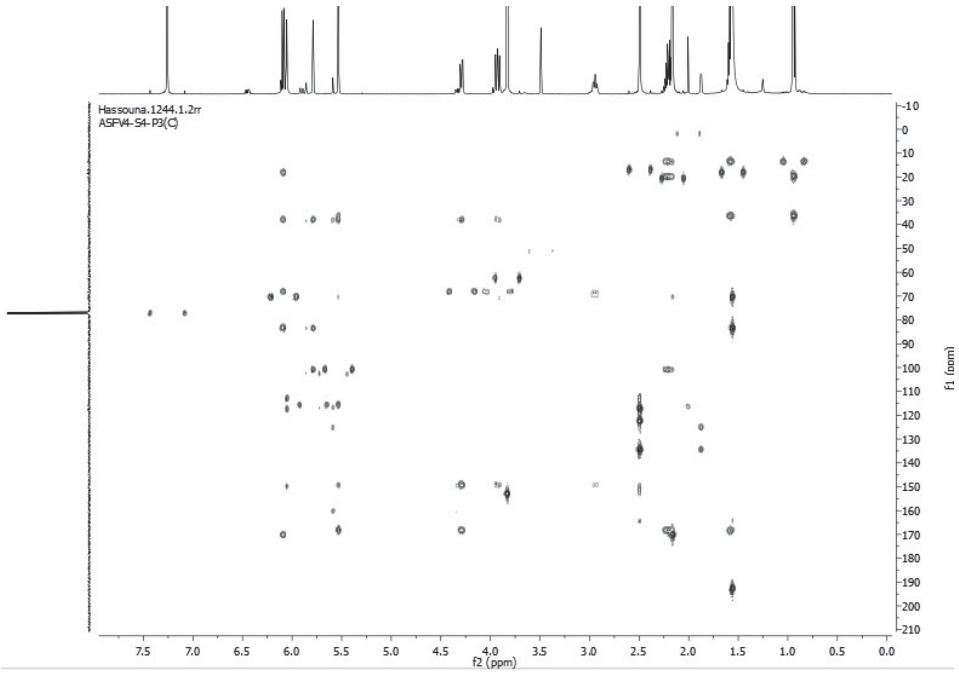

14

Figure S14. ROESY (600 MHz, $CDCl_3$) spectrum of compound **2**.

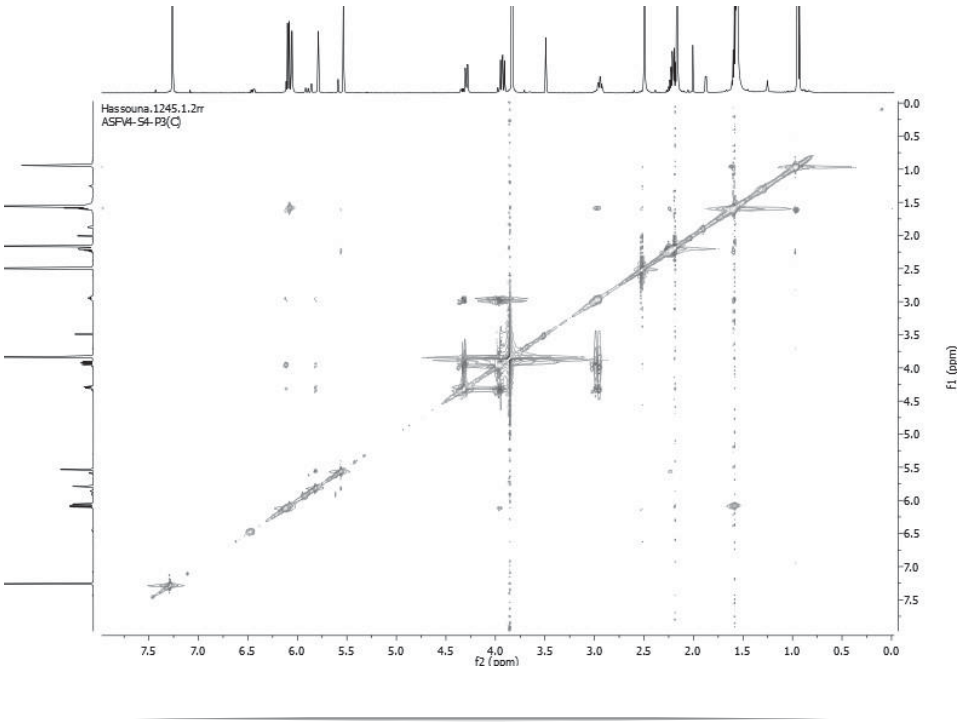

15

Figure S15. UV spectrum of compound **7**.

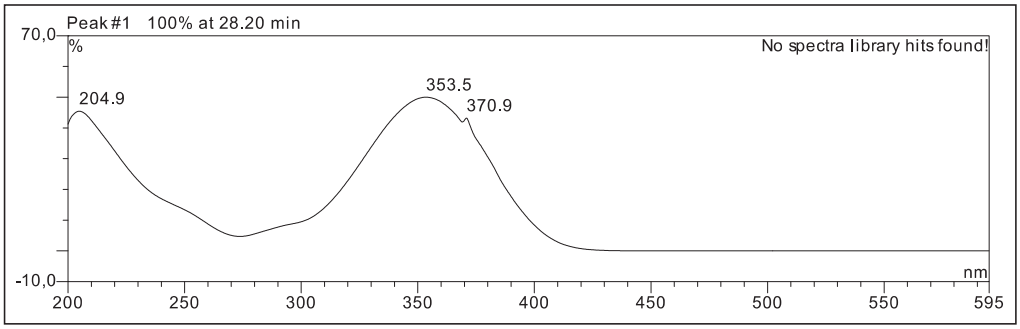

Figure S16. HRESIMS of compound **7**.

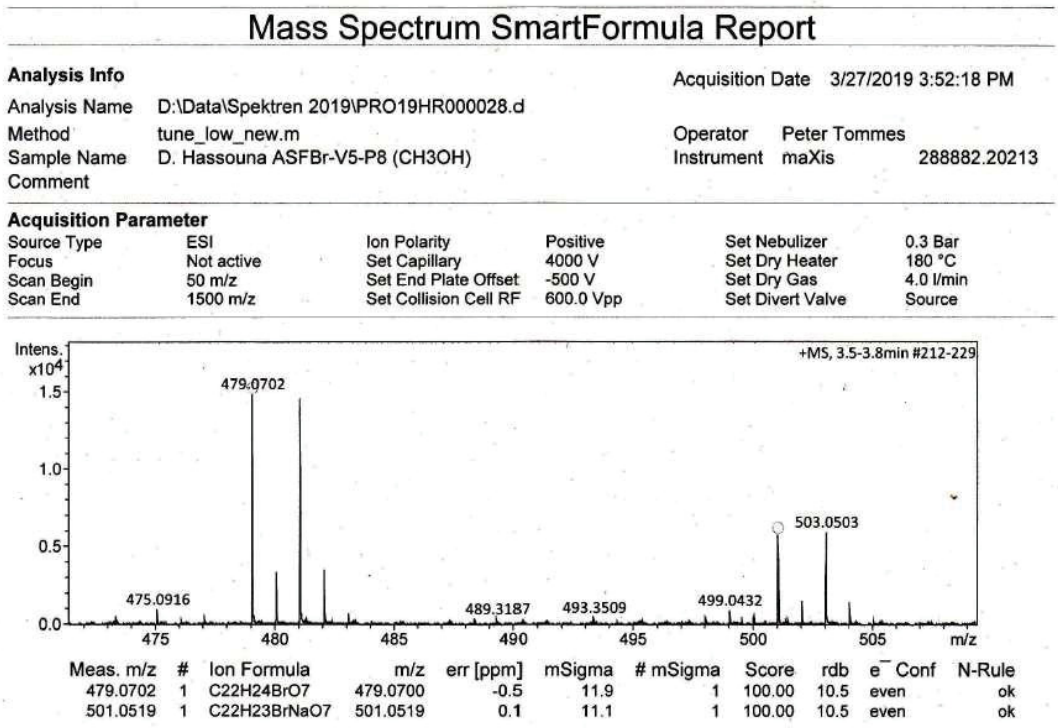

Figure S17. ^{1}H NMR (700 MHz, $CDCl_3$) spectrum of compound **7**.

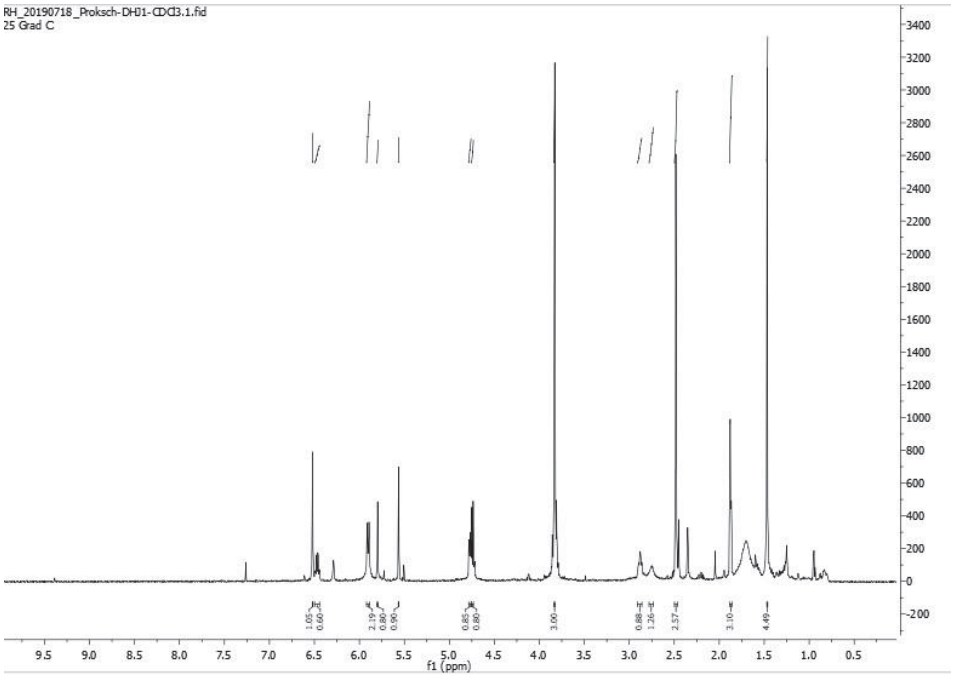

17

Figure S18. ^{13}C NMR (175 MHz, $CDCl_3$) spectrum of compound **7**.

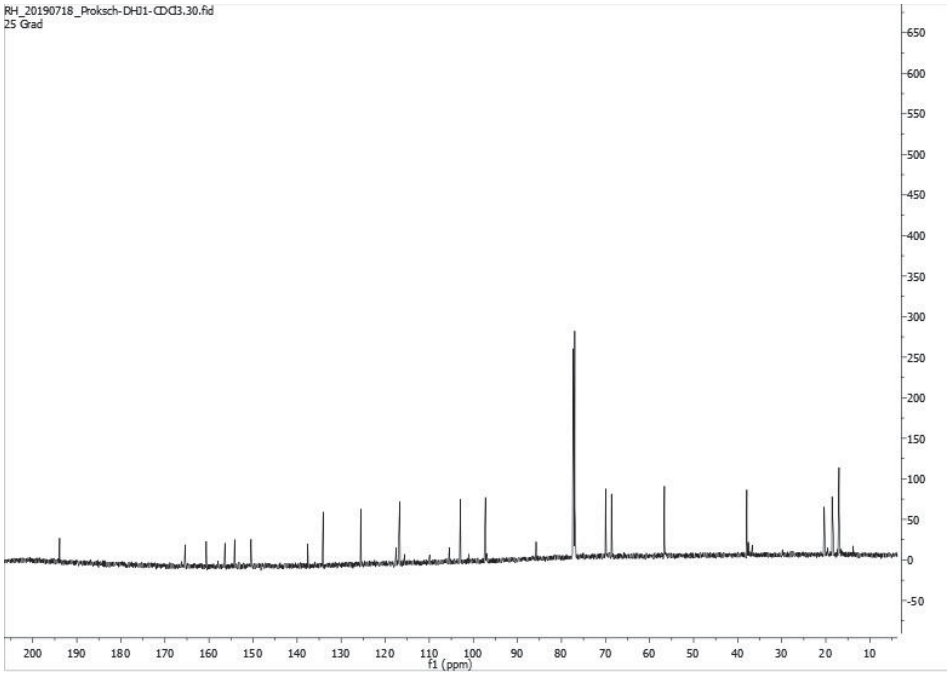

18

Figure S19. COSY (700 MHz, $CDCl_3$) spectrum of compound **7**.

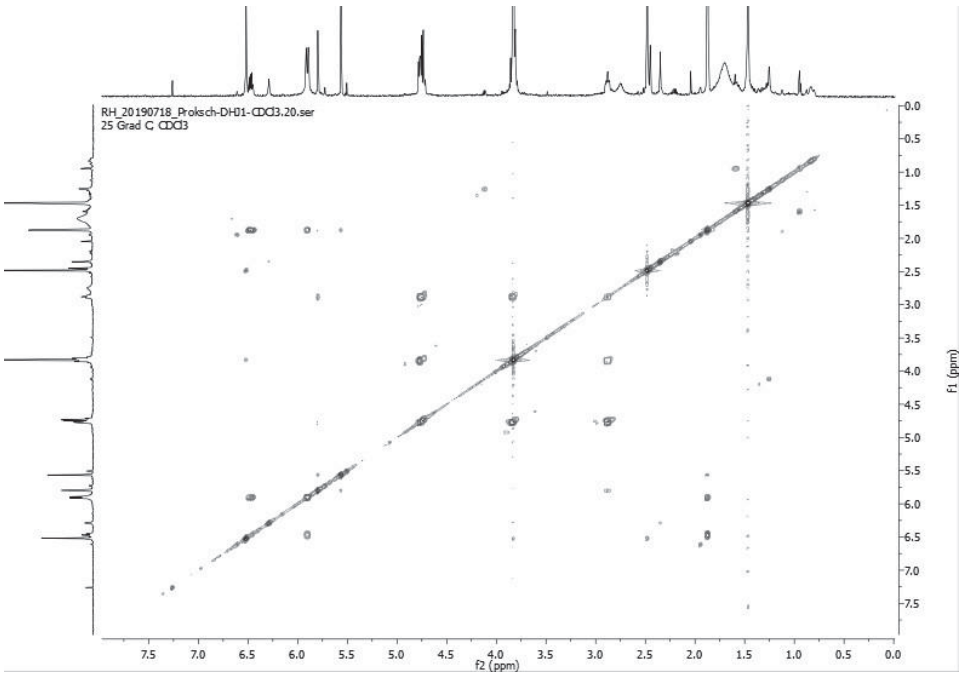

19

Figure S20. HSQC (700 MHz/175 MHz, $CDCl_3$) spectrum of compound **7**.

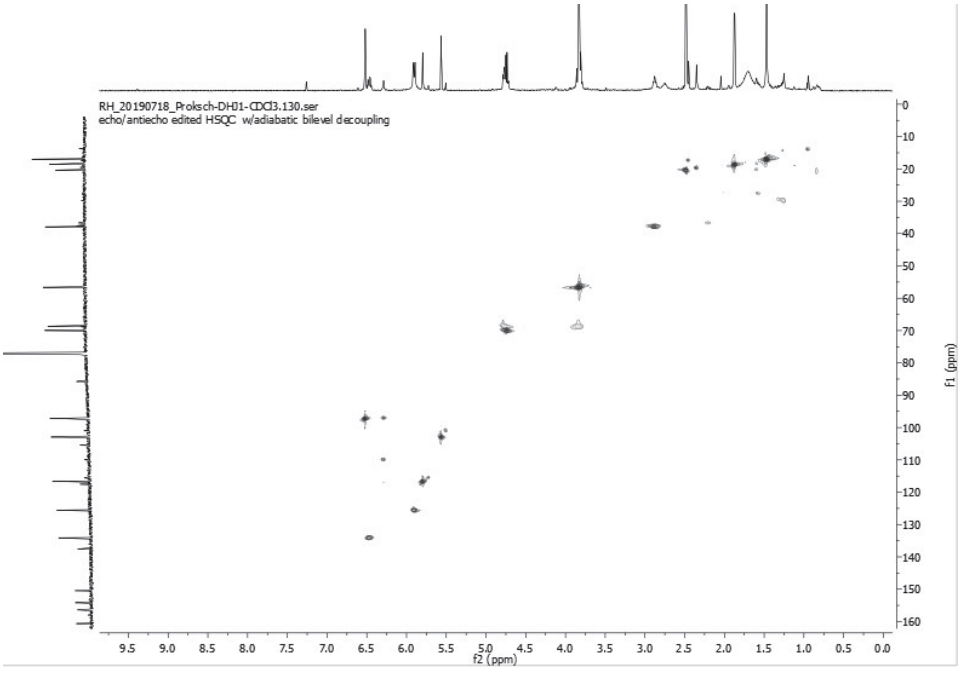

20

Figure S21. HMBC (700 MHz/175 MHz, $CDCl_3$) spectrum of compound **7**.

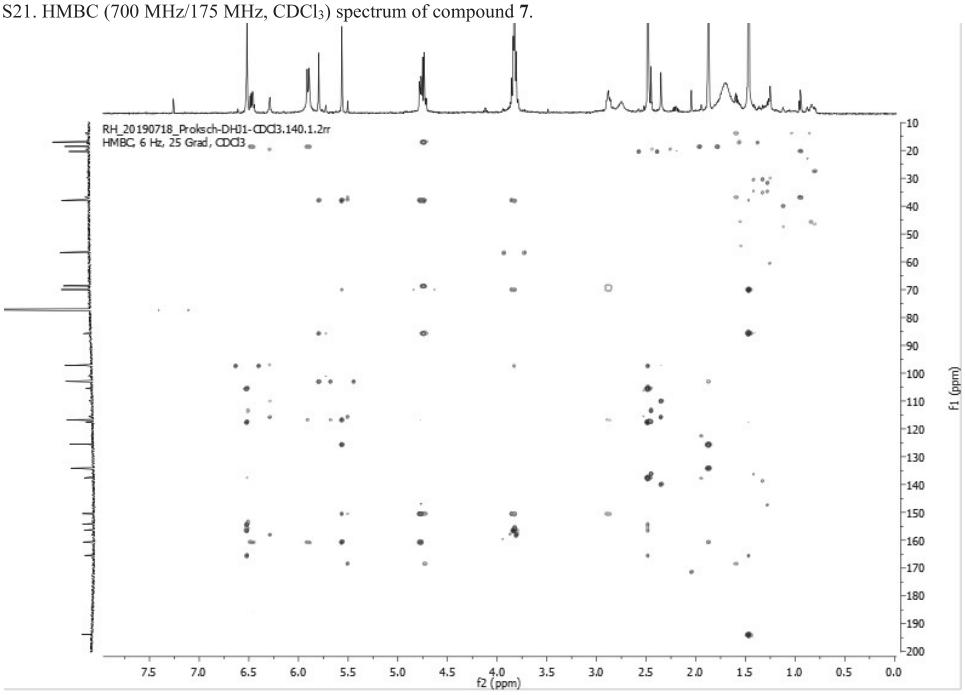

21

Figure S22. ROESY (700 MHz/175 MHz, $CDCl_3$) spectrum of compound **7**.

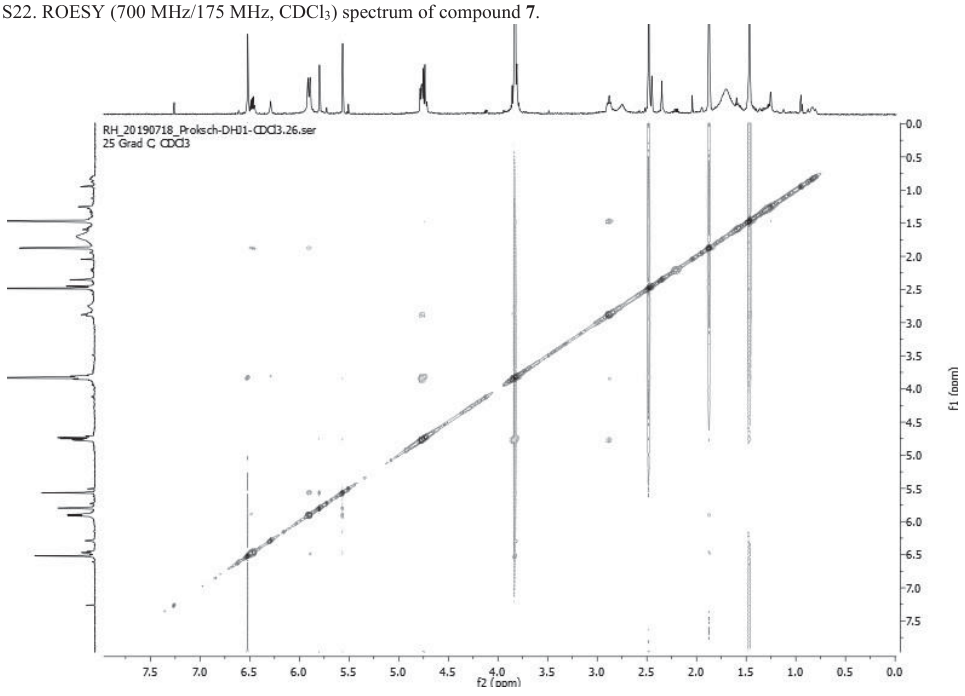

22

Figure S23. UV spectrum of compound **8**.

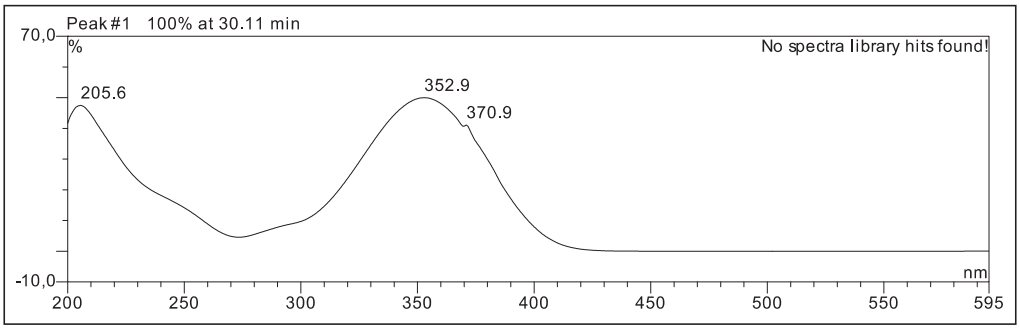

Figure S24. HRESIMS of compound **8**.

Mass Spectrum SmartFormula Report

Analysis Info

Analysis Name	D:\Data\Spektren 2019\PRO19HR000198.d	Acquisition Date	8/30/2019 12:45:23 PM
Method	tune_low_new.m	Operator	Peter Tommes
Sample Name	Hassouna ASFBr-V5-P10 II (CH3OH)	Instrument	maXis 288882.20213
Comment	25 ul in 1 ml		

Acquisition Parameter

Source Type	ESI	Ion Polarity	Positive	Set Nebulizer	0.3 Bar
Focus	Not active	Set Capillary	4000 V	Set Dry Heater	180 °C
Scan Begin	50 m/z	Set End Plate Offset	-500 V	Set Dry Gas	4.0 l/min
Scan End	1500 m/z	Set Collision Cell RF	600.0 Vpp	Set Divert Valve	Source

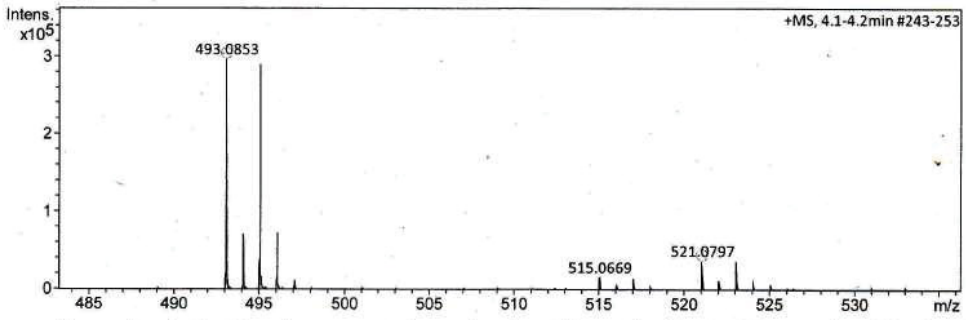

Meas. m/z	#	Ion Formula	m/z	err [ppm]	mSigma	# mSigma	Score	rdb	e⁻ Conf	N-Rule
256.9806	1	C10H10BrO3	256.9808	0.6	22.8	1	100.00	5.5	even	ok
493.0853	1	C20H18BrN10O	493.0843	-2.0	12.1	1	74.41	16.5	even	ok
	2	C23H26BrO7	493.0856	0.8	12.7	2	100.00	10.5	even	ok
521.0797	1	C24H26BrO8	521.0806	1.6	48.1	1	98.38	11.5	even	ok
	2	C21H18BrN10O2	521.0792	-1.0	52.4	2	100.00	17.5	even	ok

Figure S25. ^{1}H NMR (600 MHz, $CDCl_3$) spectrum of compound **8**.

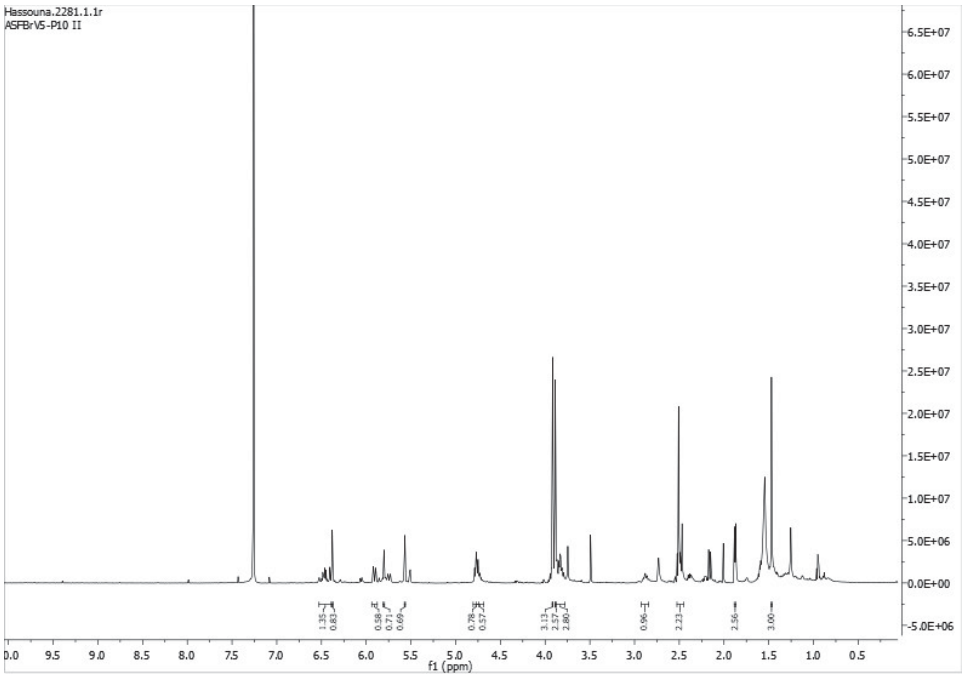

24

Figure S26. COSY (600 MHz, $CDCl_3$) spectrum of compound **8**.

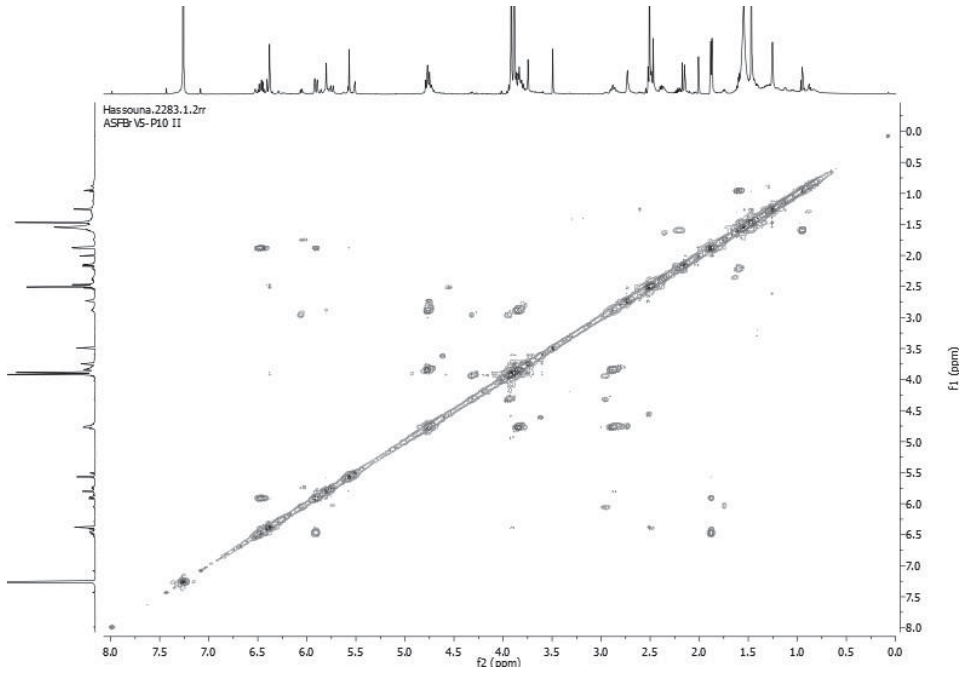

25

Figure S27. HSQC (600 MHz/150 MHz, $CDCl_3$) spectrum of compound **8**.

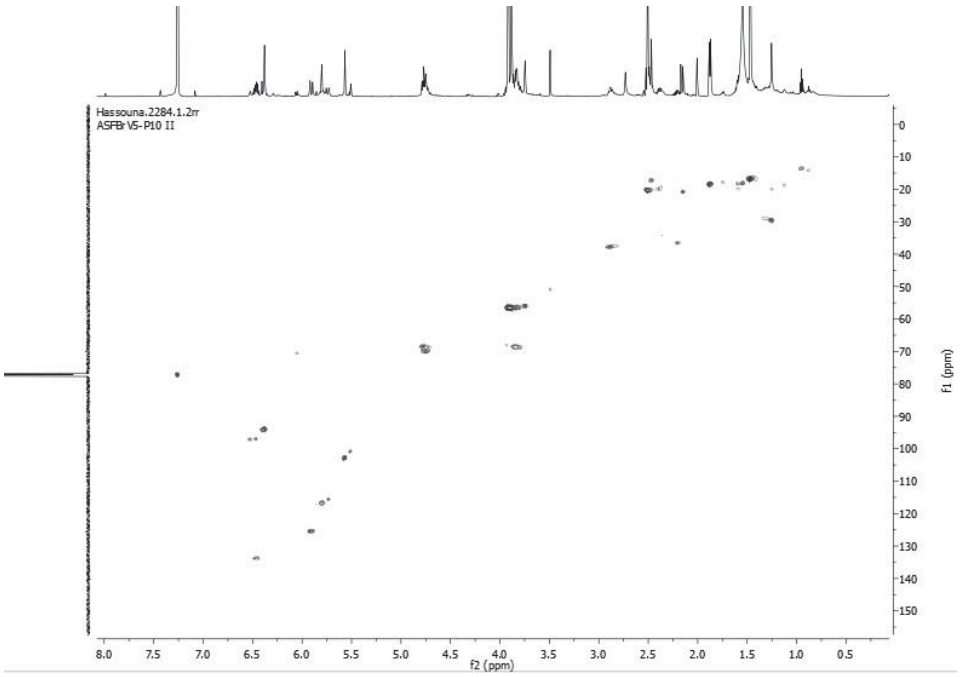

26

Figure S28. HMBC (600 MHz/150 MHz, $CDCl_3$) spectrum of compound **8**.

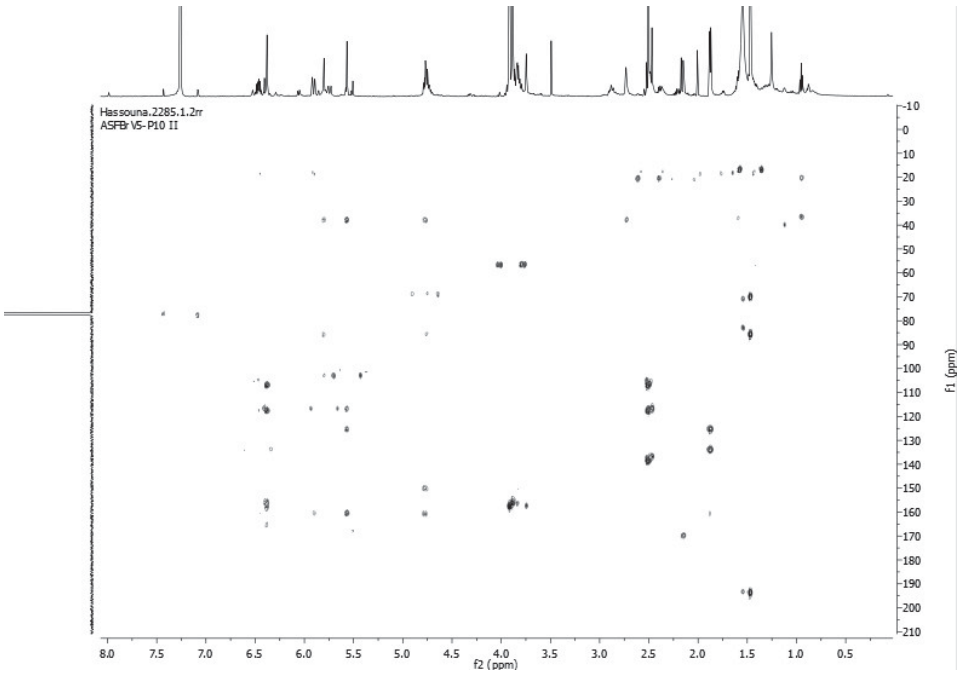

27

Figure S29. ROESY (600 MHz, $CDCl_3$) spectrum of compound **8**.

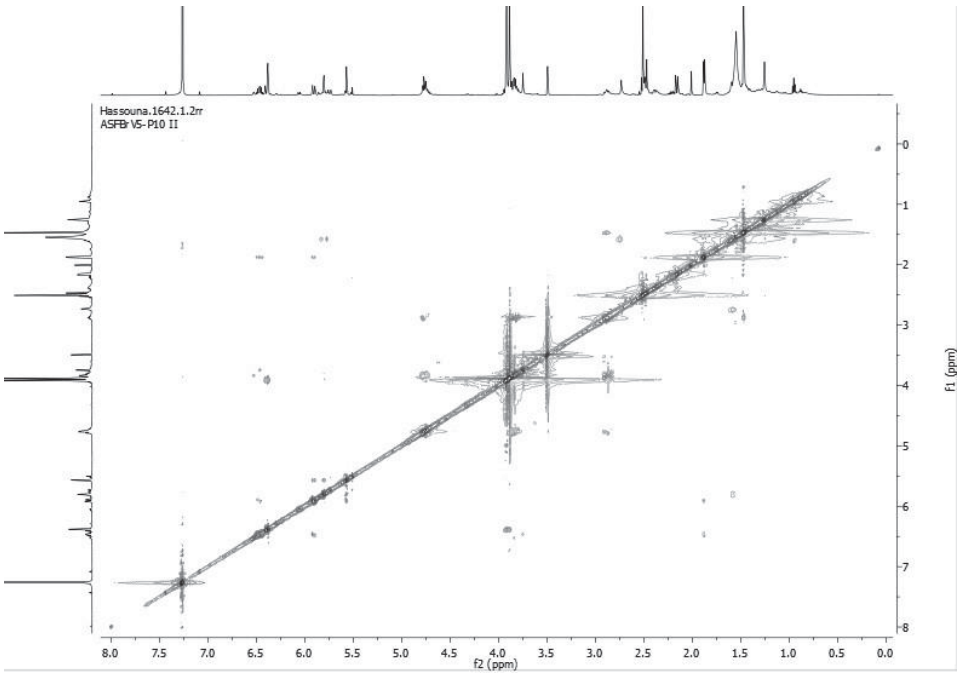

28

Figure S30. UV spectrum of compound **9**.

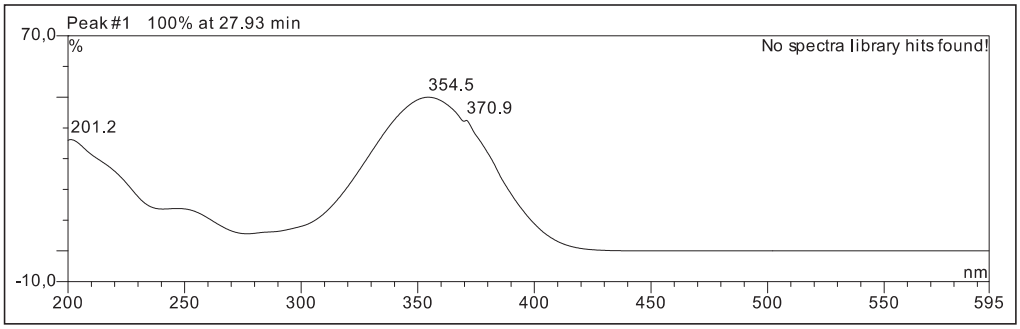

Figure S31. HRESIMS of compound **9**.

Mass Spectrum SmartFormula Report

Analysis Info

Analysis Name	D:\Data\Spektren 2019\PRO19HR000029.d	Acquisition Date	3/28/2019 8:30:17 AM
Method	tune_low_new.m	Operator	Peter Tommes
Sample Name	D. Hassouna ASFBr-V5-P9 (CH3OH)	Instrument	maXis 288882.20213
Comment			

Acquisition Parameter

Source Type	ESI	Ion Polarity	Positive	Set Nebulizer	0.3 Bar
Focus	Not active	Set Capillary	4000 V	Set Dry Heater	180 °C
Scan Begin	50 m/z	Set End Plate Offset	-500 V	Set Dry Gas	4.0 l/min
Scan End	1500 m/z	Set Collision Cell RF	600.0 Vpp	Set Divert Valve	Source

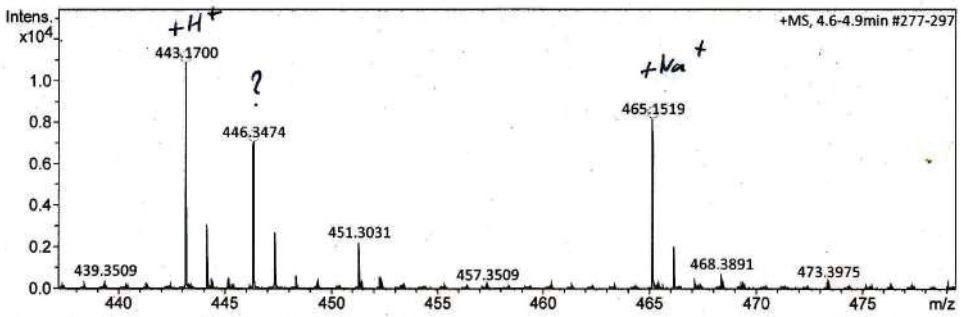

Meas. m/z	#	Ion Formula	m/z	err [ppm]	mSigma	# mSigma	Score	rdb	e⁻ Conf	N-Rule
443.1700	1	C24H27O8	443.1700	0.0	9.7	1	100.00	11.5	even	ok
446.3474	1	C24H48NO6	446.3476	0.6	66.1	1	100.00	1.5	even	ok
	2	C23H45N5NaO2	446.3465	-1.8	66.8	2	75.02	3.5	even	ok
465.1519	1	C24H26NaO8	465.1520	0.3	10.2	1	100.00	11.5	even	ok

Figure S32. ^{1}H NMR (700 MHz, $CDCl_3$) spectrum of compound **9**.

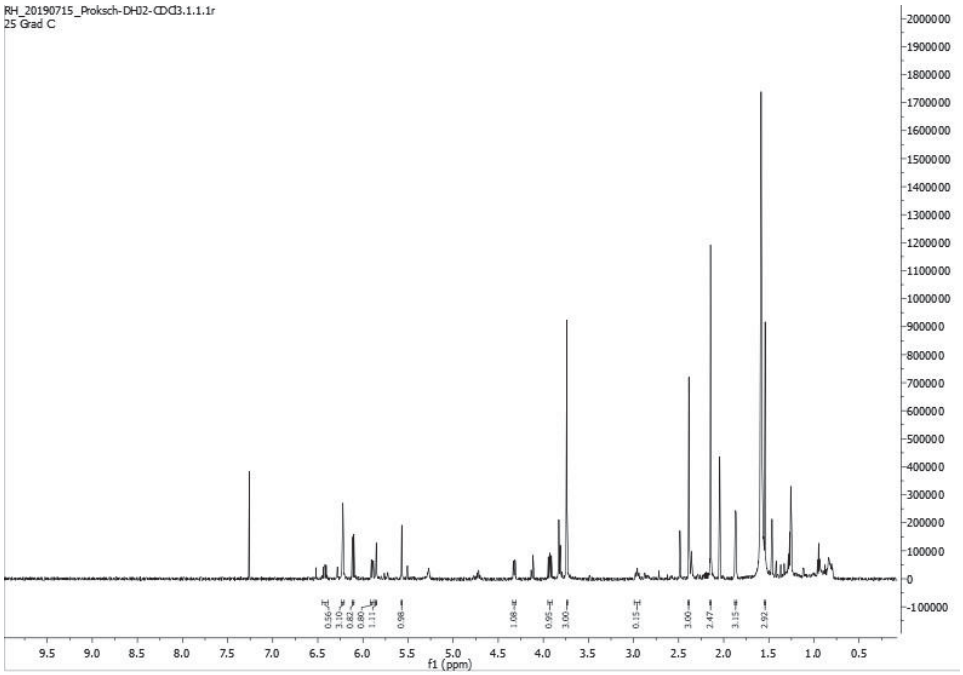

30

Figure S33. ^{13}C NMR (175 MHz, $CDCl_3$) spectrum of compound **9**.

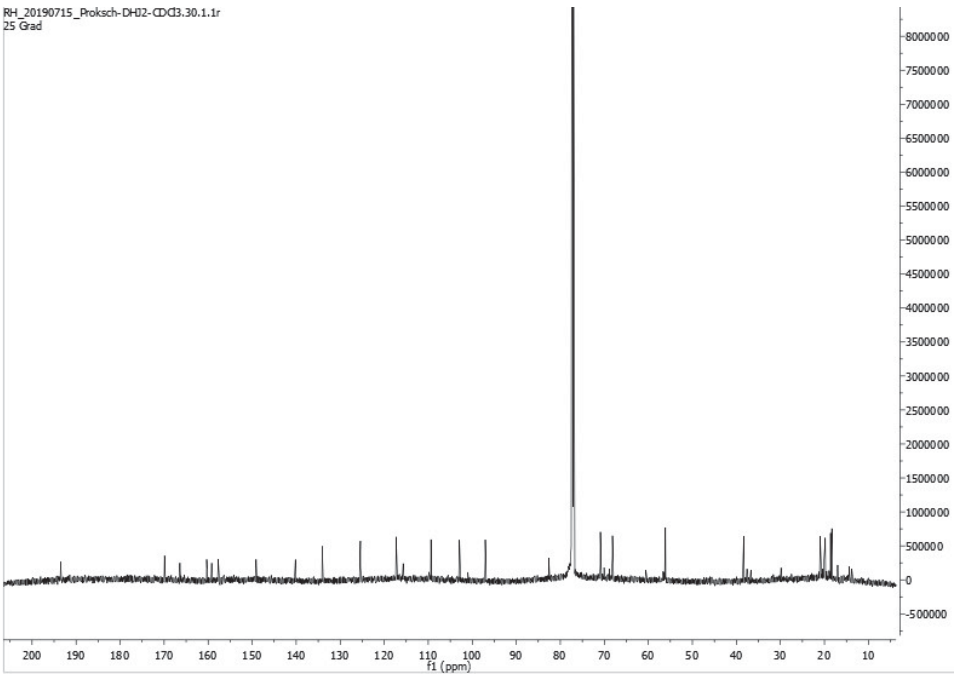

31

Figure S34. COSY (700 MHz, $CDCl_3$) spectrum of compound **9**.

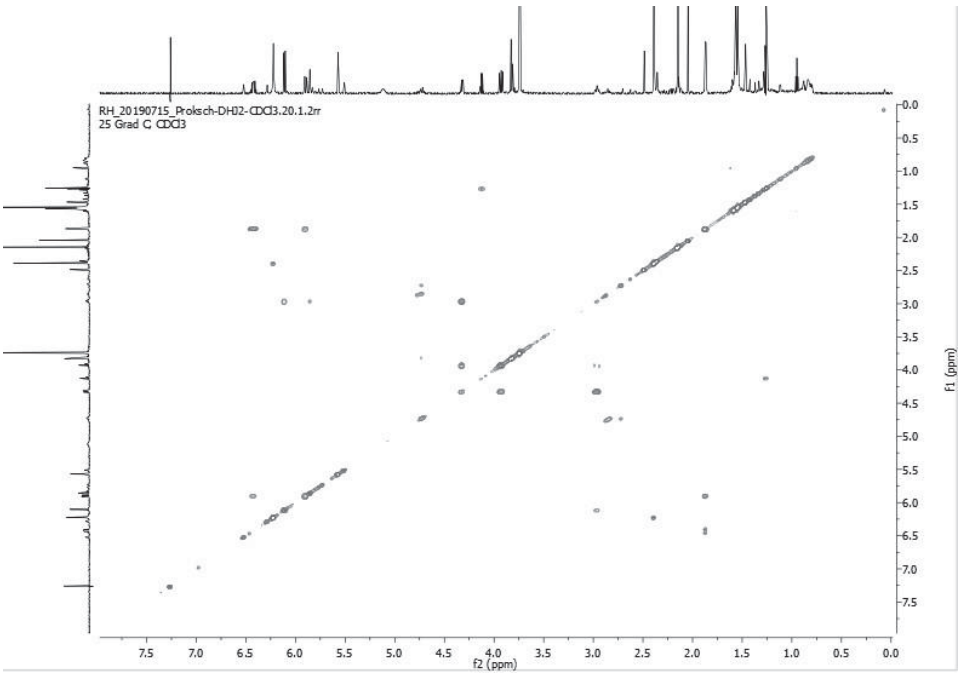

32

Figure S35. HSQC (700 MHz/175 MHz, $CDCl_3$) spectrum of compound **9**.

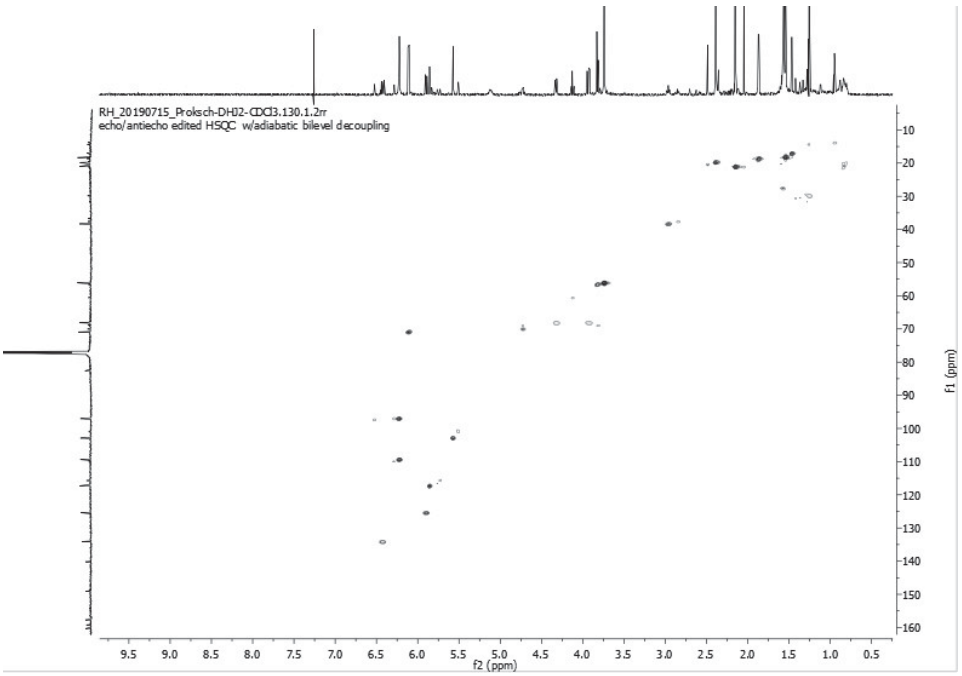

33

Figure S36. HMBC (700 MHz/175 MHz, $CDCl_3$) spectrum of compound **9**.

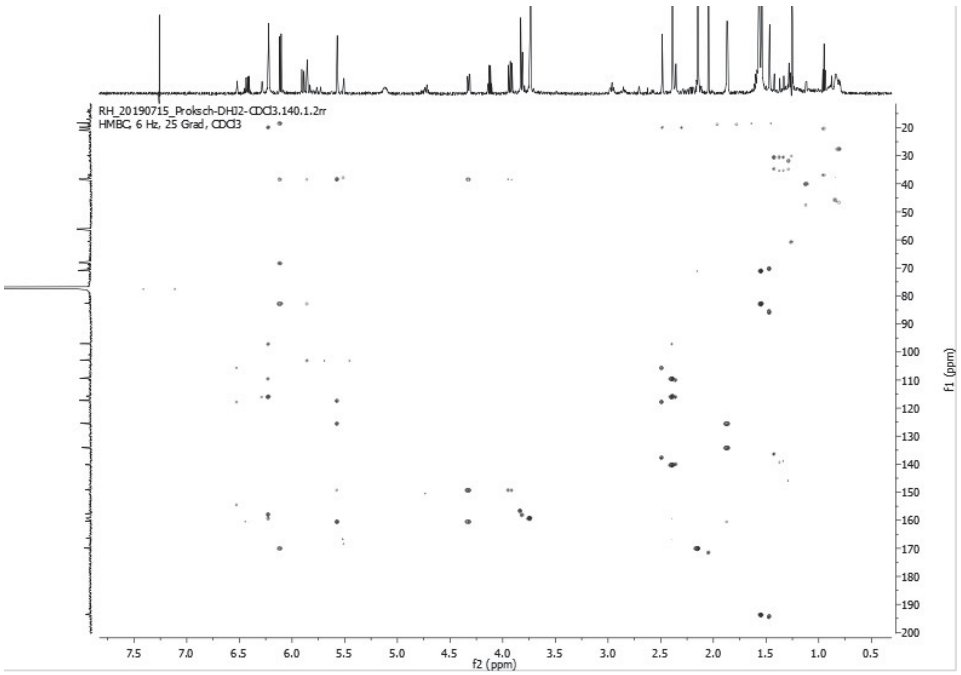

34

Figure S37. ROESY (700 MHz, $CDCl_3$) spectrum of compound **9**.

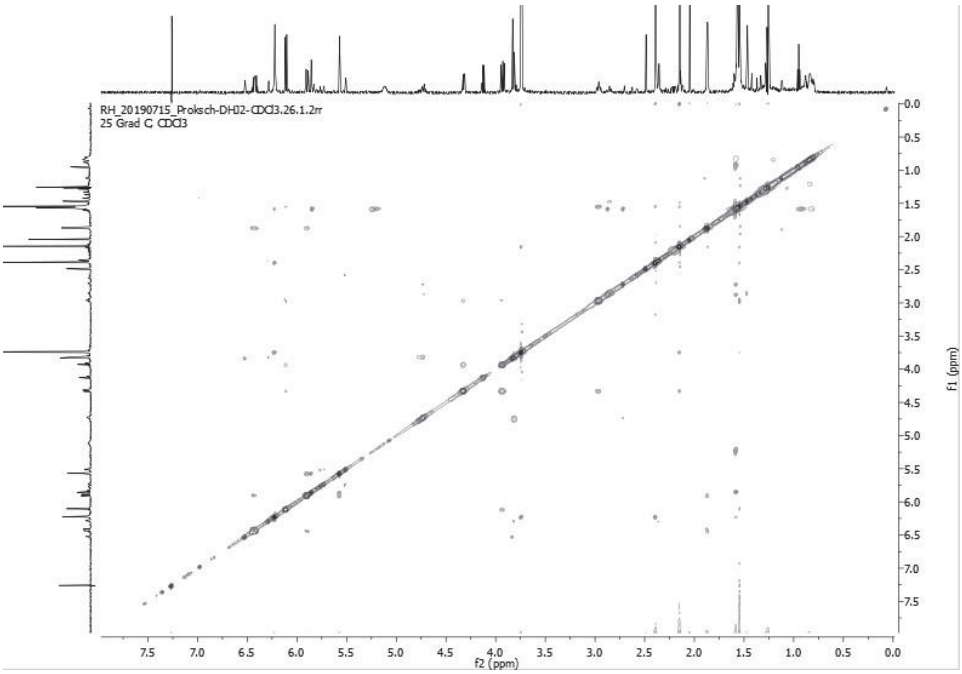

35

Figure S38. Section of the packing diagram over an extended unit cell of compound **5** (50% thermal elipsoids) determined by single-crystal x-ray diffraction. Hydrogen bonds are shown in dashed yellow lines.

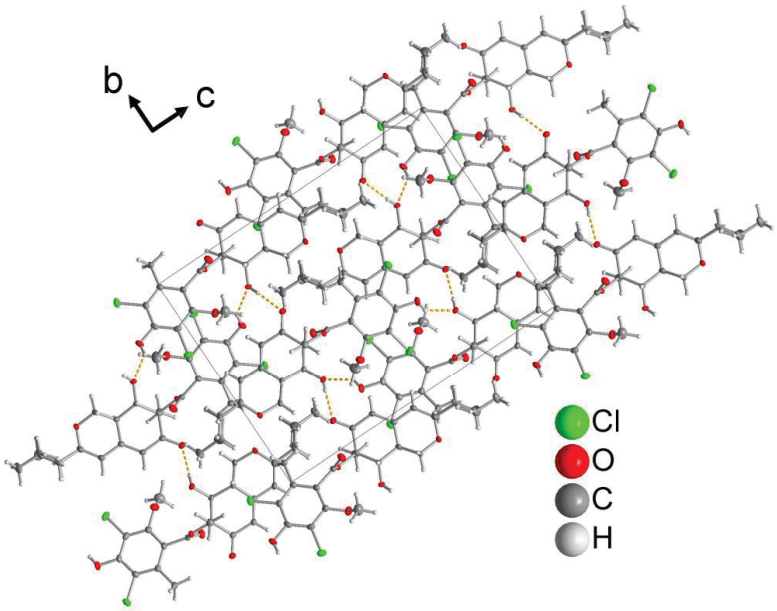

36

Figure S39. NFκB inhibitory potential of the compounds **1**, **3, 4**, **5**, **6**, **7**, **8**, **9** and **11**. Quantification of NFκB-dependent luciferase activity was performed by NFκB inhibition assay. In short, NFκB-MDA-MB-231 cells were pre-treated with the twofold serial diluted compound starting with 400 µM (**3**, **6**, **11**) or 200 µM to 0.78 µM (**1**, **4**, **5**, **7**, **9**, **11**) or left untreated (**Neg**). TNFα incubation induced NFκB activation, with untreated cells showing the maximal NFκB activity (**TNFα**). For RLU normalization, the RLU at the lowest concentration (0.78 µM) in each individual experiment was set as 100 %. Each data point represents the mean of at least three independent experiments. After the logarithmic transformation of the compound concentration in molar, nonlinear regression analysis without curve fitting was applied for data illustration using GraphPad Prism (GraphPad Software, San Diego, USA; Version 8.1.2). (M) Compound concentration in molar.

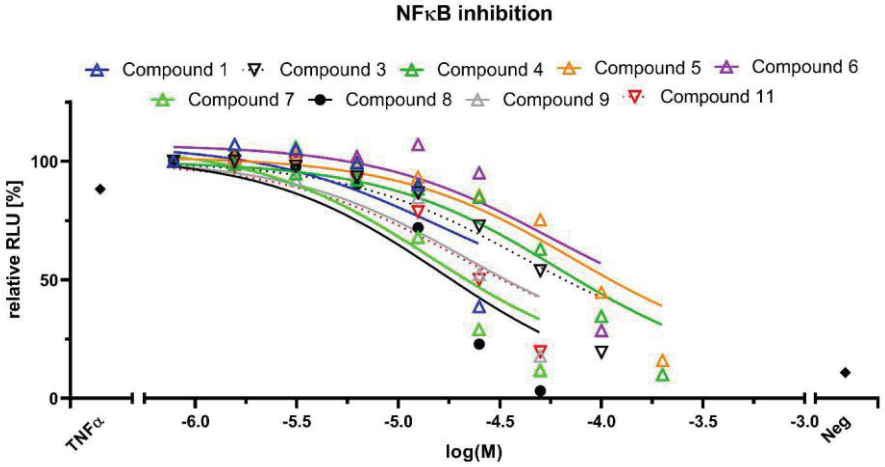

37

Figure S40. Potency in NFκB inhibition versus cytotoxicity. The scatterplot displays the pIC50 for the cell viability plotted against the pIC50 for the NFκB inhibition assay for the compounds **1**, **3**, **4**, **5**, **6**, **7**, **8**, **9** and **11**. The pIC_{50} value is determined as the negative decadic logarithm of the IC_{50}, which was calculated by nonlinear regression analysis without curve fitting using GraphPad Prism (GraphPad Software, San Diego, USA; Version 8.1.2). Compounds above the dotted line show greater potency in NFκB inhibition vs. cell viability and vice versa.

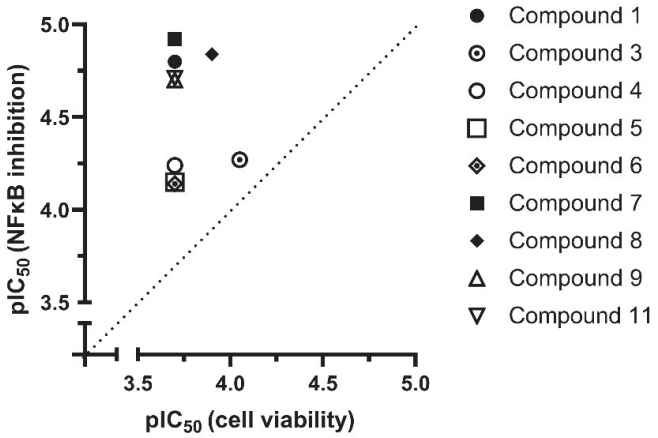

Table S1: Crystal data for compound **5**.

CCDC number	1976223
Empirical formula	$C_{22}H_{24}C_2O_7$
M [g mol^{-1}]	471.31
Crystal size [mm^3]	0.3 x 0.3 x 0.3
Temperature [K]	140
θ range [°] (completeness)	3.9 – 65.9 (0.99)
h; k; l range	±9; -14 – 16; -21 – 22
Crystal system	Orthorhombic
Space group	$P2_12_12_1$
a [Å]	8.1520(5)
b [Å]	14.1088(9)
c [Å]	18.7346(12)
α [°]	90.0
β [°]	90.0
γ [°]	90.0
V [Å^3]	2154.8(2)
Z	4
Dcalc [mg m^{-3}]	1.453
μ (Cu Kα) [mm^{-1}]	3.08
F(000)	984
Max./min. transmission	0.753 / 0.600
Reflections collected	26106
Independent reflect. (Rint)	3718
Data/restraints/parameters	3718 / 311 / 0
Max./min. Δρ [eÅ^{-3}] [a]	-0.22 / 0.43
R_1/wR_2 [I>2σ(I)] [b]	0.026 / 0.069
R_1/wR_2 [all data] [b]	0.026 / 0.069
Goodness-of-fit on F^2 [c]	1.03
Flack parameter [d]	0.016(5)

[a] Largest difference peak and hole; [b] $R_1 = [\sum(||F_o| - |F_c||)/\sum|F_o|]$; $wR_2 = [\sum[w(F_o^2 - F_c^2)^2]/\sum[w(F_o^2)^2]]^{1/2}$; [c] Goodness-of-fit $= [\sum[w(F_o^2 - F_c^2)^2]/(n - p)]^{1/2}$; [d] Absolute structure parameter.

Table S2. Fractional atomic coordinates and isotropic or equivalent isotropic displacement parameters (Å^2) for compound **5**.

	x	*y*	*z*	U_{iso}*/U_{eq}	Occ. (<1)
Cl1	0.24321 (8)	0.81549 (4)	1.04217 (3)	0.03219 (17)	
O1	0.5589 (4)	0.69409 (13)	0.53721 (10)	0.0493 (7)	
O1"	0.2929 (2)	0.53104 (14)	0.82263 (9)	0.0280 (4)	
C1"	0.3988 (3)	0.55041 (16)	0.86460 (12)	0.0197 (5)	
C1A	0.5101 (5)	0.70018 (19)	0.61155 (13)	0.0388 (8)	
H1AA	0.389878	0.691728	0.615360	0.047*	
H1AB	0.537897	0.763740	0.630398	0.047*	
Cl2	0.39219 (8)	0.46808 (5)	1.13798 (3)	0.02943 (16)	
O2	0.5498 (2)	0.38313 (11)	0.78063 (9)	0.0257 (4)	
O2"	0.3218 (2)	0.73236 (13)	0.89865 (10)	0.0303 (4)	
C2"	0.3698 (3)	0.57644 (17)	0.94185 (12)	0.0205 (5)	
O3	0.5598 (2)	0.55473 (11)	0.84990 (8)	0.0181 (3)	
O3"	0.2951 (2)	0.66247 (14)	1.15017 (9)	0.0262 (4)	
C3	0.5456 (5)	0.6063 (2)	0.50865 (14)	0.0372 (7)	
C3"	0.3220 (3)	0.66943 (17)	0.95431 (13)	0.0221 (5)	
C3'	0.4783 (5)	0.6862 (3)	0.31316 (14)	0.0468 (9)	
H3'A	0.402981	0.733835	0.293872	0.056*	
H3'B	0.451852	0.623986	0.292861	0.056*	
H3'C	0.591316	0.703135	0.300684	0.056*	
H3"O	0.245 (5)	0.711 (3)	1.155 (2)	0.045 (10)*	
O4	0.6083 (2)	0.71764 (12)	0.76564 (9)	0.0224 (4)	
C4	0.5357 (3)	0.52728 (18)	0.54849 (12)	0.0253 (5)	
H4	0.514439	0.468460	0.525616	0.030*	
C4"	0.2934 (3)	0.69915 (17)	1.02408 (14)	0.0226 (5)	
C4A	0.5564 (3)	0.52915 (17)	0.62462 (12)	0.0193 (5)	
H4O	0.557 (5)	0.760 (3)	0.752 (2)	0.048 (11)*	
C5	0.5467 (3)	0.45072 (16)	0.66601 (12)	0.0198 (5)	
H5	0.528414	0.391237	0.643617	0.024*	
C5"	0.3139 (3)	0.63701 (18)	1.08111 (12)	0.0197 (5)	

C6	0.5628 (3)	0.45355 (16)	0.74267 (12)	0.0182 (5)	
C6"	0.3654 (3)	0.54475 (17)	1.06651 (12)	0.0198 (5)	
C7	0.6131 (3)	0.54889 (16)	0.77595 (11)	0.0179 (5)	
C7"	0.3956 (3)	0.51319 (16)	0.99741 (12)	0.0203 (5)	
C8	0.5449 (3)	0.63334 (15)	0.73403 (12)	0.0175 (5)	
H8	0.422487	0.633599	0.737541	0.021*	
C8"	0.1640 (4)	0.7509 (2)	0.86995 (18)	0.0431 (7)	
H8"A	0.172803	0.799089	0.832466	0.065*	
H8"B	0.091529	0.773985	0.907890	0.065*	
H8"C	0.118724	0.692472	0.849679	0.065*	
C8A	0.5954 (3)	0.62553 (16)	0.65544 (12)	0.0218 (5)	
H8A	0.716405	0.636047	0.651994	0.026*	
C9	0.7995 (3)	0.55032 (18)	0.78099 (13)	0.0242 (5)	
H9A	0.846684	0.543759	0.733123	0.036*	
H9B	0.836613	0.497662	0.811049	0.036*	
H9C	0.835308	0.610455	0.802039	0.036*	
C9"	0.4537 (4)	0.41479 (18)	0.98344 (13)	0.0278 (6)	
H9"A	0.458174	0.403747	0.931836	0.042*	
H9"B	0.377677	0.369501	1.005353	0.042*	
H9"C	0.563290	0.406388	1.003953	0.042*	
C1'A	0.5597 (12)	0.6085 (3)	0.42905 (19)	0.0314 (18)	0.775 (19)
H1'A	0.676302	0.618190	0.416185	0.038*	0.775 (19)
H1'B	0.526074	0.545947	0.410056	0.038*	0.775 (19)
C2'A	0.4610 (8)	0.6823 (5)	0.3940 (3)	0.0348 (14)	0.775 (19)
H2'A	0.492628	0.744633	0.413960	0.042*	0.775 (19)
H2'B	0.344101	0.671564	0.405934	0.042*	0.775 (19)
C1'B	0.467 (3)	0.6112 (11)	0.4296 (7)	0.027 (4)	0.225 (19)
H1'C	0.479037	0.549208	0.405513	0.033*	0.225 (19)
H1'D	0.348780	0.626511	0.432761	0.033*	0.225 (19)
C2'B	0.553 (7)	0.6847 (19)	0.3890 (14)	0.087 (13)	0.225 (19)
H2'C	0.671573	0.670387	0.386669	0.104*	0.225 (19)
H2'D	0.538411	0.747193	0.412247	0.104*	0.225 (19)

Table S3. Atomic displacement parameters (Å^2) for compound **5**.

	U^{11}	U^{22}	U^{33}	U^{12}	U^{13}	U^{23}
Cl1	0.0442 (4)	0.0200 (3)	0.0323 (3)	0.0081 (3)	0.0045 (3)	-0.0070 (2)
O1	0.120 (2)	0.0177 (9)	0.0104 (8)	-0.0031 (12)	0.0016 (11)	0.0000 (7)
O1"	0.0299 (9)	0.0345 (10)	0.0196 (8)	-0.0048 (8)	0.0009 (7)	-0.0044 (8)
C1"	0.0300 (12)	0.0145 (11)	0.0147 (10)	-0.0003 (10)	0.0004 (10)	-0.0010 (9)
C1A	0.088 (2)	0.0173 (13)	0.0114 (11)	0.0047 (14)	-0.0014 (13)	-0.0024 (10)
Cl2	0.0390 (3)	0.0322 (3)	0.0171 (3)	0.0051 (3)	-0.0005 (2)	0.0059 (2)
O2	0.0435 (10)	0.0141 (8)	0.0197 (8)	-0.0005 (7)	-0.0004 (8)	0.0014 (7)
O2"	0.0374 (10)	0.0263 (10)	0.0271 (10)	0.0031 (8)	0.0031 (8)	0.0060 (8)
C2"	0.0271 (11)	0.0190 (11)	0.0155 (11)	-0.0006 (9)	0.0041 (10)	-0.0026 (9)
O3	0.0259 (8)	0.0174 (8)	0.0110 (7)	0.0009 (6)	0.0014 (6)	-0.0010 (6)
O3"	0.0345 (10)	0.0285 (10)	0.0158 (9)	0.0020 (8)	0.0052 (7)	-0.0067 (7)
C3	0.073 (2)	0.0224 (13)	0.0163 (12)	0.0002 (14)	0.0015 (13)	-0.0033 (10)
C3"	0.0278 (12)	0.0189 (12)	0.0194 (12)	0.0008 (10)	0.0027 (10)	0.0010 (10)
C3'	0.074 (2)	0.0469 (19)	0.0195 (14)	0.0284 (17)	-0.0023 (14)	0.0035 (13)
O4	0.0379 (9)	0.0118 (8)	0.0175 (8)	0.0005 (8)	-0.0054 (7)	-0.0028 (7)
C4	0.0429 (14)	0.0179 (12)	0.0152 (11)	0.0005 (11)	0.0006 (10)	-0.0049 (9)
C4"	0.0264 (12)	0.0159 (11)	0.0255 (12)	0.0019 (9)	0.0045 (10)	-0.0049 (10)
C4A	0.0237 (11)	0.0166 (11)	0.0175 (11)	0.0009 (9)	0.0029 (9)	-0.0036 (9)
C5	0.0282 (11)	0.0142 (11)	0.0171 (11)	0.0004 (10)	0.0015 (9)	-0.0036 (9)
C5"	0.0197 (10)	0.0243 (12)	0.0152 (11)	-0.0002 (9)	0.0035 (9)	-0.0053 (10)
C6	0.0219 (11)	0.0144 (11)	0.0182 (11)	0.0023 (9)	0.0026 (9)	-0.0016 (9)
C6"	0.0218 (11)	0.0215 (12)	0.0162 (11)	0.0013 (9)	0.0009 (9)	0.0020 (9)
C7	0.0265 (11)	0.0155 (11)	0.0116 (10)	0.0013 (9)	0.0013 (9)	-0.0022 (9)
C7"	0.0250 (11)	0.0179 (11)	0.0180 (11)	0.0008 (9)	0.0023 (9)	-0.0013 (9)
C8	0.0263 (11)	0.0121 (10)	0.0143 (10)	-0.0005 (9)	-0.0004 (9)	-0.0028 (9)
C8"	0.0405 (16)	0.0493 (18)	0.0396 (17)	0.0110 (14)	0.0018 (14)	0.0076 (14)
C8A	0.0376 (13)	0.0140 (11)	0.0138 (11)	-0.0037 (10)	0.0030 (10)	-0.0021 (9)
C9	0.0245 (12)	0.0245 (12)	0.0235 (12)	0.0019 (10)	-0.0018 (10)	-0.0021 (10)
C9"	0.0462 (15)	0.0183 (12)	0.0190 (12)	0.0030 (12)	0.0069 (11)	-0.0019 (10)
C1'A	0.054 (5)	0.0257 (19)	0.0148 (18)	0.009 (2)	0.000 (2)	-0.0013 (13)
C2'A	0.049 (3)	0.041 (3)	0.014 (2)	0.014 (3)	-0.002 (2)	-0.0002 (19)
C1'B	0.013 (9)	0.053 (9)	0.016 (6)	-0.002 (6)	-0.002 (6)	-0.013 (6)
C2'B	0.18 (4)	0.040 (11)	0.038 (11)	-0.02 (2)	0.04 (2)	0.009 (9)

Table S4. Geometric parameters (Å, º) for compound **5**.

Cl1—C4"	1.725 (2)	C4A—C5	1.354 (3)
O1—C3	1.353 (3)	C4A—C8A	1.511 (3)
O1—C1A	1.451 (3)	C5—C6	1.443 (3)
O1"—C1"	1.199 (3)	C5—H5	0.9500
C1"—O3	1.342 (3)	C5"—C6"	1.395 (4)
C1"—C2"	1.512 (3)	C6—C7	1.538 (3)
C1A—C8A	1.506 (4)	C6"—C7"	1.391 (3)
C1A—H1AA	0.9900	C7—C9	1.523 (3)
C1A—H1AB	0.9900	C7—C8	1.532 (3)
Cl2—C6"	1.735 (2)	C7"—C9"	1.490 (3)
O2—C6	1.226 (3)	C8—C8A	1.533 (3)
O2"—C3"	1.370 (3)	C8—H8	1.0000
O2"—C8"	1.419 (4)	C8"—H8"A	0.9800
C2"—C7"	1.387 (3)	C8"—H8"B	0.9800
C2"—C3"	1.388 (3)	C8"—H8"C	0.9800
O3—C7	1.454 (3)	C8A—H8A	1.0000
O3"—C5"	1.351 (3)	C9—H9A	0.9800
O3"—H3"O	0.80 (4)	C9—H9B	0.9800
C3—C4	1.344 (4)	C9—H9C	0.9800
C3—C1'A	1.496 (4)	C9"—H9"A	0.9800
C3—C1'B	1.614 (14)	C9"—H9"B	0.9800
C3"—C4"	1.392 (4)	C9"—H9"C	0.9800
C3'—C2'A	1.523 (6)	C1'A—C2'A	1.470 (8)
C3'—C2'B	1.55 (4)	C1'A—H1'A	0.9900
C3'—H3'A	0.9800	C1'A—H1'B	0.9900
C3'—H3'B	0.9800	C2'A—H2'A	0.9900
C3'—H3'C	0.9800	C2'A—H2'B	0.9900
O4—C8	1.426 (3)	C1'B—C2'B	1.46 (4)
O4—H4O	0.77 (4)	C1'B—H1'C	0.9900
C4—C4A	1.436 (3)	C1'B—H1'D	0.9900
C4—H4	0.9500	C2'B—H2'C	0.9900
C4"—C5"	1.392 (4)	C2'B—H2'D	0.9900
C3—O1—C1A	114.3 (2)	C2"—C7"—C6"	117.7 (2)
O1"—C1"—O3	125.4 (2)	C2"—C7"—C9"	121.1 (2)
O1"—C1"—C2"	124.8 (2)	C6"—C7"—C9"	121.2 (2)

O3—C1"—C2"	109.79 (19)	O4—C8—C7	107.72 (18)
O1—C1A—C8A	110.9 (2)	O4—C8—C8A	111.21 (19)
O1—C1A—H1AA	109.5	C7—C8—C8A	109.82 (18)
C8A—C1A—H1AA	109.5	O4—C8—H8	109.3
O1—C1A—H1AB	109.5	C7—C8—H8	109.3
C8A—C1A—H1AB	109.5	C8A—C8—H8	109.3
H1AA—C1A—H1AB	108.1	O2"—C8"—H8"A	109.5
C3"—O2"—C8"	114.1 (2)	O2"—C8"—H8"B	109.5
C7"—C2"—C3"	121.6 (2)	H8"A—C8"—H8"B	109.5
C7"—C2"—C1"	122.6 (2)	O2"—C8"—H8"C	109.5
C3"—C2"—C1"	115.8 (2)	H8"A—C8"—H8"C	109.5
C1"—O3—C7	119.03 (17)	H8"B—C8"—H8"C	109.5
C5"—O3"—H3"O	113 (3)	C1A—C8A—C4A	108.9 (2)
C4—C3—O1	123.0 (2)	C1A—C8A—C8	110.5 (2)
C4—C3—C1'A	125.1 (3)	C4A—C8A—C8	112.05 (19)
O1—C3—C1'A	111.7 (3)	C1A—C8A—H8A	108.4
C4—C3—C1'B	121.4 (6)	C4A—C8A—H8A	108.4
O1—C3—C1'B	110.8 (6)	C8—C8A—H8A	108.4
O2"—C3"—C2"	119.0 (2)	C7—C9—H9A	109.5
O2"—C3"—C4"	121.3 (2)	C7—C9—H9B	109.5
C2"—C3"—C4"	119.3 (2)	H9A—C9—H9B	109.5
C2'A—C3'—H3'A	109.5	C7—C9—H9C	109.5
C2'A—C3'—H3'B	109.5	H9A—C9—H9C	109.5
H3'A—C3'—H3'B	109.5	H9B—C9—H9C	109.5
C2'A—C3'—H3'C	109.5	C7"—C9"—H9"A	109.5
H3'A—C3'—H3'C	109.5	C7"—C9"—H9"B	109.5
H3'B—C3'—H3'C	109.5	H9"A—C9"—H9"B	109.5
C8—O4—H4O	108 (3)	C7"—C9"—H9"C	109.5
C3—C4—C4A	121.9 (2)	H9"A—C9"—H9"C	109.5
C3—C4—H4	119.0	H9"B—C9"—H9"C	109.5
C4A—C4—H4	119.0	C2'A—C1'A—C3	114.6 (5)
C5"—C4"—C3"	120.7 (2)	C2'A—C1'A—H1'A	108.6
C5"—C4"—Cl1	118.49 (19)	C3—C1'A—H1'A	108.6
C3"—C4"—Cl1	120.71 (19)	C2'A—C1'A—H1'B	108.6
C5—C4A—C4	123.2 (2)	C3—C1'A—H1'B	108.6
C5—C4A—C8A	121.9 (2)	H1'A—C1'A—H1'B	107.6
C4—C4A—C8A	114.9 (2)	C1'A—C2'A—C3'	114.7 (5)

C4A—C5—C6	122.8 (2)	C1'A—C2'A—H2'A	108.6
C4A—C5—H5	118.6	C3'—C2'A—H2'A	108.6
C6—C5—H5	118.6	C1'A—C2'A—H2'B	108.6
O3"—C5"—C4"	123.6 (2)	C3'—C2'A—H2'B	108.6
O3"—C5"—C6"	118.0 (2)	H2'A—C2'A—H2'B	107.6
C4"—C5"—C6"	118.3 (2)	C2'B—C1'B—C3	109 (2)
O2—C6—C5	123.2 (2)	C2'B—C1'B—H1'C	110.0
O2—C6—C7	119.8 (2)	C3—C1'B—H1'C	110.0
C5—C6—C7	116.9 (2)	C2'B—C1'B—H1'D	110.0
C7"—C6"—C5"	122.3 (2)	C3—C1'B—H1'D	110.0
C7"—C6"—Cl2	119.76 (18)	H1'C—C1'B—H1'D	108.4
C5"—C6"—Cl2	117.92 (18)	C1'B—C2'B—C3'	107 (3)
O3—C7—C9	103.80 (18)	C1'B—C2'B—H2'C	110.2
O3—C7—C8	109.62 (17)	C3'—C2'B—H2'C	110.2
C9—C7—C8	112.6 (2)	C1'B—C2'B—H2'D	110.2
O3—C7—C6	110.85 (18)	C3'—C2'B—H2'D	110.2
C9—C7—C6	107.64 (19)	H2'C—C2'B—H2'D	108.5
C8—C7—C6	112.06 (18)		

Table S5. Hydrogen-bond geometry (Å, º) for compound **5**.

D—H···*A*	*D*—H	H···*A*	*D*···*A*	*D*—H···*A*
O3"—H3"*O*···Cl1	0.80 (4)	2.58 (4)	2.989 (2)	113 (3)
O3"—H3"*O*···O4^{i}	0.80 (4)	2.11 (4)	2.769 (2)	139 (3)
O4—H4*O*···O2^{ii}	0.77 (4)	2.04 (4)	2.804 (2)	171 (4)

Symmetry codes: (i) *x*-1/2, -*y*+3/2, -*z*+2; (ii) -*x*+1, *y*+1/2, -*z*+3/2.

Chapter 4 - A new dibenzoxepin and a new natural isocoumarin from the marine-derived fungus *Aspergillus falconensis*

Reprint from "**Dina H. El-Kashef**, Fadia S. Youssef, Werner E.G. Müller, Wenhan Lin, Marian Frank, Zhen Liu and Peter Proksch (2020). A new dibenzoxepin and a new natural isocoumarin from the marine-derived fungus *Aspergillus falconensis*. *Bioorganic & medicinal chemistry*." Submitted and currently is under revision.

4.1 Publication Manuscript

Submitted and is under revision in "Bioorganic & Medicinal Chemistry"

Impact Factor: 3.073 (2019)

Overall contribution to this publication: First author, laboratory work including, cultivation and extraction, compound isolation, structure elucidation, and manuscript preparation.

Bioorganic & Medicinal Chemistry
journal homepage: www.elsevier.com

A new dibenzoxepin and a new natural isocoumarin from the marine-derived fungus *Aspergillus falconensis*

Dina H. El-Kashef [a,b], Fadia S. Youssef [a,c], Werner E.G. Müller [d], Wenhan Lin [e], Marian Frank [a,*], Zhen Liu [a,*] and Peter Proksch [a,f,*]

[a]*Institute of Pharmaceutical Biology and Biotechnology, Faculty of Mathematics and Natural Sciences, Heinrich-Heine-University Duesseldorf, 40225 Duesseldorf, Germany.*
[b]*Department of Pharmacognosy, Faculty of Pharmacy, Minia University, 61519 Minia, Egypt.*
[c]*Department of Pharmacognosy, Faculty of Pharmacy, Ain Shams University Abbassia, 11566 Cairo, Egypt*
[d]*Institute of Physiological Chemistry, Johannes Gutenberg University Mainz, 55128 Mainz, Germany.*
[e]*State Key Laboratory of Natural and Biomimetic Drugs, Peking University, Beijing 100191, China.*
[f]*Hubei Key Laboratory of Natural Products Research and Development, College of Biological and Pharmaceutical Sciences, China Three Gorges University, Yichang 443002, China.*

ARTICLE INFO

Article history:
Received
Received in revised form
Accepted
Available online

Keywords:
Aspergillus falconensis
OSMAC
Molecular docking
Cytotoxicity
Polyketides

ABSTRACT

Fermentation of the marine-derived fungus *Aspergillus falconensis*, isolated from sediment collected from the Red Sea, Egypt on solid rice medium containing 3.5% NaCl yielded a new dibenzoxepin derivative (**1**) and a new natural isocoumarin (**2**) along with six known compounds (**3** - **8**). Changes in the metabolic profile of the fungus were induced by replacing NaCl with 3.5% $(NH_4)_2SO_4$ that resulted in the accumulation of three further known compounds (**9** – **11**), which were not detected when the fungus was cultivated in the presence of NaCl. The structures of the new compounds were elucidated by HRESIMS and 1D/2D NMR as well as by comparison with the literature. Molecular docking was conducted for all isolated compounds on crucial enzymes involved in the formation, progression and metastasis of cancer which included human cyclin-dependent kinase 2 (CDK-2), human DNA topoisomerase II (TOP-2) and matrix metalloproteinase 13 (MMP-13). Diorcinol (**7**), sulochrin (**9**) and monochlorosulochrin (**10**) displayed notable stability within the active pocket of CDK-2 with free binding energy (ΔG) equals to -25.72, -25.03 and -25.37 Kcal/mol, respectively whereas sulochrin (**9**) exerted the highest fitting score within MMP-13 active center (ΔG = -33.83 Kcal/mol). *In vitro* cytotoxic assessment using MTT assay showed that sulochrin (**9**) exhibited cytotoxic activity versus L5178Y mouse lymphoma cells with an IC_{50} value of 5.1 µM.

1. Introduction

The marine environment has gained considerable attention in the last decades with regard to bioprospecting as exemplified by 12 clinically approved marine-derived drugs that mostly originate from marine microbes or from marine invertebrates whereas numerous further compounds are under clinical investigation or in preclinical status.[1] Marine-derived fungi which have come into the focus of bioprospecting only within the last two decades or so [2-5] have yielded a plethora of structurally unique bioactive metabolites as exemplified by the discovery of halimide. Halimide has served as a lead structure for plinabulin that is currently in clinical phase III for the treatment of non-small cell lung cancer.[6, 7]

In continuation of our ongoing research on marine-derived fungi,[5, 8, 9] the fungal strain *Aspergillus falconensis*, isolated from marine sediment collected at a depth of 25 m from the Canyon at Dahab, Red Sea, Egypt, was found to be a prolific producer of structurally diverse secondary metabolites including halogenated azaphilones.[10]

In the present study, a new dibenzoxepin derivative (**1**) and a new natural isocoumarin (**2**) together with six known compounds (**3** - **8**) were isolated from *A. falconensis* following fermentation of the fungus on solid rice medium containing 3.5% NaCl. Replacing NaCl by 3.5% $(NH_4)_2SO_4$ was performed as an OSMAC (**O**ne **S**train **Ma**ny **C**ompounds) approach aiming to trigger the expression of silent genes with concomitant production of compounds that were undetected in the fungal culture under normal conditions [11]. This led to three further known compounds (**9** – **11**), which were undetected in the fungal culture containing 3.5% NaCl. *In silico* virtual studies were conducted on critical enzymes involved in the formation, progression and metastasis of cancer which are human cyclin-dependent kinase 2 (CDK-2), human DNA topoisomerase II (TOP-2) and matrix

metalloproteinase 13 (MMP-13) in an effort to find new entities combating cancer and to interpret their probable mode of action. This was paralleled by an *in vitro* cytotoxicity assessment using MTT assay against mouse lymphoma cells which were used as an experimental model in addition to the molecular docking approach.

2. Results and discussion

Our previous chemical exploration of the marine-derived fungus *Aspergillus falconensis* yielded a group of azaphilone derivatives.[10] During our ongoing chemical investigation of the fungus, a new dibenzoxepin derivative (**1**), a new natural isocoumarin (**2**) in addition to six known compounds (**3** - **8**) including arugosin C (**3**),[12] dichlorodiaportin (**4**),[13] desmethyldiaportinol (**5**),[14] questin (**6**),[15] diorcinol (**7**),[16] and 4-hydroxybenzaldehyde (**8**)[17] were isolated after cultivating the fungus on solid rice medium containing 3.5% NaCl.

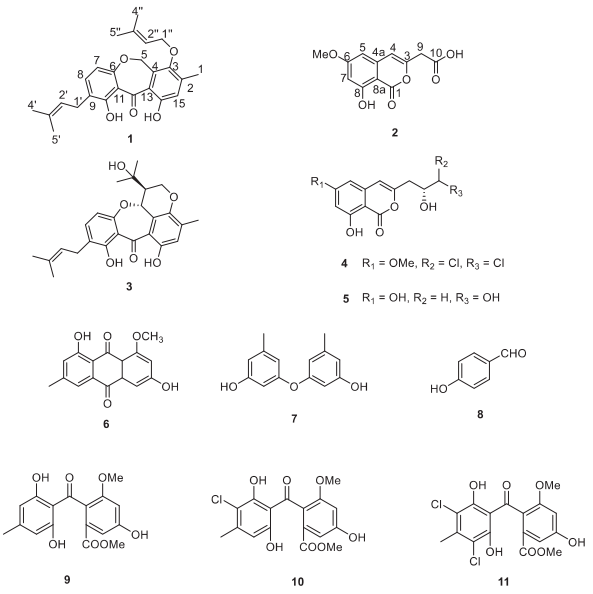

Figure 1. Structures of compounds isolated from *Aspergillus falconensis*.

Compound **1** was isolated as yellow crystalline needles. Its molecular formula was established as $C_{25}H_{28}O_5$ by HRESIMS, which requires 12 degrees of unsaturation. The ^{1}H NMR spectrum showed the signals of five methyl groups resonating at δ_H 1.72 (s, H_3-5"), 1.75 (s, H_3-5'), 1.76 (s, H_3-4'), 1.81 (s, H_3-4"), and 2.46 (s, H_3-1), three methylene groups at δ_H 3.39 (d, J = 7.5 Hz, H_2- 1'), 4.45 (d, J = 7.2 Hz, H_2- 1"), and 5.09 (s, H_2-5), two olefinic protons at δ_H 5.33 (m, H-2'), and 5.62 (m, H-2"), three aromatic protons at δ_H 6.85 (d, J = 8.5 Hz, H-7), 7.28 (s, H-15), and 7.48 (d, J = 8.5 Hz, H-8) in addition to a chelated hydroxyl group resonating at δ_H 12.93 (s, 10-OH). The ^{13}C NMR chemical shifts (**Table 1**) assigned from HSQC and HMBC cross peaks indicated the presence of 12 aromatic carbon resonances C-2 (δ_C 142.6), C-3 (δ_C 152.5), C-4 (δ_C 134.3, C), C-6 (δ_C 154.0), C-7 (δ_C 105.7), C-8 (δ_C 137.0), C-9 (δ_C 123.1), C-10 (δ_C 158.9), C-11 (δ_C 108.5), C-13 (δ_C 117.9), C-14 (δ_C 154.1), and C-15 (δ_C 119.4), one carbonyl group C-12 (δ_C 206.0), and 12 further oxygenated or non-oxygenated aliphatic carbon signals. Analysis of the HMBC and COSY correlations (Figure **2**) revealed four distinct subunits of the carbon scaffold. Two isoprenyl residues were established based on their distinctive pattern of deshielded methyl signals H_3-4'/ H_3-5' and H_3-4"/ H_3-5" that show HMBC correlations to their respective olefinic carbons C-2' and C-2" which are in turn connected to methylene units H_2-1' and H_2-1" as revealed by COSY correlation from H-2' and H-2" respectively. Furthermore, the methylene unit C-1" (δ_C 72.2) was strongly deshielded relative to C-1' (δ_C 27.1), suggesting a connection to an oxygen at C-1" rather than to a carbon as found for C-1'. This was confirmed by HMBC correlation of H_2-1" to an oxygenated aromatic carbon C-3 (δ_C 152.5), establishing it as an isoprenylphenylether, while the HMBC correlation of H_2-1' revealed the connection of C-1' to the aromatic carbon C-9 (δ_C 123.1). The substitution patterns of the aromatic systems were established based on the HMBC and COSY correlations of signals of H-7, H-8 and H-15, as well as of the methylene H_2-5, the aromatic methyl H_3-1 and the phenol OH-10. Protons H-7 and H-8 are situated in an *ortho* position as shown by their *J*-coupling (8.5 Hz). Thus, their combined J_3-HMBC correlations reveal oxygenated aromatic carbons C-10 (δ_C 158.9) and C-6 (δ_C 154.0) as well as aromatic quaternary carbons C-9 (δ_C 123.1) and C-11 (δ_C 108.5) and confirm the position of C-1'. The distinct ^{1}H-NMR signal of OH-10 allowed detection of HMBC correlations to C-9, C-10 and C-11 which pinpointed this hydroxyl group to position 10 and indicated the presence of a chelating carbonyl C-12 (δ_C 206.0) connected to C-11 that is necessary for a hydrogen bond formation. The second aromatic system was revealed to be pentasubstituted due to the presence of only one more aromatic proton which was detected at H-15. The strong J_3 HMBC correlation of H-15 to C-13 (δ_C 117.9) and C-3 (δ_C 152.5) matched those of the methylene H_2-5, establishing a para position for these signals. The deshielded chemical shift of C-5 (δ_C 57.1) and the remaining HMBC correlations of H_2-5 to C-6 (δ_C 154.0) and C-4 (δ_C 134.3) indicated a connection of the two aromatic systems between C-4 and C-6 via an oxygen at C-6. The remaining aromatic methyl H_3-1 is positioned between C-15 and the isoprenylether carrying C-3 as indicated by HMBC correlations of H_3-1 to C-2 (δ_C 142.6), C-3 and C-15. Finally, carbon C-14 (δ_C 154.1) was assigned based on the weaker J_2 HMBC correlation of H-15 and identified as a hydroxyl moiety based on its chemical shift and the molecular formula. The connection between C-12 and C-13 accounted for the last missing degree of unsaturation. Thus, compound **1** was elucidated as shown. These findings were in agreement with the presence of a (6-7-6) tricyclic system of the dibenzo[*b,e*]oxepin-11(6*H*)-one skeleton with isoprenyl subunits[18] corresponding to the required 12 degrees of unsaturation. Moreover, similar prenylated polyketides, arugosins G and H, had previously been isolated from the marine-derived fungus *Aspergillus nidulans* (syn. *Emericella nidulans* var. *acristata*)[19]. Since the new compound (**1**) is a derivative of the co-isolated known compound (**3**), arugosin C, we propose the name arugosin O for compound (**1**).

Table 1. ^{1}H and ^{13}C NMR data of compound **1**[a]

No.	δ_C, type[b]	δ_H (J in Hz)
1	17.7, CH_3	2.46, s
2	142.6, C	
3	152.5, C	
4	134.3, C	
5	57.1, CH_2	5.09, s
6	154.0, C	
7	105.7, CH	6.85, d, J = 8.5
8	137.0, CH	7.48, d, J = 8.5
9	123.1, C	
10	158.9, C	
11	108.5, C	
12	206.0, C	
13	117.9, C	
14	154.1, C	
15	119.4, CH	7.28, s
1'	27.1, CH_2	3.39, d, J = 7.5

2'	121.8, CH	5.33, m
3'	133.4, C	
4'	25.8, CH_3	1.76, s
5'	17.8, CH_3	1.75, s
1"	72.2, CH_2	4.45, d, J = 7.2
2"	119.6, CH	5.62, m
3"	139.1, C	
4"	25.9, CH_3	1.81, s
5"	18.1, CH_3	1.72, s
10-OH		12.93, s

[a] Measured in $CDCl_3$ (^1H at 600 MHz and ^{13}C at 150 MHz).

[b] Data are extracted from the HSQC and HMBC spectra.

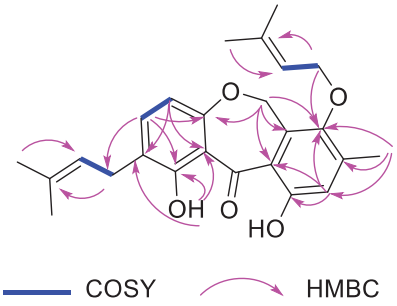

Figure 2. COSY (blue lines) and key HMBC (arrows) correlations of **1**

Compound **2** 2-(8-Hydroxy-6-methoxyisochromen-3'-yl) acetic acid is reported here for the first time from nature and was hitherto only known from synthesis.[20]

In an OSMAC approach, NaCl was replaced by 3.5% $(NH_4)_2SO_4$ that was added to solid rice medium. Interestingly, this induced the production of three further known metabolites (**9** – **11**) including sulochrin (**9**),[21] monochlorosulochrin (**10**),[21] dihydrogeodin (**11**).[21]

In an effort to find new entities combating cancer and to identify their probable mode of action, molecular docking was performed on human cyclin-dependent kinase 2 (CDK-2), human DNA topoisomerase II (TOP-2) and matrix metalloproteinase 13 (MMP-13) that are implicated in cancer formation.

Human cyclin-dependent kinases represent a group of enzymes that effectively control the progression and transcription of the cell cycle. CDK2 is a serine-threonine kinase that strictly binds to two regulatory cyclins namely, A and E. CDK2- cyclin E complex is incorporated in the G1 to S-phase transition. Its complex with cyclin A leads to cell cycle progression through the S to M-phase. Thus, inhibition of CDK2 significantly arrests cell proliferation at G2/M-phase.[22] All docked compounds revealed a certain degree of stability in the active sites of CDK-2 as illustrated in Table 2 except for compound (**1**) that showed unfavorable interaction manifested by the positive value of (ΔG). Diorcinol (**7**), sulochrin (**9**) and monochlorosulochrin (**10**) displayed notable stability within the active pocket of CDK-2 with free binding energy (ΔG) equal to -25.72, -25.03 and -25.37 Kcal/mol, respectively compared to doxorubicin (ΔG = - 40.79 Kcal/mol) and CK8(N-[4-(2,4-dimethyl-thiazol-5-yl)-pyrimidin-2-yl]-N',N'-dimethyl-benzene-1,4-diamine), a potent CDK-2 inhibitor that had been co-crystalized with CDK-2, which revealed a ΔG value of -39.34 Kcal/mol. Diorcinol (**7**) exhibited the highest fitting score which is mainly attributed to the formation of several bonds with the amino acid residues at the active site. These bonds are represented by the formation of three conventional H- bonds with Glu 81, Phe 82 and Leu 83 in addition to the formation of four π-bonds between the Ile 10, Val 18, Ala 31 and Leu 134 and the phenolic OH moieties present in the molecule. Furthermore, four hydrophobic alkyl interactions between the CH_3 groups in the molecule and Lys 89, Ala 31, Val 18 and Phe 80 exist (**Figure 3A**). Doxorubicin in comparison forms four H- bonds with Leu 83, Gln 85, His 84 and Lys 89 in addition to multiple π-bonds with Ala 144, Val 18, Leu 13, Ile 10, Asp 26 and van der Waals interactions with Gln 131 and Asp 145 (**Figure 3B**). CK8 on the other hand forms one hydrogen bond with Leu 83, a van der Waals interaction with His 84 and eight π-bonds with Val 18, Ile 10 and Leu 134 (**Figure 3C**). Thus, Leu 83 is a fundamental amino acid residue that is crucial for enzyme inhibition. Sulochrin (**9**) forms five conventional H-bonds with Lys 9, Lys 89, Asp 86, His 84, π-alkyl and alkyl- alkyl interactions with Ala 31, Leu 134, Ile 10 in addition to C-H bond with Glu 8 with multiple van der Waals interactions. Meanwhile, monochlorosulochrin (**10**) forms four conventional H-bonds with Ile 10, Lys 89, Lys 9 in addition to C-H bond with Glu 12 and Gly 11 together with van der Waals interactions (**Figure S13**).

Table 2. Free binding energies (ΔG) of compounds isolated from *Aspergillus falconensis* within the active sites human cyclin-dependent kinase 2 (CDK-2), DNA topoisomerase II (TOP-2) and Matrix metalloproteinase 13 (MMP-13) employing *in silico* virtual screening expressed using kcal/mol

Compound	CDK-2	TOP-2	MMP-13
Arugosin O (**1**)	8.72	32.626	6.81
Compound (**2**)	- 22.30	-8.99	-23.08
Arugosin C (**3**)	-7.61	13.57	4.66
Dichlorodiaportin (**4**)	-20.32	-4.64	-23.75
Desmethyldiaportinol (**5**)	-20.46	-4.75	-22.12
Questin (**6**)	-9.12	6.36	-10.22
Diorcinol (**7**)	**- 25.72**	-13.91	-31.10
4-Hydroxybenzaldehyde (**8**)	- 17.74	**-14.28**	-19.64
Sulochrin (**9**)	- 25.03	-12.11	**-33.83**
Monochlorosulochrin (**10**)	- 25.37	-9.31	-33.31
Dihydrogeodin (**11**)	- 21.68	-6.48	FD
Doxorubicin (TOP-2 inhibitor)	- 40.79	-16.28	-16.31
CK8 (CDK-2 inhibitor)	-39.34	ND	ND
PB4 (MMP-13 inhibitor)	ND	ND	-72.51

Positive values indicate unfavorable interaction
FD: fail to dock
ND: Not done
CK8: N-[4-(2,4-dimethyl-thiazol-5-yl)-pyrimidin-2-yl]-N',N'-dimethyl-benzene-1,4-diamine
PB4: N,N'-bis (4-fluoro-3-methylbenzyl) pyrimidine-4,6-dicarboxamid

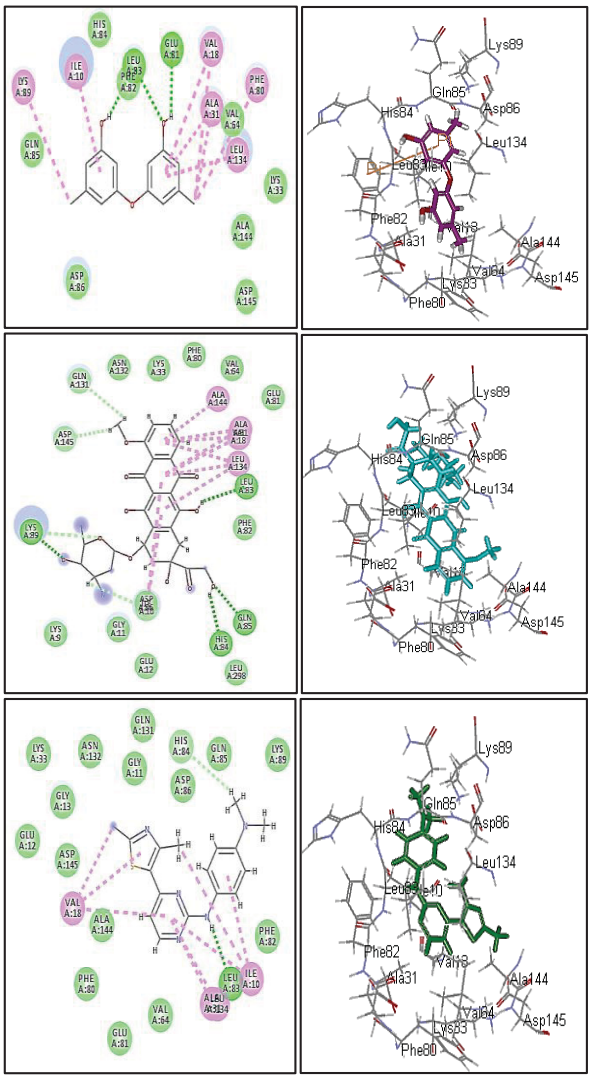

Figure 3: 2D and 3D binding modes of the (A) Diorcinol (**7**), (B) Doxorubicin and (C) CK8 (CDK-2 inhibitor) within the active pockets of CDK-2.

Human DNA topoisomerase II controls the vital cellular functions *via* triggering significant alterations regarding the topology of chromosomal DNA. It forms transient double-stranded breaks in the DNA molecule that enables the strands to cross each other to unwind DNA thus constituting an important role for cell survival. Multiple efficient antitumor drugs inhibit this enzyme.[23] Regarding human DNA topoisomerase II, mild interaction exists between the active centers of the enzyme and the docked compounds except for compounds (**1**) and (**3**) that revealed unfavorable interaction**.** On the contrary, diorcinol (**7**), 4-hydroxybenzaldehyde (**8**) and sulochrin (**9**) displayed a certain stability within the active sites with free binding energy of -13.91 -14.28 and -12.11 Kcal/mol, respectively similar to that exerted by doxorubicin (ΔG = - 16.28). Doxorubicin was previously reported to exhibit its antitumor potential *via* its notable inhibition of DNA topoisomerase II.[24] Hydroxybenzaldehyde (**8**) exerted the highest fitting score as evident by the formation of two H- bonds, one of which between the carbonyl moiety of the compound and Arg 503 while the other exists between its phenolic OH and Lys 505 in addition to the formation of one van der Waals interaction with Gly 504 and one π- bond with Arg 503 (**Figure 4A**). Doxorubicin forms four conventional H- bonds with Arg 503, Lys 505, Asn 520 and Glu 522 in addition to two van der Waals interactions with Ile 506 and Gly 504 together with hydrophobic interaction with Gln 778 and Lys 505. This in turn reflects the necessity of hydrogen bond formation with Arg 503 and Lys 505 for the inhibitory activity (**Figure 4B**). Sulochrin (**9**) forms two H-bonds with Arg 503 and Lys 505, C-H bond with Glu 522 in addition to the formation of π- anion bond between Glu 522 and aromatic ring and some van der Waals interactions. However, monochlorosulochrin (**10**) forms one H-bond and one π-alkyl bond with Arg 503 in addition to C-H bond with Arg 503, Glu 522 and Gly 504 and van der Waals interactions (**Figure S14**).

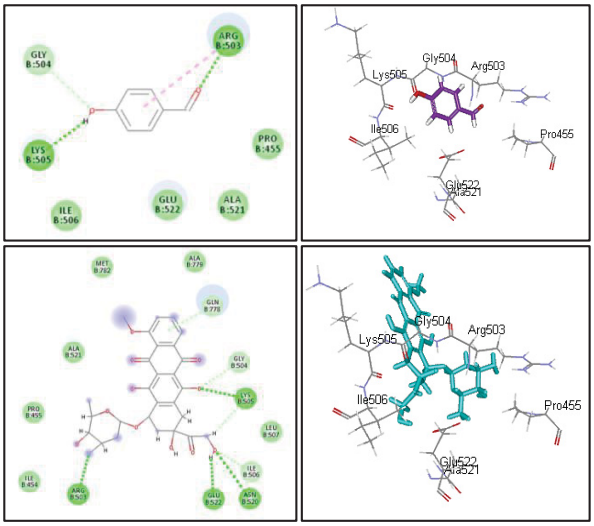

Figure 4: 2D and 3D binding modes of the (A) 4- Hydroxybenzaldehyde (**8**) and (B) Doxorubicin within the active pockets of TOP-2

Matrix metalloproteinases (MMPs) are capable of degrading extracellular matrix of vital components that is considered as a crucial factor for the growth of malignant tumor and is mainly associated with their invasive character, metastasis and angiogenesis as well. Matrix metalloproteinase inhibitors represent a completely different new therapeutic approach for counteracting tumor growth relative to other anti-cancer drugs.[25] Concerning matrix metalloproteinase 13, one enzyme of the MMP family, sulochrin **(9)** showed considerable interaction with MMP-13 with ΔG equal to -33.83 Kcal/mol superior to that exerted by doxorubicin that revealed free binding energy of -16.31 Kcal/mol. However, PB4, a MMP-13 inhibitor that had been co-crystalized with MMP-13, showed a ΔG value of -72.51 Kcal/mol. The fitting of sulochrin (**9**) to MMP-13 active sites can be explained by the formation of multiple bonds between the compound and the amino acid residues at the active site. These bonds are represented by a H-bond with Pro 236, a π-π interaction with Phe 252, and five van der Waals interactions with Leu 239, Phe 241 and Gly 237 in addition to the formation of a hydrophobic π- bond between the aromatic ring and Leu 218 and hydrophobic interactions between the alkyl groups and Lys 249 and His 222 (Figure **5A**). PB4 in comparison forms four hydrogen bonds with Thr 245, Thr 247, Lys 140 and Leu 239 in addition to several π-bonds with His 222, Tyr 244 and Phe252 together with numerous hydrophobic interactions as illustrated in Figure **5B**. Monochlorosulochrin (**10**) also showed tight binding at the active sites owing to the formation of one H- bond with Pro236, π-π bond with Phe252, alkyl interactions between Tyr 246, Leu 218 and chlorine moiety and between His 222, Lys 249 and CH_3 moieties **(Figure S15).**

In vitro cytotoxic assessment of the isolated compounds using mouse lymphoma cells was performed to ascertain the results obtained from molecular docking. The benzophenone derivative, sulochrin (**9**), was found to possess cytotoxic activity against the mouse lymphoma cell line L5178Y with an IC_{50} value of 5.1 µM. The activity of this compound may possibly be attributed to its CDK-2, TOP-2 and MMP-13 inhibitory action as evidenced by the molecular docking results. However, further studies of the isolated compounds using target specific assays as CDK2 and MMP inhibition assays are recommended to further ascertain the results obtained from docking experiments.

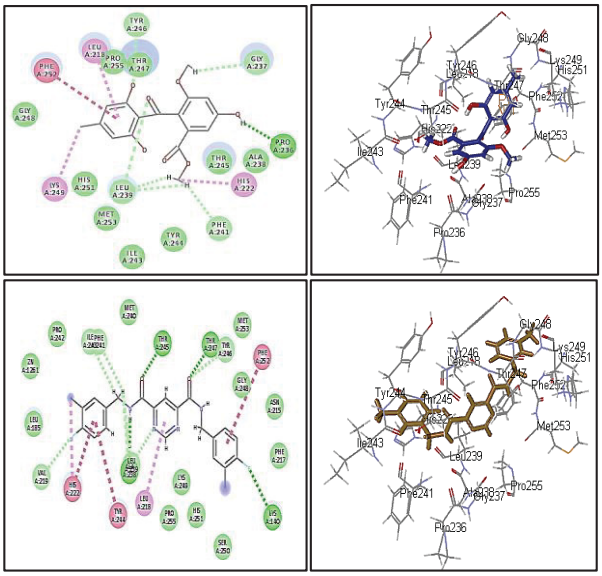

Figure 5: 2D and 3D binding modes of the (A) sulochrin (**9**) and (B) PB4 (MMP-13 inhibitor) within the active pockets of MMP-13

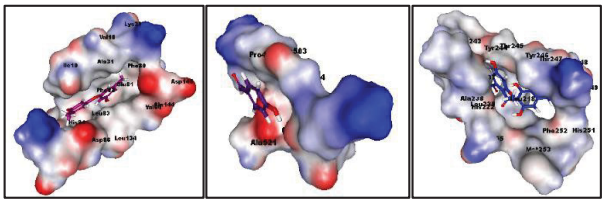

Figure 6: Diorcinol (**7**) in the active pocket of CDK-2 (A), 4-hydroxybenzaldehyde (**8**) in the active pocket of TOP-2 (B) and sulochrin (**9**) in the active pocket of MMP-13

3. Experimental

3.1. General experimental procedures

Optical rotations were measured on a Jasco P-2000 polarimeter after the compounds were dissolved in optically pure solvents (Uvasol, Merck Chemicals, Darmstadt, Germany). All NMR spectra (^{1}H, ^{13}C and 2D) were recorded on a Bruker Avance 600 MHz NMR spectrometer (Bruker BioSpin GmbH, Rheinstetten, Germany). Low-resolution mass spectra (ESI) were recorded with an Ion-Trap-API Finnigan LCQ Deca (Thermo Quest) mass spectrometer, while HRESIMS spectra were measured on a FTHRMS-Orbitrap (Thermo-Finnigan) mass spectrometer. HPLC analysis was performed using a Dionex UltiMate3400 SD with an LPG-3400SD pump with a photodiode array detector (DAD3000RS) and a Knauer Eurospher C_{18} analytical column (125 × 4 mm). Compounds were purified using semi-preparative HPLC on the VWR Hitachi Chromaster HPLC system, 5160 Pump; 5410 UV detector; Eurosphere-100 C_{18}, 300 mm × 8 mm, Knauer, Germany) utilizing MeOH and H_2O as eluents with a flow rate of 5 mL/min. Column chromatography was used for subsequent fractionation of the crude extract using different stationary phases including silica gel 60 M (Merck MN), silica gel 60 RP-18 (40-63 µm) and Sephadex LH-20 (25-100 µm). TLC plates were used for monitoring the collected fractions which resulted from column chromatography and spots were detected at 254 and 365 nm followed by anisaldehyde spray reagent.

3.2. Fungal material

The marine-derived fungus *A. falconensis* was isolated from marine sediment collected at a depth of 25 m from the Canyon at Dahab, Red Sea, Egypt in November 2016. The fungus was identified as *A. falconensis* (GenBank accession No. MN905375) using a molecular protocol as described previously.[26] The fungal strain has been deposited in one of author´s laboratory (P.P.).

3.3. Cultivation and extraction

The fungus was fermented on solid rice medium in 10 1L Erlenmeyer flasks. For preparation of solid medium, 100 g rice (Oryza Milchreis), 100 mL of demineralized water, and 3.5 g of sea salt (NaCl) were combined followed by autoclaving at 121°C for 20 min. Then, the fungus was inoculated on the sterile rice medium after cooling to room temperature. The culture was left to grow at 20°C under static conditions for 21 days.

Each flask was infused with 600 mL EtOAc, then the solid medium was cut into small pieces and shaken for 8 hours followed by filtration and evaporation of EtOAc till dryness. The weight of the crude EtOAc extract was 16 g.

3.4. OSMAC experiment

The cultivation and extraction procedures in the OSMAC experiment were the same as described before except for changing the incorporated inorganic salt from 3.5% NaCl to 3.5% $(NH_4)_2SO_4$ and cultivating the fungus on three flasks instead of ten. After evaporation of the solvent, 990 mg of EtOAC extract was yielded.

3.5. Isolation of compounds

The initial crude extract (16 g) obtained from cultivating the fungus on solid rice medium with 3.5% NaCl was subjected to silica gel vacuum liquid chromatography (VLC) utilizing a step gradient elution of n-hexane/EtOAc and CH_2Cl_2/MeOH to afford 12 fractions (ASFV1 to ASFV-12). Fractions ASFV-2 and ASFV-3 were combined (10.6 g). Fraction ASFV2/3 was further subjected to another VLC on silica gel with n-hexane/EtOAc as mobile phase affording 10 subfractions (ASFV2/3-V1 to ASFV2/3-V10). Subfraction ASFV2/3-V5 (217 mg) was further purified by semi-preparative HPLC using gradient elution with MeOH-H_2O mixtures (from 55:45 to 95:5 in 20 minutes) to afford compound (**1**) (7.1 mg). Fraction ASFV-4 (874 mg) was subjected to Sephadex LH20 column chromatography utilizing CH_2Cl_2–MeOH (1:1) as mobile phase which afforded eight subfractions (ASFV4-S1 to ASFV4-S8). Subfraction ASFV4-S5 (139.6 mg) was purified by semi-preparative HPLC using gradient elution with acetonitrile-H_2O (containing 0.1% formic acid) from 60:40 to 95:5 in 22 minutes affording arugosin C (**3**) (6.4 mg), and dichlorodiaportin (**4**) (2 mg). Subfraction ASFV4-S6 was combined with ASFV4-S7 (137.8 mg) then separated by semi-preparative HPLC utilizing gradient elution with MeOH-H_2O mixtures (48:52 to 80:20) to afford diorcinol (**7**) (15 mg), and 4-hydroxy benzaldehyde (**8**) (3.8 mg). Fraction ASFV-6 (686.1 mg) was subjected to RP-VLC column using H_2O-MeOH gradient

elution affording 10 subfractions (ASFV6-R1 to ASFV6-R10). Subfraction ASFV6-R7 (110 mg) was purified by semi-preparative HPLC using a gradient of MeOH-H_2O containing 0.1% formic acid from 67:33 to 80:20 in 20 minutes affording questin (**6**) (5.7 mg). Fraction ASFV10 (2.3 g) was further separated by column chromatography on Sephadex LH-20 with CH_2Cl_2–MeOH (1:1) as mobile phase affording seven subfractions (ASFV10-S1 to ASFV10-S7). Subfractions ASFV10-S5 and ASFV10-S6 were combined (130.8 mg) then subjected to semi-preparative HPLC with a gradient of MeOH-H_2O from 45:55 to 65:35 affording desmethyldiaportinol (**5**) (2.1 mg), and the new natural product compound (**2**) (2.2 mg).

The chromatographic work up of the EtOAc extract (990 mg) obtained from the OSMAC experiment with 3.5 % $(NH_4)_2SO_4$, followed the same procedure as described before for the EtOAc crude extract obtained from the initial fermentation on solid rice medium with NaCl. Subsequent purification of the obtained fractions on a silica gel column chromatography, a Sephadex LH20 column chromatography and semi-preparative HPLC with a gradient of MeOH-H_2O containing 0.1% formic acid afforded compound (**9**) (2 mg), compound (**10**) (0.7 mg), and compound (**11**) (3.2 mg).

3.6. Compound characterization

Arugosin O (**1**): Yellow needle crystals; UV (MeOH) λ_{max} 269.2, 236.2, and 202.8 nm; ^{1}H and ^{13}C NMR data, Table 1; HRESIMS *m/z* 409.2022 $[M + H]^+$ (calcd for $C_{25}H_{29}O_5$, 409.2015).

2-(8-Hydroxy-6-methoxyisochromen-3'-yl) acetic acid (**2**): Brown oil; UV (MeOH) λ_{max} 327.9, 277.7, and 243.5 nm; ^{1}H NMR (600 MHz, DMSO-d_6) δ 10.93 (1H, s, 8-OH), 6.66 (1H, s, H-4), 6.64 (1H, d, J = 2.3 Hz, H-5), 6.56 (1H, d, J = 2.3 Hz, H-7), 3.86 (3H, s, 6-OC$\underline{H}_3$), 3.61 (2H, s, H-9); ^{13}C NMR (150 MHz, DMSO) δ 169.8 (C-10), 166.6 (C-6), 165.0 (C-1), 162.6 (C-8), 151.3 (C-3), 139.1 (C-4a), 106.5 (C-4), 101.7 (C-8a), 100.8 (C-7), 99.2 (C-5), 56.0 (6-O$\underline{C}H_3$), 38.6 (CH_2-9); HRESIMS *m/z* 251.0553 $[M + H]^+$ (calcd for $C_{12}H_{11}O_6$, 251.0550). *In Silico* Virtual Screening Studies

3.7. In Silico virtual screening studies

Molecular docking experiments for the main constituents isolated from *Aspergillus falconensis* were performed on human cyclin-dependent kinase 2 (CDK-2) (PDB ID 1PXP, 2.30 Å), human DNA topoisomerase II (TOP-2) (PDB ID 4G0U, 2.70 Å), and matrix metalloproteinase 13 (MMP-13) (PDB ID 1XUD, 1.8Å). Virtual screening was done on the previously listed enzymes which were downloaded from protein data bank (www.pdb.org) using Discovery Studio 2.5 (Accelrys Inc., San Diego, CA, USA) adopting C-docker protocol. Free binding energies were computed as previously reported for the most stable docking poses.[27, 28]

3.8. Cytotoxicity assay

Cytotoxicity was tested against L5178Y mouse lymphoma cells utilizing the MTT (3-(4,5-dimethylthiazol-2-yl)-2,5-diphenyltetrazoliumbromide) assay, in comparison to untreated controls, as previously described.[29] As negative control, 0.1% ethylene glycol monomethyl ether in DMSO was utilized in this experiment. For the positive control, the depsipeptide kahalalide F (4.3 µM) was used. Experiments were repeated three times and carried out in triplicate.

Acknowledgments

D.H.E. gratefully acknowledges the Egyptian Government (Ministry of Higher Education) for awarding a doctoral scholarship. Financial support by the Manchot Foundation and by the DFG (Project number 270650915, GRK 2158) to P.P. is gratefully acknowledged. In addition, we wish to thank Dr. Dent. Abdel Rahman O. El Mekkawi, EFR, PADI IDC staff instructor, founder of I Dive Tribe, Dahab, South Sinai – Egypt, for collecting the sediment sample.

References and notes

Supplementary Material

Supplementary material (HPLC chromatograms, UV spectra, HRESIMS analyses, ^{1}H NMR, ^{13}C NMR, HSQC and HMBC spectra for compounds 1 and 2 and COSY spectrum of compound **1** can be found, in the online version, at -----

1. http://midwestern.edu/departments/marinepharmacology/clinical-pipeline.xml (accessed 04.08.2020).
2. Smith, C. J.; Abbanat, D.; Bernan, V. S.; Maiese, W. M.; Greenstein, M.; Jompa, J.; Tahir, A.; Ireland, C. M., *J Nat Prod* **2000**, *63*, 142-145.
3. Park, Y. C.; Gunasekera, S. P.; Lopez, J. V.; McCarthy, P. J.; Wright, A. E., *J Nat Prod* **2006**, *69*, 580-584.
4. Liu, H.; Edrada-Ebel, R.; Ebel, R.; Wang, Y.; Schulz, B.; Draeger, S.; Müller, W. E.; Wray, V.; Lin, W.; Proksch, P., *J Nat Prod* **2009**, *72*, 1585-1588.
5. Frank, M.; Özkaya, C. F.; Müller, E. G. W.; Hamacher, A.; Kassack, U. M.; Lin, W.; Liu, Z.; Proksch, P., *Mar Drugs* **2019**, *17*, 99.
6. Ebada, S. S.; Proksch, P., Marine-Derived Fungal Metabolites. In Springer Handbook of Marine Biotechnology, Kim, S.-K., Ed. Springer Berlin Heidelberg: Berlin, Heidelberg, 2015; pp 759-788.
7. https://www.beyondspringpharma.com/ChannelPage/index.aspx. (accessed 22.01.2020).
8. El-Kashef, D. H.; Daletos, G.; Plenker, M.; Hartmann, R.; Mandi, A.; Kurtan, T.; Weber, H.; Lin, W.; Ancheeva, E.; Proksch, P., *J Nat Prod* **2019**, *82*, 2460-2469.
9. Mokhlesi, A.; Hartmann, R.; Kurtan, T.; Weber, H.; Lin, W.; Chaidir, C.; Müller, W. E. G.; Daletos, G.; Proksch, P., *Mar Drugs* **2017**, *15*, 356.
10. El-Kashef, D. H.; Youssef, F. S.; Hartmann, R.; Knedel, T.-O.; Janiak, C.; Lin, W.; Reimche, I.; Teusch, N.; Liu, Z.; Proksch, P., *Mar Drugs* **2020**, *18*, 204.
11. Romano, S.; Jackson, S. A.; Patry, S.; Dobson, A. D. W., *Marine Drugs* **2018**, *16*, 244.
12. Hawas, U. W.; El-Beih, A. A.; El-Halawany, A. M., *Arch. Pharm. Res.* **2012**, *35*, 1749-1756.
13. Larsen, T. O.; Breinholt, J., *J Nat Prod* **1999**, *62*, 1182-1184.
14. Aly, A. H.; Edrada-Ebel, R.; Wray, V.; Müller, W. E.; Kozytska, S.; Hentschel, U.; Proksch, P.; Ebel, R., *Phytochemistry* **2008**, *69*, 1716-1725.
15. Chaudhary, N. K.; Pitt, J. I.; Lacey, E.; Crombie, A.; Vuong, D.; Piggott, A. M.; Karuso, P., *J Nat Prod* **2018**, *81*, 1517-1526.
16. Sanchez, J. F.; Chiang, Y. M.; Szewczyk, E.; Davidson, A. D.; Ahuja, M.; Elizabeth Oakley, C.; Woo Bok, J.; Keller, N.; Oakley, B. R.; Wang, C. C., *Mol Biosyst* **2010**, *6*, 587-593.
17. Gomez-Betancur, I.; Zhao, J. P.; Tan, L.; Chen, C.; Yu, G.; Rey-Suarez, P.; Preciado, L., *Mar Drugs* **2019**, *17*, 401.
18. Sun, T. Y.; Kuang, R. Q.; Chen, G. D.; Qin, S. Y.; Wang, C. X.; Hu, D.; Wu, B.; Liu, X. Z.; Yao, X. S.; Gao, H., *Molecules* **2016**, *21*, 1184.
19. Kralj, A.; Kehraus, S.; Krick, A.; Eguereva, E.; Kelter, G.; Maurer, M.; Wortmann, A.; Fiebig, H. H.; Konig, G. M., *J Nat Prod* **2006**, *69*, 995-1000.
20. Matsumoto, N.; Nakashima, T.; Isshiki, K.; Kuboki, H.; Hirano, S. I.; Kumagai, H.; Yoshioka, T.; Ishizuka, M.; Takeuchi, T., *J. Antibiot.* **2001**, *54*, 285-296.
21. Inamori, Y.; Kato, Y.; Kubo, M.; Kamiki, T.; Takemoto, T.; Nomoto, K., *Chem. Pharm. Bull.* **1983**, *31*, 4543-4548.

22. Hall, C. R.; Bisi, J. E.; Strum, J. C., Inhibition of CDK2 overcomes primary and acquired resistance to CDK4/6 inhibitors. AACR: 2019.
23. Chikamori, K.; G Grozav, A.; Kozuki, T.; Grabowski, D.; Ganapathi, R.; K Ganapathi, M., *Curr Cancer Drug Targets* **2010**, *10*, 758-771.
24. Cutts, S. M.; Nudelman, A.; Rephaeli, A.; Phillips, D. R., *IUBMB life* **2005**, *57*, 73-81.
25. Vihinen, P.; Ala-aho, R.; Kahari, V.-M., *Curr Cancer Drug Targets* **2005**, *5*, 203-220.
26. Kjer, J.; Debbab, A.; Aly, A. H.; Proksch, P., *Nat Protoc* **2010**, *5*, 479-490.
27. Labib, R.; Youssef, F.; Ashour, M.; Abdel-Daim, M.; Ross, S., *Molecules* **2017**, *22*, 1384.
28. Janibekov, A. A.; Youssef, F. S.; Ashour, M. L.; Mamadalieva, N. Z., *Ind Crops Prod* **2018**, *118*, 142-148.
29. Ashour, M.; Edrada, R.; Ebel, R.; Wray, V.; Watjen, W.; Padmakumar, K.; Müller, W. E.; Lin, W. H.; Proksch, P., *J Nat Prod* **2006**, *69*, 1547-1553.

4.2 Supporting Information

Supplementary Material

A new dibenzoxepin and a new natural isocoumarin from the marine-derived fungus *Aspergillus falconensis*

Dina H. El-Kashef [a,b], Fadia S. Youssef [a,c], Werner E.G. Müller [d], Wenhan Lin [e], Marian Frank [a,*], Zhen Liu [a,*] and Peter Proksch [a,f,*]

[a]*Institute of Pharmaceutical Biology and Biotechnology, Faculty of Mathematics and Natural Sciences, Heinrich-Heine-University Duesseldorf, 40225 Duesseldorf, Germany.*
[b]*Department of Pharmacognosy, Faculty of Pharmacy, Minia University, 61519 Minia, Egypt.*
[c]*Department of Pharmacognosy, Faculty of Pharmacy, Ain Shams University Abbassia, 11566 Cairo, Egypt*
[d]*Institute of Physiological Chemistry, Johannes Gutenberg University Mainz, 55128 Mainz, Germany.*
[e]*State Key Laboratory of Natural and Biomimetic Drugs, Peking University, Beijing 100191, China.*
[f]*Hubei Key Laboratory of Natural Products Research and Development, College of Biological and Pharmaceutical Sciences, China Three Gorges University, Yichang 443002, China.*

Contents

Figure S1. HPLC chromatogram (A) and UV spectrum (B) of compound **1**.

A)

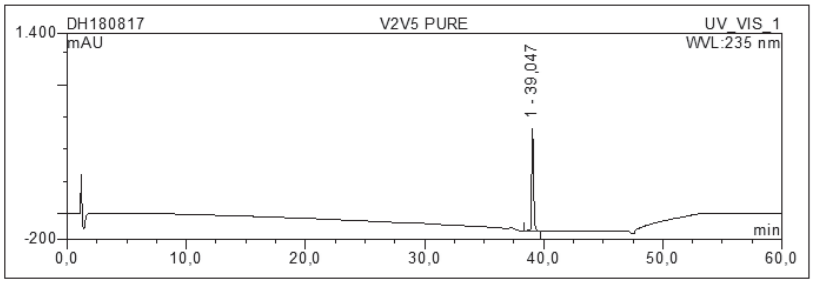

B)

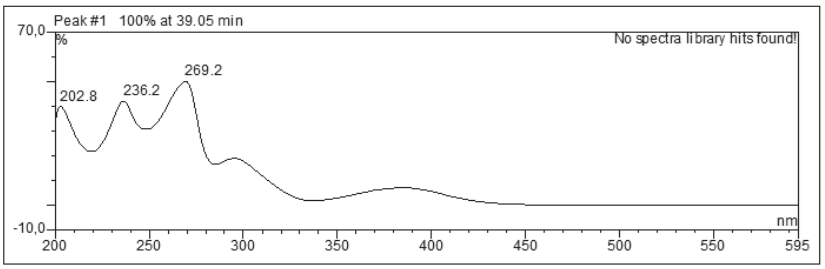

Figure S2. HRESIMS of compound **1**.

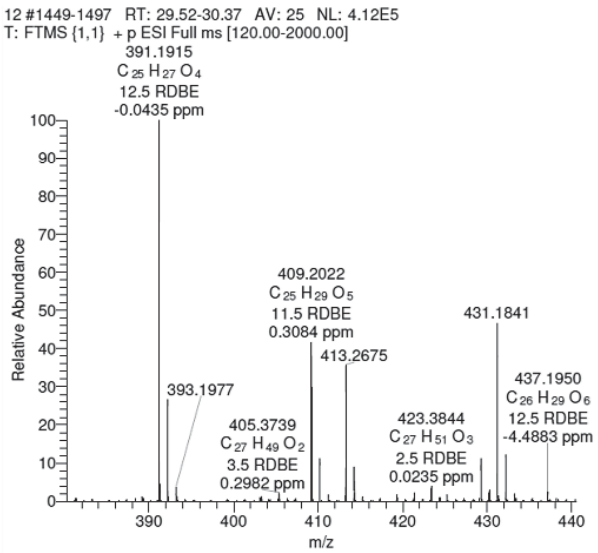

Figure S3. ^{1}H NMR (600 MHz, $CDCl_3$) Spectrum of Compound **1**.

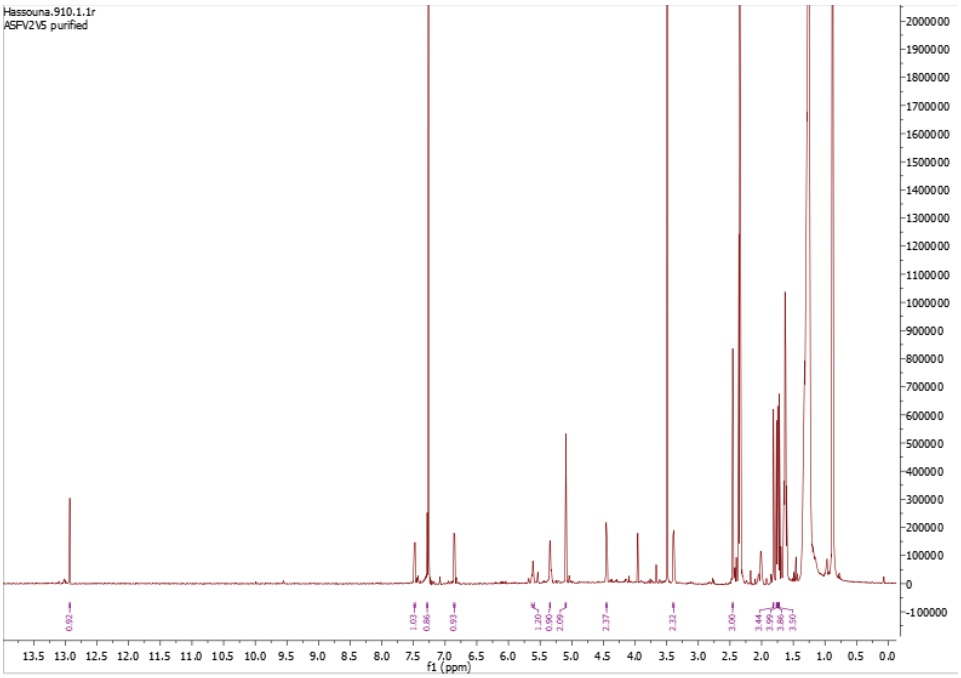

4

Figure S4. COSY (600 MHz, $CDCl_3$) spectrum of compound **1**.

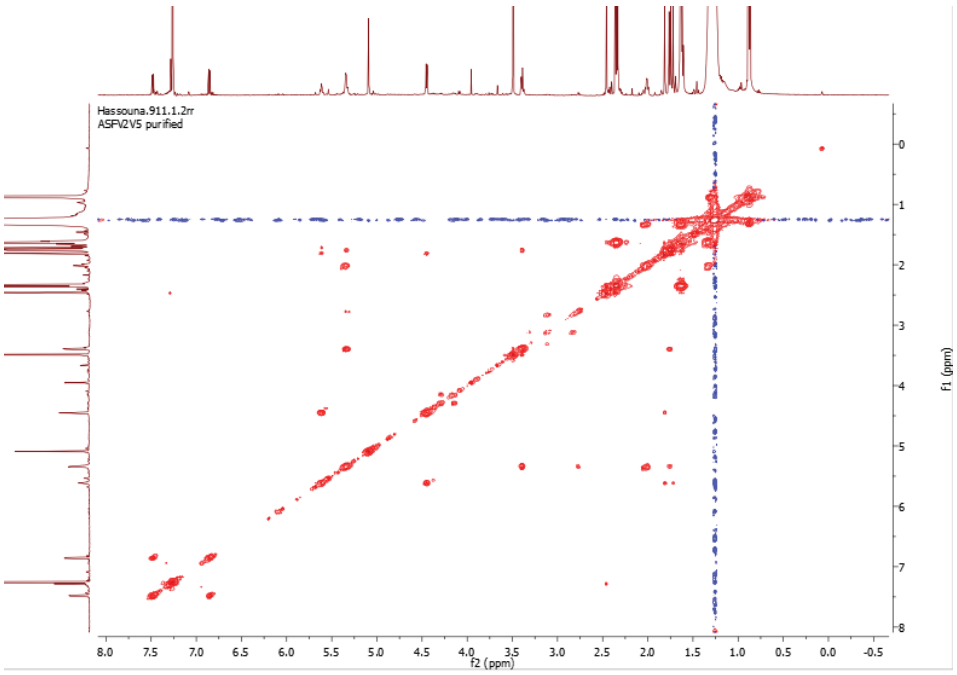

5

Figure S5. HSQC (600 MHz/150 MHz, $CDCl_3$) spectrum of compound **1**.

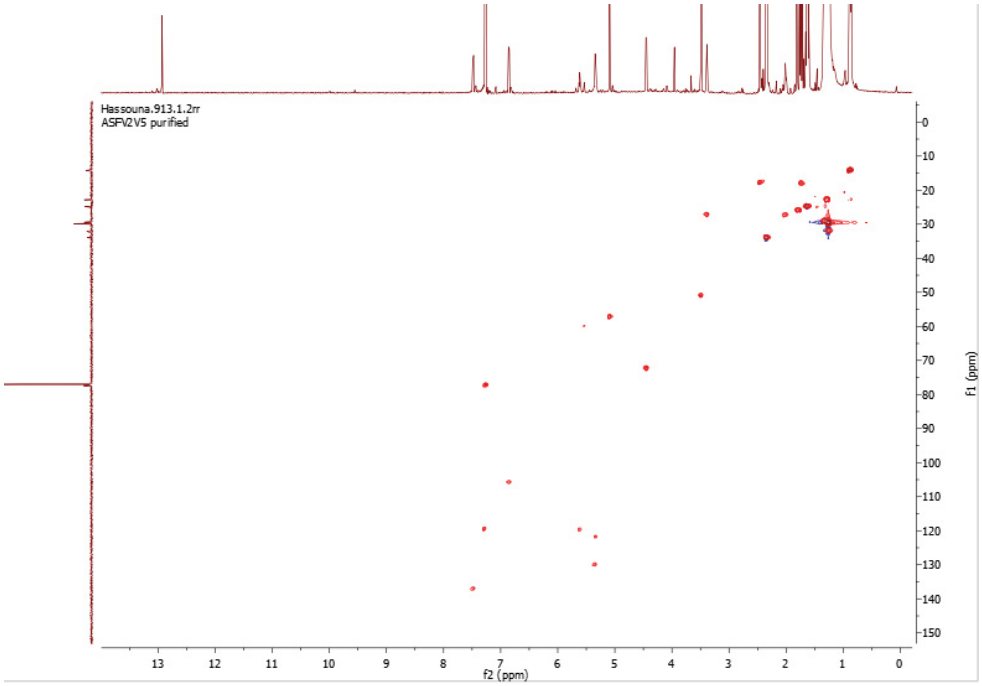

6

Figure S6. HMBC (600 MHz/150 MHz, $CDCl_3$) spectrum of compound **1**.

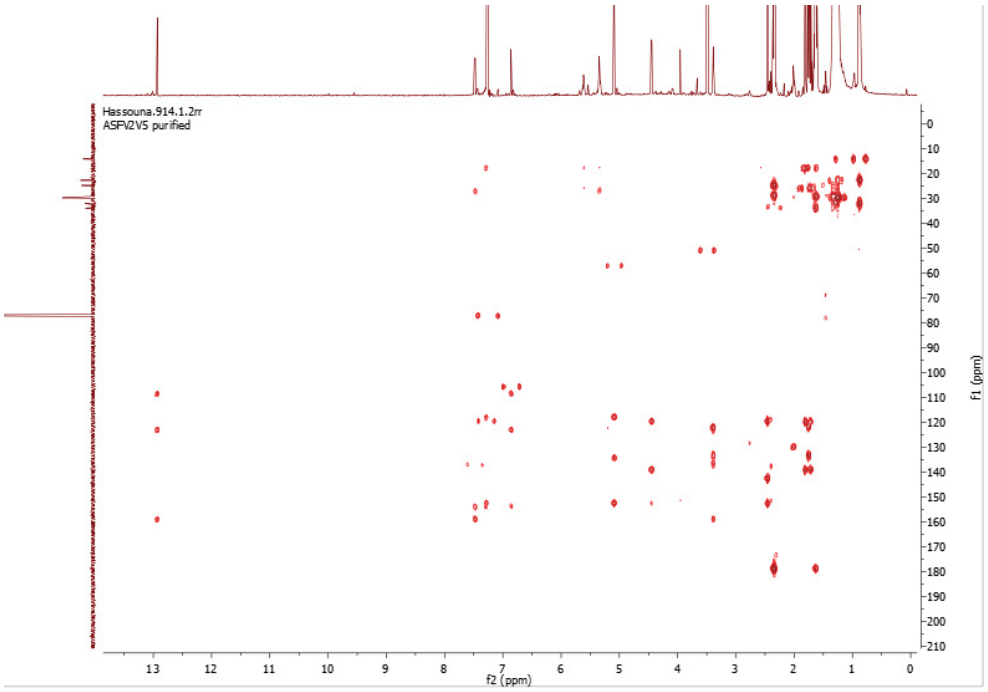

7

Figure S7. HPLC chromatogram (A) and UV spectrum (B) of compound **2**.

A)

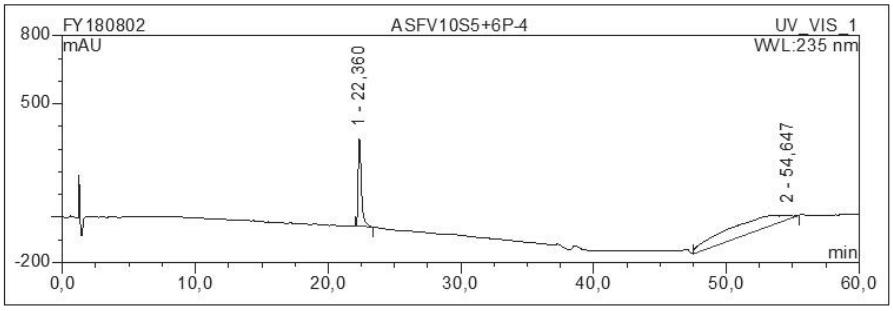

B)

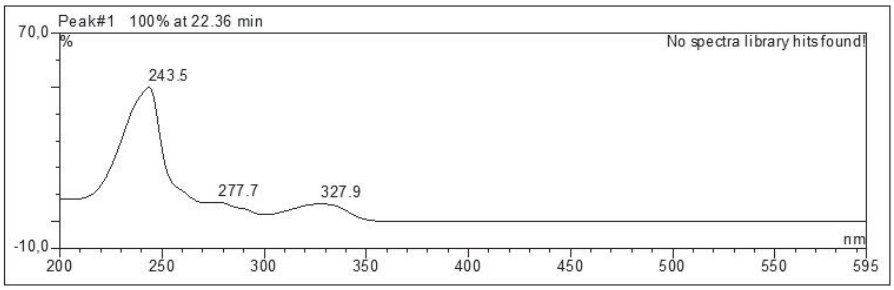

Figure S8. HRESIMS of compound **2**.

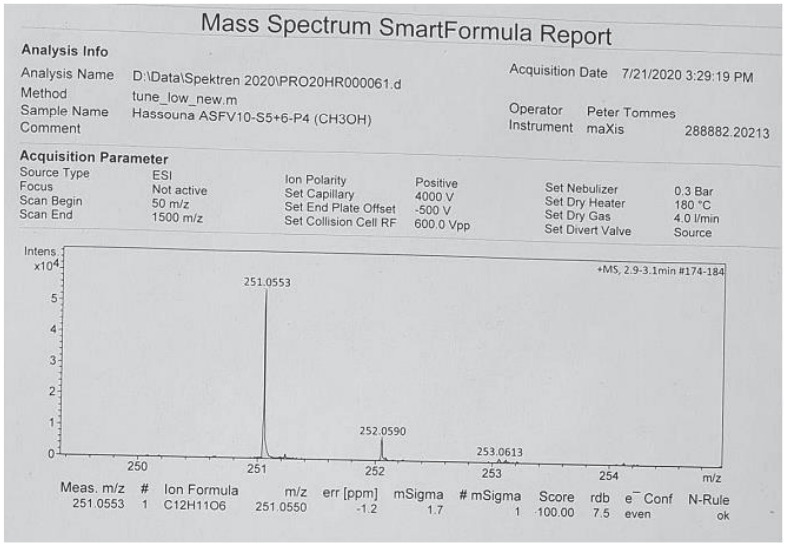

Figure S9. ^{1}H NMR (600 MHz, DMSO-d_6) spectrum of compound **2**.

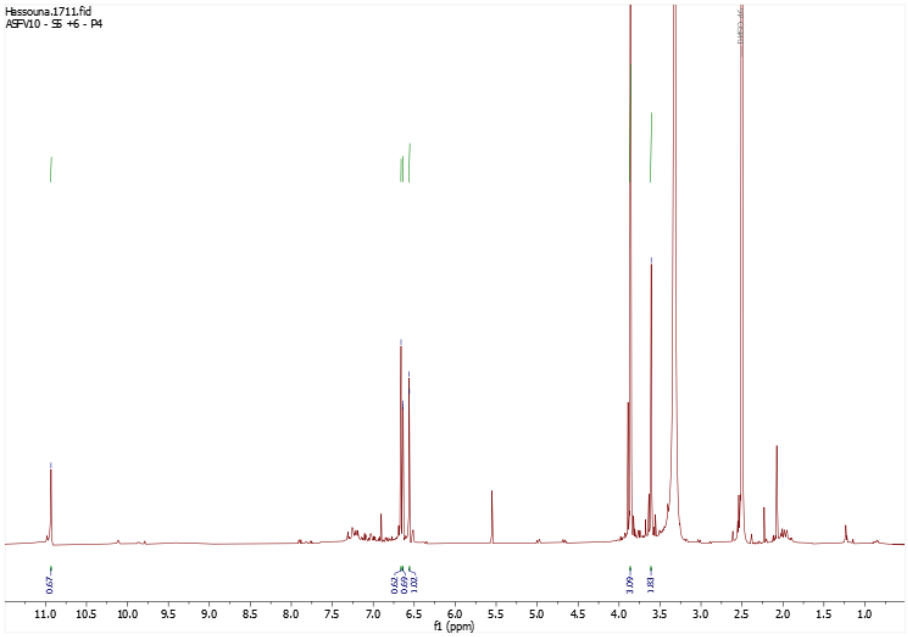

9

Figure S10. ^{13}C NMR (150 MHz, DMSO-d_6) spectrum of compound **2**.

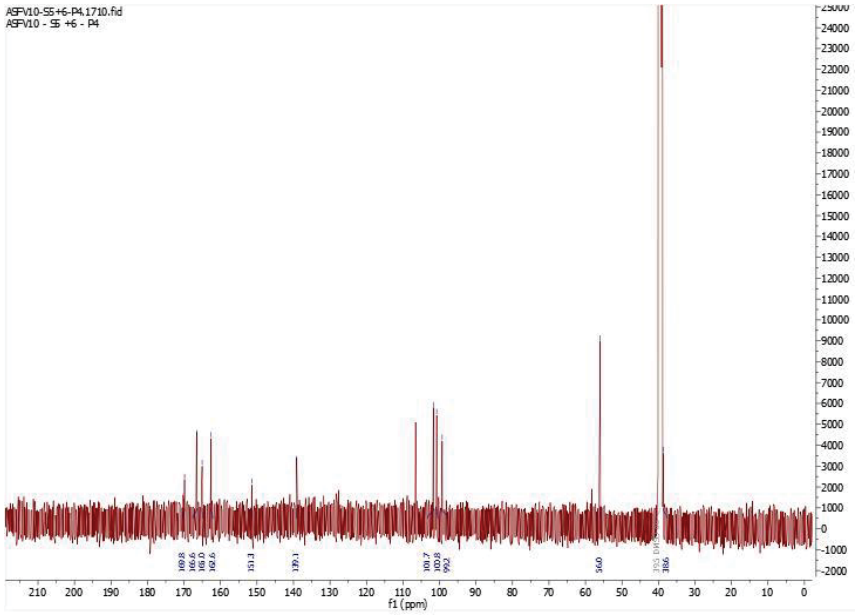

10

Figure S11. HSQC (600 MHz/150 MHz, DMSO-d_6) spectrum of compound **2**.

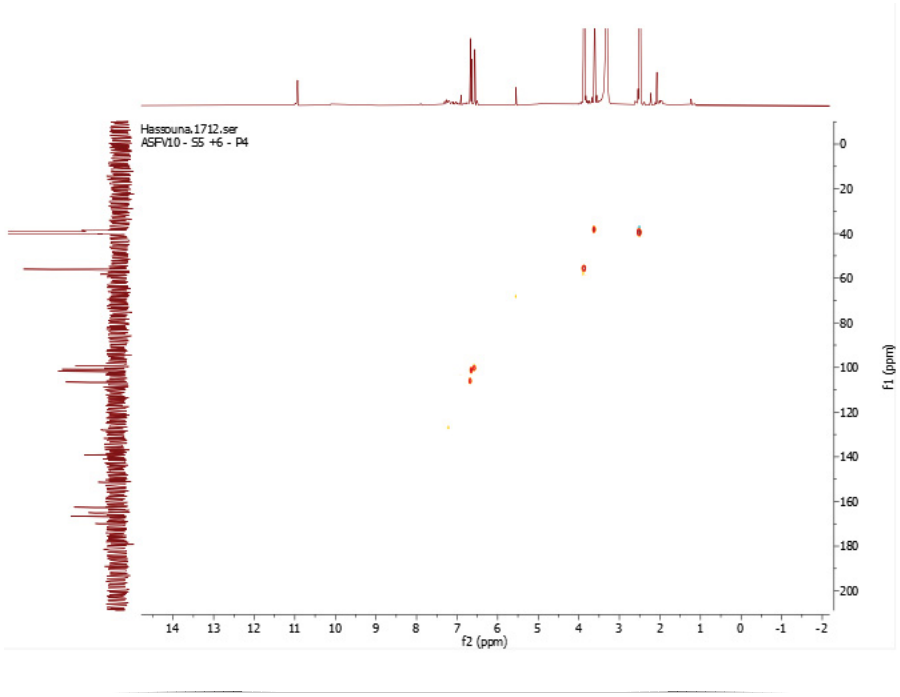

11

Figure S12. HMBC (600 MHz/150 MHz, DMSO-d_6) spectrum of compound **2**.

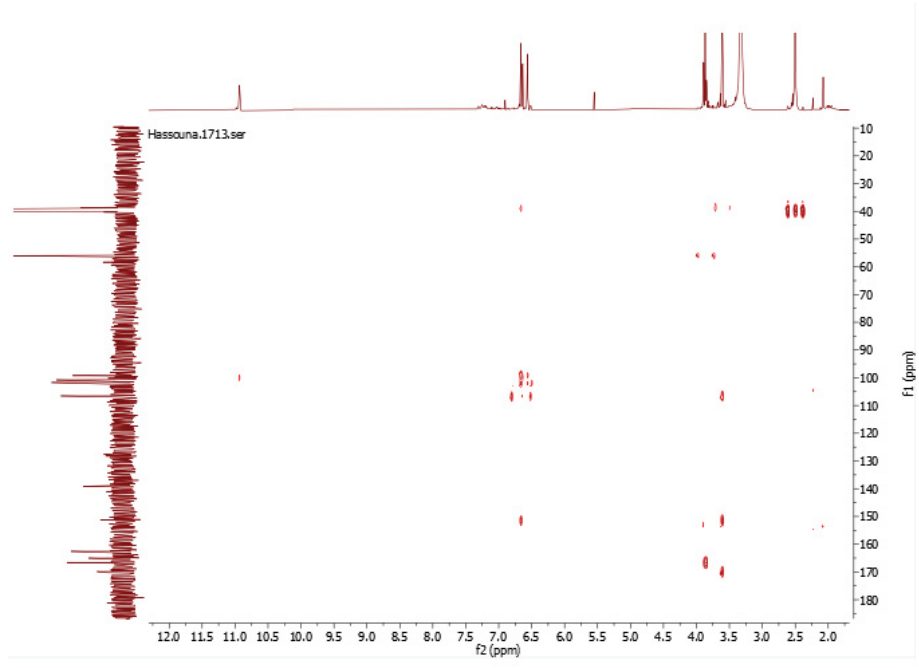

12

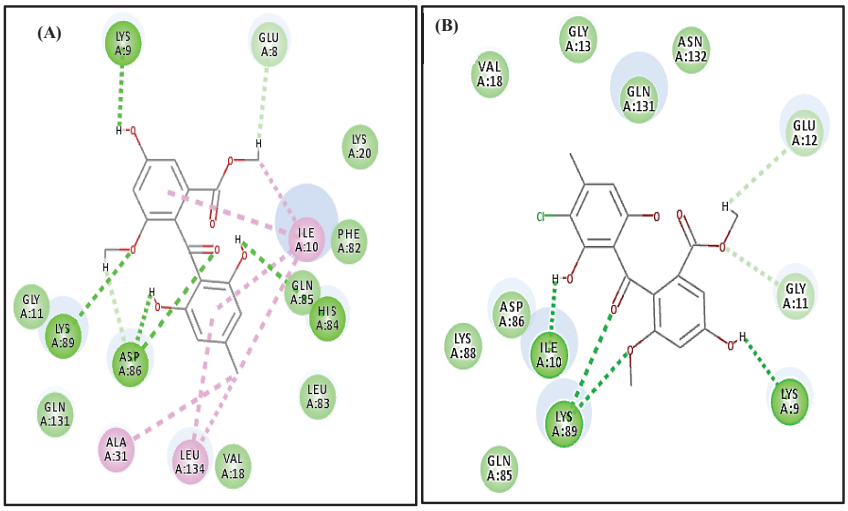

Figure S13: 2D binding modes of the (A) sulochrin (**9**) and (B) monochlorosulochrin (**10**) within the active pocket of CDK-2.

13

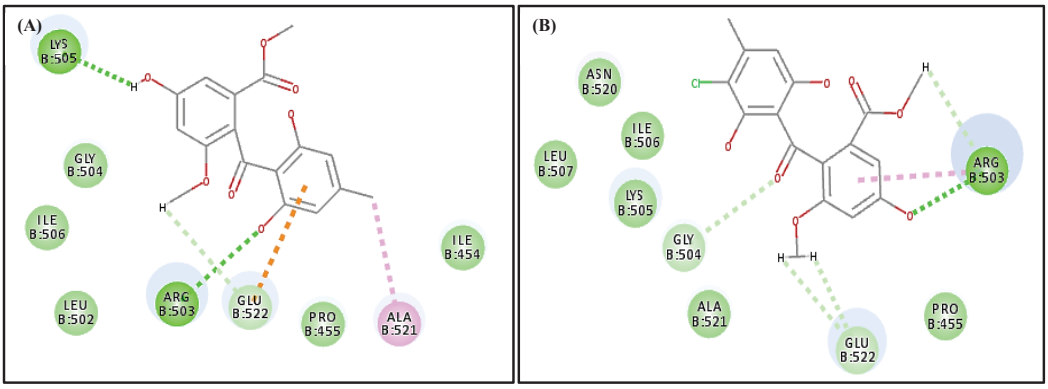

Figure S14: 2D binding modes of the (A) sulochrin (**9**) and (B) monochlorosulochrin (**10**) within the active pocket of TOP-2.

14

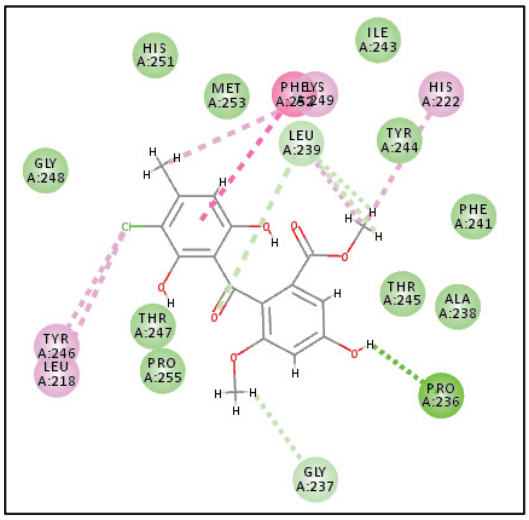

Figure S15. 2D binding mode of the monochlorosulochrin (**10**) in the active pocket of MMP-13

Chapter 5 - General Discussion

5.1 Underexplored Fungi from Unusual Sources

Fungi from "exotic" or extreme habitats are considered as a treasure for isolating fascinating compounds which could serve as potential candidates for drug discovery and development. Generally, an extreme habitat is referred to when organisms live at high or low pH, high or low temperature, high pressure and/or high salinity (Wilson *et al.* 2009). Organisms from such harsh habitats have developed special defences against the surrounding environment in order to survive and to be able to grow and reproduce, including the production of many interesting molecules ranging from simple secondary metabolites to complex compounds (Wilson *et al.* 2009, Chávez *et al.* 2015). For instance, marine conditions (e.g. salinity, high hydrostatic pressure, low temperature, low oxygen levels, light deficiency), especially in the deep-sea environment, are considered as harsh conditions for organisms to survive in. Consequently, fungi from such environments are expected to produce structurally unique compounds with potential biological and pharmacological activities (Rateb *et al.* 2011, Shin 2020).

For instance, from the marine-derived fungus *Aspergillus insulicola*, obtained from a Hawaiian marine-sediment, a novel hexacyclic dipeptide, azonazine, was isolated. The compound exhibited anti-inflammatory activity through inhibiting both NF-κB luciferase with IC_{50} value of 8.37 μM and nitrite production with IC_{50} value of 13.70 μM (Wu *et al.* 2010).

5.1.1 Investigation of New Secondary Metabolites from Marine Fungi

Marine-derived fungi are contributing significantly to the field of natural products' chemistry and represent a valuable source for isolating new secondary metabolites with unusual structural features exhibiting diverse bioactivities (Shin 2020). Aiming to investigate underexplored fungi from exotic sources, two marine fungal strains from different sources were examined in this doctoral thesis. The first investigated marine–derived fungus, *Metarhizium marquandii*, was isolated from seawater sediment collected from the North Sea, Germany. The North Sea covers a surface area of 575,000 km^2. However, its biosphere is considered as an underexplored habitat and poorly investigated for the production of secondary metabolites (Lee 1980, Lysek *et al.* 2002, König *et al.* 2006, Schulz *et al.* 2011). Excitingly, fungi from the genus *Metarhizium*

are soil-borne, mostly infect soil-dwelling insects and are considered as entomopathogens which have been frequently used worldwide in several agricultural and disease-vector control programs (Bidochka *et al.* 2001, Scholte *et al.* 2004). Whilst isolating the genus *Metarhizium* from a marine source is not common and only reported in few publications (Cabrera *et al.* 2006, Boot *et al.* 2007). Moreover, our search with databases such as Scifinder revealed that the species *Metarhizium marquandii* is rarely investigated and only few metabolites have been reported from it (syn. *Paecilomyces marquandii*) (Radics *et al.* 1987, Cabrera *et al.* 2006). Accordingly, the fungus *M. marquandii* was of high interest to be studied for inspecting its secondary metabolite production and for exploring the North Sea as a fruitful source for isolating new structural entities. Fascinatingly, chemical investigation of the fungus yielded structurally unique natural products of different chemical classes (polyketides, alkaloids and butenolides), Moreover, three of the isolated compounds, marqualide, (±)-peniphenone E and aflaquinolone I, are new natural products from which marqualide possesses an unusual methylenebistetronic acid group that is unprecedented in nature. Determination of absolute configuration of the isolated compounds is discussed and explained separately in **chapter 5.3.**

From a different ecological habitat, the Red Sea, Egypt, the second chosen fungus for study in this thesis, *Aspergillus falconensis*, was obtained. The Red Sea is an extremely productive source of new biologically active marine secondary metabolites. Over the last decade, great interest from marine natural products' experts was given to the Red Sea resulting in the isolation and characterization of more than 600 marine natural products so far (Abou El-Ezz *et al.* 2017, El-Hossary *et al.* 2020). These marine natural products were mainly obtained from marine invertebrates (sponges and soft corals) and marine microbes (fungi and bacteria) comprising different compound classes such as terpenes, sterols, peptides, alkaloids, polyketides, macrolides, flavonoids, polyacetylenes, quinones and fatty acids and exerting impressive biological activities (Hawas *et al.* 2016, El-Hossary *et al.* 2020).

Generally, the genus *Aspergillus*, which is composed of more than 300 species, has proven to be a prolific source for high diversity of bioactive natural products and it is one of the main genera contributing to fungal secondary metabolites (Bugni *et al.* 2004, Zin *et al.* 2016, Elad *et al.* 2018). Although the genus *Aspergillus* is considered as a terrestrial genus, this genus is very tolerant to high NaCl concentrations (Tresner *et al.*

1971). Therefore, species belonging to genera *Aspergillus* as well as *Penicillium* are considered as dominant fungi inhabiting the marine environment and they are the most studied genera among all marine-derived fungi (Imhoff 2016). Nevertheless, the genus *Aspergillus* obtained from the Red Sea is poorly studied and only few publications report metabolite production and the bioactivities exerted by the isolated secondary metabolites (Abd El-Hady *et al.* 2015, El-Gendy *et al.* 2015, Ahmed *et al.* 2017, Asfour *et al.* 2019). Thus, the second investigated fungus in this thesis, *Aspergillus falconensis*, obtained from the Red Sea, Egypt, was chosen for study. Noteworthy to mention that in this study *A. falconensis* is investigated for the first time from a marine origin. The fungus was obtained from a marine sediment collected at a water depth of 25 m from the canyon at Dahab, Red Sea, Egypt to demonstrate how fungi from exotic habitats could be producers of diverse remarkable secondary metabolites with potential biological activities. During this work various natural products belonging to different classes of compounds were isolated including azaphilone derivatives (falconensins) besides many phenolic compounds classified as dibenzoxepin derivatives (arugosin C and O), isocoumarin derivatives (2-(8-Hydroxy-6-methoxyisochromen-3'-yl) acetic acid, dichlorodiaportin and desmethyldiaportinol), phenolic aldehyde (4-hydroxybenzaldehyde), anthraquinone (questin) and diphenyl ether (diorcinol). This result supports the high potential of the biosynthetic machinery of the genus *Aspergillus* (Bugni *et al.* 2004). Besides, in order to diversify the metabolite production and to activate silent biogenetic clusters, the OSMAC approach was implemented and succeeded in improving the metabolic profile of the fungus and in isolating biologically active secondary metabolites including further new azaphilone derivatives and accumulation of benzophenone derivatives (sulochrin, monochlorosulochrin and dihydrogeodin). The results of the OSMAC experiments are discussed in **chapters 5.2.1** and **5.2.2**. Additionally, *in silico* and *in vitro* studies were conducted on the isolated phenolic secondary metabolites from the fungus.

Molecular docking of the isolated phenolic compounds was performed on different enzymes associated with cancer formation such as human cyclin-dependent kinase 2 (CDK-2), human DNA topoisomerase II (TOP-2) and matrix metalloproteinase 13 (MMP-13) with the aim of discovering new anticancer entities through prediction of interaction between compounds with the active pocket of enzymes (Horňák *et al.* 1999). To further support molecular docking results, *in vitro* cytotoxic MTT assays against

mouse lymphoma cell line L5178Y were conducted and showed that sulochrin, one of the isolated phenolic compounds, exhibited cytotoxic activity with an IC_{50} value of 5.1 μM. Additionally, the isolated azaphilone derivatives (falconensins) were evaluated for their anti-inflammatory activity through NF-κB inhibitory assay against the triple negative breast cancer cell line MDA-MB-231. The results of this activity is discussed separately in **chapter 5.4**.

5.2 Exploring the Structural Diversity of Fungal Secondary Metabolites by Implementing OSMAC Approaches

Fungal secondary metabolites represent a bioprospecting source for drug discovery by offering a huge diversity of compounds (Keller 2019). Under standard cultivation conditions, not all fungal gene clusters are transcribed and many of these gene clusters are considered "silent" as exemplified by the difference between the number of identified gene clusters as the potential producers of fungal secondary metabolites and the actual number of isolated secondary metabolites from the same fungus (Daletos *et al.* 2017, Romano *et al.* 2018). In order to activate silent biogenetic gene clusters and to increase the diversity of fungal secondary metabolites, OSMAC approaches can be employed (Daletos *et al.* 2017, Pan *et al.* 2019). In the current study, the marine-derived fungus, *Aspergillus falconensis*, was subjected to numerous OSMAC experiments in order to explore the potential of its biosynthetic machinery for the production of interesting new secondary metabolites through activation of silent biogenetic gene clusters.

5.2.1 OSMAC Approach and Halogenation in Marine Natural Products

Due to the fact that halogen atoms are abundant in sea and ocean water, halogenated secondary metabolites are commonly present in marine organisms (*e.g.* marine fungi) (Gribble 1998, Huang *et al.* 2012). Therefore, OSMAC experiments with changing the incorporated halogen sources are an interesting approach for diversification of metabolites (Chen *et al.* 2019, Frank *et al.* 2019). In the current study, two new dichlorinated azaphilones, falconensins O and P, together with the known dichlorinated azaphilone derivatives (falconensin A, M, N and H), were isolated following fermentation of *Aspergillus falconensis* on solid rice medium containing 3.5% sodium chloride which is similar to the salinity of sea water. Since bromine atoms are also present in sea water but in a less concentration than chlorine atoms (only 0.065 parts per thousand) and because halogenating enzymes (flavin-dependent halogenases

or haloperoxidases) could also incorporate bromine rather than chlorine atoms (Mclachlan *et al.* 1967, Sureram *et al.* 2013), an OSMAC experiment by replacing the incorporated NaCl in the rice medium with 3.5% sodium bromide was conducted in an attempt to produce new brominated derivatives. Remarkably, two new brominated azaphilones, falconensins Q and R, were produced following this OSMAC experiment. One additional observational consequence of adding bromine to the culture medium was the isolation of new non-halogenated azaphilone, falconensin S (figure 5).

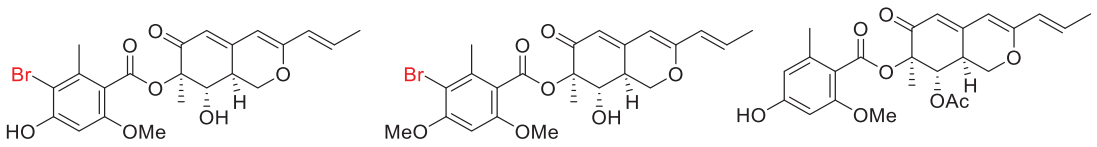

Falconensin Q Falconensin R Falconensin S

Figure 5. Brominated and non- brominated azaphilones from OSMAC experiment.

Although the isolated chlorinated and brominated azaphilones showed very similar UV spectra, their retention times in the HPLC chromatograms were very different. Moreover, the characteristic isotope patterns corresponding to chlorine and bromine atoms were clearly indicated in mass spectra of the isolated compounds from solid rice media containing 3.5% NaCl or 3.5% NaBr, respectively. The overall change in the metabolic profile of *A. falconensis* after altering halogen salts added to rice medium was detected in HPLC chromatograms of crude extracts after conducting different OSMAC experiments (figure 6).

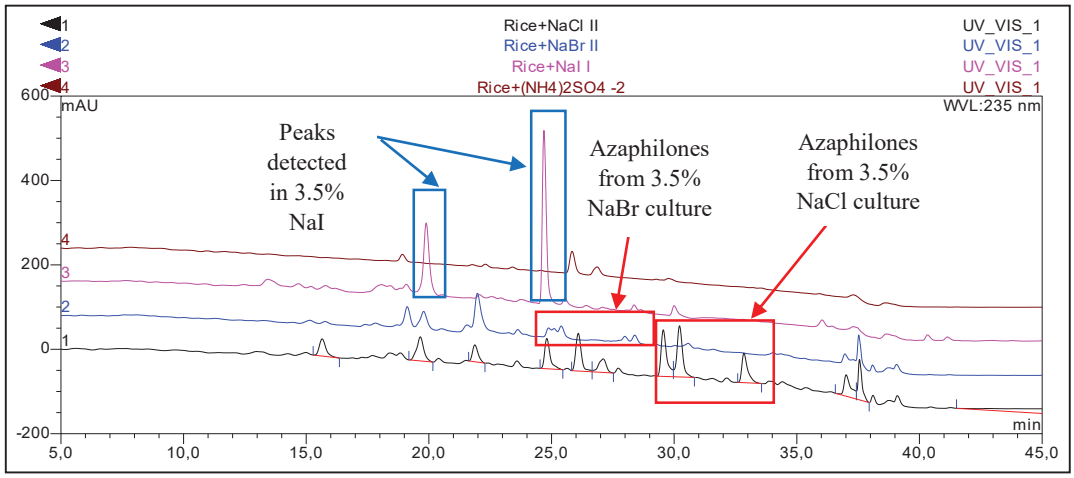

Figure 6: HPLC overlay of different rice medium extracts of *Aspergillus falconensis* supplemented with different salts.

To demonstrate whether halogenating enzymes are able to utilize other halogen substrates such as iodide and fluoride, other OSMAC experiments were conducted on the fungus *A. falconensis* by incorporating 3.5% sodium iodide or 3.5% sodium fluoride into solid rice medium.

Strikingly, in the 3.5% NaI containing culture, the fungus did not produce any iodinated metabolites. Moreover, no azaphilones were detected in the fermentation culture but, only two peaks corresponding to non-halogenated low molecular weight compounds were observed. The two compounds were also detected in control culture but upregulated in the 3.5% NaI culture (Figure 6). Unfortunately, these two peaks were not isolated due to their instability during isolation procedures. In general, iodinated natural products are relatively rare and very few examples are known in nature (Gribble 1998, Anderson *et al.* 2006). To the best of our knowledge, only one study described the isolation of iodinated natural products from marine fungi following an OSMAC experiment on the marine-derived fungus *Trichoderma* cf. *brevicompactum* after incorporating 3.0% NaI in the culture medium (Yamazaki *et al.* 2015).

Furthermore, we found that the fungus did not grow in the 3.5% NaF supplemented culture indicating the toxic effect of fluoride ions on fungi (Li *et al.* 2013).

Therefore, we speculate that halogenation of the isolated azaphilones was conducted by halogenating enzymes which could utilize chlorine and bromine but not

iodine. Since flavin-dependent halogenases catalyze regioselective halogenation of aromatic natural products and can incorporate halogens such as chlorine and bromine but not iodine (Neubauer *et al.* 2018) and because halogenation of orsellinic acid, a biosynthetic intermediate of falconensins, is known to be utilized via $FADH_2$-dependent halogenase (Sureram *et al.* 2013), we assume that the fungus *Aspergillus falconensis* harbours $FADH_2$-dependent halogenases that are catalyzing halogenation in the aromatic orsellinate moiety of isolated azaphilones and not haloperoxidases (which could incorporate iodine besides chlorine and bromine) (Sureram *et al.* 2013).

Generally, substitution of chlorine with bromine in microbial metabolites has been reported several times in the literature (Huang *et al.* 2012, Wang *et al.* 2016) and could be attributed to the higher reactivity of Br^- than Cl^- ions (Cruz *et al.* 2015). However, very few examples report the isolation of brominated azaphilone derivatives from fungi. The aforementioned examples are exclusively reported from different *Penicillium* species namely, *P. multicolor*, *P. janthinellum*, *P. canescens* (Matsuzaki *et al.* 1998, Chen *et al.* 2019, Frank *et al.* 2019). It is worth to mention that the current study represents the first isolation of brominated azaphilones from the genus *Aspergillus*. In addition, among those few examples of brominated azaphilone derivatives, the current study is the only example which demonstrates bromination in the orsellinate moiety substituent not directly in the azaphilone core nucleus. Moreover, the isolated azaphilone derivatives from *A. falconensis* are structurally unique with halogenation in the orsellinate substituent and not in C-5 as shown in all the previously reported halogenated azaphilone derivatives (Gao *et al.* 2013).

The current work demonstrated how halogen incorporation utilizing the OSMAC approach led to directed biosynthesis and targeted isolation of new halogenated and non-halogenated natural products exemplifying that marine-derived fungi are very suitable producers of diverse fascinating natural products with potential biological activities as discussed in **chapter 5.4**. Our study also reflects that bio-halogenation could be induced in a controlled fashion in which chlorinated metabolites are isolated from NaCl supplemented cultures and brominated derivatives are isolated from NaBr supplemented cultures. Since halogenated natural products are reported to possess a variety of bioactivities where the introduction of halogens has a direct impact on the structure activity relationship of compounds (Gribble 1998), bio-halogenation is very important in drug design and development. For example, in the antibiotic vancomycin,

the presence of chlorine atoms is essential for its anti-infectious activity against drug-resistant strains (Harris *et al.* 1985).

5.2.2 OSMAC Approach and Ammonium Sulfate as a Nitrogen Source

Inspired by the diverse isolated compounds from *A. falconensis* obtained by changing halogens added to solid rice medium, incorporation of an inorganic salt as ammonium sulfate (nitrogen source) to the rice medium, was introduced as another OSMAC approach. Replacing the incorporated salt in rice medium from 3.5% NaCl to 3.5% $(NH_4)_2SO_4$ led to a profound change in the metabolic profile of the fungus. Remarkably, the fungus did not produce any azaphilone derivative and only benzophenone derivatives were accumulated as the main metabolites namely, sulochrin, monochlorosulochrin and dihydrogeodin. Azaphilones, which are fungal polyketides containing a highly oxygenated pyrone-quinone bicyclic core structure with a quaternary center, are known as fungal pigments. They are responsible for the bright yellow or red colour of culture media (Gao *et al.* 2013). When *A. falconensis* was cultured on 3.5% $(NH_4)_2SO_4$ supplemented medium, the colour of the culture changed and did not show the characteristic bright yellow colour of azaphilones indicating their absence in $(NH_4)_2SO_4$ cultures (figure 7). Therefore, we postulate that in the presence of ammonium sulfate, the gene cluster responsible for production of azaphilone derivatives, falconensins, is silent. Moreover, ammonium sulfate is reported to inhibit the growth of fungi not directly due to increasing the extracellular pH values but through the release of toxic free ammonia to the culture medium where the germination ratio of fungi decreases linearly by increasing ammonia concentration (Depasquale *et al.* 1990).

Excitingly, ammonium sulfate concentration in cultivation medium of the fungus *Rhizopus oryzae* is reported to have a pronounced impact on phenolic content production (Schmidt *et al.* 2012). This finding is in agreement with our results where incorporation of ammonium sulfate to the culture medium of the fungus *Aspergillus falconensis* induced only accumulation of phenolic metabolites (figure 8).

An interesting observation was the isolation of chlorinated phenolic compounds (monochlorosulochrin and dihydrogeodin) from the 3.5% $(NH_4)_2SO_4$ supplemented culture. Therefore, we assume that the fungus could utilize trace chlorine ions (perhaps

from tap water) present in the solid rice medium through the activity of halogenating enzymes.

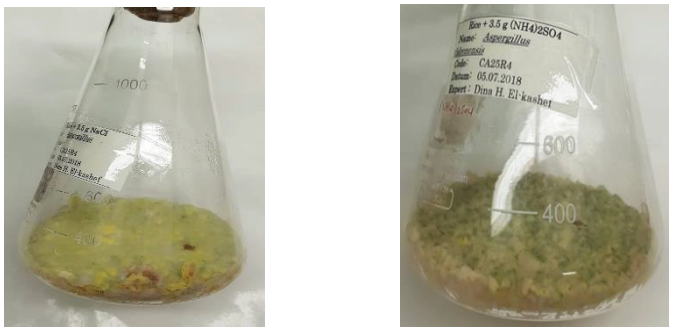

A) **B)**

Figure 7. **A)** *A. falconensis* culture on solid rice medium with 3.5% NaCl. **B)** *A. falconensis* culture on solid rice medium with 3.5% $(NH_4)_2SO_4$.

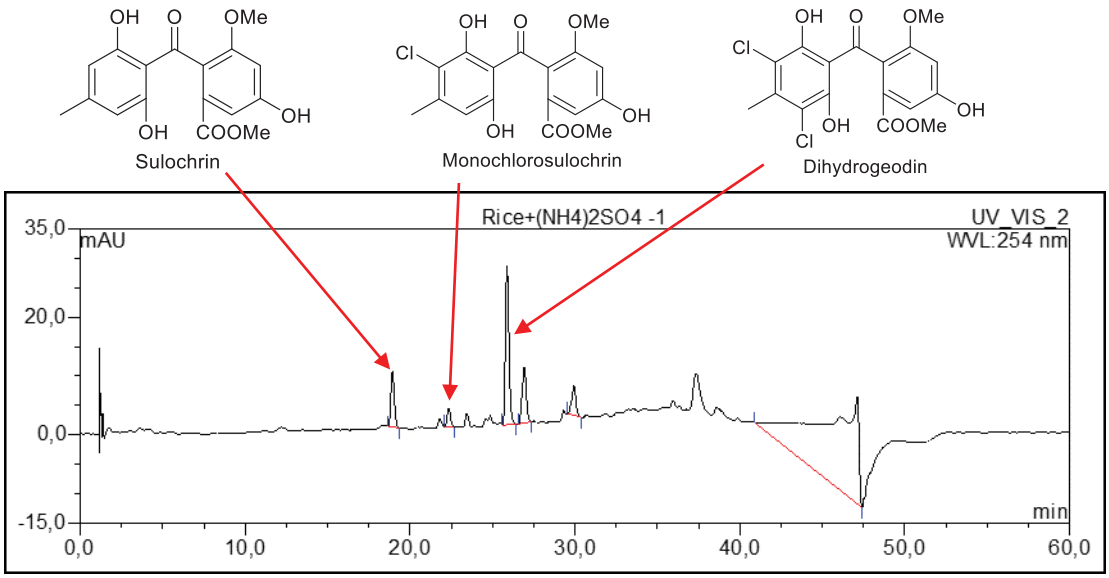

Figure 8: HPLC chromatogram of 3.5% $(NH_4)_2SO_4$ supplemented rice medium of *Aspergillus falconensis.*

Phenolic natural products have been reported to possess potent anticancer activity during both *in vivo* and *in vitro* studies. At high doses, natural phenolics are less toxic and safer than many synthetic and semi-synthetic compounds. Consequently, the search for natural phenolic compounds as anticancer agents is of high importance (Anantharaju *et al.* 2016). In the current study, with the purpose of finding possible candidates with

anticancer activity, molecular docking of the isolated phenolic compounds from both sodium chloride and ammonium sulfate supplemented cultures (excluding azaphilone derivatives), was performed on several enzymes linked with cancer development. Molecular docking, which is a computational method, offers an overview on the interaction of compounds with specific targets involved in diseases such as cancer. This *in silico* method is very important in saving time and resources by allowing to conduct the successive bioassays only on promising candidates. Therefore, it represents a viable basis for drug development (De Vita *et al.* 2020).

Amongst all the docked compounds, sulochrin, isolated from the ammonium sulfate culture of *A. falconensis*, showed stability within the active sites of (CDK-2), (TOP-2) and (MMP-13) with free binding energy (ΔG) of -25.03, -12.11 and -33.83 Kcal/mol, respectively. In addition, to further ascertain the docking results, an *in vitro* cytotoxic evaluation against L5178Y mouse lymphoma cells utilizing the MTT assay, was conducted. Sulochrin exhibited significant cytotoxic activity with an IC_{50} value of 5.1 µM. This result for sulochrin is exciting because the compound was previously reported to be inactive against several animal and human cell lines (Smetanina *et al.* 2011, Xie *et al.* 2015, Zheng *et al.* 2019). Thus, the isolated phenolic compounds, including sulochrin are recommended for further studies and assays to additionally explore the possible targets and the exact mechanism of action which later would help in introducing new lead compounds for drug development.

5.2.3 Plausible Biosynthetic Pathway of Azaphilones (Falconensins A, H, I, K, M-S)

A plausible biosynthetic pathway of falconensin derivatives obtained from *A. falconensis* is proposed to be polyketide-based like most pigments produced by fungi. The polyketide pathway is responsible for the formation of the chromophore main structure of azaphilone pigments from one starter unit (acetic acid) and five chain extender units (malonic acid) (Osmanova *et al.* 2010). After the formation of the hexaketide intermediate (**A**), 2, 7 aldol condensation takes place to generate the first aromatic ring (**B**) as proposed by Chen *et al* (Chen *et al.* 2017). Successive reduction, dehydration and oxidation, constructed a pyran ring in the intermediate (**D**) (Chen *et al.* 2017). Orsellinic acid which constitutes the benzoate part of the hydrogenated falconensins, is known to be derived from the polyketide pathway from one acetate unit

and three malonate units (Sureram *et al.* 2013, Chen *et al.* 2020). Following condensation of the intermediate (**D**) and orsellinic acid, subsequent acetylation and deacetylation take place forming intermediate (**G**) (Chen *et al.* 2017). We assume that enzyme-mediated halogenation takes place by $FADH_2$-dependent halogenases which are responsible for incorporating halogen atoms such as, chlorine and bromine into aromatic compounds activated for electrophilic attack (van Pée 2012).

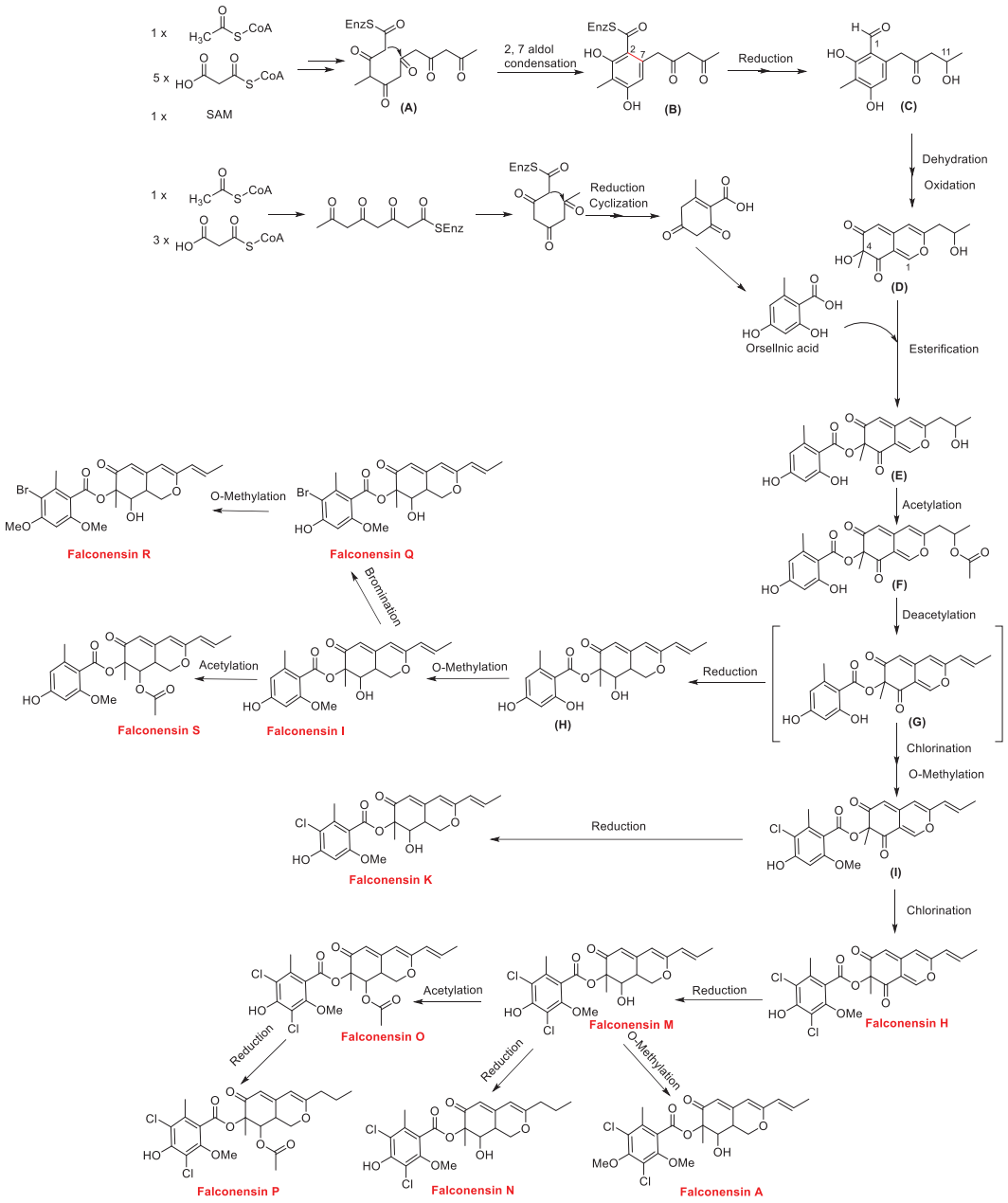

Figure 9: Proposed biosynthesis of falconensins A, H, I, K, M-S

5.3 Challenges in Absolute Configuration Assignment

As pointed out earlier in **chapter 1.3**, determination of the absolute configuration of chiral natural products is essential for full characterization of compounds and is a cornerstone in interaction between compounds and receptors and hence, in drug design and development. From the studied marine-derived fungus *Metarhizium marquandii*, the absolute configuration of the novel terrestric acid derivative, marqualide, was assigned to be 5*R*,9*S*,5′*R* by a combination of modified Mosher's method and time-dependent density functional theory-electronic circular dichroism (TDDFT-ECD) calculations at different levels (figure 10). The *S* absolute configuration of the hydroxyl group at C-9 was established utilizing modified Mosher's method after measuring the chemical shift differences between the formed *R* and *S* esters. The absolute configuration at C-5 and C-5′ in the two γ-lactone rings was established to be 5*R* and 5′*R* based on the solution TDDFT-ECD method. TDDFT is considered to be the method of choice and the most widely used method for ECD calculations being able to keep the balance between computational efforts and accuracy. Therefore, ECD solutions provide trustworthy conformational ensembles in determination of AC of natural products (Petrovic *et al.* 2010, Mándi *et al.* 2019). The first conducted step in ECD calculations should be initial conformational analysis to get the lowest energy conformers which in the case of marqualide afforded 135 and 147 conformers. This initial analysis was carried out by Merck Molecular Force Field (MMFF) conformational search. The second step involves geometry reoptimizations of the obtained conformers at different levels using TDDF calculations of the ECD spectra of the conformers. The principle relies on comparing the calculated and experimental ECD spectra. If both spectra show close matching, the conclusion for AC elucidation is considered reliable (Li *et al.* 2010).

Moreover, AC assignment of marqualide demonstrated the importance of intramolecular hydrogen bonding in stabilizing conformers and in influencing ECD features. Determination of AC of marqualide represents an example how modified Mosher's method and ECD method can be complementary.

Terrestric acid hydrate is a known natural product first isolated from *Penicillium terrestre* Jensen in 1963 (Birkinshaw *et al.* 1936). However, its absolute configuration was unknown. In the current study, the 5*R*,9*S* absolute configuration was assigned to terrestric acid hydrate isolated from the studied fungus *M. marquandii* (figure 10).

Based on biogenetic considerations that terrestric acid hydrate is a building block or a precursor of the previously described co-isolated compound, marqualide, the AC at C-9 was assumed to be 9*S* since terrestric acid hydrate did not succeed to convert to Mosher esters. Therefore, TDDFT-ECD calculations were conducted on (5*R*,9*S*) and (5*S*,9*S*) conformers to fully characterize the AC of the compound.

In contrast to our expectations that the chiral center C-5 of the γ-lactone ring chromophore should govern the ECD spectrum regardless the effect of the remote chiral C-9, both chosen diastereomers for solution ECD calculations, (5*R*,9*S*) and (5*S*,9*S*), reproduced a good fit with the experimental ECD spectrum. Therefore, *S* absolute configuration is unambiguously assigned to C-9 while, AC at C-5 is tentatively determined based on the better fit of the computed ECD spectra of (5*R*,9*S*) with the experimental ECD spectrum, a result which is in agreement with the assigned (5*R*,9*S*,5′*R*) of the related compound marqualide.

This finding sheds light on the influence of a flexible side-chain with no chromophore but with a remote chirality center and a chelating group that could form intramolecular hydrogen bonds on the features of ECD spectra. Therefore, our result rules out the assumption that flexible side-chains with no chromophores could be neglected or truncated to decrease the number of conformers and to simplify ECD calculations (Mándi *et al.* 2019).

Another example demonstrating how AC is assigned through combination of more than one method involves the AC elucidation of aflaquinolone I. The absolute configuration of aflaquinolone I, isolated from the studied fungus *M. marquandii*, was deduced to be (3*R*,4*R*) on the basis of a combination of OR, ECD, and VCD calculations (figure 10).

Analyzing ROESY spectrum for relative configuration determination, which determines the overall molecular conformation (Pescitelli *et al.* 2009), revealed a cofacial orientation between H-3 and the aromatic protons, H-12 and H-16 which is similar to other known analogues such as aflaquinolone A (Neff *et al.* 2012). On the other hand, conducting ECD method did not give a solid assignment of AC. Therefore, SOR calculations were conducted on the (3*S*,4*S*) conformer. SOR results adopted negative sign for conformers with different orientation of the aryl group at C-4. This

result is important since the previously published results for (3*S*,4*S*)-aflaquinolone F with $[\alpha]^{25}_{D}$ value of +10 (*c* 0.19, MeOH) and (3*S*,4*S*)-14-hydroxyaflaquinolone F with $[\alpha]^{20}_{D}$ value of −33 (*c* 0.15, MeOH), were conflicting (Neff *et al.* 2012, An *et al.* 2013).

Finally, to further support elucidating AC of aflaquinolone I, Vibrational Circular Dichroism (VCD) method in combination with DFT calculations was conducted as a complimentary approach to SOR and ECD. In conclusion, AC of aflaquinolone I was deduced to be (3*R*,4*R*) which is opposite to the reported (3*S*,4*S*) absolute configuration of the related aflaquinolones A-G, demonstrating an example for the phenomenon of chiral switch in natural products (Agranat *et al.* 2002).

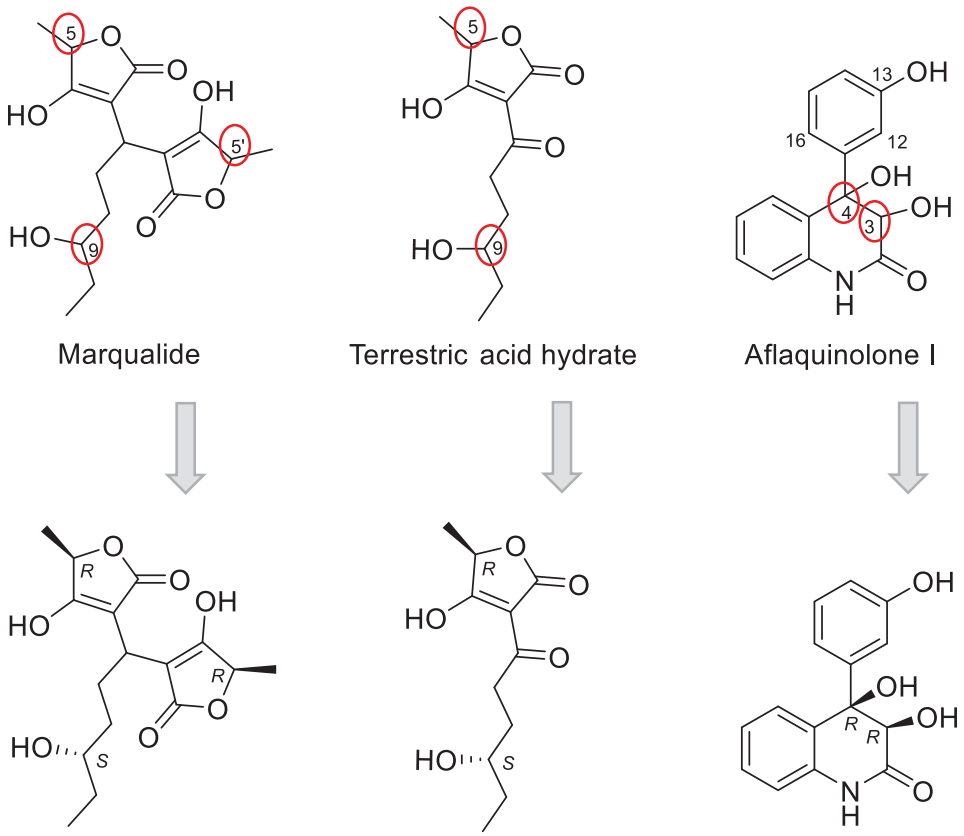

Figure 10: Absolute configurations of compounds isolated from *M. marquandii*

From the other studied marine-derived fungus, *Aspergillus falconensis*, a group of azaphilone derivatives, namely falconensins, were isolated. These azaphilone derivatives are bearing three stereocenters. Inspection of the interproton *J* values ($^{3}J_{H-H}$) around the bonds which connect the stereocenters at C-7, C-8 and C-8a, together

with analysis of NOE correlations, concluded the assignment of relative configuration which is the same for all isolated azaphilone derivatives.

Moreover, the 7*R*, 8*S*, and 8a*S* absolute configuration (figure 11) was deduced on the basis of SOR measurements which is consistent with the reported positive SOR values of falconensin derivatives with the 7*R*, 8*S*, and 8a*S* AC (Itabashi *et al.* 1992, Itabashi *et al.* 1996).

The established AC at C-7, C-8 and C-8a was further confirmed by single crystal X-ray diffraction analysis anomalous dispersion of one of the isolated known compounds (falconensin N). Although Mosher's Method and Cotton effects of CD curves had been utilized to elucidate the absolute configuration of the reported known falconensin derivatives (Itabashi *et al.* 1992, Itabashi *et al.* 1996), our study represents the first report for a crystal structure for any of these compounds.

Therefore, X-ray analysis can be used in combination with chiroptical methods, such as SOR measurement, to determine AC of natural products where the two techniques strengthen each other (Mándi *et al.* 2019).

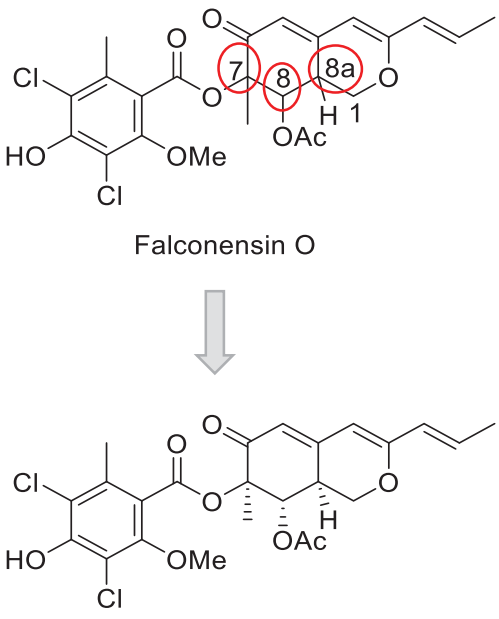

Figure 11: Absolute configurations of falconensin O, one of the isolated falconensin derivatives from *A. falconensis*

In summary, the results of AC determination of compounds isolated from *Metarhizium marquandii* and *Aspergillus falconensis* demonstrate how absolute configuration determination of chiral natural products relies on a strategy that should be planned based on many considerations. Although, many methods are available as discussed in **chapter 1.3**, no single method is valid for all kinds of chiral compounds and the choice of the appropriate method is crucial. Nevertheless, sometimes a combination of two of more methods is required for a solid conclusion of AC of a compound.

5.4 NF-κB Inhibitory Activity against the Triple Negative Breast Cancer Cell Line MDA-MB-231

Chronic inflammation may lead to cancer progression. Since the transcription factor NF-κB is the master regulator of inflammatory disorders and its constitutive activation is associated with tumor development, the blockage of its signalling pathway represents a potential target for the development of therapies (Agrawal *et al.* 2018). Many phytochemicals and their analogues have been reported to have significant inhibitory effects of NF-κB signalling pathway (Gupta *et al.* 2018, Rajagopal *et al.* 2018). Various reports suggested that azaphilones possess anti-inflammatory activity via inhibition of nitric oxide production (Luo *et al.* 2017) or via inhibition of tumor necrosis factor alpha (TNFα)-induced nuclear factor kappa B (NF-κB) in RAW 264.7 cells (Youn *et al.* 2015). Moreover, Yu et al. reported that the azaphilone, conellin A, obtained from the goose dung derived fungus *Coniella fragariae* exhibited significant inhibition of NF-κB activity in the triple negative breast cancer cell line MDA-MB-231 with an IC_{50} value of 4.4 μM (Yu *et al.* 2018). The azaphilone derivatives falconensins A-N isolated from *Emericella falconensis* and *Emericella fruticulosa* are reported to inhibit the inflammatory activity of 12-O-tetradecanoylphorbol-13-acetate (TPA)-induced inflammatory ear oedema in mice in a similar degree as the control indomethacin, which is known for its anti-inflammatory and anti-tumor promoting effect (Yasukawa *et al.* 2008).

In the present study, the isolated falconensin derivatives were evaluated in an *in vitro* anti-inflammatory assay against the triple negative breast cancer (TNBC) cell line MDA-MB-231. TNBC represents an aggressive clinical phenotype of breast cancer with poorer survival rate than non-TNBC. Additionally, no targeted agents are available

for it so far (Pal *et al.* 2011). In this type of cancers, aberrant activation of the pro-inflammatory transcription factor NF-κB is associated with tumor aggressiveness (Agrawal *et al.* 2018). Hence, blockade of NF-κB activation may hold a promise for developing therapies for TNBC.

Strikingly, the tested falconensin derivatives isolated from *Aspergillus falconensis* (falconensins A, H, I, M-O, Q-S) showed inhibition of NF-κB signaling in the TNBC cell line MDA-MB-231 based on their IC_{50} values ranging from (11.9 ± 2.1 – 72.0 ± 28.1) μM. The new azaphilone derivative, falconensin Q, was the most potent azaphilone derivative with an IC_{50} of 11.9 ± 2.1 μM. To exclude that inhibition of NF-κB signaling is attributed to the cytotoxic effect of the tested compounds, cell viability cytotoxic assay was performed which indicated that the tested falconensin derivatives showed a higher potency for NF-κB inhibition than its cytotoxic activity. Therefore, we recommend performing further studies on the isolated metabolites which could serve as possible candidates for drug discovery and development from natural sources.

Conclusion and Prospect

Marine organisms harbour highly interesting diverse natural products. The results of this dissertation support how marine fungi are fruitful producers of new structural entities and bioactive compounds. The two major projects included in this thesis feature two different marine fungi from different habitats, which had proven that not only underexplored fungal genera are interesting for study but also that already intensively studied genera represent a promising source for new bioactive natural products. The OSMAC approach helped in diversifying the metabolic profiles of fungi and the production of new biologically active secondary metabolites. The promising results obtained from OSMAC experiments, suggest further modifications of culture media and conditions to enhance activation of silent gene clusters to produce other diverse metabolites. The production of bioactive natural products could support the continued quest for new drug leads. The marine environment, in particular marine fungi, represent an untapped resource for new structural scaffolds and promising bioactive natural products and are expected to have a higher contribution in pharmaceutical development in the near future.

References (for Chapter 1 and 5)

Abd El-Hady, F. K., M. S. Abdel-Aziz, K. H. Shaker, Z. A. El-Shahid and L. S. Ibrahim (2015). "Antioxidant, acetylcholinesterase and α-Glucosidase potentials of metabolites from the marine fungus *Aspergillus unguis* RSPG_204 associated with the sponge (Agelas sp.)." *International Journal of Pharmaceutical Sciences Review and Research* **30** (1): 272-278.

Abou El-Ezz, R., A. Ibrahim, E. Habib, H. Kamel, M. Afifi, H. Hassanean and S. Ahmed (2017). "Review of natural products from marine organisms in the Red Sea." *International Journal of Pharmaceutical Sciences and Research* **8** (3): 940.

Adpressa, D. A. and S. Loesgen (2016). "Bioprospecting chemical diversity and bioactivity in a marine derived *Aspergillus terreus*." *Chemistry & biodiversity* **13** (2): 253-259.

Agranat, I., H. Caner and J. Caldwell (2002). "Putting chirality to work: the strategy of chiral switches." *Nature Reviews Drug Discovery* **1** (10): 753-768.

Agrawal, A. K., E. Pielka, A. Lipinski, M. Jelen, W. Kielan and S. Agrawal (2018). "Clinical validation of nuclear factor kappa B expression in invasive breast cancer." *Tumor Biology* **40** (1): 1010428317750929.

Ahmed, E. F., M. E. Rateb, L. T. Abou El-Kassem and U. W. Hawas (2017). "Anti-HCV Protease of Diketopiperazines Produced by the Red Sea Sponge-Associated Fungus *Aspergillus versicolor*." *Applied biochemistry and microbiology* **53** (1): 101-106.

Amend, A., G. Burgaud, M. Cunliffe, V. P. Edgcomb, C. L. Ettinger, M. Gutiérrez, J. Heitman, E. F. Hom, G. Ianiri and A. C. Jones (2019). "Fungi in the marine environment: Open questions and unsolved problems." *MBio* **10** (2) e01189-18.

An, C. Y., X. M. Li, H. Luo, C. S. Li, M. H. Wang, G. M. Xu and B. G. Wang (2013). "4-Phenyl-3,4-dihydroquinolone derivatives from *Aspergillus nidulans* MA-143, an endophytic fungus isolated from the mangrove plant *Rhizophora stylosa*." *Journal of Natural Products* **76** (10): 1896-1901.

Anantharaju, P. G., P. C. Gowda, M. G. Vimalambike and S. V. Madhunapantula (2016). "An overview on the role of dietary phenolics for the treatment of cancers." *Nutrition journal* **15** (1): 99.

Anderson, J. R. and S. K. Chapman (2006). "Molecular mechanisms of enzyme-catalysed halogenation." *Molecular BioSystems* **2** (8): 350-357.

Arora, D., P. Gupta, S. Jaglan, C. Roullier, O. Grovel and S. Bertrand (2020). "Expanding the chemical diversity through microorganisms co-culture: Current status and outlook." *Biotechnology Advances* **40**: 107521.

Asfour, H. Z., Z. A. Awan, A. A. Bagalagel, M. A. Elfaky, R. F. Abdelhameed and S. S. Elhady (2019). "Large-scale production of bioactive Terrein by *Aspergillus terreus* strain S020 isolated from the Saudi coast of the Red Sea." *Biomolecules* **9** (9): 480.

B'Hymer, C., M. Montes-Bayon and J. A. Caruso (2003). "Marfey's reagent: Past, present, and future uses of 1-fluoro-2,4-dinitrophenyl-5-L-alanine amide." *Journal of separation science* **26** (1-2): 7-19.

Balkwill, F. and A. Mantovani (2001). "Inflammation and cancer: back to Virchow?" *The Lancet* **357** (9255): 539-545.

Bergmann, W. and D. Burke (1955). "Marine products. XXXIX. The nucleosides of sponges. III. Spongothymidine and spongouridine." *The Journal of Organic Chemistry* **20**: 1501-1507.

Bergmann, W. and R. J. Feeney (1951). "Contributions to the study of marine products. XXXII. The nucleosides of sponges. I." *The Journal of Organic Chemistry* **16** (6): 981-987.

Bertrand, S., N. Bohni, S. Schnee, O. Schumpp, K. Gindro and J.-L. Wolfender (2014). "Metabolite induction via microorganism co-culture: a potential way to enhance chemical diversity for drug discovery." *Biotechnology Advances* **32** (6): 1180-1204.

Bhushan, R. and H. Brückner (2004). "Marfey's reagent for chiral amino acid analysis: a review." *Amino acids* **27** (3-4): 231-247.

Bidochka, M. J., A. M. Kamp, T. M. Lavender, J. Dekoning and J. N. De Croos (2001). "Habitat association in two genetic groups of the insect-pathogenic fungus *Metarhizium anisopliae*: uncovering cryptic species?" *Applied and Environmental Microbiology* **67** (3): 1335-1342.

Birkinshaw, J. H. and H. Raistrick (1936). "Studies in the biochemistry of micro-organisms: Isolation, properties and constitution of terrestric acid (ethylcarolic acid), a metabolic product of *Penicillium terrestre* Jensen." *Biochemical Journal* **30** (12): 2194-2200.

Blunt, J. W., A. R. Carroll, B. R. Copp, R. A. Davis, R. A. Keyzers and M. R. Prinsep (2018). "Marine natural products." *Natural Product Reports* **35** (1): 8-53.

Bode, H. B., B. Bethe, R. Höfs and A. Zeeck (2002). "Big effects from small changes: possible ways to explore nature's chemical diversity." *ChemBioChem* **3** (7): 619-627.

Boot, C. M., T. Amagata, K. Tenney, J. E. Compton, H. Pietraszkiewicz, F. A. Valeriote and P. Crews (2007). "Four classes of structurally unusual peptides from two marine-derived fungi: structures and bioactivities." *Tetrahedron* **63** (39): 9903-9914.

Bugni, T. S. and C. M. Ireland (2004). "Marine-derived fungi: a chemically and biologically diverse group of microorganisms." *Natural Product Reports* **21** (1): 143-163.

Cabrera, G. M., M. Butler, M. A. Rodriguez, A. Godeas, R. Haddad and M. N. Eberlin (2006). "A sorbicillinoid urea from an intertidal *Paecilomyces marquandii*." *Journal of Natural Products* **69** (12): 1806-1808.

Cao, F., Z.-H. Meng, X. Mu, Y.-F. Yue and H.-J. Zhu (2019). "Absolute configuration of bioactive azaphilones from the marine-derived fungus *Pleosporales* sp. CF09-1." *Journal of Natural Products* **82** (2): 386-392.

Carroll, A. R., B. R. Copp, R. A. Davis, R. A. Keyzers and M. R. Prinsep (2020). "Marine natural products." *Natural Product Reports* **37** (2): 175-223.

Chávez, R., F. Fierro, R. O. García-Rico and I. Vaca (2015). "Filamentous fungi from extreme environments as a promising source of novel bioactive secondary metabolites." *Frontiers in Microbiology* **6**: 903.

Chen, C., H. Tao, W. Chen, B. Yang, X. Zhou, X. Luo and Y. Liu (2020). "Recent advances in the chemistry and biology of azaphilones." *RSC Advances* **10** (17): 10197-10220.

Chen, M., Y.-Y. Zheng, Z.-Q. Chen, N.-X. Shen, L. Shen, F.-M. Zhang, X.-J. Zhou and C.-Y. Wang (2019). "NaBr-Induced Production of Brominated Azaphilones and Related Tricyclic Polyketides by the Marine-Derived Fungus *Penicillium janthinellum* HK1-6." *Journal of Natural Products* **82** (2): 368-374.

Chen, W., R. Chen, Q. Liu, Y. He, K. He, X. Ding, L. Kang, X. Guo, N. Xie, Y. Zhou, Y. Lu, R. J. Cox, I. Molnar, M. Li, Y. Shao and F. Chen (2017). "Orange, red, yellow: biosynthesis of azaphilone pigments in *Monascus* fungi." *Chemical Science* **8** (7): 4917-4925.

Cheung, R. C. F., T. B. Ng and J. H. Wong (2015). "Marine peptides: Bioactivities and applications." *Marine Drugs* **13** (7): 4006-4043.

Cichewicz, R. H. (2010). "Epigenome manipulation as a pathway to new natural product scaffolds and their congeners." *Natural Product Reports* **27** (1): 11-22.

Cruz, J. o. C., M. Iorio, P. Monciardini, M. Simone, C. Brunati, E. Gaspari, S. I. Maffioli, E. Wellington, M. Sosio and S. Donadio (2015). "Brominated variant of the lantibiotic NAI-107 with enhanced antibacterial potency." *Journal of Natural Products* **78** (11): 2642-2647.

Dale, J. A. and H. S. Mosher (1973). "Nuclear magnetic resonance enantiomer regents. Configurational correlations via nuclear magnetic resonance chemical shifts of diastereomeric mandelate, O-methylmandelate, and. alpha.-methoxy-. alpha.-trifluoromethylphenylacetate (MTPA) esters." *Journal of the American Chemical Society* **95** (2): 512-519.

Daletos, G., W. Ebrahim, E. Ancheeva, M. El-Neketi, W. Lin and P. Proksch (2017). "Microbial co-culture and OSMAC approach as strategies to induce cryptic fungal biogenetic gene clusters." In: *Chemical Biology of Natural Products;* Newman, D. J., Cragg, G. M., Grothaus, P. G. (Eds.); CRC Press: Boca Raton, FL, USA, 2017, 233–284. ISBN 9781439841945.

De Vita, S., S. Terracciano, I. Bruno and M. G. Chini (2020) "From Natural compounds to bioactive molecules through NMR and in Silico methodologies." *European Journal of Organic Chemistry.*

Depasquale, D. A. and T. J. Montville (1990). "Mechanism by which ammonium bicarbonate and ammonium sulfate inhibit mycotoxigenic fungi." *Applied and Environmental Microbiology* **56** (12): 3711-3717.

Dyshlovoy, S. A. and F. Honecker (2019). "Marine Compounds and Cancer: The First Two Decades of XXI Century." *Marine Drugs* **18** (1): 20.

Ebada, S. S. and P. Proksch (2015). Marine-derived fungal metabolites. In: *Hb25_Springer Handbook of Marine Biotechnology*. S.-K. Kim (Ed.); Berlin, Heidelberg, Springer Berlin Heidelberg, 759-788, ISBN 978-3-642-53970-1

El-Gendy, B. E. M. and M. E. Rateb (2015). "Antibacterial activity of diketopiperazines isolated from a marine fungus using t-butoxycarbonyl group as a simple tool for purification." *Bioorganic & Medicinal Chemistry Letters* **25** (16): 3125-3128.

El-Hossary, E. M., M. Abdel-Halim, E. S. Ibrahim, S. M. Pimentel-Elardo, J. R. Nodwell, H. Handoussa, M. F. Abdelwahab, U. Holzgrabe and U. R. Abdelmohsen (2020). "Natural products repertoire of the Red Sea." *Marine Drugs* **18** (9): 457.

El-Kashef, D. H., G. Daletos, M. Plenker, R. Hartmann, A. Mándi, T. Kurtán, H. Weber, W. Lin, E. Ancheeva and P. Proksch (2019). "Polyketides and a dihydroquinolone alkaloid from a marine-derived strain of the fungus *Metarhizium marquandii*." *Journal of Natural Products* **82** (9): 2460-2469.

El-Kashef, D. H., F. S. Youssef, R. Hartmann, T.-O. Knedel, C. Janiak, W. Lin, I. Reimche, N. Teusch, Z. Liu and P. Proksch (2020). "Azaphilones from the Red Sea fungus *Aspergillus falconensis*." *Marine Drugs* **18** (4): 204.

Elad, D. and E. Segal (2018). "Diagnostic aspects of veterinary and human aspergillosis." *Frontiers in Microbiology* **9** :1303.

Elnaggar, M. S., S. S. Ebada, M. L. Ashour, W. Ebrahim, W. E. Müller, A. Mándi, T. Kurtán, A. Singab, W. Lin and Z. Liu (2016). "Xanthones and sesquiterpene derivatives from a marine-derived fungus *Scopulariopsis* sp." *Tetrahedron* **72** (19): 2411-2419.

FDA (1992). "FDA's policy statement for the development of new stereoisomeric drugs." *Chirality* **4** (5): 338-340.

Florey, H. W. (1955). "Antibiotic products of a versatile fungus." *Annals of internal medicine* **43** (3): 480-490.

Frank, M., R. Hartmann, M. Plenker, A. Mándi, T. Kurtán, F. C. Özkaya, W. E. G. Müller, M. U. Kassack, A. Hamacher, W. Lin, Z. Liu and P. Proksch (2019). "Brominated Azaphilones from the Sponge-Associated Fungus *Penicillium canescens* Strain 4.14.6a." *Journal of Natural Products* **82** (8): 2159-2166.

Fuchser, J. and A. Zeeck (1997). "Secondary metabolites by chemical screening .34. Aspinolides and aspinonene/aspyrone co-metabolites, new pentaketides produced by *Aspergillus ochraceus*." *Liebigs Annalen-Recueil* (1): 87-95.

Gao, J. M., S. X. Yang and J. C. Qin (2013). "Azaphilones: chemistry and biology." *Chemical Reviews* **113** (7): 4755-4811.

Gerwick, W. H. and B. S. Moore (2012). "Lessons from the past and charting the future of marine natural products drug discovery and chemical biology." *Chemistry & Biology* **19** (1): 85-98.

Gribble, G. W. (1998). "Naturally occurring organohalogen compounds." *Accounts of Chemical Research* **31** (3): 141-152.

Guo, W., J. Peng, T. Zhu, Q. Gu, R. A. Keyzers and D. Li (2013). "Sorbicillamines A–E, nitrogen-containing sorbicillinoids from the deep-sea-derived fungus *Penicillium* sp. F23–2." *Journal of Natural Products* **76** (11): 2106-2112.

Gupta, S. C., A. B. Kunnumakkara, S. Aggarwal and B. B. Aggarwal (2018). "Inflammation, a double-edge sword for cancer and other age-related diseases." *Frontiers in immunology* **9**: 2160.

Gupta, S. C., C. Sundaram, S. Reuter and B. B. Aggarwal (2010). "Inhibiting NF-κB activation by small molecules as a therapeutic strategy." *Biochimica et Biophysica Acta (BBA)-Gene Regulatory Mechanisms* **1799** (10-12): 775-787.

Hara, S., H. Okabe and K. Mihashi (1987). "Gas-liquid chromatographic separation of aldose enantiomers as trimethylsilyl ethers of methyl 2-(polyhydroxyalkyl)-thiazolidine-4 (*R*)-carboxylates." *Chemical and Pharmaceutical Bulletin* (Tokyo) **35** (2): 501-506.

Harris, C. M., R. Kannan, H. Kopecka and T. M. Harris (1985). "The role of the chlorine substituents in the antibiotic vancomycin: preparation and characterization of mono- and didechlorovancomycin." *Journal of the American Chemical Society* **107** (23): 6652-6658.

Hawas, U. W., E. F. Ahmed, A. Halwany, A. Atif, W. Ahmed and L. T. Abou El-Kassem (2016). "Bioactive metabolites from the Egyptian Red Sea fungi with potential anti-HCV protease effect." *Chemistry of Natural Compounds* **52** (1): 104-110.

Horňák, V., R. Dvorský and E. Šturdík (1999). "Receptor-ligand interaction and molecular modelling." *General Physiology and Biophysics* **18**: 231-248.

Hoye, T. R., C. S. Jeffrey and F. Shao (2007). "Mosher ester analysis for the determination of absolute configuration of stereogenic (chiral) carbinol carbons." *Nature Protocols.* **2** (10): 2451-2458.

https://www.midwestern.edu/departments/marinepharmacology/clinical-pipeline.xml. Last Revised (June 2020).

Hu, G.-P., J. Yuan, L. Sun, Z.-G. She, J.-H. Wu, X.-J. Lan, X. Zhu, Y.-C. Lin and S.-P. Chen (2011). "Statistical research on marine natural products based on data obtained between 1985 and 2008." *Marine Drugs* **9** (4): 514-525.

Huang, H., F. Wang, M. Luo, Y. Chen, Y. Song, W. Zhang, S. Zhang and J. Ju (2012). "Halogenated Anthraquinones from the Marine-Derived Fungus *Aspergillus* sp. SCSIO F063." *Journal of Natural Products* **75** (7): 1346-1352.

Hyde, K. D., E. G. Jones, E. Leaño, S. B. Pointing, A. D. Poonyth and L. L. Vrijmoed (1998). "Role of fungi in marine ecosystems." *Biodiversity & Conservation* **7** (9): 1147-1161.

Imhoff, J. F. (2016). "Natural products from marine fungi—Still an underrepresented resource." *Marine Drugs* **14** (1): 19.

Itabashi, T., K. Nozawa, M. Miyaji, S.-i. Udagawa, S. Nakajima and K.-i. Kawai (1992). "Falconensins A, B, C, and D, New Compounds Related to Azaphilone, from *Emericella falconensis*." *Chemical & Pharmaceutical Bulletin* **40** (12): 3142-3144.

Itabashi, T., N. Ogasawara, K. Nozawa and K. Kawai (1996). "Isolation and structures of new azaphilone derivatives, falconensins E-G, from *Emericella falconensis* and absolute configurations of falconensins A-G." *Chemical & Pharmaceutical Bulletin* **44** (12): 2213-2217.

Jiménez, C. (2018). Marine natural products in medicinal chemistry, *ACS Medicinal Chemistry Letters* **9** (10): 959-961.

Keller, N. P. (2019). "Fungal secondary metabolism: regulation, function and drug discovery." *Nature Reviews Microbiology* **17** (3): 167-180.

Ko, J., B. I. Morinaka and T. F. Molinski (2011). "Faulknerynes A− C from a Bahamian sponge *Diplastrella* sp.: Stereoassignment by critical application of two exciton coupled CD methods." *Journal of Organic Chemistry* **76** (3): 894-901.

Kong, L. Y. and P. Wang (2013). "Determination of the absolute configuration of natural products." *Chinese journal of natural medicines* **11** (3): 193-198.

König, G. M., S. Kehraus, S. F. Seibert, A. Abdel-Lateff and D. Müller (2006). "Natural products from marine organisms and their associated microbes." *ChemBioChem* **7** (2): 229-238.

Lee, A. J. (1980). Chapter 14 North Sea: Physical Oceanography. In: *The North-West European Shelf Seas: The Sea Bed and the Sea in Motion II. Physical and Chemical Oceanography, and Physical Resources*; F. T. Banner, M. B. Collins and K. S. Massie (Eds.); Elsevier. (**1980**) **24**: 467-493, ISBN 0422-9894.

Li, S., K. D. Smith, J. H. Davis, P. B. Gordon, R. R. Breaker and S. A. Strobel (2013). "Eukaryotic resistance to fluoride toxicity mediated by a widespread family of fluoride export proteins." *Proceedings of the National Academy of Sciences USA* **110** (47): 19018-19023.

Li, X.-C., D. Ferreira and Y. Ding (2010). "Determination of absolute configuration of natural products: Theoretical calculation of electronic circular dichroism as a tool." *Current Organic Chemistry* **14** (16): 1678-1697.

Ling-Yi, K. and W. Peng (2013). "Determination of the absolute configuration of natural products." *Chinese Journal of Natural Medicines* **11** (3): 193-198.

Luo, J. G., Y. M. Xu, D. C. Sandberg, A. E. Arnold and A. A. Gunatilaka (2017). "Montagnuphilones A–G, Azaphilones from Montagnulaceae sp. DM0194, a fungal

endophyte of submerged roots of *Persicaria amphibia*." *Journal of Natural Products* **80** (1): 76-81.

Lysek, N., E. Rachor and T. Lindel (2002). "Isolation and structure elucidation of deformylflustrabromine from the North Sea bryozoan *Flustra foliacea*." *Zeitschrift für Naturforschung C* **57** (11-12): 1056-1061.

Mándi, A. and T. Kurtán (2019). "Applications of OR/ECD/VCD to the structure elucidation of natural products." *Natural Product Reports* **36** (6): 889-918.

Marmann, A., A. H. Aly, W. Lin, B. Wang and P. Proksch (2014). "Co-cultivation—a powerful emerging tool for enhancing the chemical diversity of microorganisms." *Marine Drugs* **12** (2): 1043-1065.

Matsumori, N., M. Murata and K. Tachibana (1995). "Conformational analysis of natural products using long-range carbon-proton coupling constants: Three-dimensional structure of okadaic acid in solution." *Tetrahedron* **51** (45): 12229-12238.

Matsuzaki, K., H. Tahara, J. Inokoshi, H. Tanaka, R. Masuma and S. Omura (1998). "New brominated and halogen-less derivatives and structure-activity relationship of azaphilones inhibiting gp120-CD4 binding." *The Journal of Antibiotics* (Tokyo) **51** (11): 1004-1011.

Mayer, A. M., K. B. Glaser, C. Cuevas, R. S. Jacobs, W. Kem, R. D. Little, J. M. McIntosh, D. J. Newman, B. C. Potts and D. E. Shuster (2010). "The odyssey of marine pharmaceuticals: a current pipeline perspective." *Trends in pharmacological sciences* **31** (6): 255-265.

Mclachlan, J. and J. S. Craigie (1967). "Bromide, a substitute for chloride in a marine algal medium." *Nature* **214** (5088): 604-605.

Menna, M., C. Imperatore, A. Mangoni, G. Della Sala and O. Taglialatela-Scafati (2019). "Challenges in the configuration assignment of natural products. A case-selective perspective." *Natural Product Reports* **36** (3): 476-489.

Molinski, T. F. and B. I. Morinaka (2012). "Integrated approaches to the configurational assignment of marine natural products." *Tetrahedron* **68** (46): 9307-9343.

Neff, S. A., S. U. Lee, Y. Asami, J. S. Ahn, H. Oh, J. Baltrusaitis, J. B. Gloer and D. T. Wicklow (2012). "Aflaquinolones A-G: secondary metabolites from marine and fungicolous isolates of *Aspergillus* spp." *Journal of Natural Products* **75** (3): 464-472.

Netzker, T., J. Fischer, J. Weber, D. J. Mattern, C. C. König, V. Valiante, V. Schroeckh and A. A. Brakhage (2015). "Microbial communication leading to the activation of silent fungal secondary metabolite gene clusters." *Frontiers in Microbiology* **6**: 299.

Neubauer, P. R., C. Widmann, D. Wibberg, L. Schröder, M. Frese, T. Kottke, J. Kalinowski, H. H. Niemann and N. Sewald (2018). "A flavin-dependent halogenase from metagenomic analysis prefers bromination over chlorination." *PloS one* **13** (5): e0196797.

Newman, D. J. and G. M. Cragg (2016). "Natural products as sources of new drugs from 1981 to 2014." *Journal of Natural Products* **79** (3): 629-661.

Newton, G. G. and E. P. Abraham (1955). "Cephalosporin C, a new antibiotic containing sulphur and D-alpha-aminoadipic acid." *Nature* **175** (4456): 548.

Nicholson, B., G. K. Lloyd, B. R. Miller, M. A. Palladino, Y. Kiso, Y. Hayashi and S. T. C. Neuteboom (2006). "NPI-2358 is a tubulin-depolymerizing agent: in-vitro evidence for activity as a tumor vascular-disrupting agent." *Anti-Cancer Drugs* **17** (1): 25-31.

Niu, S., D. Liu, Z. Shao, P. Proksch and W. Lin (2018). "Eremophilane-type sesquiterpenoids in a deep-sea fungus *Eutypella* sp. activated by chemical epigenetic manipulation." *Tetrahedron* **74** (51): 7310-7325.

Ohtani, I., T. Kusumi, M. O. Ishitsuka and H. Kakisawa (1989). "Absolute configurations of marine diterpenes possessing a xenicane skeleton. An application of an advanced Mosher's method." *Tetrahedron Letters* **30** (24): 3147-3150.

Osmanova, N., W. Schultze and N. Ayoub (2010). "Azaphilones: a class of fungal metabolites with diverse biological activities." *Phytochemistry Reviews* **9** (2): 315-342.

Pal, S. K., B. H. Childs and M. Pegram (2011). "Triple negative breast cancer: unmet medical needs." *Breast Cancer Research and Treatment* **125** (3): 627-636.

Pan, R., X. Bai, J. Chen, H. Zhang and H. Wang (2019). "Exploring structural diversity of microbe secondary metabolites using OSMAC strategy: A literature review." *Frontiers in Microbiology* **10**: 294.

Pereira, R. B., N. M. Evdokimov, F. Lefranc, P. Valentão, A. Kornienko, D. M. Pereira, P. B. Andrade and N. G. M. Gomes (2019). "Marine-derived anticancer agents: Clinical benefits, innovative mechanisms, and new targets." *Marine Drugs* **17** (6): 329.

Pescitelli, G., T. Kurtan, U. Flörke and K. Krohn (2009). "Absolute structural elucidation of natural products—A focus on quantum-mechanical calculations of solid-state CD spectra." *Chirality:* **21** (1E): E181-E201.

Petrovic, A. G., A. Navarro-Vazquez and J. L. Alonso-Gomez (2010). "From relative to absolute configuration of complex natural products: interplay between NMR, ECD, VCD, and ORD assisted by ab initio calculations." *Current Organic Chemistry* **14** (15): 1612-1628.

Radics, L., M. Kajtar-Peredy, C. G. Casinovi, C. Rossi, M. Ricci and L. Tuttobello (1987). "Leucinostatins H and K, two novel peptide antibiotics with tertiary amine-oxide terminal group from *Paecilomyces marquandii* isolation, structure and biological activity." *The Journal of Antibiotics* (Tokyo) **40** (5): 714-716.

Rajagopal, C., M. B. Lankadasari, J. M. Aranjani and K. B. Harikumar (2018). "Targeting oncogenic transcription factors by polyphenols: A novel approach for cancer therapy." *Pharmacological Research* **130**: 273-291.

Rateb, M. E. and R. Ebel (2011). "Secondary metabolites of fungi from marine habitats." *Natural Product Reports* **28** (2): 290-344.

Romano, S., S. A. Jackson, S. Patry and A. D. W. Dobson (2018). "Extending the "One Strain Many Compounds"(OSMAC) principle to marine microorganisms." *Marine Drugs* **16** (7): 244.

Sashidhara, K. V., K. N. White and P. Crews (2009). "A selective account of effective paradigms and significant outcomes in the discovery of inspirational marine natural products." *Journal of Natural Products* **72** (3): 588-603.

Schmidt, C. G. and E. B. Furlong (2012). "Effect of particle size and ammonium sulfate concentration on rice bran fermentation with the fungus *Rhizopus oryzae*." *Bioresource Technology* **123**: 36-41.

Scholte, E. J., B. G. Knols, R. A. Samson and W. Takken (2004). "Entomopathogenic fungi for mosquito control: a review." *Journal of Insect Science* **4**: 19.

Schulz, D., B. Ohlendorf, H. Zinecker, R. Schmaljohann and J. F. Imhoff (2011). "Eutypoids B− E produced by a *Penicillium* sp. strain from the North Sea." *Journal of Natural Products* **74** (1): 99-101.

Scott, A., K. Khan, J. Cook and V. Duronio (2004). "What is "inflammation"? Are we ready to move beyond Celsus?" *British Journal of Sports Medicine* **38** (3): 248-249.

Seco, J. M., E. Quinoá and R. Riguera (2004). "The assignment of absolute configuration by NMR." *Chemical Reviews* **104** (1): 17-118.

Shin, H. J. (2020). "Natural Products from Marine Fungi.",.*Marine Drugs* **18** (5): 230.

Smetanina, O. F., A. N. Yurchenko, A. I. Kalinovsky, M. A. Pushilin, N. N. Slinkina, E. A. Yurchenko and S. S. Afiyatullov (2011). "4-Methoxy-3-methylgoniothalamin from marine-derived fungi of the genus *Penicillium*." *Russian Chemical Bulletin* **60** (4): 760-763.

Song, C. E. (2009). "An overview of cinchona alkaloids in chemistry." In: *Cinchona alkaloids in synthesis and catalysis, ligands, immobilization and organocatalysis*; Weinheim. C. E. S. (Ed.); WILEY-VCH Verlag GmbH & Co. KGaA, **2009**, ch1: 1-10, ISBN 9783527628179.

Sureram, S., C. Kesornpun, C. Mahidol, S. Ruchirawat and P. Kittakoop (2013). "Directed biosynthesis through biohalogenation of secondary metabolites of the marine-derived fungus *Aspergillus unguis*." *RSC Advances* **3** (6): 1781-1788.

Tanaka, T., T. Nakashima, T. Ueda, K. Tomii and I. Kouno (2007). "Facile discrimination of aldose enantiomers by reversed-phase HPLC." *Chemical and Pharmaceutical Bulletin* (Tokyo) **55** (6): 899-901.

Tresner, H. D. and J. A. Hayes (1971). "Sodium chloride tolerance of terrestrial fungi." *Applied Microbiology* **22** (2): 210-213.

Uchoa, P. K. S., A. T. A. Pimenta, R. Braz-Filho, M. de Oliveira, N. N. Saraiva, B. S. F. Rodrigues, L. H. Pfenning, L. M. Abreu, D. V. Wilke, K. G. D. Florencio and M. A. S. Lima (2017). "New cytotoxic furan from the marine sediment-derived fungi *Aspergillus niger*." *Natural Product Research* **31** (22): 2599-2603.

van Pée, K.-H. (2012). "Chapter Twelve - Enzymatic Chlorination and Bromination." In: *Methods in Enzymology*. D. A. Hopwood (Ed.); Academic Press: Elsevier, **2012**, **516**: 237-257, ISBN 0076-6879.

Wang, H., H. Dai, C. Heering, C. Janiak, W. Lin, R. S. Orfali, W. E. G. Müller, Z. Liu and P. Proksch (2016). "Targeted solid phase fermentation of the soil dwelling fungus *Gymnascella dankaliensis* yields new brominated tyrosine-derived alkaloids." *RSC Advances* **6** (85): 81685-81693.

Wang, Y., J. Zheng, P. Liu, W. Wang and W. Zhu (2011). "Three new compounds from *Aspergillus terreus* PT06-2 grown in a high salt medium." *Marine Drugs* **9** (8): 1368-1378.

Zin W. W., W., C. Prompanya, S. Buttachon and A. Kijjoa (2016). "Bioactive secondary metabolites from a Thai collection of soil and marine-derived fungi of the genera *Neosartorya* and *Aspergillus*." *Current Drug Delivery* **13** (3): 378-388.

Watanabe, T., K. Izaki and H. Takahashi (1982). "New polyenic antibiotics active against gram-positive and-negative bacteria." *The Journal of Antibiotics* (Tokyo) **35** (9): 1148-1155.

Wiese, J. and J. F. Imhoff (2019). "Marine bacteria and fungi as promising source for new antibiotics." *Drug Development Research* **80** (1): 24-27.

Wilson, Z. E. and M. A. Brimble (2009). "Molecules derived from the extremes of life." *Natural Product Reports* **26** (1): 44-71.

Wu, Q. X., M. S. Crews, M. Draskovic, J. Sohn, T. A. Johnson, K. Tenney, F. A. Valeriote, X. J. Yao, L. F. Bjeldanes and P. Crews (2010). "Azonazine, a novel dipeptide from a Hawaiian marine sediment-derived fungus, *Aspergillus insulicola*." *Organic Letters* **12** (20): 4458-4461.

Xie, F., X. B. Li, J. C. Zhou, Q. Q. Xu, X. N. Wang, H. Q. Yuan and H. X. Lou (2015). "Secondary metabolites from *Aspergillus fumigatus*, an endophytic fungus from the liverwort Heteroscyphus tener (Steph.) Schiffn." *Chemistry & Biodiversity* **12** (9): 1313-1321.

Yamazaki, H., H. Rotinsulu, R. Narita, R. Takahashi and M. Namikoshi (2015). "Induced production of halogenated epidithiodiketopiperazines by a marine-derived *Trichoderma* cf. *brevicompactum* with sodium halides." *Journal of Natural Products* **78** (10): 2319-2321.

Yasukawa, K., T. Itabashi, K.-i. Kawai and M. Takido (2008). "Inhibitory effects of falconensins on 12-O-tetradecanoylphorbol-13-acetate-induced inflammatory ear edema in mice." *Journal of Natural Medicines* **62** (3): 384-386.

Yoshida, S., K. Kito, T. Ooi, K. Kanoh, Y. Shizuri and T. Kusumi (2007). "Four pimarane diterpenes from marine fungus: chloroform incorporated in crystal lattice for absolute configuration analysis by X-ray." *Chemistry Letters* **36** (11): 1386-1387.

Youn, U. J., T. Sripisut, E. J. Park, T. P. Kondratyuk, N. Fatima, C. J. Simmons, M. M. Wall, D. Sun, J. M. Pezzuto and L. C. Chang (2015). "Determination of the absolute configuration of chaetoviridins and other bioactive azaphilones from the endophytic fungus *Chaetomium globosum*." *Bioorganic & Medicinal Chemistry Letters* **25** (21): 4719-4723.

Yu, H., J. Sperlich, A. Mándi, T. Kurtán, H. Dai, N. Teusch, Z.-Y. Guo, K. Zou, Z. Liu and P. Proksch (2018). "Azaphilone derivatives from the fungus Coniella fragariae inhibit NF-kappaB activation and reduce tumor cell migration." *Journal of Natural Products* **81** (11): 2493-2500.

Zheng, C.-J., H.-X. Liao, R.-Q. Mei, G.-L. Huang, L.-J. Yang, X.-M. Zhou, T.-M. Shao, G.-Y. Chen and C.-Y. Wang (2019). "Two new benzophenones and one new natural amide alkaloid isolated from a mangrove-derived fungus *Penicillium citrinum*." *Natural Product Research* **33** (8): 1127-1134.

List of Abbreviations

Abbreviation	
$[\alpha]_D$	Specific optical rotation at the sodium D-line
Ara-A	9-β-D-arabinofuranosyladenine
Ara-C	Cytosine arabinoside
5-AC	5-Azacytidine
ADC	Antibody-drug Conjugates
Axl RTK	AXL receptor tyrosine kinase
AC	Absolute configuration
Å	Angström
Arg	Arginine
Asn	Asparagine
A. falconensis	*Aspergillus falconensis*
BCMA	B-cell maturation antigen
BLAST	Basic local alignment search tool
Br−	Bromine ion
br	Broad
CDK-2	Cyclin-dependent kinase 2
Ca^{+2}	Calcium ion
Calcd.	Calculated
°C	Degrees Celsius
CIN	Chemotherapy-induced neutropenia
CDAs	Chiral derivatizing agents
CD	Circular Dichroism
CD71	Cluster of differentiation 71
$CDCl_3$	Deuterated chloroform
CEs	Cotton effects
CH_2Cl_2, DCM	Dichloromethane
$CHCl_3$	Chloroform
CK8	N-[4-(2,4-dimethyl-thiazol-5-yl)-pyrimidin-2-yl]-N',N' dimethyl- benzene-1,4-diamine
CLSI	Clinical and laboratory standards institute
COSY	Correlation spectroscopy
Cm^{-1}	Centimeter
Cl−	Chlorine ion
Cu-Kα	Copper K-alpha
COX-2	Cyclooxygenase-2
C–H	Carbon-hydrogen
d	Doublet signal
dd	Doublet of doublet signal
ddd	Doublet of doublet of doublet signal
dddd	Doublet of doublet of doublet of doublet signal
1D	One dimensional
2D	Two dimensional
DFT	Density functional theory
DNA	Deoxyribonucleic acid
DNMT	DNA methyl transferase
D_2O	Deuterated water
DMSO	Dimethyl sulfoxide

ECD	Electronic circular dichroism
ECCD	Exciton chirality circular dichroism
ENPP3	Ectonucleotide pyrophosphatase/phosphodiesterase 3
EEF1A2	Eukaryotic translation elongation factor 1 alpha 2
EtOAc	Ethyl acetate
ESIMS	Electrospray ionization mass spectrometry
e.g.	Exempli gratia, meaning “for example”
et al.	Et alia, meaning “and others”
$FADH_2$	1,5-Dihydro-flavin adenine dinucleotide
FDA	Food and Drug Administration
FDAA	1-Fluoro-2,4-dinitrophenyl-5-$_L$-alanine amide
FD	Failed to dock
FT-IR	Fourier-transform infrared spectroscopy
g	Gram
GLC	Gas-liquid chromatography
Glu	Glutamate
Gly	Glycine
Gln	Glutamine
ΔG	Gibbs free energy
h	Hour (s)
H-bond	Hydrogen bond
HRESIMS	High-resolution electrospray ionization mass spectrometry
HDAC	Histone-deacetylase
HER2	Human epidermal growth factor receptor 2
Hz	Herz
HMBC	Heteronuclear multiple-bond correlation
HPLC	High performance liquid chromatography
HSQC	Heteronuclear single quantum coherence
His	Histidine
IC_{50}	Half maximal inhibitory concentration
IGF-1R	Insulin-like growth factor-1 receptor
Ile	Isoleucine
ITS	Internal transcribed spacer
IR	Infrared
i.d.	Inner diameter
Kcal	Kilocalorie
KJ	kilojoule
KBr	Potassium bromide
KI	Potassium iodide
Km^2	Square kilometre
L	Liter
Leu	Leucine
Lys	Lysine
m	Multiplet signal
m	Meter
M	Molar
MHz	Megahertz
mL	Milliliter
mm	Millimeter
m/z	Mass per charge

MMM	Modified Mosher's method
µg	Microgram
µM	Micromolar (10^{-6} mol/L)
MMP-13	Matrix metalloproteinase 13
MMAE	Monomethyl auristatin E
MMAF	Monomethyl auristatin F
c-Met	Mesenchymal-epithelial transition factor
mmol	Millimole
MeCN	Acetonitrile
MeOH	Methanol
MMFF	Merck molecular force field
min	Minute (s)
MPDB	Malt peptone dextrose broth
MTPA	*α*-Methoxy-*α*-trifluoromethylphenylacetic acid
MTPA-Cl	*α*-Methoxy-*α*-trifluoromethylphenylacetyl chloride
MPA	Methoxyphenylacetic acid
MTT	3-(4,5-Dimethylthiazol-2-yl)-2,5-diphenyltetrazolium bromide
M. marquandii	*Metarhizium marquandii*
NA	Not available
NaCl	Sodium chloride
NaBr	Sodium bromide
NaF	Sodium fluoride
NaI	Sodium iodide
NaPi2b	Sodium-dependent phosphate transport protein 2b
NCBI	The National center for biotechnology information
ND	Not done
NF-κB	Nuclear factor kappa-light-chain-enhancer of activated B cells
NH_3	Ammonia
nm	Nanometer
NMR	Nuclear magnetic resonance
NOE	Nuclear Overhauser effect
NOESY	Nuclear Overhauser effect spectroscopy
NP	Natural product
NSCLC	Non-small-cell lung carcinoma
$(NH_4)_2SO_4$	Ammonium sulfate
OR	Optical rotation
ORD	Optical rotatory dispersion
OSMAC	One Strain Many Compounds
Phe	Phenylalanine
PB4	N,N'-bis (4-fluoro-3-methylbenzyl) pyrimidine-4,6-dicarboxamid
PDB	Potato dextrose broth
PDYB	Potato dextrose yeast broth
pIC_{50}	$-\log_{10}$ (half maximal inhibitory concentration)
Pro	Proline
π-bond	Pi bond
PYG	Peptone yeast glucose broth
ppm	Patrs per million

q	Quartet
ROESY	Rotating-frame nuclear Overhauser effect correlation spectroscopy
RP	Reversed phase
ROR2	Receptor tyrosine kinase-like Orphan receptor 2
s	Singlet
sh	Showlder
SAHA	Suberoylanilide hydroxamic acid
SBHA	Suberoyl bishydroxamic acid
SAM	S-adenosyl-methionin
SOR	Specific optical rotation
STAT3	Signal transducer and activator of transcription 3
sp.	Species
t	Triplet signal
td	Triplet of doublet
TDDFT	Time-dependent density functional theory
Thr	Threonine
TLC	Thin-layer chromatography
TMS	Trimethylsilyl group
TOP-2	Human DNA topoisomerase II
TNBC	Triple-negative breast cancer
TNFα	Tumor necrosis factor alpha
TPA	Tissue plasminogen activator
Tyr	Tyrosine
UDB	Universal NMR Database
UV/Vis	Ulta-violet/Visible
VCD	Vibrational Circular Dichroism
VEGF	Vascular endothelial growth factor
VLC	Vacuum liquid chromatography
w/v	Weight per Volume
XRD	X-ray diffraction analysis

List of Publications

1. **Dina H. El-Kashef**, Georgios Daletos, Malte Plenker, Rudolf Hartmann, Attila Mándi, Tibor Kurtán, Horst Weber, Wenhan Lin, Elena Ancheeva, and Peter Proksch (**2019**). Polyketides and a dihydroquinolone alkaloid from a marine-derived strain of the fungus *Metarhizium marquandii*. *Journal of natural products*, 82 (9), 2460-2469.

Overall contribution to this publication: First author, laboratory work including, compound isolation, structure elucidation, and preparation of manuscript

2. **Dina H. El-Kashef**, Fadia S. Youssef, Rudolf Hartmann, Tim-Oliver Knedel, Christoph Janiak, Wenhan Lin, Irene Reimche, Nicole Teusch, Zhen Liu, and Peter Proksch (**2020**). Azaphilones from the Red Sea Fungus *Aspergillus falconensis*. *Marine Drugs*, 18 (4), 204.

Overall contribution to this publication: First author, laboratory work including, cultivation and extraction, compound isolation, structure elucidation, and preparation of manuscript.

3. **Dina H. El-Kashef**, Fadia S. Youssef, Werner E.G. Müller, Wenhan Lin, Marian Frank, Zhen Liu and Peter Proksch (**2020**). A new dibenzoxepin and a new natural isocoumarin from the marine-derived fungus *Aspergillus falconensis*. *Bioorganic & medicinal chemistry*. (Submitted and currently under revision).

Overall contribution to this publication: First author, laboratory work including, cultivation and extraction, compound isolation, structure elucidation, and manuscript preparation.

4. Jana Deitersen, **Dina H. El-Kashef**, Peter Proksch, and Björn Stork (**2019**). Anthraquinones and autophagy–Three rings to rule them all?. *Bioorganic & medicinal chemistry*, 27 (20), 115042.

5. Sherif S. Ebada, **Dina H. El-Kashef**, Werner E.G. Müller, and Peter Proksch (**2019**). Cytotoxic eudesmane sesquiterpenes from *Crepis sancta*. *Phytochemistry Letters*, 33, 46-48.

6. Kenneth G. Ngwoke, **Dina H. El-Kashef**, Georgios Daletos, Elena Ancheeva, Zhen Liu, Festus BC Okoye, Charles O. Esimone, and Peter Proksch (**2020**). *R*-Hexitronic acid, a new tetronic acid derivative isolated from a soil fungus FG9RK. *Natural Product Research*, 1-6.

7. Feng Pan, **Dina H. El-Kashef**, Rainer Kalscheuer, Werner E.G. Müller, Jungho Lee, Michael Feldbrügge, Attila Mándi, Tibor Kurtán, Zhen Liu, Wei Wu and Peter Proksch (**2020**). Cladosins L-O, new hybrid polyketides from the endophytic fungus *Cladosporium sphaerospermum* WBS017. *European Journal of Medicinal Chemistry*, 191, 112159.

8. Sherif S. Ebada, Nariman A. Al-Jawabri, Fadia S. Youssef, **Dina H. El- Kashef**, Tim-Oliver Knedel, Amgad Albohy, Michal Korinek, Tsong-Long Hwang, Bing-Hung Chen, Guan-Hua Lin, Chia-Yi Lin, Sa'ed M. Aldalaien, Ahmad M. Disi, Christoph Janiak and Peter Proksch (**2020**). Anti-inflammatory, antiallergic and COVID-19 protease inhibitory activities of phytochemicals from the Jordanian hawksbeard: identification, structure–activity relationships, molecular modeling and impact on its folk medicinal uses. *RSC Advances*, 10, 38128-38141.

Conferences

Dina H. El-Kashef, Georgios Daletos, Malte Plenker, Rudolf Hartmann, Attila Mándi, Tibor Kurtán, Horst Weber, Wenhan Lin, Elena Ancheeva and Peter Proksch (**2019**). Polyketides and a Dihydroquinolone Alkaloid from a Marine-Derived Strain of the Fungus *Metarhizium marquandii*. Marine Drugs, Poster presentation at the XVI International Symposium on Marine Natural Products & XI European Conference on Marine Natural Products, September 1st-5th, Peniche, Portugal.

Acknowledgement

To the almighty God **"ALLAH"** who has granted me all these graces to fulfill this work and who supported and blessed me by His power and His mercy in all my life. To Him I extend my heartfelt thanks.

My sincere appreciation and deepest thanks to Prof. Dr. Dres. h.c. Peter Proksch for giving me the precious opportunity to pursue my doctoral studies in his research group at the Institute of Pharmaceutical Biology and Biotechnology, Heinrich Heine University, Düsseldorf. His encouragement, unforgettable support, priceless advices, direct guidance were always the energy driven to me to perform well and to achieve my goals. In addition, his direct insights in the field of natural products and his continuous seeking for scientific distinction will always be a model for inspiration to me. I am deeply grateful to him for the chances given to me for fruitful collaborations with other research groups. I also wish to express my thanks to Mrs. Dr. Proksch for her support, nice meetings and help in providing samples that ended up with a successful project.

I extend my deepest thanks to my mentor Prof. Dr. Matthias Kassack, from the institute of Pharmaceutical and Medicinal Chemistry, Heinrich Heine University, Düsseldorf, for giving me the honour to be my second supervisor and for co-reviewing my thesis.

I wish to express my appreciation to Prof. Dr. Rainer Kalscheuer, from the Institute of Pharmaceutical Biology and Biotechnology, Heinrich Heine University, Düsseldorf, for performing antimicrobial assays.

I would like to express my cordial thanks to Prof. Dr. Nicole Teusch and Ms. Irene Reimche (Department of Biomedical Sciences, Faculty of Human Sciences, University of Osnabrück) for their collaboration in the cytotoxicity and anti-inflammatory assays.

My appreciation goes to Prof. Dr. Werner E.G. Müller (Institute of Physiological Chemistry, Johannes Gutenberg University, Mainz) for performing cytotoxicity assays against mouse lymphoma cell line L5178Y.

My sincere appreciation and deepest thanks to Prof. Dr. Wenhan Lin (State Key Laboratory of Natural and Biomimetic Drugs, Peking University, Beijing, China) for fruitful discussions and ideas and for solving complex NMR problems. My special

thanks to Prof. Dr. Bingui Wang (Laboratory of Experimental Marine Biology, Institute of Oceanology, Chinese Academy of Science, China) for constructive discussions and advises.

I want to thank Prof. Dr. Tibor Kurtán and Dr. Attila Mándi (Department of Organic Chemistry, University of Debrecen, Hungary) for their effort in ECD and VCD measurements and calculations.

I wish to express my appreciation to Prof. Dr. Christoph Janiak and Dr. Tim-Oliver Knedel (Institute of Inorganic Chemistry and Structural Chemistry, Heinrich Heine University, Düsseldorf) for their collaboration on X-ray crystallography analysis.

I also wish to express my thanks to Dr. Rudolph Hartmann and Mr. Malte Plenker (Institute of Complex Systems, Forschungszentrum, Jülich) for performing NMR measurements on very small amounts of complicated compounds and helping in structure elucidation of my compounds.

My thanks go to Prof. Dr. Björn Stork and Ms. Jana Deitersen (Institute of Molecular Medicine I, Medical Faculty, Heinrich Heine University, Düsseldorf) for the nice collaboration.

I am deeply indebted to Dr. Sigrun Wegener-Feldbrügge (Junior Scientist and International Researcher Center (JUNO), Heinrich Heine University, Düsseldorf) for her continuous help and support which had started even before I came to Germany. I also wish to express my thanks to PD Dr. Katrin Henze (personal assistant of the dean, faculty of mathematics and natural sciences, Heinrich Heine University, Düsseldorf) for her help and concern.

I am grateful to Dr. Georgios Daletos for his help and valuable advices in structure elucidation of my compounds and in rechecking my data.

I wish to extend my thanks to Dr. Elena Ancheeva for constructive suggestions, fruitful discussions and revising my first manuscript.

My appreciation and thanks go to Dr. Zhen Liu for his valuable suggestions and precious discussions regarding structure elucidation of isolated compounds and his efforts in manuscripts' revisions.

I extend my deepest thanks, appreciation and heartfelt gratitude to Assoc. Prof. Dr. Sherif S. Ebada (Department of Pharmacognosy, Faculty of Pharmacy, Ain-Shams University, Cairo, Egypt) for fruitful discussions and successful collaborations.

I also wish to express my thanks to Dr. Marian Frank for nice discussions, scientific advices, rechecking my data and his kind help in translating the abstract of my thesis to German.

Many thanks go to Dr. Nam M. Tran-Cong for inspiring discussions and kind help during my Ph.D. study time. I also wish to thank Dr. Haiqian Yu for his continuous support and his help during submission of my thesis. My sincere appreciation goes to Dr. Yang Liu for her scientific guidance when I first joined the research group.

I would like to express my cordial thanks to Ms. Kim Thao Le for her continuous help and remarkable support throughout my Ph.D. time.

My thanks go to my laboratory partner Dr. Harwoko Harwoko for the nice scientific discussions and for sharing ideas with me.

My appreciation goes to Mrs. Claudia Eckelskemper for her administrative help whenever needed and to our team of technicians Mrs. Simone Miljanovic, Mrs. Simone Mönninghoff-Pützer, Mrs. Katja Friedrich, Ms. Linda Wiegand, Mrs. Maryam Masrouri and Mrs. Heike Goldbach-Gecke for their support and help during my Ph.D. time.

My heartfelt thanks go to my former colleagues and postdocs for the happy times, supportive atmosphere at the institute and the valuable friendships that developed during this time: Dr. Mariam Moussa, Dr. Nada Abdel-Wahab, Dr. Fadia S. Youssef, Dr. Amin Mokhlesi, Dr. Daowan Lai, Dr. Hao Wang, Dr. Miada Fouad Abdelwahab Sakr, Ms. Flaminia Mazzone, Dr. Hajar Heydari, Dr. Catalina Perez Hemphill, Dr. Feng Pan, Dr. Han Xiao, Mr. Lei Wang, Mrs. Nihal Aktas, Dr. Peter Eze, Dr. Ramsay Kadeem, Dr. Sergi Herve Akone, Mr. Viktor Simons, Dr. Ni Putu Ariantari, Dr. Rini Muharini, Dr. Shuai Liu, Mr. Tino Seidemann, Ms. Xiaoqin Yu and Mrs. Ying Gao. I wish to thank Mr. Jens Hagenow and Ms. Milica Elek for their assistances and advices for chemical synthesis.

I would like to express my cordial thanks and profound gratitude to Prof. Dr. Mostafa Ahmed Fouad (Department of Pharmacognosy, Faculty of Pharmacy, Minia

University, Egypt) for introducing me to the research group of Prof. Dr. Dres. h.c. Peter Proksch.

My profound appreciation to the Egyptian Ministry of Higher Education, Missions Office for awarding a doctoral scholarship.

My deep thanks to all my colleagues, technical staff and all the family of Pharmacognosy Department, Faculty of Pharmacy, Minia University, for their encouragement and help.

This journey would not have been possible without the support of my family. To my family, thank you for encouraging me in all of my pursuits and inspiring me to follow my dreams. My grand indebtedness to my parents, my husband Amro, my lovely son Mohammed and my brothers, who supported me emotionally with their unfailing love, spiritual support, continuous prayers and encouragement. I always knew that you believed in me and wanted the best for me.

To All of You, Thank You Very Much

و آخر دعوانا أن الحمد لله ربّ العالمين